Heavy-Quark Pair Production at Hadron Colliders: Transverse-Momentum Resummation NNLO Corrections and Azimuthal Asymmetries

---

Dissertation

zur

Erlangung der naturwissenschaftlichen Doktorwürde
(Dr. sc. nat.)

vorgelegt der

Mathematisch-naturwissenschaftlichen Fakultät

der

Universität Zürich

von

Hayk Sargsyan

aus

Armenien

Promotionskomitee

Prof. Dr. Massimiliano Grazzini (Vorsitz und Leitung der Dissertation)
Prof. Dr. Thomas Gehrmann
Prof. Dr. Stefano Pozzorini
Prof. Dr. Adrian Signer

Zürich, 2017

Abstract

The Standard Model (SM) of particle physics successfully describes the known elementary particles and their interactions through electroweak and strong forces. Despite extensive tests, no evidence of beyond-the-Standard-Model phenomena has been observed, and the discovery of the Higgs boson in 2012 crowns the SM as one of the most successful theories of modern physics. Being the heaviest known particle, the top quark is expected to play a special role in many extensions of the SM, and the thorough understanding of its signatures and properties is of utmost importance to shed light on the mechanism of spontaneous electroweak symmetry breaking and to control the backgrounds in New Physics searches. The main method to obtain quantitative predictions in particle physics is perturbation theory, which relies on the expansion of observables in powers of the relevant coupling constant and on the truncation of the series at some fixed order. The computation of the coefficients of the perturbative series is a highly non-trivial task, its difficulty increasing dramatically with the order. In addition, the fixed-order computation of some observables in Quantum Chromodynamics leads to non-physical predictions at phase space boundaries, due to the large logarithmic contributions related to the infrared behaviour of the theory. A well known example of such an observable is the transverse-momentum (q_T) spectrum of high-mass systems. A related observable that may not be computable in fixed-order perturbation theory is the azimuthal distribution. The logarithmically- enhanced contributions in the fixed-order computation of this observable are related to the azimuthal correlations of the corresponding transverse-momentum distribution at low q_T. To obtain a reliable prediction for this class of observables the standard fixed-order perturbation theory can be improved through a resummation procedure, which aims at summing the logarithmically-enhanced contributions to all perturbative orders.

In this thesis we consider the computation of higher-order corrections to heavy-quark production at hadron colliders, its transverse-momentum spectrum, and the ensuing azimuthal correlations. In particular, we exploit our understanding on the singular behavior of the transverse-momentum spectrum to obtain new results on the second order perturbative contributions to this process in Quantum Chromodynamics. We also present quantitative predictions for the transverse-momentum spectrum of the top-quark pair at next-to-leading logarithmic accuracy, and a first comparison to experimental data. We finally provide a general discussion of azimuthal asymmetries for a wide class of processes, by presenting new quantitative results for the case of top-quark production.

Zusammenfassung

Das Standardmodell (SM) der Teilchenphysik umfasst eine erfolgreiche Beschreibung der bekannten Elementarteilchen und ihrer Wechselwirkungen durch elektroschwache und starke Kräfte. Trotz umfangreicher Untersuchungen wurde kein Hinweis darauf gefunden, dass Phänomene existieren, die über das SM hinausgehen. Die Entdeckung des Higgs-Bosons im Jahr 2012 krönte das SM schliesslich als eine der erfolgreichsten Theorien der modernen Physik. Als schwerstes bekanntes Teilchen kommt dem Top-Quark in vielen Erweiterungen des SM eine besondere Rolle zu: Ein gründliches Verständnis seiner Signatur und Eigenschaften sind enorm wichtig, um Aufschluss über den Mechanismus der spontanen elektroschwachen Symmetriebrechung zu geben und die Hintergrundstrahlung von Physik jenseits des Standardmodells zu steuern. Die wichtigste Methode, um quantitative Vorhersagen in der Teilchenphysik zu erhalten, ist Störungstheorie. Sie beruht auf der Entwicklung von Observablen in Potenzen der relevanten Kopplungskonstante sowie auf dem Abbruch der Reihe zu einer festen Ordnung. Die Berechnung der Koeffizienten der Störungsreihe ist eine höchst nichttriviale Aufgabe, da die damit verbundene Schwierigkeit drastisch mit der Ordnung steigt. Darüber hinaus führt die Berechnung einiger Observablen zu fester Ordnung in der Quantenchromodynamik zu nichtphysikalischen Vorhersagen an Grenzpunkten des Phasenraums, was auf die grossen logarithmischen Beiträge im infraroten Bereich der Theorie zurückzuführen ist. Ein wohlbekanntes Beispiel einer solchen Observable ist das Spektrum des Transversalimpulses (q_T) eines massereichen Systems. Eine verwandte Observable, deren Berechnung in Störungstheorie zu fester Ordnung nicht möglich sein dürfte, ist die azimutale Verteilung. Die logarithmisch verstärkten Beiträge dieser Observable bei der Berechnung zu fester Ordnung sind verknüpft mit den azimutalen Korrelationen der entsprechenden Transversalimpulsverteilung für kleines q_T. Um eine verlässliche Vorhersage für diese Klassen von Observablen zu erhalten, kann die klassiche Störungstheorie zu fester Ordnung durch eine sogenannte Resummation verbessert werden, welche darauf abzielt, die logarithmisch verstärkten Beiträge zu allen Ordnungen der Störungstheorie zu summieren.

In dieser Thesis betrachten wir die Berechnung von Korrekturen höherer Ordnung zur Produktion schwerer Quarks an Hadronen-Beschleunigern sowie deren Transversalimpulsspektrum und der sich ergebenden azimutalen Korrelationen. Besonderen Wert legen wir auf ein Verständnis des singulären Verhaltens des Transversalimpulsspektrums, um neue Ergebnisse zu Beiträgen zweiter Ordnung Störungstheorie zu diesem Prozess in der Quantenchromodynamik zu erhalten. Wir präsentieren zudem quantitative Vorhersagen für das Transversalimpulsspektrum des Top-Quark-Paars zu nächst-zu-führender logarithmischer Genauigkeit sowie einen ersten Vergleich mit experimentellen Daten. Schliesslich diskutieren wir in allgemeiner Form azimutale Asymmetrien für eine grosse Klasse an Prozessen, indem wir neue quantitative Ergebnisse für den Fall der Top-Quark-Produktion vorstellen.

Contents

Chapter 1

Introduction

The properties and interactions of all known elementary particles can be described within a single theoretical framework, known as the Standard Model (SM). The SM incorporates the constituents of matter, the quarks and the leptons, as well as their interactions through electroweak and strong forces. The electroweak sector of the SM is described by the Glashow-Weinberg-Salam model [1–3], which is based on the unification of Quantum Electrodynamics (QED) [4–7] and weak interactions. Its mathematical formulation is based on the $\mathrm{SU}(2)_L \times \mathrm{U}(1)_Y$ gauge symmetry group of weak left-handed isospin and hypercharge. The strong interactions of quarks and gluons are described by Quantum Chromodynamics (QCD) [8–10], which is based on the $\mathrm{SU}(3)_C$ colour symmetry group. The interactions of the elementary particles are realised through the force-carriers of the theory, the gauge bosons, whose properties are fundamentally different from those of fermions. The masses of the gauge bosons in the SM are generated through the so-called electroweak symmetry breaking (EWSB) mechanism [11–15] proposed in mid-1960s. The scalar particle, the Higgs boson, predicted by the EWSB mechanism was the last building block of the SM, and it has eluded the experimental detection until recently. On July 4th 2012 the ATLAS and CMS collaborations at the Large Hadron Collider (LHC) have announced the discovery of a new scalar resonance [16, 17] of mass about 125 GeV. The measurements of the properties of this resonance are in a very good agreement with what expected for the SM Higgs boson. Combined with the high-precision SM tests during the last decades at the particle colliders like LEP, HERA, the Tevatron and the LHC, the Higgs boson discovery makes the SM the most successful theory of modern physics.

Despite being a mathematically complete theory accommodating almost all known experimental data available to date, the SM is believed to be a mere effective theory, valid only at the presently accessible energies. The first major and obvious problem of the SM as the fundamental theory of our universe, is that it describes the interactions of the elementary particles only through three out of the four fundamental forces, the gravitational interaction being left out. Furthermore, it does not explain the hierarchical

pattern of fermion masses. For example, the top quark (t), the heaviest known particle, is more than five orders of magnitude heavier than the electron e and more than thirty times heavier than the next heaviest quark, the bottom quark (b).

Besides the aforementioned shortcomings of the SM, there are other severe problems that call for New Physics (NP). Cosmological and astrophysical observations and computer simulations show that the particles described by the SM account for less than 5 % percent of the content of the universe. The remaining energy of the universe is assigned to the so-called dark matter (DM) and the dark energy. One possible explanation of the DM is that it could be due to an unknown stable, massive, electrically neutral and very weakly interacting particle. The SM does not include any dark matter candidate particle.

One of the conceptual limitations of the SM is the so-called hierarchy problem [18, 19], which is related to the unnaturally small value of the Higgs boson mass $m_H \approx 125\,\text{GeV}$. When computing the radiative corrections to the Higgs mass squared, one encounters quadratically divergent contributions coming from self-energy corrections. This means that the Higgs mass should be naturally of the order of the cut-off of the model, i.e., the scale at which NP should show up. Without a NP contribution appearing at relatively low energy, the parameters of the SM need to be fine-tuned, in order to accommodate the experimentally observed value of the Higgs mass.

A special role in the SM is played by the top quark, which is predominantly produced through the $t\bar{t}$ pair production process at hadron colliders. Due to its large mass of about 173.3 GeV, and, consequently, large Yukawa coupling, the top quark has the largest contribution among all the fermions to the hierarchy problem. It is also the only quark that decays before hadronization, thus allowing to study the properties of the 'bare' quark, through its decay products. Because of its special role in the SM, the precise understanding of top-quark properties, and, in particular, the accurate knowledge of inclusive and differential cross sections for $t\bar{t}$ production is crucial also for beyond-the-Standard-Model (BSM) searches, since top-quark production is a background to many NP signatures.

Following its discovery twenty years ago [20], the top quark has been under an intensive study at the Tevatron. The two general-purpose experiments at the LHC, ATLAS and CMS, have analysed the data collected during the first run of the LHC at center of mass energies $\sqrt{s} = 7$ and $8\,\text{TeV}$ [21–24]. The combination of all these results already provides important measurements for various top-quark observables. The LHC has already started accumulating data at $\sqrt{s} = 13\,\text{TeV}$. With the increased luminosity and energy, many more top-quark pairs will be produced. As a result, the experimental uncertainties will be substantially reduced, enabling us to do precision studies on top-quark physics, which calls for precision predictions from the theory side.

To obtain high-precision theoretical predictions is, however, a highly non-trivial task, since the equations defining the SM can not be solved in closed form. The framework

to obtain quantitative predictions in particle physics is provided by perturbation theory, i.e. the possibility of organising the computation of cross sections of scattering processes as a fixed order expansion in powers of the relevant coupling constant. Of the various perturbative corrections that can be considered, those from the strong interactions are often the most important. The leading term in this expansion is called the leading order (LO) contribution, followed by the next-to-leading order (NLO), next-to-next-to-leading order (NNLO), and so forth. While in most of the cases the LO contribution to the cross section or any other properly defined observable is relatively straightforward, it only gives an order-of-magnitude estimate. To obtain a realistic estimate of the observable at least the NLO, and more often the NNLO computation is required.

The calculation of the higher-order contributions in the series expansion requires the computation of radiative corrections to the LO process. At NLO it includes the computation of the *virtual*, or *loop* (one more particle running in a closed loop), and *real* (one more particle in the final state) corrections. Separately, these contributions are ill-defined. The virtual corrections contain *ultraviolet* (UV) divergences, which are cured by renormalization, as well as *infrared* (IR) divergences, while the real corrections contain only IR divergences. Although according to the Bloch-Nordseck [25] and Kinoshita-Lee-Nauenberg (KLN) theorems [26, 27] the IR divergences are guaranteed to cancel out once the virtual and real corrections are combined, for any properly defined observable, their presence at intermediate stages does not permit a straightforward implementation of numerical techniques.

A general framework to handle and cancel IR singularities is provided by the so-called *subtraction methods*. The main idea of the subtraction methods is to reorganise the intermediate steps of the calculation in such a way that all phase-space integrations are finite and can be performed numerically. At NLO in QCD, two process-independent subtraction schemes are available: Catani-Seymour dipole subtraction [28–30], and the FKS subtraction [31]. Nowadays, the implementation of general NLO subtraction schemes has been combined with codes capable of numerically computing tree-level and one-loop amplitudes for a given process [32–34]. This important step in principle allows a complete automation of the NLO computations.

At NNLO the situation is much more involved. Various methods have been proposed and used to handle the IR singularities at the NNLO level for different classes of processes. The formalisms of *colourful* subtraction [35, 36] and *antenna* subtraction [37–42] are more related to NNLO extensions of the established NLO formulations of the subtraction method mentioned above. The *Stripper* formalism [43–45] is a combination of the subtraction method with numerical techniques based on *sector decomposition* [46, 47]. Variants of the subtraction methods are the q_T subtraction formalism [48] and the recently proposed *N-jettiness* subtraction [49–51].

This thesis addresses the computation of higher-order corrections to heavy-quark pro-

duction at hadron colliders, its transverse-momentum spectrum, and the ensuing azimuthal correlations. As far as $t\bar{t}$ production is concerned, the theoretical efforts for obtaining precision predictions started almost thirty years ago with the calculation of the NLO corrections to this process [52–56]. To go one order higher in perturbation theory, as already mentioned, is a formidable task and only recently the calculation of the NNLO QCD corrections to the inclusive $t\bar{t}$ cross section was completed [57–60]. The total cross section, however, is an ideal quantity, while the experiments always have finite acceptances. Moreover, the total cross section does not give a full picture of the dynamics of the process. Thus, besides the total cross section, the differential cross sections are of a great importance for precision studies. One example of such observable is the invariant mass distribution of the $t\bar{t}$ pair, for which precise predictions have been worked out in Ref. [61]. Recently, differential results for the top-quark charge asymmetry have been presented at NNLO accuracy [62], followed by differential results for top-quark pair production at the LHC [63] and the Tevatron [64] in NNLO QCD. The NNLO computations in Refs. [57–60, 62–64] for $t\bar{t}$ production have been performed by using the Stripper method [43]. Parallely, an ongoing effort is being carried out by using the antenna subtraction method [40,65], which led to the NNLO fully differential computation of $t\bar{t}$ production in the $q\bar{q}$ channel [66, 67] at leading colour and including the light-quark contributions.

Despite being a powerful tool, fixed-order perturbation theory sometimes cannot provide physically meaningful predictions. In the case of semi-inclusive observables, when more than one energy scale is involved, large logarithmic terms involving the ratio of the different scales appear, which may invalidate the fixed-order expansion. An important example is the transverse momentum (q_T) spectrum of a system with large invariant mass M. When $q_T \sim M$ the standard perturbative treatment is applicable. At small transverse momenta, $q_T \ll M$, large logarithmic contributions of the form $\alpha_S^n \log^m(M^2/q_T^2)$ ($m = 2n, \ldots, 1$) appear that lead to the breakdown of the fixed-order perturbative expansion. Eventually, the fixed-order computation of the transverse-momentum spectrum leads to a divergent cross section as $q_T \to 0$.

The unphysical (divergent) behavior of the transverse-momentum spectrum in fixed-order perturbation theory has been known for long time. A less known issue regards the corresponding divergent behaviour of azimuthal distributions for a large class of processes at hadron colliders. The class of processes which exhibit this problem includes $t\bar{t}, Vj, jj, \gamma\gamma, \ldots$, while, for instance, the azimuthal distributions for the Drell-Yan (DY) process are computable in fixed-order perturbation theory (see e.g. Ref. [68] and references therein). As it will be shown in this thesis, the divergent behaviour of azimuthal correlations in fixed-order calculations is directly related to the *azimuthal correlations* of the transverse-momentum spectrum at low q_T for these processes. The latter issue has been first noted in Ref. [69] for the processes that are driven by gluon fusion at LO. This unphysical behaviour of fixed-order perturbative QCD at small values of q_T and the consequent divergence of the q_T integrated azimuthal correlations requires some deeper understanding in order to achieve a QCD prediction for physically measurable azimuthal distributions.

The nowadays standard mechanism to obtain reliable perturbative predictions for the transverse-momentum spectrum at small q_T is the so-called *resummation* of the large logarithmic contributions to all orders in $\alpha_{\rm S}$. In its core, the resummation of the large logarithmic contributions is realised through their all-order *exponentiation*. In QCD, the transverse-momentum resummation has been originally proposed and applied to the hadroproduction processes of colourless systems F with large invariant mass [70–82]. In more recent years the techniques and methods of Soft Collinear Effective Theory (SCET) [83–85] have been developed and applied to transverse-momentum resummation for this class of processes [86–92].

Recently, the transverse-momentum resummation formalism has been extended to the production of heavy-quark pairs $Q\bar{Q}$ at hadron colliders in SCET [93, 94], and using the traditional QCD resummation framework [95]. The main complication of transverse-momentum resummation for the production of a heavy-quark pair with respect to the production of a colourless system F is related to the appearance of additional soft singularities due to the final-state radiation. The structure of these singularities is much more involved due to the non-trivial *colour correlations* between the final-state heavy quarks and initial-final state interferences. This poses technical complications for its application to numerical computations, which is one of the objectives of this thesis. As it will be shown, the contribution from the final-state soft radiation needs a special treatment due to the non-diagonal structure of colour-correlations.

An important difference between the work in Refs. [93, 94] and the work in Ref. [95] regards the treatment of the azimuthal angle $\phi(\mathbf{q_T})$ of the transverse-momentum vector $\mathbf{q_T}$ of the $Q\bar{Q}$ pair and the azimuthal angles $\phi(\mathbf{p_{T}}_{3,4})$ of the transverse-momentum vectors $\mathbf{p_{T}}_{3,4}$ of the heavy quarks. While the analysis in Refs. [93, 94] is limited to the study of the q_T spectrum after the integration over these azimuthal angles, the results in Ref. [95] are valid at the fully-differential level with respect to the kinematics of the produced heavy quarks, with the full control of the ensuing *azimuthal correlations* $\phi(\mathbf{q_T}) - \phi(\mathbf{p_{T}}_{3,4})$ at small q_T. The full control over the azimuthal correlations is crucial in the view of our study of the azimuthal distributions. In particular, in the case of $t\bar{t}$ production, we show that with the extension of our transverse-momentum resummation formalism to deal with the azimuthal correlations at small q_T, we can predict finite azimuthal distributions that can be measured at hadron colliders [96]. Moreover, the azimuthal correlations at small q_T have also a non-trivial effect on the azimuthally-averaged q_T cross section for $t\bar{t}$ production starting from NNLL+NNLO accuracy, and on the inclusive cross section starting from NNLO. The effect of azimuthal correlation terms on the averaged cross section has been first studied in Ref. [69] for the production processes of colourless systems that are mediated by the gluon fusion subprocess at LO. As it is shown in this thesis, this effect is more complicated in the case of heavy-quark production, requiring a computation of non-trivial integrals over the azimuthal angle.

Besides its phenomenological relevance in obtaining physical predictions at small q_T, the

transverse-momentum resummation formalism has also a direct application to the fixed-order calculations in the framework of the q_T subtraction method [48]. The q_T subtraction method exploits the analytical knowledge of the singularity structure of the cross section at small q_T, which is given by the resummation formulae, to construct IR subtraction counterterms to handle and cancel the IR divergences at the NLO and NNLO level. By using the transverse-momentum resummation formalism for hadroproduction of colourless high-mass systems, the method has been successfully applied to the fully differential computation of NNLO QCD corrections to several hard-scattering processes of this class [48, 97–107].

With the extension of the transverse-momentum resummation formalism to heavy-quark pair production [95], a formulation of the q_T subtraction method for this process becomes feasible. In this thesis we carry out two major steps in this direction. We first compute the IR counterterms that are needed for the NNLO calculation of heavy-quark pair hadroproduction, to complete the computation of the NNLO QCD corrections to top-quark pair production in all off-diagonal channels [108]. Then, we consider the diagonal channels by showing, for the first time, the cancellation of the singularities between the NLO $t\bar{t}$+jet cross section and the corresponding subtraction counterterm. Technically, this is the most delicate part of the calculation, and it provides a crucial check of the entire framework. The completion of the NNLO computation in the diagonal channels will be possible once the NNLO hard-collinear functions will be available. The computations performed in this thesis require the evaluation of Born-level and one-loop colour-correlated UV renormalised amplitudes, combined with the proper IR subtraction operators and, at the same time, the use of existing NLO automated codes for the $t\bar{t}$ + jet process. In particular, we use the Munich code [109], which provides a fully automated implementation of the NLO dipole subtraction formalism [28, 30] as well as an interface to the one-loop generator OpenLoops [32]. The computations presented here can straightforwardly be extended to the production of massive-quark pairs of different flavour (e.g. bottom-quark pair). Moreover, with relatively little additional input they can be extended to the production processes of the kind $Q\bar{Q}F$, with F being a colourless (set of) particle(s).

The thesis is organized as follows. In Chapter 2 we give a short overview of the main aspects of QCD. In particular, the concepts of *confinement* and *asymptotic freedom* are outlined, and the factorization of QCD IR singularities is discussed with some detail. In Chapter 3 we sketch the transverse-momentum resummation formalism for the production of colourless systems with large invariant mass. We outline the physical differences between the processes that are mediated by the $q\bar{q}$ annihilation and gluon fusion subprocesses at LO. In particular, the issue of azimuthal correlations at small transverse momenta is introduced in Section 3.4.1, and in Section 3.4.2 we show their non-vanishing impact on the azimuthally-averaged cross section. In Chapter 4 we discuss the transverse-momentum resummation for the production of heavy-quark pairs at hadron colliders. In Section 4.1 we sketch the all-order resummation formula of Ref. [95]. Section 4.2 outlines the azimuthal structure of the resummed cross section. In particular, in Section 4.2.1 we present the explicit form of the azimuthal correlations at small q_T in NLO QCD and we provide the

resummation formula at NLL+NLO accuracy. In Section 4.2.2 we show the contribution of the azimuthal correlation terms at NNLO and we analytically compute the azimuthal integrals, which are crucial for the computation of the transverse-momentum resummed cross section at NNLL+NNLO accuracy and the NNLO QCD corrections in the framework of the q_T subtraction method. Starting from Section 4.3 we present the treatment of colour-correlated contributions in our computation. In particular, we fix the colour basis in Section 4.3 and present the explicit expressions for the soft anomalous dimension matrices in the chosen basis. Since the soft anomalous dimension matrices are not diagonal in colour space, we present the general algorithm of its diagonalization that is needed for the numerical implementation of the resummed q_T spectrum. In Section 4.5 and 4.6 we consider the azimuthally-averaged cross section and present the explicit expressions for the resummed and finite contributions at NNLL+NNLO, including the contributions from the azimuthally-correlated terms. We conclude the Chapter by presenting our numerical results for the resummed q_T spectrum at NLL+NLO accuracy in Section 4.7, and a first comparison to ATLAS data. Chapter 5 is devoted to the extension of the q_T subtraction method for the heavy-quark pair production process. We sketch the main building blocks of the method and present our numerical results at NLO and NNLO, by showing, for the first time, the cancellation of IR singularities in all partonic channels. In Chapter 6 we discuss the inapplicability of the fixed-order perturbation theory in providing physical predictions for azimuthal distributions for a large class of processes. In Section 6.1 we present our solution to the problem in the transverse-momentum resummation framework, extended to deal with azimuthal correlations at small q_T. We also present here quantitative results for fixed-order and resummed azimuthal correlations. Chapter 7 provides a brief summary and an outlook.

This thesis is the subject of three publications. The NNLO computation for heavy-quark pair production in the framework of the q_T subtraction method is documented in Ref. [108]. The numerical study of the resummed transverse-momentum spectrum of heavy-quark pairs will be published soon [110]. Finally, we are close to finalizing a detailed paper on the issue of the azimuthal asymmetries in general, along with the first numerical studies of the resummed azimuthal distributions for heavy-quark pair production [96].

Chapter 2

Quantum Chromodynamics

Quantum Chromodynamics (QCD) is the theory of strong interactions, one of the four fundamental forces of nature. It describes the interactions of quarks via their *colour* quantum numbers, mediated by the gauge bosons of the theory – the *gluons*. It is similar in structure to Quantum Electrodynamics (QED), but with an important difference: QCD is described by a non-Abelian gauge group, SU(3), which allows for self-interactions of gluons. In the following, we sketch the historical developments towards the establishment of QCD and outline the main properties of the theory, such as *confinement* and *asymptotic freedom*.

The existence of approximately point-like constituents inside hadrons (protons and neutrons, in particular) was demonstrated by the classic electron deep inelastic scattering experiments performed at Stanford Linear Accelerator Center (SLAC) [111, 112]. To explain this phenomenon, the *parton model* was proposed, in which the constituents of hadrons were identified with partons, that we now know to be the quarks and the gluons. Hadrons are categorized into two families: baryons (proton, neutron, etc.) and mesons (pion, kaon, etc.). The observed baryons are interpreted as bound states of three quarks qqq, while mesons are formed from a quark-antiquark pair $q\bar{q}$. There are three families of quarks, each family containing one up-type and one down-type quark (2.1).

$$\begin{pmatrix} u \\ d \end{pmatrix}, \quad \begin{pmatrix} c \\ s \end{pmatrix}, \quad \begin{pmatrix} t \\ b \end{pmatrix}. \tag{2.1}$$

The quarks are referred to by their *flavours*, and called u (up), d (down), c (charm), s (strange), t (top) and b (bottom). The up-type quarks (u, c and t) carry an electrical charge of $+2/3$ and the down-type quarks (d, s and b) carry an electrical charge of $-1/3$, in the units of the electron charge.

In the naive quark model, that is, without assigning a colour charge to the quarks,

there is a difficulty in constructing the low-lying baryon states, such as the pion-nucleon resonance Δ^{++}, which is of spin 3/2. Based on its charge, isospin and strangeness, Δ^{++} is formed by three u-quarks. Moreover, for the state of Δ^{++}, with the third component of the total angular momentum $J_3 = 3/2$, all three u-quarks must also have their spins aligned up

$$|\Delta++, J_3 = \frac{3}{2}\rangle = |u\uparrow, u\uparrow, u\uparrow\rangle \ . \tag{2.2}$$

This assignment runs into a problem, because the quarks are assumed to be fermions and, hence, according to the *Pauli exclusion principle*, the same quantum state cannot be occupied by more than one quark with the same quantum numbers. This forces one to assume the existence of a hidden degree of freedom for quarks, the colour, to distinguish the otherwise identical three quarks. By introducing the additional colour quantum number, it is then easy to construct a totally antisymmetric state for Δ^{++}

$$|\Delta++, J_3 = \frac{3}{2}\rangle = \epsilon_{ijk}\,|u^i\uparrow, u^j\uparrow, u^k\uparrow\rangle \ , \tag{2.3}$$

where the indices i, j and k are the quark colour indices and ϵ_{ijk} is the totally antisymmetric tensor. For the construction of baryon states, like in Eq. (2.3), one needs at least three colours for the quarks. There is, in fact, experimental evidence, that the quarks have exactly three colours. The two most well-known indirect evidences for the colour degree of freedom are the decay $\pi \to \gamma\gamma$ and e^+e^- annihilation into hadrons.

Since the colour degree of freedom are not observed in the experiments, one may assume that the hadronic phenomena are unaltered under the colour transformations. The colour symmetry group is assumed to be the SU(3) group, and all the hadrons are in the colour-singlet states of SU(3). The corresponding colour-singlet state for the mesons can be constructed similarly to the baryon case in Eq. (2.3)

$$|M\rangle = \frac{1}{\sqrt{3}}\delta_{ij}\,|q^i\bar{q}^j\rangle \ . \tag{2.4}$$

The fact that the colour is not directly observable means that the quarks are confined to the inside of hadrons and are not observed as isolated states. This is known as quark *confinement* postulate.

Because of the confinement of quarks it was highly doubted that the parton model could be used for perturbative studies of strong interactions. The situation changed fundamentally with the discovery of asymptotic freedom in non-Abelian gauge theories in 1973 [8,9], which eventually led us to QCD. The asymptotic freedom predicts the coupling constant of strong interactions to be small at high energies so that the quarks behave as free particles at asymptotic energies. We discuss the property of asymptotic freedom in a bit more detail in Section 2.3, when we present the running of the strong coupling constant.

2.1 The Lagrangian of QCD

The QCD Lagrangian density has the following form

$$\mathcal{L}_{\rm QCD} = \mathcal{L}_{\rm classic} + \mathcal{L}_{\rm gauge-fix} + \mathcal{L}_{\rm ghost}\,. \tag{2.5}$$

The expression for the classical Lagrangian density $\mathcal{L}_{\rm classic}$ is

$$\mathcal{L}_{\rm classic} = -\frac{1}{4}F^a_{\mu\nu}F^{a,\mu\nu} + \sum_{\rm flavours}\bar{q}_i(i\not{D}_{ij} - m_q\delta_{ij})q_j\,. \tag{2.6}$$

These terms describe the interaction of quarks with mass m_q and gluons. The quark fields q_i are in the triplet representation of the colour group ($i = 1, 2, 3$). $F^a_{\mu\nu}$ is the gluon field strength tensor and is given by

$$F^a_{\mu\nu} = \partial^\mu A^a_\nu - \partial^\nu A^a_\mu - g_{\rm S}f^{abc}A^b_\mu A^c_\nu\,, \tag{2.7}$$

where $g_{\rm S}$ is the strong coupling of QCD and f^{abc} ($a, b, c = 1, \ldots, 8$) are the structure constants of the SU(3) colour group. It is the third 'non-Abelian' term on the right-hand side of Eq. (2.7) that distinguishes QCD from QED, giving rise to trilinear and quadrilinear gluon self-interactions. $\not{D}$ in Eq. (2.6) is the short-hand notation for $\gamma_\mu D^\mu$, and D^μ is the covariant derivative. Acting on triplet and octet fields the covariant derivative takes the following form in terms of the gluon field A^μ_a

$$D^\mu_{ij} = \partial^\mu\delta_{ij} + ig_{\rm S}A^\mu_c t^c_{ij}\,, \quad D^\mu_{ab} = \partial^\mu\delta_{ab} + ig_{\rm S}A^\mu_c T^c_{ab}\,, \tag{2.8}$$

where t^c and T^c are the generators of SU(3) in the fundamental and adjoint representations respectively and satisfy the following relations:

$$\left[t^a, t^b\right] = if^{abc}t^c\,, \quad \left[T^a, T^b\right] = if^{abc}T^c\,, \quad (T^a)_{bc} = -if^{abc}\,. \tag{2.9}$$

By convention, the SU(N) matrices are normalized in the following way:

$$\mathrm{Tr}(t^a t^b) = T_R\delta^{ab}\,, \quad T_R = \frac{1}{2}\,. \tag{2.10}$$

With this choice one gets the following relations for the colour matrices:

$$\sum_a t^a_{ij}t^a_{jk} = C_F\delta_{ik}\,, \quad C_F = \frac{N^2-1}{2N}\,, \tag{2.11}$$

$$\mathrm{Tr}(T^cT^d) = \sum_{a,b} f^{abc}f^{abd} = C_A\delta^{cd}\,, \quad C_A = N\,. \tag{2.12}$$

While the first term $\mathcal{L}_{\rm classic}$ in Eq. (2.5) generates the dynamics of quarks, the last two terms are needed for the consistent quantization of the theory. The key point is that it is

impossible to define the propagator for the gluon field in an unambiguous way and, thus, one needs to choose a specific gauge. The gauge-fixing Lagrangian density $\mathcal{L}_{\text{gauge-fix}}$ can be written as

$$\mathcal{L}_{\text{gauge-fix}} = -\frac{1}{2\xi} G(A)\,, \tag{2.13}$$

where the choice $G(A) = |\partial_\mu A^{a,\mu}|^2$ leads to the covariant gauges and $G(A) = |n_\mu A^{a,\mu}|^2$ (n^μ being some light-like reference vector) leads to the axial gauges. If a covariant gauge-fixing term is used, the gluon field has non-physical longitudinal degrees of freedom, which must be subtracted. This is achieved by introducing the *ghost* fields through the following Lagrangian

$$\mathcal{L}_{\text{ghost}} = \bar{c}^a(-\partial^2\delta^{ac} - g_{\text{S}}\partial^\mu f^{abc} A^b_\mu)c^c\,, \tag{2.14}$$

where the ghost fields c^a are complex scalar fields which obey Fermi statistics. Ghosts only appear as virtual particles in loops, never as physical external states. They decouple completely from the theory if an axial gauge is used.

2.2 General structure of perturbative QCD cross sections

In Quantum Field Theories, and in QCD in particular, the general mechanism of obtaining theoretical predictions is based on the perturbative expansion of cross section in powers of the coupling constant, provided that the latter is small. In this section we briefly sketch the general structure of QCD cross sections. For simplicity, let us consider a scattering process in QCD with two initial-state and m final-state massless particles. We write the cross section $\sigma(k_1, k_2)$ as a power series expansion in the QCD coupling constant $\alpha_{\text{S}} = g_{\text{S}}^2/(4\pi)$:

$$\begin{aligned}\sigma(k_1, k_2; \{p_i\}; \alpha_{\text{S}}) = \alpha_{\text{S}}^k \Big[&\sigma^{(\text{LO})}(k_1, k_2; \{p_i\}) + \alpha_{\text{S}}\,\sigma^{(\text{NLO})}(k_1, k_2; \{p_i\}) \\ &+ \alpha_{\text{S}}^2\,\sigma^{(\text{NNLO})}(k_1, k_2; \{p_i\}) + \cdots\Big]\,,\end{aligned} \tag{2.15}$$

where k_1 and k_2 are the momenta of the initial-state partons, and p_i are the final-state momenta. Under the assumption of small coupling constant, a first estimate of the cross section for the given reaction can be obtained by taking into account only the lowest order cross section $\sigma^{(\text{LO})}$. This is the leading order (LO) approximation and the cross section at this order can be computed by

$$\sigma^{(\text{LO})} = \int_m d\sigma^{\text{B}}\,, \tag{2.16}$$

where the Born-level cross section σ^{B} is simply a product of the m-particle phase space measure $d\Phi^{(m)}$, the tree-level matrix element $\mathcal{M}_m^{(0)}(\{p_i\})$ and some measurement function $\mathcal{J}^m(\{p_i\})$

$$d\sigma^{\text{B}} = d\Phi^{(m)}|\mathcal{M}_m^{(0)}(\{p_i\})|^2\mathcal{J}^m(\{p_i\})\,. \tag{2.17}$$

The m-particle phase space measure in Eq. (2.17) can be written in the following form:

$$d\Phi^{(m)} = \frac{(2\pi)^4}{4F} \prod_{i=1}^{m} \frac{d^4 p_i}{(2\pi)^3} \delta_+(p_i^2) \delta^4(k_1 + k_2 - \sum_{i=1}^{m} p_i) \,, \tag{2.18}$$

with the incoming flux F defined as $F = \sqrt{(k_1 + k_2)^2}/2$.

The matrix element $\mathcal{M}_m^{(0)}(\{p_i\})$ in Eq. (2.17) is the Born-level scattering amplitude, which is computed based on the Feynman rules that can be derived from the QCD Lagrangian of Eq. (2.5). The measurement function $\mathcal{J}^m(\{p_i\})$ is some phase space function that defines the physical quantity we want to compute.

The LO approximation in most cases gives only an order of magnitude estimate of the cross section. For a reliable prediction the higher order terms in the expansion (2.15) must be included in the computation. At next-to-leading order (NLO) there are two types of corrections to the LO process: real (one more parton in the final state) and virtual (one more parton running in a closed loop).

$$\sigma^{(\mathrm{NLO})}(k_1, k_2; \{p_i\}) = \int_{m+1} d\sigma^{\mathrm{R}} + \int_m d\sigma^{\mathrm{V}} \,. \tag{2.19}$$

Similar to Eq (2.17), the cross sections for the real and virtual corrections can be written as

$$\begin{aligned} d\sigma^{\mathrm{R}} &= d\Phi^{(m+1)} |\mathcal{M}_{m+1}^{(0)}|^2 \mathcal{J}^{m+1}(\{p_i\}) \,, \\ d\sigma^{\mathrm{V}} &= d\Phi^{(m)} \left[\mathcal{M}_m^{(1)} \mathcal{M}_m^{(0)\dagger} + \mathcal{M}_m^{(1)\dagger} \mathcal{M}_m^{(0)} \right] \mathcal{J}^m(\{p_i\}) \,, \end{aligned} \tag{2.20}$$

where $d\Phi^{(m+1)}$ and $\mathcal{J}^{m+1}(\{p_i\})$ are now defined for $m+1$ final-state particles.

Both the real and virtual corrections separately have divergent behaviour in some phase space regions. The calculation of loop corrections usually is accompanied with integrals which diverge in the limit when the loop momentum goes to infinity. These singularities are known as *ultraviolet* (UV) divergences and for renormalizable theories like QCD can be removed through the *renormalization* procedure, which consists in a redefinition of the bare couplings and masses in the Lagrangian of Eq. (2.5) (see Sections 2.3 and 2.4).

Besides the UV divergences, the QCD scattering amplitudes also contain *infrared* (IR) singularities. In the case of virtual corrections the IR divergences, as in the case of UV divergences, originate from the integration over the loop momentum, but in this case the divergences are related to the small momentum $k \to 0$ limit. The IR singularities in the case of the real corrections arise after the integration of the scattering amplitudes over the phase space of the additional soft or collinear gluon, radiated from the external legs. As we will see in Section 2.5 the IR singularities cancel out for sufficiently inclusive QCD processes with no initial-state hadrons, after summing the virtual and real corrections. The case of

QCD processes with initial-state hadrons is more involved and the perturbative calculation is accompanied with some left-over initial-state collinear divergences, which, however, can be handled by an appropriate redefinition of hadronic structure functions (see Section 2.7).

2.3 The running coupling constant

To introduce the concept of running coupling constant, let us consider a dimensionless physical observable R which depends on a single physical scale Q. Let us also assume that the scale Q is much larger than the mass of any particle involved in the process, and, thus, one can neglect them. This means, that Q is the only variable that has a mass dimension. And since R is dimensionless, one naturally expects that R should not depend on Q.

As we have mentioned in Section 2.2 the virtual corrections to the LO process suffer from UV divergences, which need to be removed through the renormalization. The renormalization procedure introduces an unphysical scale, μ_R, which is the scale at which the subtraction of UV divergences is performed. Due to the presence of this new scale μ_R, R is not constant in Q, but can rather depend on the ratio Q^2/μ_R^2. Moreover, R also implicitly depends on the renormalization scale through the running coupling $\alpha_{\rm S}(\mu_R)$. However, since μ_R is an arbitrary parameter, physical observables cannot depend on it. This leads to a number of *renormalization group* (RG) equations. The μ independence of R can be written in the following way

$$\mu^2 \frac{\partial}{\partial \mu^2} R(Q^2/\mu^2, \alpha_{\rm S}) \equiv \left[\mu^2 \frac{\partial}{\partial \mu^2} + \mu^2 \frac{\partial \alpha_{\rm S}}{\partial \mu^2} \frac{\partial}{\partial \alpha_{\rm S}} \right] R = 0 \,. \tag{2.21}$$

One can write Eq. (2.21) in a more compact form

$$\left[-\frac{\partial}{\partial t} + \beta(\alpha_{\rm S}) \frac{\partial}{\partial \alpha_{\rm S}} \right] R(e^t, \alpha_{\rm S}) = 0 \,, \tag{2.22}$$

by introducing the following notations

$$t = \ln\left(\frac{Q^2}{\mu^2}\right) \,, \quad \beta(\alpha_{\rm S}) = \mu^2 \frac{\partial \alpha_{\rm S}}{\partial \mu^2} \,. \tag{2.23}$$

The first-order partial differential equation (2.22) can be solved by implicitly defining a new function, the *running coupling* $\alpha_{\rm S}(Q^2)$

$$t = \int_{\alpha_{\rm S}(\mu^2)}^{\alpha_{\rm S}(Q^2)} \frac{d\alpha_{\rm S}}{\beta(\alpha_{\rm S})} \,. \tag{2.24}$$

Differentiating Eq. (2.24) one finds

$$\frac{\partial \alpha_{\rm S}(Q^2)}{\partial t} = \beta(\alpha_{\rm S}(Q^2)) \,, \quad \frac{\partial \alpha_{\rm S}(Q^2)}{\partial \alpha_{\rm S}} = \frac{\beta(\alpha_{\rm S}(Q^2))}{\beta(\alpha_{\rm S})} \,, \tag{2.25}$$

and therefore $R(1, \alpha_S(Q^2))$ is a solution of Eq. (2.22), which means that all the scale dependence of R enters through the running coupling constant $\alpha_S(Q^2)$. The dependence of the running coupling $\alpha_S(Q^2)$ on the scale Q is described by the RG equation:

$$\frac{d \ln \alpha_S(Q)}{d \ln Q^2} = \beta(\alpha_S(Q)) = -\sum_{n=0}^{\infty} \beta_n \left(\frac{\alpha_S}{\pi}\right)^{n+1} , \tag{2.26}$$

where the coefficients of the QCD *beta function* β are computable in perturbation theory. The exact expression of the first two coefficients, β_0 and β_1 is [113]

$$\beta_0 = \frac{1}{12}(11C_A - 2n_f) , \quad \beta_1 = \frac{1}{24}(17C_A^2 - 5C_A n_f - 3C_F n_f) , \tag{2.27}$$

where n_f is the number of active light flavours[†]. Here we see the effect of the non-Abelian interactions in QCD, namely that β_0, unlike to corresponding QED coefficient, is positive for $n_f \leq 16$.

Eq. (2.26) has an analytical solution only at the lowest order, which reads

$$\alpha_S(Q^2) = \frac{\alpha_S(\mu_0^2)}{1 + \alpha_S(\mu_0^2)\frac{\beta_0}{\pi} \ln(Q^2/\mu_0^2)} . \tag{2.28}$$

Evidently, the absolute value of the strong coupling constant is not computable in perturbation theory. However, if the strong coupling constant is measured at some scale μ_0, by using Eq. (2.28) or the higher-order solutions of Eq. (2.26), one can compute its value at any other scale, for instance at the mass of the Z boson, m_Z. Fig. 2.1 depicts the world average of the value of $\alpha_S(m_Z^2)$, extracted from different measurements at different energy scales Q [114]. The line depicts the theory prediction in Eq. (2.28) of the running.

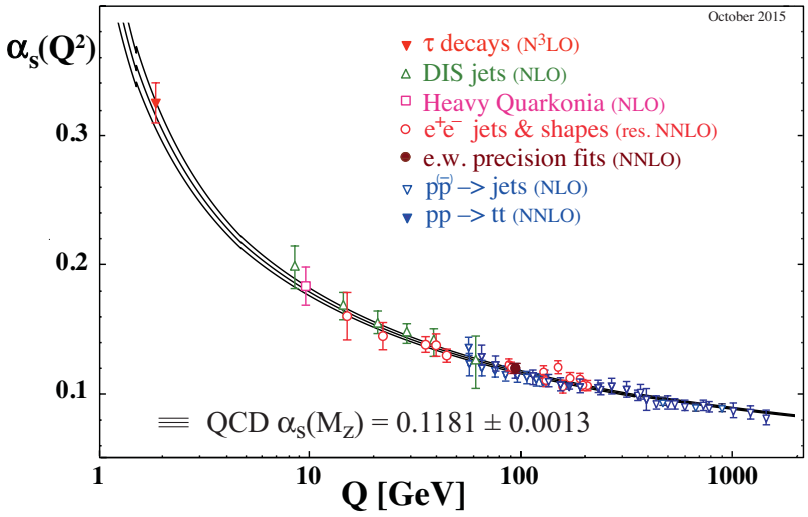

Figure 2.1: Summary of measurements of α_S as a function of the energy scale Q.

[†]For example, $n_f = 5$ for the top-quark pair production process.

The crucial consequence of Eq. (2.28) and the fact that $\beta_0 > 0$ is that α_S decreases with the energy, as it is shown in Fig. 2.1, meaning that $\alpha_S(Q^2) \to 0$ at asymptotic energies $Q \to \infty$. This is the fundamental property of QCD, the asymptotic freedom mentioned in the beginning of this chapter, which justifies the validity of perturbation theory at sufficiently high energies. At small energies, however, α_S becomes large and perturbation theory breaks down. One could get an order of magnitude estimate of the scale Λ_{QCD} where this happens by requiring the denominator of the solution in Eq. (2.28) to vanish, which gives about $\Lambda_{QCD} \sim 200\,\text{MeV}$. Thus, $\alpha_S(Q^2)$ becomes large and perturbation theory breaks down for scales comparable with the masses of light hadrons ($Q \simeq 1\,\text{GeV}$). This could be an indication that the confinement of quarks and gluons inside the hadrons is actually a consequence of the growth of the coupling at low scales.

2.4 Quark masses

Having discussed the QCD coupling in Section 2.3, we now turn to the discussion of other physical parameters in the QCD Lagrangian of Eq. (2.5), namely, the quark masses. The masses in the Lagrangian, as for the coupling constant, are not physical quantities. The physical masses can be defined only after renormalization. In QED the lepton masses are defined through their classical limit. This procedure, however, is not applicable to the quarks, because the quarks are not observable, and, thus, their masses cannot be measured directly, but must be determined indirectly, through their impact on hadronic properties. Moreover, any quantitative statement on the value of a quark mass must make reference to the particular theoretical framework that is used to define it. One can define the quark masses in a close analogy with the QCD coupling constant. Let us consider for simplicity the case in which there is one flavour of quark with renormalized mass m. Examining the scale dependence of the dimensionless physical observable R, one gets the following RG equation for the quark mass:

$$\frac{\mu^2}{m}\frac{\partial m}{\partial \mu^2} = -\gamma_m(\alpha_S) = -\sum_{n=1}^{\infty} \gamma_m^{(n)} \left(\frac{\alpha_S}{\pi}\right)^n , \tag{2.29}$$

where $\gamma_m(\alpha_S)$ is the mass anomalous dimension, which is known to four-loop order in perturbation theory [115, 116]. The mass anomalous dimension depends on the renormalization scheme. The explicit expression for its first two coefficients in the most commonly used renormalization scheme, $\overline{\text{MS}}$, reads:

$$\gamma_m^{(1)} = 1\,, \qquad \gamma_m^{(2)} = \frac{101}{24} - \frac{5n_f}{36}\,. \tag{2.30}$$

The solution of Eq. (2.29) is given by

$$m(Q) = m(\mu)\exp\left[-\int_{\alpha_S(\mu)}^{\alpha_S(Q)} d\alpha_S \frac{\gamma_m(\alpha_S)}{\beta(\alpha_S)}\right] , \tag{2.31}$$

which, at first perturbative order in the $\overline{\text{MS}}$ scheme simplifies to

$$\overline{m}(Q) = \overline{m}(\mu) \left[\frac{\alpha_{\text{S}}(\mu)}{\alpha_{\text{S}}(Q)} \right]^{\frac{1}{\beta_0}} , \tag{2.32}$$

where by $\overline{m}$ we denoted the running mass in the $\overline{\text{MS}}$ scheme.

An alternative scheme of defining the quark masses is the *pole mass*. In this scheme one defines the quark mass m to be the pole of the propagator $i(\not{p} + m)/(p^2 - m^2)$ to all orders. This is close to one's physical picture of mass, and is very useful for the processes with the characteristic scales $Q \sim m$, but it turns out that it is similar to a running mass scheme with μ of order m and therefore generates large logarithms and large truncation error for $Q \gg m$. The pole mass m and the $\overline{\text{MS}}$ mass $\overline{m}$ are related to each other. At first non-trivial order the relation is given by

$$m = \overline{m}(\overline{m}) \left(1 + C_F \frac{\alpha_{\text{S}}(\overline{m})}{\pi} + \mathcal{O}(\alpha_{\text{S}}^2) \right) , \tag{2.33}$$

where $\alpha_{\text{S}}(\overline{m})$ is the QCD coupling constant in the $\overline{\text{MS}}$ scheme.

For all numerical calculations in this thesis we assume the light quarks (u, d, s, c, b) to be massless and we choose the pole mass for the top quark $m_t = 173.3\,\text{GeV}$.

2.5 Infrared singularities in QCD

As we have discussed in Section 2.2, the QCD corrections to the scattering processes are accompanied with UV and IR singularities. We have mentioned that the UV divergences are handled by the renormalization procedure, leading to the redefinition of the bare couplings and masses of the QCD Lagrangian. In this section we briefly sketch the structure of QCD IR singularities. As a test case we consider the first-order QCD corrections to a classical process, electron-positron annihilation into quark and antiquark pair $e^+(q_1)\, e^-(q_2) \to q(p_1)\, \bar{q}(p_2)$. At the Born level it is a purely QED process and the cross section is given by

$$\sigma_0 = \frac{4\pi\alpha^2}{Q^2} N_c \sum e_q^2 , \tag{2.34}$$

where the sum runs over the different flavours of the quarks, α is the QED coupling constant, $Q^2 = 2\, q_1 \cdot q_2$ is the center of mass energy of the e^+e^- pair and e_q are the electrical charges of the quarks. As it was mentioned in Section 2.2, at NLO real and virtual corrections to the LO process must be computed. Let us first consider the real QCD corrections to the Born process, when a gluon with momentum p_3 is radiated from

one of the quark lines. For the kinematics of the real radiation one can use the following variables

$$x_i = \frac{2\,p_i \cdot Q}{Q^2}\,, \tag{2.35}$$

which are the energy fractions $x_i = 2E_i/Q$ of three partons in the center of mass frame, and hence are positive quantities $x_i > 0$. They also obey the following constraint

$$x_1 + x_2 + x_3 = \frac{2\sum p_i \cdot Q}{Q^2} = 2\,, \tag{2.36}$$

due to the energy conservation. One can also relate these energy fractions to the scattering angles. For example

$$2\,p_1 \cdot p_3 = Q^2 - 2\,p_2 \cdot Q = Q^2(1 - x_2) = 2E_1E_g(1 - \cos\theta_{13})\,, \tag{2.37}$$

where E_1 and E_g are the energies of the quark and the extra radiated gluon and θ_{13} is the angle between them. Since $1 - \cos\theta_{ij}$ is positive, it follows from Eq. (2.37) that the energy fractions are also bounded from above $x_i < 1$. To compute the cross section for the real radiation one needs to compute the integral of the matrix element over the three-body phase space. The three-body phase space measure Φ_3 can be written as

$$d\Phi_3 = \frac{1}{(2\pi)^5}\,\frac{Q^2}{32}\,d\phi\,d(\cos\beta)\,d\gamma\,dx_1\,dx_2\,dx_3\,\delta(2 - x_1 - x_2 - x_3)\,, \tag{2.38}$$

where ϕ, β and γ are the Euler angles. Using the variables in Eq. (2.35) the real cross section, integrated over the Euler angles, can be written as

$$\sigma_{\rm R} = \int_0^1 dx_1\,dx_2\,dx_3\,\delta(2 - x_1 - x_2 - x_3)\,|\overline{\mathcal{M}_{\rm real}(x_1, x_2, x_3)}|^2\,, \tag{2.39}$$

where the matrix element $\mathcal{M}_{\rm real}(x_1, x_2, x_3)$ is easy to compute and is given as follows

$$|\overline{\mathcal{M}_{\rm real}(x_1, x_2, x_3)}|^2 = \sigma_0\,C_F\,\frac{\alpha_{\rm S}}{2\pi}\,\frac{x_1^2 + x_2^2}{(1 - x_1)(1 - x_2)}\,. \tag{2.40}$$

One can see that the integrals over x_1 and x_2 are divergent along the boundaries $x_{1,2} = 1$. From the relation between the energy fractions and the angles in Eq. (2.37) we see that the singularities come from the regions of phase space where the gluon is collinear with the quark or antiquark ($\theta_{13} \to 0$, or $\theta_{23} \to 0$, corresponding to the limits $x_1 \to 1$ or $x_2 \to 1$), or where the gluon is soft, $E_g/Q \to 0$ ($x_1 \to 1$ and $x_2 \to 1$, or, alternatively, $x_3 \to 0$). Since in the real world one does not really integrate up to $x_{1,2} = 1$, but rather up to some physical cutoff of the order of $1 - \Lambda_{\rm QCD}/Q$, the infrared singularities are not real (from mathematical point of view) singularities. We indeed get

$$\alpha_{\rm S}(Q^2)\int_0^{1-\Lambda_{\rm QCD}/Q}\frac{dx}{1 - x} = \alpha_{\rm S}(Q^2)\ln\left(\frac{Q}{\Lambda_{\rm QCD}}\right)\,, \tag{2.41}$$

which is finite, but spoils the perturbative expansion, since $\alpha_{\rm S}(Q^2)\ln(Q/\Lambda_{\rm QCD})$ can be of the order of one even for small QCD coupling $\alpha_{\rm S}(Q^2)$. In other words, the existence of the IR singularities in the real matrix element means that there are non-perturbative phenomena in the calculation which are not power suppressed at high energies, thus breaking the factorization pattern into short and long distance physics. The apparent breakdown of the factorization formula is cured once the virtual corrections are also considered. The virtual corrections are very similar to the real corrections as far as the matrix elements are considered. However, the kinematics of the virtual corrections is different, because of the absence of the extra radiated parton in the final state, so the momentum conservation takes the same form as in the Born case. The cross section for the virtual corrections can be written as

$$\sigma_{\rm V} = \int_0^1 dx_1 dx_2 \delta(2-x_1-x_2) \int_0^\infty dx_3 |\overline{\mathcal{M}_{\rm virtual}}|^2 \,, \tag{2.42}$$

where the integration over x_3 is over the energy fraction of the particle running in the loop, which is unconstrained. To understand better the origin of the IR divergences in this case let us split the integration over the loop momentum into two pieces

$$\int_0^\infty dx_3 \cdots = \int_1^\infty dx_3 \cdots + \int_0^1 dx_3 \cdots \,. \tag{2.43}$$

The first integration on the right-hand side of Eq. (2.43) gives rise to the UV divergences, while the second integration is responsible for the IR divergences and has the same form as the integrals for the real correction in Eq. (2.39). Both the UV and the IR divergences can be regularised using, for example, dimensional regularization, where one computes the integrals in $d = \mu = 4 - 2\epsilon$ dimensions. In this regularization method the singularities show up as explicit poles in ϵ. Performing the integrations in Eqs (2.39) and (2.42) gives

$$\sigma_{\rm R} = \sigma_0 N_c \sum e_q^2 C_F \frac{\alpha_{\rm S}}{2\pi} H(\epsilon) \left[\frac{2}{\epsilon^2} + \frac{3}{\epsilon} + \frac{19}{2}\right] \,, \tag{2.44}$$

and

$$\sigma_{\rm V} = \sigma_0 N_c \sum e_q^2 C_F \frac{\alpha_{\rm S}}{2\pi} H(\epsilon) \left[-\frac{2}{\epsilon^2} - \frac{3}{\epsilon} - 8\right] \,, \tag{2.45}$$

where $H(\epsilon)$ is some function of Euler Gamma functions of ϵ which is finite in the $\epsilon \to 0$ limit. One can see that the IR poles of real and virtual corrections are exactly the same with the opposite sign. Thus, once added together, the $\mathcal{O}(\alpha_{\rm S})$ corrections are finite. The cancellation of IR divergences between the real and virtual corrections to the e^+e^--annihilation process is a direct consequence of the Kinoshita-Lee-Nauenberg (KLN) theorem [25–27], which states that IR divergences cancel out in transition probabilities when summing over all the degenerate initial and final states.

2.6 Infrared factorization of QCD amplitudes

In this section we review the infrared behaviour of tree-level QCD scattering amplitudes at the first order in the QCD coupling, α_S. At this order the structure of infrared singularities has been known for long time. To set the notation, we consider a tree-level matrix element $\mathcal{M}_m$ with m final-state QCD partons (massless quarks and gluons) with momenta $p_1, \ldots, p_m$, which has the following general structure

$$\mathcal{M}^{c_1,\ldots,c_m;s_1,\ldots,s_m}_{a_1,\ldots,a_m}(p_1,\ldots,p_m)\,, \tag{2.46}$$

where $\{c_1,\ldots,c_m\}$, $\{s_1,\ldots,s_m\}$ and $\{a_1,\ldots,a_m\}$ respectively denote the colour, spin and flavour indices of the m external particles. There are $a = 1,\ldots,N_c^2-1$ different colours for each gluons and $\alpha = 1,..,N_c$ different colours for each quark or antiquark. We use the conventional dimensional regularisation (CDR) scheme with $d = 4-2\epsilon$ space-time dimensions and consider two helicity states for the fermions and $d-2$ helicity states for gluons. Thus, we denote the spin indices as $s = 1,2$ for quarks and $\mu = 1,\ldots,d$ for gluons. We also define the spin-polarization tensor

$$\mathcal{T}^{s_1 s_1'}_{a_1,\ldots,a_m} = \sum_{\text{spins}\neq s_1,s_1'}\ \sum_{\text{colours}} \mathcal{M}^{c_1,\ldots,c_m;s_1,\ldots,s_m}_{a_1,\ldots,a_m}\left[\mathcal{M}^{c_1,\ldots,c_m;s_1',\ldots,s_m}_{a_1,\ldots,a_m}\right]^\dagger\,, \tag{2.47}$$

which is the square of the matrix element in Eq. (2.46), summed over all spins except s_1 and summed over all colours.

2.6.1 Factorisation in the collinear limit

We now consider the singular collinear limit of the m-particle tree-level amplitude of Eq. (2.46) which is realized when the momenta of two partons, for example, p_1 and p_2, become parallel. To define this collinear limit we use the following parametrization of momenta:

$$\begin{aligned} p_1^\mu &= z p^\mu + k_\perp^\mu - \frac{k_\perp^2}{z}\frac{n^\mu}{2\,p\cdot n}\,,\\ p_2^\mu &= (1-z)p^\mu - k_\perp^\mu - \frac{k_\perp^2}{1-z}\frac{n^\mu}{2\,p\cdot n}\,, \end{aligned} \tag{2.48}$$

where the light-like ($p^2=0$) vector p^μ denotes the collinear direction and n^μ is an auxiliary light-like vector which is necessary to specify how the collinear direction is approached. With this parametrization the scalar product of the momenta p_1 and p_2 becomes

$$s_{12} \equiv 2\,p_1\cdot p_2 = -\frac{k_\perp^2}{z(1-z)}\,, \tag{2.49}$$

and, thus, the collinear limit corresponds to $k_\perp^\mu \to 0$. In this limit the square of the matrix element in Eq. (2.46) behaves as follows

$$|\overline{\mathcal{M}_{a_1,a_2,\ldots,a_m}(p_1,p_2,\ldots,p_m)}|^2 \xrightarrow{k_\perp\to 0} \frac{2}{s_{12}}\,4\pi\mu^{2\epsilon}\,\alpha_{\rm S}\,\hat{P}^{s_1 s_1'}_{a_1 a_2}(z,k_\perp;\epsilon)\,\mathcal{T}^{s_1 s_1'}_{a,a_3,\ldots,a_m}(p,\ldots)\,, \quad (2.50)$$

where μ is the dimensional-regularization scale and $\mathcal{T}^{s_1 s_1'}_{a,a_3,\ldots,a_m}$ is the spin-polarization tensor, defined in Eq. (2.47), with the partons a_1 and a_2 replaced by a single parton a. The parton a carries the quantum numbers of the pair a_1+a_2 in the collinear limit. Thus, its momentum is p^μ and its other quantum numbers are obtained according to the following rule: Gluon + anything gives anything and quark + antiquark gives gluon.

The kernel $\hat{P}^{s_1 s_1'}_{a_1 a_2}(z,k_\perp;\epsilon)$ is the d-dimensional spin-dependent AP splitting function. The exact expressions of these splitting functions for different flavours are given by

$$\hat{P}^{ss'}_{qg}(z,k_\perp;\epsilon) = \hat{P}^{ss'}_{\bar{q}g}(z,k_\perp;\epsilon) = \delta_{ss'} C_F \left[\frac{1+z^2}{1-z} - \epsilon\,(1-z)\right], \quad (2.51)$$

$$\hat{P}^{ss'}_{gq}(z,k_\perp;\epsilon) = \hat{P}^{ss'}_{g\bar{q}}(z,k_\perp;\epsilon) = \delta_{ss'} C_F \left[\frac{1+(1-z)^2}{z} - \epsilon\,z\right], \quad (2.52)$$

$$\hat{P}^{\mu\nu}_{q\bar{q}}(z,k_\perp;\epsilon) = \hat{P}^{\mu\nu}_{\bar{q}q}(z,k_\perp;\epsilon) = T_R \left[-g^{\mu\nu} + 4z\,(1-z)\,\frac{k_\perp^\mu k_\perp^\nu}{k_\perp^2}\right], \quad (2.53)$$

$$\hat{P}^{\mu\nu}_{gg}(z,k_\perp;\epsilon) = 2C_A \left[-g^{\mu\nu}\left(\frac{z}{1-z}+\frac{1-z}{z}\right) - 2\,(1-\epsilon)\,z\,(1-z)\,\frac{k_\perp^\mu k_\perp^\nu}{k_\perp^2}\right]. \quad (2.54)$$

The AP splitting functions in Eqs. (2.51)–(2.54) are in general matrices acting on the spin indices s and s' of the parton a. In the case of fermionic parent partons (Eqs. (2.51) and (2.52)) the splitting functions are proportional to the unity matrix in the spin indices. The situation is more involved in the case of collinear splitting of gluons, leading to non-trivial *spin correlations*. Due to these spin correlations the spin-average square of the matrix element $\mathcal{M}_{a,\ldots,a_m}(p,\ldots,p_m)$ cannot be simply factorized on the right-hand side of Eq. (2.50).

2.6.2 Factorisation in the soft limit

Unlike the collinear radiation, the emission of a soft gluon does not affect the spin of the radiating hard partons. It does, however, affect their colour because the gluon always carries some colour charge. For this reason the soft-gluon emission does not factorize exactly, as it does the soft-photon emission in QED, and leads to non-trivial colour correlations.

In the following we will derive the factorization formula for a generic tree-level QCD matrix element with $m+1$ external QCD massless partons $\mathcal{M}^{c_1,\ldots,c_m;c}_{m+1}(p_1,\ldots,p_m;q)$, when

one of the gluons with momentum q and colour c becomes soft [117,118]. We note that the coupling of the gluon to any internal parton is not singular in the soft limit. It can, thus, be neglected, and we need to consider only the emission of a soft gluon from the external legs.

We first consider the emission of a soft gluon from a final-state quark with momentum p_i and colour α. The matrix element $\mathcal{M}_{m+1}^{c_1,\ldots,c_m;c}(p_1,\ldots,p_m;q)$ has the following form in this case:

$$\mathcal{M}_{m+1}^{\alpha;c}(p_i;q) = g_{\mathrm{S}}\mu^{\epsilon}\bar{u}(p_i)(t^c)_{\alpha\beta}\varepsilon_{\mu}(q)\gamma^{\mu}\frac{\not{p}_i+\not{q}}{(p_i+q)^2}\widetilde{\mathcal{M}}_m^{\beta}\,, \tag{2.55}$$

where $\bar{u}$ is the Dirac spinor of quark i, (t^c) is the colour-charge matrix in the fundamental representation and $\widetilde{\mathcal{M}}_m^{\beta}$ is the the m-particle matrix element with the on-shell quark i replaced by an off-shell quark: $\mathcal{M}_m^{\beta} = \bar{u}(p_i)\widetilde{\mathcal{M}}_m^{\beta}$. In the soft limit, $q \to 0$, one gets

$$\begin{aligned}\mathcal{M}_{m+1}^{\alpha;c}(p_i;q) &\simeq g_{\mathrm{S}}\mu^{\epsilon}\bar{u}(p_i)\varepsilon_{\mu}(q)\gamma^{\mu}\frac{\not{p}_i}{2\,p_i\cdot q}(t^c)_{\alpha\beta}\widetilde{\mathcal{M}}_m^{\beta} \\ &= g_{\mathrm{S}}\mu^{\epsilon}\bar{u}(p_i)\varepsilon_{\mu}(q)\frac{2p_i^{\mu}-\not{p}_i\gamma^{\mu}}{2\,p_i\cdot q}(t^c)_{\alpha\beta}\widetilde{\mathcal{M}}_m^{\beta} \\ &= g_{\mathrm{S}}\mu^{\epsilon}\varepsilon_{\mu}(q)\left[\frac{p_i^{\mu}}{p_i\cdot q}\right](t^c)_{\alpha\beta}\mathcal{M}_m^{\beta}\,,\end{aligned} \tag{2.56}$$

where we first used the Clifford algebra to interchange the gamma matrices then the Dirac equation $\bar{u}(p_i)\not{p}_i = 0$ for massless fermions. As anticipated, in the soft limit the $(m+1)$-particle matrix element factorizes into the m-particle matrix element, up to colour correlations. The factorization formula in Eq. (2.56) is the same also in the case of soft-gluon emission from initial-state antiquark. In the case of initial-state quark and final-state antiquark, only the colour-charge matrix $t^c_{\alpha\beta}$ changes: $t^c_{\alpha\beta} \to \bar{t}^c_{\alpha\beta} = -t^c_{\beta\alpha}$.

We now proceed with the case when the soft gluon is emitted from the external gluon. In this case the matrix element $\mathcal{M}_{m+1}^{c_1,\ldots,c_m;c}(p_1,\ldots,p_m;q)$ can be written in the following way:

$$\mathcal{M}_{m+1}^{a;c}(p_i;q) = \mu^{\epsilon}\varepsilon_{\lambda}(p_i)\varepsilon_{\nu}(q)\frac{id_{\mu\sigma}(p_i+q)}{(p_i+q)^2}V^{\mu\nu\lambda}(p+q,-q,-p)\widetilde{\mathcal{M}}_m^{a,\sigma}\,, \tag{2.57}$$

where $d_{\mu\sigma}(p_i+q)$ is the gluon polarization tensor and $\widetilde{\mathcal{M}}_m^{\sigma}$ is the the m-particle matrix element with the on-shell gluon i replaced by an off-shell gluon: $\mathcal{M}_m^{a} = \varepsilon_{\sigma}(p_i)\widetilde{\mathcal{M}}_m^{a,\sigma}$. The tensor $V^{\mu\nu\lambda}(p+q,-q,-p)$ is the triple-gluon vertex, which reads

$$V^{\mu\nu\lambda} = -g_{\mathrm{S}}f^{abc}\left[g^{\mu\lambda}(2p_i+q)^{\nu} + g^{\lambda\nu}(q-p_i)^{\mu} + g^{\nu\mu}(-p_i-2q)^{\lambda}\right]\,, \tag{2.58}$$

where f^{abc} is the colour-charge matrix in the adjoint representation. In the soft limit, $q \to 0$, Eq. (2.57) simplifies to

$$\mathcal{M}_{m+1}^{a;c}(p_i;q) \simeq\ -g_{\mathrm{S}}f^{abc}\mu^{\epsilon}\varepsilon_{\lambda}(p_i)\varepsilon_{\nu}(q)\frac{id_{\mu\sigma}(p_i)}{2\,p_i\cdot q}\left[2g^{\mu\lambda}p_i^{\nu} - g^{\lambda\nu}p_i^{\mu} - g^{\nu\mu}p_i^{\lambda}\right]\widetilde{\mathcal{M}}_m^{a,\sigma}\,. \tag{2.59}$$

The factorization formula is most easily derived in a *physical gauge*, where the longitudinal (unphysical) polarizations of the gluon vanish. In this gauge the gluon polarization tensor $d_{\mu\sigma}(p_i)$ has the following form

$$d^{\mu\sigma}(p_i) = -g^{\mu\sigma} + \frac{p_i^\mu n^\sigma + p_i^\sigma n^\mu}{p_i \cdot n}\,, \tag{2.60}$$

where the light-like vector n^μ satisfies the relation $n \cdot \varepsilon(p_i) = 0$. It is easy to see that only the first term in the square bracket on the right-hand side of Eq. (2.59) gives non-vanishing contribution, and we get

$$\begin{aligned}\mathcal{M}^{a;c}_{m+1}(p_i;q) \simeq\ & g_{\rm S}\mu^\epsilon \varepsilon_\nu(q)\left[\frac{p_i^\nu}{p_i\cdot q}\right]\left(if^{abc}\right)\varepsilon_\sigma(p_i)\widetilde{\mathcal{M}}^{a,\sigma}_m \\ &= g_{\rm S}\mu^\epsilon \varepsilon_\nu(q)\left[\frac{p_i^\nu}{p_i\cdot q}\right]\left(if^{abc}\right)\mathcal{M}^{a}_m\,.\end{aligned} \tag{2.61}$$

One can see an apparent similarity between the factorization formulae in the quark channel (Eq. (2.56)) and in the gluon channel (Eq. (2.61)), the only difference being in the colour-charge matrices. We can write the soft-gluon factorization in a general way, by introducing a colour basis $\{|c_1,\ldots,c_m\rangle\}$ (see, for example, Ref. [29]), such that the matrix element in Eq. (2.46) is given by

$$\mathcal{M}_{c_1,\ldots,c_m}(p_1,\ldots,p_m) = \langle c_1,\ldots,c_m|\mathcal{M}(p_1,\ldots,p_m)\rangle\ . \tag{2.62}$$

For the discussion in this section we do not need to specify the basis, so $\{|c_1,\ldots,c_m\rangle\}$ is an abstract basis in colour space and the ket $|\mathcal{M}(p_1,\ldots,p_m)\rangle$ is a vector in this space[†]. The square of the matrix element, summed over the spins and colours of the partons, can be written as

$$|\mathcal{M}(p_1,\ldots,p_m)|^2 = \langle\mathcal{M}(p_1,\ldots,p_m)|\mathcal{M}(p_1,\ldots,p_m)\rangle\ . \tag{2.63}$$

To describe the colour correlations due to soft gluon emission in a general way, we associate a colour operator $\boldsymbol{T}_i$ with the emission from each parton i. If the colour index of the emitted gluon is a, the colour-charge operator is:

$$\boldsymbol{T}_i \equiv \langle a|\,T_i^a\,. \tag{2.64}$$

The action of this operator onto the colour space is defined by

$$\langle c_1,\ldots,c_i,\ldots,c_m,a|\boldsymbol{T}_i|b_1,\ldots,b_i,\ldots,b_m\rangle = \delta_{c_1b_1},\ldots,T^a_{b_ic_i},\ldots,\delta_{c_mb_m}\,, \tag{2.65}$$

where $T^a_{bc} = if^{bac}$, if the emitting parton is a gluon, $T^a_{\alpha\beta} = t^a_{\alpha\beta}$ if the emitting parton is a final-state quark or an initial-state antiquark and $T^a_{\alpha\beta} = -t^a_{\beta\alpha}$ in the case of an initial-state quark or a final-state antiquark.

[†]In Section 4.3, however, when we consider the colour structure of the heavy-quark production matrix element, we will specify the basis and will give some more details on the colour algebra.

By definition, each vector $|\mathcal{M}(p_1,\ldots,p_m)\rangle$, defined by Eq. (2.62), is a colour singlet state. Therefore, colour conservation implies

$$\sum_{i=1}^{m} \boldsymbol{T}_i \,|\mathcal{M}(p_1,\ldots,p_m)\rangle = 0\,. \tag{2.66}$$

The exchange of a gluon between two partons i and j is given by the following colour algebra:

$$T_i^a T_j^a \equiv \mathbf{T}_i\cdot\mathbf{T}_j = \mathbf{T}_j\cdot\mathbf{T}_i\,, \quad \text{if } i\neq j; \qquad \mathbf{T}_i^2 = C_i\,, \tag{2.67}$$

where C_i is the Casimir operator and equal to $C_i = C_A = N_c$ if i is a gluon and $C_i = C_F = (N_c^2-1)/2N_c$ if i is a quark or antiquark.

We can now summarize the factorization formulae in Eqs. (2.56) and (2.61) in one expression:

$$\langle a|\mathcal{M}(q,p_1,\ldots,p_m)\rangle \simeq g_{\rm S}\mu^{\epsilon}\varepsilon_\mu(q)\boldsymbol{J}^\mu(q)\,|\mathcal{M}(p_1,\ldots,p_m)\rangle\,, \tag{2.68}$$

where the factor $\boldsymbol{J}^\mu(q)$ is the tree-level eikonal current and is given by

$$\boldsymbol{J}^\mu(q) = \sum_{i=1}^{m} \mathbf{T}_i \frac{p_i^\mu}{p_i\cdot q}\,. \tag{2.69}$$

Though we have used a specific gauge (the physical gauge) to arrive at the factorization formula in Eq. (2.61), we note that the factorization formula is actually gauge invariant. This is because of an important property of the eikonal current $\boldsymbol{J}^\mu(q)$, namely, its conservation. To see this, let us consider the action of $q_\mu\boldsymbol{J}^\mu(q)$ operator on the vector $|\mathcal{M}(p_1,\ldots,p_m)\rangle$:

$$q_\mu\boldsymbol{J}^\mu(q)\,|\mathcal{M}(p_1,\ldots,p_m)\rangle = \sum_{i=1}^{m}\mathbf{T}_i\,|\mathcal{M}(p_1,\ldots,p_m)\rangle = 0\,, \tag{2.70}$$

where the last equality follows from colour conservation (Eq. (2.66)). As we mentioned earlier, the choice of the physical gauge was motivated from the simplicity of the calculation because of the absence of longitudinal polarizations of the soft gluon. A gauge transformation is equivalent to adding a longitudinal component to the polarization vector of the soft gluon through the replacement $\varepsilon_\mu(q)\to\varepsilon_\mu(q)+\lambda q_\mu$. However, the current conservation of the eikonal current (Eq.(2.70)) implies that this replacement does not affect the factorization formula in Eq. (2.68).

By squaring Eq. (2.68) and summing over the gluon polarizations we arrive at the well-known soft-gluon factorization formula for the squared tree-level amplitude:

$$|\mathcal{M}(q,p_1,\ldots,p_m)|^2 \simeq g_{\rm S}^2\mu^{2\epsilon}2\sum_{i,j=1}^{m}\mathcal{S}_{ij}(q)|\mathcal{M}_{(i,j)}(p_1,\ldots,p_m)|^2\,, \tag{2.71}$$

where $\mathcal{S}_{ij}(q)$ is the eikonal function and is given by

$$\mathcal{S}_{ij}(q) = \frac{p_i \cdot p_j}{2\,(p_i \cdot q)(p_j \cdot q)} = \frac{s_{ij}}{s_{iq}\, s_{jq}}\,, \tag{2.72}$$

and $|\mathcal{M}_{(i,j)}(p_1, \ldots, p_m)|^2$ is the square of colour-correlated tree-level amplitude, which is defined as follows:

$$|\mathcal{M}_{(i,j)}(p_1, \ldots, p_m)|^2 \equiv \langle \mathcal{M}(p_1, \ldots, p_m) | \mathbf{T}_i \cdot \mathbf{T}_j | \mathcal{M}(p_1, \ldots, p_m) \rangle\ . \tag{2.73}$$

To summarize, in this section we have derived the soft-gluon factorization formula of the tree-level QCD amplitudes with external massless QCD partons to leading order in α_S. It is easy to show that in the case of massive quarks and antiquarks the factorization formula in Eq. (2.68) is exactly the same at this order. The differences arise starting from 1-loop order. The soft-gluon factorization formula at 1-loop order with massless QCD partons has been derived in Ref. [119]. For massive quarks the corresponding results have been computed in Ref. [120].

2.7 QCD perturbation theory at hadron colliders

The perturbative expansion in Eq. (2.15) relies on the assumption of small coupling constant α_S. Because of asymptotic freedom, for large values Q of transferred momentum the hadrons behave as a collection of weakly interacting particles, quarks and gluons, and the perturbative expansion is justified. At small scales, however, the colour interaction becomes very strong, confining the quarks inside the hadrons, and perturbation theory breaks down. If one is not interested in the details of the interaction at small scales, or in other words, if one considers a 'sufficiently inclusive' process, than the parton picture can be used to describe that process. The parton picture essentially consists in the factorization of short and long distance phenomena. As an example one can consider the hadronic cross section in e^+e^- annihilation, which is completely inclusive over the final state. The hadrons in the final state are produced first by the production of a $q\bar{q}$ pair, sketched in Section 2.5. The quarks then evolve, eventually fragmenting into hadrons. The perturbative stage of the evolution is controlled by a large scale of the order of the center of mass energy of e^+e^- pair. The hadronization contribution gives rise only to power-suppressed corrections of the order $\mathcal{O}\left(\frac{\Lambda}{Q}\right)$, and hence can be neglected as long as the high-energy behaviour of the total cross section is considered.

The parton model picture has been the first attempt to describe the factorization properties of high-energy collisions. To make it explicit, let us consider an inclusive hadron-hadron hard-scattering process,

$$h_1(P_1) + h_2(P_2) \to H(Q) + X\,, \tag{2.74}$$

where the colliding hadrons h_1 and h_2 have the momenta P_1 and P_2, H denotes the observed high-mass particle or system of particles (vector bosons, Higgs bosons, heavy quarks, jets, etc.) and X stands for any unobserved particles produced by the collision of hadrons. Q is the characteristic hard scale of the scattering process under consideration, which can be set, for example, by the invariant mass of the produced high-mass system. The dependence on other measured kinematic variables is implicitly understood. According to the naive parton model picture, the cross section for this process can be symbolically written as

$$\sigma^H(P_1, P_2; Q) = \sum_{a,b} \int dx_1\, dx_2\, f_{a/h_1}(x_1)\, f_{b/h_2}(x_2)\, \hat{\sigma}^H_{ab}(x_1 P_1, x_2 P_2; \alpha_S(Q))\,, \tag{2.75}$$

where $f_{a/h}(x)$ is the parton distribution function (PDF), which represents the probability of finding the parton a inside the hadron h, and $\hat{\sigma}^H_{ab}$ is the cross section of the hard-scattering process $a+b \to H+X$, which can be computed according to the perturbative expansion in Eq. (2.15). The importance of this picture is that, though the structure functions $f_{a/h}(x)$ are non-perturbative objects, they are universal, i.e. they depend only on the hadron. Therefore, they can be measured for one process and then used as an input to make predictions for other processes involving the same hadron. The factorization formula of Eq. (2.75), however, fails beyond LO QCD because of the more complicated pattern of QCD IR singularities than that described in Section 2.5. In particular, it turns out that for the processes with initial-state hadrons, the IR singularities do not cancel even after summing the virtual and real corrections. Note that the fact of non-cancellation of initial-state collinear singularities does not contradict the KLN theorem, since the underlying hard-scattering process $a + b \to H + X$ is not completely inclusive over the initial state.

The fact that the structure functions $f_{a/h}$ are not computable in perturbation theory allows us to assume that the PDFs defined in the naive parton model are not physical quantities, but need to be redefined, analogously to the redefinition of masses and the coupling constant in the customary UV renormalization procedure. This is possible, in particular, thanks to the universal factorization of the collinear singularities (see Section 2.6 for more details). The renormalization of bare PDFs introduces an arbitrary unphysical scale, μ_F, which represents the scale up to which the initial-state collinear singularities are reabsorbed into the PDFs, characterised by $k_T < \mu_F$. The QCD factorization formula for the hadronic cross section for the process (2.74) can be written as:

$$\begin{aligned}\sigma^H(P_1, P_2; Q) = &\sum_{a,b} \int dx_1\, dx_2\, f_{a/h_1}(x_1, \mu_F^2)\, f_{b/h_2}(x_2, \mu_F^2)\, \hat{\sigma}^H_{ab}(x_1 P_1, x_2 P_2; \alpha_S(Q), \mu_F^2) \\ &+ \mathcal{O}\left(\left(\frac{\Lambda_{\mathrm{QCD}}}{Q}\right)^p\right)\,,\end{aligned} \tag{2.76}$$

where Λ_{QCD} is the characteristic scale of QCD, below which perturbation theory is not valid. Hence, the term $\mathcal{O}\left(\left(\frac{\Lambda_{\mathrm{QCD}}}{Q}\right)^p\right)$ on the right-hand side of Eq. (2.76) generically denotes non-perturbative contributions, such as hadronization effects, multiparton interactions, etc. Both the partonic cross section $\hat{\sigma}_{ab}(\mu_F^2)$ and the parton distribution functions (PDFs)

$f_{a/h}(x, \mu_F^2)$ of the colliding hadrons in Eq. (2.76) depend on the factorization scale μ_F. However, the dependence should be such that it cancels in the hadronic cross section $\sigma(P_1, P_2; Q)$, since it is the physical cross section and cannot depend on the unphysical scale. Nonetheless, in a fixed-order computation only finitely many terms in the small coupling expansion of $\hat{\sigma}_{ab}(\mu_F)$ in Eq. (2.15) are kept, and the μ_F dependence remains. Together with the residual dependence on the renormalisation scale μ_R, this dependence is often used to obtain an estimate for the yet uncalculated higher-order contributions.

It should be noted that, even though μ_F is an arbitrary scale, in a real calculation one should take care on the choice of its value. The reason is that the higher-order corrections to the partonic cross section in Eq. (2.15) contain logarithms of the form, $\alpha_S^n \ln(Q/\mu_F)^n$. These logarithmic contributions can be large if μ_F is chosen very different from the hard scale Q, thus spoiling the perturbative expansion in Eq. (2.15). Therefore, the factorization scale should be chosen of the order of the hard scale of the process $\mu_F \sim Q$.

As non-perturbative quantities, the PDFs cannot be obtained from first principles. However, the scale-dependence on μ_F arises from perturbative physics at the separation scale and can thus be computed using QCD perturbation theory by means of the Dokshitzer-Gribov-Lipatov-Altarelli-Parisi (DGLAP) evolution equations [121–123]

$$Q^2 \frac{d}{dQ^2} f_{a/h}(x, Q^2) = \sum_b \int_x^1 \frac{dz}{z} P_{ab}(\alpha_S(Q^2), z) f_{a/h}(x/z, Q^2)\,, \tag{2.77}$$

where $P_{ab}(\alpha_S(Q^2), z)$ are the *Altarelli-Parisi* (AP) *splitting functions*. These functions are universal, they only depend on the species of partons involved in the splitting process and have the following perturbative expansion in α_S

$$P_{ab}(\alpha_S, z) = \sum_{n=1}^{\infty} \left(\frac{\alpha_S}{2\pi}\right)^n P_{ab}^{(n)}(z)\,. \tag{2.78}$$

To leading order in α_S the AP splitting functions are [123]

$$P_{qq}^{(1)}(z) = C_F \left[\frac{1+z^2}{1-z}\right]_+\,, \tag{2.79}$$

$$P_{qg}^{(1)}(z) = T_R \left[z^2 + (1-z)^2\right]\,, \tag{2.80}$$

$$P_{gq}^{(1)}(z) = C_F \left[\frac{1+(1-z)^2}{z}\right]\,, \tag{2.81}$$

$$P_{gg}^{(1)}(z) = 2C_A \left[\frac{z}{(1-z)_+} + \frac{1-z}{z} + z(1-z)\right] + \delta(1-z)\beta_0\,. \tag{2.82}$$

The 'plus-distribution' of a function $f(z)$ is defined as

$$\int_0^1 dz [f(z)]_+ g(z) = \int_0^1 dz [f(z) - f(1)] g(z)\,, \tag{2.83}$$

where $g(z)$ is a test function and it is regular at $z = 1$.

2.8 Soft-gluon effects in multi-scale processes

Up to now we have considered QCD processes with only one hard scale Q. We have seen in this case that the soft singularities in real and virtual corrections cancel each other for infrared-safe quantities. However, when more than one scale is present, the emission of soft gluons can still be relevant and lead to large logarithmic contributions. As an example, let us consider the production of a jet with small invariant mass in e^+e^- collisions. It is a two-scale problem, where the mass of the jet m_J^2 is much smaller than the center of mass energy of the e^+e^- pair Q^2. At the LO the final-state quark and the antiquark are produced back-to-back. One of them can be identified as the jet of measured mass. We denote the momentum of the jet at the LO by p, the energy in the center of mass frame is equal to $E_p = Q/2$, and the mass of the jet is zero $m_{\rm jet}^2 = 0$. At the NLO one has to consider real and virtual corrections to the LO process. The real correction is due to the emission of an on-shell gluon with momentum q and energy ω, radiated by one of the final-state quarks at an angle θ. The differential probability of such a radiation in the soft-collinear limit is

$$dw_{\rm real}^{(1)} = C_F \frac{\alpha_{\rm S}}{\pi} \frac{d\omega}{\omega} \frac{d\theta^2}{\theta^2} \,. \tag{2.84}$$

It has a double-logarithmic spectrum, with $d\omega/\omega$ being the bremsstrahlung spectrum and $d\theta^2/\theta^2$ being the collinear-splitting spectrum.

The virtual correction is due to the self-energy diagram, where a virtual gluon is emitted and then reabsorbed by the same quark. Because of unitarity, the differential probability of the virtual radiation is equal to the real one, but with the opposite sign, thus ensuring the cancellation of the singularities, according to the KLN theorem

$$dw_{\rm real}^{(1)} = -dw_{\rm virt}^{(1)} \,. \tag{2.85}$$

Summing the virtual and real corrections, the cross section can be written as

$$\sigma = \sigma^{(0)} \left\{ 1 + C_F \frac{\alpha_{\rm S}}{\pi} \int_0^{E_p} \frac{d\omega}{\omega} \int_0^1 \frac{d\theta^2}{\theta^2} \left[\Theta(m_J^2 - m_{\rm jet}^2) - 1 \right] + \mathcal{O}(\alpha_{\rm S}^2) \right\} , \tag{2.86}$$

where the Heaviside theta function $\Theta(m_J^2 - m_{\rm jet}^2)$ is due to the constraint on the invariant mass of the jet, which is equal to $m_{\rm jet}^2 = 2p \cdot q = 2\omega E_p(1 - \cos\theta) \sim \omega E_p \theta^2$ for the real emission kinematics. The -1 in $\left[\Theta(m_J^2 - m_{\rm jet}^2) - 1\right]$ is due to the virtual contribution, where the constraint $m_{\rm jet}^2 \ll m_J^2$ is automatically fulfilled, because $m_{\rm jet}^2 = 0$ for the LO kinematics. As one expects, the real and virtual contributions are separately divergent in the soft ($\omega \to 0$ or $z \to 1$) and collinear ($\theta \to 0$) limits. Using the following identity

$$\Theta(m_J^2 - \omega E_p \theta^2) - 1 = -\Theta(\omega E_p \theta^2 - m_J^2) \,, \tag{2.87}$$

one basically finds that the sum of the real and virtual corrections results in regularising the soft and collinear divergences. Indeed, from Eq. (2.87) we find that $\theta^2 > m_J^2/(\omega E_p)$

and $\omega > m_J^2/E_p$, such that the cross section in Eq. (2.86) can be written as

$$\sigma = \sigma^{(0)} \left\{ 1 - C_F \frac{\alpha_S}{\pi} \int_{m_J^2/E_p}^{E_p} \frac{d\omega}{\omega} \int_{m_J^2/(\omega E_p)}^{1} \frac{d\theta^2}{\theta^2} + \mathcal{O}(\alpha_S^2) \right\} , \tag{2.88}$$

which is now finite and can be integrated to give

$$\sigma = \sigma^{(0)} \left[1 - C_F \frac{\alpha_S}{2\pi} \ln^2 \frac{Q^2}{4m_J^2} + \mathcal{O}(\alpha_S^2) \right] . \tag{2.89}$$

We see that despite the cancellation of IR divergences, the cross section in Eq. (2.89) contains a two-scale logarithm $\ln^2(Q^2/4m_J^2)$, which can be large in the regime $m_J^2 \ll Q^2$, because of a strong kinematical suppression of the real radiation. As a result, $\alpha_S \ln^2(Q^2/4m_J^2)$ can be ~ 1 even for small coupling constant $\alpha_S \ll 1$, thus spoiling the convergence of the fixed-order expansion. To obtain reliable phenomenological results in such situations one needs to find a technique to improve the perturbation expansion. Such a technique is called *resummation*: the large logarithmic contributions arising in the fixed-order expansion are (re)-summed to all orders by introducing a modified expansion parameter of the form $\alpha_S L$, L being the large logarithm.

Chapter 3

Transverse-momentum resummation

The transverse-momentum (q_T) spectrum of high-mass systems produced at hadron colliders is another example of a quantity which suffers from large logarithmic contributions in fixed-order computations. At every order n in the perturbative expansion of the transverse-momentum spectrum one finds logarithmic terms of the form

$$\alpha_{\rm S}^n \ln(M^2/q_T^2)^m \,, \quad m = 2n, \dots 1 \,, \tag{3.1}$$

where M is the invariant mass of the final-state system. These logs can be large in the small-q_T region, eventually breaking the convergence of the perturbative expansion. Thus, to obtain reliable perturbative predictions of the transverse-momentum spectrum at small q_T these terms have to be resummed to all orders in $\alpha_{\rm S}$ according to the techniques developed in Refs. [70–82].

In this section we review the general formalism of transverse-momentum resummation for the production of generic colourless high-mass systems (see e.g. Ref. [82]) and we highlight the universal process-independent ingredients that will enter also in the resummation formula for the production of a heavy-quark pair. Due to colourless nature of the triggered final state, the large logarithms appearing in the fixed-order calculation of this class of processes is limited to the soft and collinear contributions from the initial-state partons and the colour algebra is simple. It factorises into the Casimir operators of the initial-state partons, while the colour-correlation terms due to the exchange of non-collinear gluons between the two partons cancel out in the soft limit. The transverse-momentum resummation in this case is well known and has been applied to number of processes of this class [124–127].

3.1 The resummation formalism

We consider the inclusive hard-scattering process

$$h_1(P_1) + h_2(P_2) \to F(\{q_i\}) + X\,, \tag{3.2}$$

where the collision of the two hadrons h_1 and h_2 with momenta P_1 and P_2 produces a final-state system F of non-strongly interacting particles (one or more), accompanied by an arbitrary and undetected final state X. We treat the colliding hadrons as massless particles and the hadronic center-of-mass energy is $\sqrt{s} = \sqrt{(P_1+P_2)^2} = \sqrt{2P_1\cdot P_2}$. The momenta of the individual particles of the system F are denoted by q_i^μ ($i = 3, 4, \ldots$) and the total momentum q^μ of the system is their sum ($q^\mu = \sum_i q_i^\mu$). In the centre-of-mass system of the collision the momentum q^μ is fully specified by the invariant mass M ($M^2 = q^2$), the two-dimensional transverse-momentum vector $\mathbf{q_T}$ (with magnitude q_T and azimuthal angle $\phi(\mathbf{q_T})$) and the rapidity $y = \frac{1}{2}\ln\frac{q\cdot P_2}{q\cdot P_1}$. If F is composed by more than one particle (for example, a dilepton), additional independent variables are needed to specify the angular distribution of the individual particles with respect to the momentum q of the final-state system. We denote the set of these additional variables by $\mathbf{\Omega}$ and we consider the following multidifferential cross section

$$\frac{d\sigma_{h_1h_2\to F+X}(s;\mathbf{q_T},y,M,\mathbf{\Omega})}{d^2\mathbf{q_T}\,dM^2\,dy\,d\mathbf{\Omega}}\,. \tag{3.3}$$

According to the QCD factorization theorem the hadronic multidifferential cross section can be written as a convolution of PDFs and partonic differential cross section

$$\begin{aligned}\frac{d\sigma_{h_1h_2\to F+X}(s;\mathbf{q_T},y,M,\mathbf{\Omega})}{d^2\mathbf{q_T}\,dM^2\,dy\,d\mathbf{\Omega}} &= \sum_{a_1,a_2}\int_0^1 d\xi_1\int_0^1 d\xi_2\, f_{a_1/h_1}(\xi_1,\mu_F^2)\, f_{a_2/h_2}(\xi_2,\mu_F^2) \\ &\quad\times \frac{d\hat\sigma_{a_1a_2\to F+X}(\hat s;\mathbf{q_T},\hat y,M,\mathbf{\Omega};\alpha_S(\mu_R^2),\mu_R^2,\mu_F^2)}{d^2\mathbf{q_T}\,dM^2\,d\hat y\,d\mathbf{\Omega}}\,,\end{aligned} \tag{3.4}$$

where $\hat y$ and $\hat s$ are the rapidity and the center-of-mass energy of the partonic scattering process which are related to the corresponding hadronic variables y and s by

$$\hat y = y - \frac{1}{2}\ln\frac{\xi_1}{\xi_2}\,,\qquad \hat s = \xi_1\xi_2 s\,. \tag{3.5}$$

It is useful to rewrite the factorization formula in Eq. (3.4) in the following way

$$\begin{aligned}\frac{d\sigma_{h_1h_2\to F+X}(s;\mathbf{q_T},y,M,\mathbf{\Omega})}{d^2\mathbf{q_T}\,dM^2\,dy\,d\mathbf{\Omega}} &= \frac{1}{s}\sum_{a_1,a_2}\int_{x_1}^1\frac{dz_1}{z_1}\int_{x_2}^1\frac{dz_2}{z_2} \\ &\quad\times f_{a_1/h_1}(x_1/z_1,\mu_F^2)\, f_{a_2/h_2}(x_2/z_2,\mu_F^2)\,\frac{d\hat\sigma_{a_1a_2\to F+X}(\mathbf{q_T},z_1,z_2;M,\mathbf{\Omega};\alpha_S(\mu_R^2),\mu_R^2,\mu_F^2)}{d^2\mathbf{q_T}\,dz_1\,dz_2\,d\mathbf{\Omega}}\,,\end{aligned} \tag{3.6}$$

where the hadronic scaling variables x_1 and x_2 are defined such that $M^2 = x_1 x_2 s$ and $y = \frac{1}{2} \ln \frac{x_1}{x_2}$. Explicitly

$$x_1 = \frac{M}{\sqrt{s}} e^{+y} , \quad x_2 = \frac{M}{\sqrt{s}} e^{-y} . \tag{3.7}$$

We have also introduced the partonic scaling variables z_1 and z_2, which are the momentum fractions of the partons entering the hard process and are defined such that $M^2 = z_1 z_2 \hat{s}$ and $\hat{y} = \frac{1}{2} \ln \frac{z_1}{z_2}$. Explicitly

$$z_1 = \frac{M}{\sqrt{\hat{s}}} e^{+\hat{y}} , \quad z_2 = \frac{M}{\sqrt{\hat{s}}} e^{-\hat{y}} . \tag{3.8}$$

In the region where $q_T \sim M$, the QCD perturbative expansion of the partonic cross section in Eq. (3.6) is controlled by a single expansion parameter, $\alpha_{\rm S}(M)$, and the standard fixed-order calculations can be safely applied. In the region $q_T \ll M$, however, the convergence of perturbative expansion is spoiled by the presence of large logarithms of the form in Eq. (3.1), which need to be resummed to all orders. To separate these two regions, therefore, we introduce the following decomposition of the hadronic cross section

$$\frac{d\sigma_{h_1 h_2 \to F+X}(s; \mathbf{q_T}, y, M, \mathbf{\Omega})}{d^2\mathbf{q_T}\, dM^2\, dy\, d\mathbf{\Omega}} = [d\sigma_F] + \frac{d\sigma^{\rm reg.}_{h_1 h_2 \to F+X}(s; \mathbf{q_T}, y, M, \mathbf{\Omega})}{d^2\mathbf{q_T}\, dM^2\, dy\, d\mathbf{\Omega}} , \tag{3.9}$$

where, in order to simplify the later presentation, we have introduced the short-hand notation $[d\sigma_F]$ for the singular component of the hadronic cross section:

$$[d\sigma_F] \equiv \frac{d\sigma^{\rm sing.}_{h_1 h_2 \to F+X}(s; \mathbf{q_T}, y, M, \mathbf{\Omega})}{d^2\mathbf{q_T}\, dM^2\, dy\, d\mathbf{\Omega}} . \tag{3.10}$$

The decomposition of the hadronic cross section into singular and regular components in Eq. (3.9) implies a corresponding decomposition of the partonic cross section

$$\frac{d\hat{\sigma}_{a_1 a_2 \to F+X}}{d^2\mathbf{q_T}\, dz_1\, dz_2\, \mathbf{\Omega}} = \frac{d\hat{\sigma}^{\rm sing.}_{a_1 a_2 \to F+X}}{d^2\mathbf{q_T}\, dz_1\, dz_2\, \mathbf{\Omega}} + \frac{d\hat{\sigma}^{\rm reg.}_{a_1 a_2 \to F+X}}{d^2\mathbf{q_T}\, dz_1\, dz_2\, \mathbf{\Omega}} , \tag{3.11}$$

where the first term on the right-hand side contains all the contributions that are enhanced (*singular*) at small q_T. In particular, besides the large logarithms, these contributions can also be proportional to $\delta^{(2)}(\mathbf{q_T})$. On the contrary, the second term on the right-hand side is *regular* order-by-order in perturbation theory as $q_T \to 0$. More precisely, the integration of $d\hat{\sigma}^{\rm reg.}_{a_1 a_2 \to F+X}/d^2\mathbf{q_T}$ over the range $0 \le q_T \le Q_0$ leads to a finite result which vanishes in the limit $Q_0 \to 0$, at each fixed order in $\alpha_{\rm S}$.

In practise, of course, one cannot compute all the logarithmic contributions in the perturbative series. In actual calculations, however, the singular component $d\hat{\sigma}^{\rm sing.}_{a_1 a_2 \to F+X}$ can, through logarithmic expansion, be systematically organized in classes of leading logarithmic (LL), next-to-leading logarithmic (NLL), next-to-next-to-leading logarithmic (NNLL)

contributions. The logarithmic expansion of the singular component $\left[d\hat{\sigma}^{\text{sing.}}_{a_1a_2\to F+X}\right]_{\text{l.a.}}$, then, needs to be consistently matched with the fixed order expansion of the regular component $\left[d\hat{\sigma}^{\text{reg.}}_{a_1a_2\to F+X}\right]_{\text{f.o.}}$ at intermediate values of q_T

$$\frac{d\hat{\sigma}_{a_1a_2\to F+X}}{d^2\mathbf{q_T}\,dz_1\,dz_2\,\mathbf{\Omega}} \to \left[\frac{d\hat{\sigma}_{a_1a_2\to F+X}}{d^2\mathbf{q_T}\,dz_1\,dz_2\,\mathbf{\Omega}}\right]_{\text{f.o+l.a}} = \left[\frac{d\hat{\sigma}^{\text{sing.}}_{a_1a_2\to F+X}}{d^2\mathbf{q_T}\,dz_1\,dz_2\,\mathbf{\Omega}}\right]_{\text{l.a}} + \left[\frac{d\hat{\sigma}^{\text{reg.}}_{a_1a_2\to F+X}}{d^2\mathbf{q_T}\,dz_1\,dz_2\,\mathbf{\Omega}}\right]_{\text{f.o}}, \tag{3.12}$$

where the regular component $\left[d\hat{\sigma}^{\text{reg.}}_{a_1a_2\to F+X}\right]_{\text{f.o.}}$ is computed by subtracting from the usual perturbative series for the partonic cross section $[d\hat{\sigma}_{a_1a_2\to F+X}]_{\text{f.o.}}$, truncated at a given fixed order in α_{S}, the perturbative truncation of the singular component at the *same* fixed order α_{S}

$$\left[\frac{d\hat{\sigma}^{\text{reg.}}_{a_1a_2\to F+X}}{d^2\mathbf{q_T}\,dz_1\,dz_2\,\mathbf{\Omega}}\right]_{\text{f.o}} = \left[\frac{d\hat{\sigma}_{a_1a_2\to F+X}}{d^2\mathbf{q_T}\,dz_1\,dz_2\,d\mathbf{\Omega}}\right]_{\text{f.o}} - \left[\frac{d\hat{\sigma}^{\text{sing.}}_{a_1a_2\to F+X}}{d^2\mathbf{q_T}\,dz_1\,dz_2\,\mathbf{\Omega}}\right]_{\text{f.o}} \tag{3.13}$$

Moreover, to maintain the full information of the perturbative calculation up to the specified fixed order, the following condition is imposed

$$\left[\left[\frac{d\hat{\sigma}^{\text{sing.}}_{a_1a_2\to F+X}}{d^2\mathbf{q_T}\,dz_1\,dz_2\,\mathbf{\Omega}}\right]_{\text{l.a}}\right]_{\text{f.o}} = \left[\frac{d\hat{\sigma}^{\text{sing.}}_{a_1a_2\to F+X}}{d^2\mathbf{q_T}\,dz_1\,dz_2\,\mathbf{\Omega}}\right]_{\text{f.o}}. \tag{3.14}$$

The resummation of large logarithmic contributions relies on the factorization of the cross section in the infrared region. As we have discussed in Section 2.6, the QCD scattering amplitudes universally factorise in the soft and collinear limits. However, the complete factorisation of the cross section requires the phase space to factorise as well. In some cases, one needs to go to some adjoint space to avoid convolutions involving energy-momentum conservation constraints. In the case of transverse-momentum, the resummation has to be carried out in the impact-parameter space (***b***-space), to correctly take into account the kinematics constraint of transverse-momentum conservation. In **b**-space the singular terms are proportional to powers of $\ln(M^2b^2)$ ($q_T^2 \ll M^2$ corresponds to $M^2b^2 \gg 1$). The transverse-momentum resummed cross section is then obtained by inverse Fourier transformation from **b**-space to $\mathbf{q_T}$-space

$$\frac{d\hat{\sigma}^{\text{sing.}}_{a_1a_2\to F+X}}{d^2\mathbf{q_T}\,dz_1\,dz_2\,\mathbf{\Omega}} = \frac{M^2}{\hat{s}}\int\frac{d^2\mathbf{b}}{(2\pi)^2}\,e^{i\mathbf{b}\cdot\mathbf{q_T}}\,\mathcal{W}^F_{a_1a_2}(\hat{s};M,z_1,z_2,\mathbf{b},\mathbf{\Omega};\alpha_{\text{S}}(\mu_R^2),\mu_R^2,\mu_F^2)\,. \tag{3.15}$$

The factor $\mathcal{W}^F_{a_1a_2}$ is the perturbative and process-dependent partonic cross section that embodies the all-order resummation of the large logarithms $\ln M^2b^2$. In general, it can depend both on the modulus of the two-dimensional vector $\mathbf{b}^2$, as well as on the azimuthal angle $\phi(\mathbf{b})$. However, as we will see in Section 3.2, for processes which are mediated by $q\bar{q}$ annihilation at the Born level, the partonic resummation factor $\mathcal{W}^F_{a_1a_2}$ depends only on $\mathbf{b}^2$ and not on the azimuthal angle $\phi(\mathbf{b})$. In these cases one can straightforwardly integrate Eq. (3.15) over $\phi(\mathbf{b})$

$$\int\frac{d^2\mathbf{b}}{2\pi}\,e^{i\mathbf{b}\cdot\mathbf{q_T}}\,F(\mathbf{b}^2) = \int_0^\infty db\;b\;J_0(bq_T)\;F(b^2)\,, \tag{3.16}$$

where $J_0(x)$ is the 0th-order Bessel function. In this way the *two*-dimensional Fourier transformation is replaced by the *one*-dimensional Bessel transformation, leading to a technical simplification of the resummation formula. More relevantly, the result in Eq. (3.16) implies that the right-hand side of Eq. (3.15) depends only on $q_T = |\mathbf{q_T}|$ and does not depend on the azimuthal angle $\phi(\mathbf{q_T})$ of $\mathbf{q_T}$. This, in particular means that $d\hat{\sigma}^{\text{sing.}}_{a_1a_2\to F+X}/d^2\mathbf{q_T}$ and $d\hat{\sigma}^{\text{sing.}}_{a_1a_2\to F+X}/dq_T^2$ are simply proportional to each other

$$\frac{d\hat{\sigma}^{\text{sing.}}_{a_1a_2\to F+X}}{d^2\mathbf{q_T}\; dz_1\; dz_2\; d\mathbf{\Omega}} = \frac{1}{\pi}\; \frac{d\hat{\sigma}^{\text{sing.}}_{a_1a_2\to F+X}}{dq_T^2\; dz_1\; dz_2\; d\mathbf{\Omega}}\,, \tag{3.17}$$

and Eq. (3.15) simplifies to

$$\frac{d\hat{\sigma}^{\text{sing.}}_{a_1a_2\to F+X}}{dq_T^2\; dz_1\; dz_2\; \mathbf{\Omega}} = \frac{M^2}{\hat{s}} \int db\; \frac{b}{2}\; J_0(bq_T)\; \mathcal{W}^F_{a_1a_2}(\hat{s}; M, z_1, z_2, b, \mathbf{\Omega}; \alpha_{\text{S}}(\mu_R^2), \mu_R^2, \mu_F^2)\,. \tag{3.18}$$

In the case of gluon fusion processes, these conclusions about azimuthal correlations at small q_T are no longer true due to spin-correlation effects. We discuss the transverse-momentum resummation in gluon fusion processes in Section 3.4. The situation becomes more involved in the case of heavy-quark production, due to additional azimuthal correlations of soft origin.

The resummed cross section $\mathcal{W}^F_{a_1a_2}$ can be organised in a simpler form in the Mellin space (N-space). The Mellin transform g_N of some function $g(z)$ with respect z is defined as

$$g_N = \int_0^1 dz\; z^{N-1}\; g(z)\,. \tag{3.19}$$

To keep the full rapidity dependence at the Born level, we define the double Mellin moments $\mathcal{W}^{N_1,N_2}$ of $\mathcal{W}$ with respect to the z_1 and z_2 variables in Eq. (3.8) at fixed M:

$$\begin{aligned}\mathcal{W}^F_{a_1a_2,\,(N_1,N_2)}(M, b, \mathbf{\Omega}; \alpha_{\text{S}}(\mu_R^2), \mu_R^2, \mu_F^2) = \int_0^1 dz_1\; z_1^{N_1-1} \int_0^1 dz_2\; z_2^{N_2-1} \\ \times\, \mathcal{W}^F_{a_1a_2}\left(\hat{s} = \frac{M^2}{z_1z_2}; M, z_1, z_2, b, \mathbf{\Omega}; \alpha_{\text{S}}(\mu_R^2), \mu_R^2, \mu_F^2\right)\,.\end{aligned} \tag{3.20}$$

The double Mellin moment $\mathcal{W}^F_{N_1,N_2}$ can be then symbolically written in the following factorised form:

$$\begin{aligned}\mathcal{W}^F_{N_1,N_2}(M, b, \mathbf{\Omega}; \alpha_{\text{S}}(\mu_R^2), \mu_R^2, \mu_F^2) = \left[d\sigma^{(0)}_{c\bar{c},\,F}\right] \mathcal{H}^F_{N_1,N_2}(M, \mathbf{\Omega}, \alpha_{\text{S}}(\mu_R^2); M^2/\mu_R^2, M^2/\mu_F^2, M^2/Q^2) \\ \times \exp\{\mathcal{G}_{N_1,N_2}(\alpha_{\text{S}}(\mu_R^2), L; M^2/\mu_R^2, M^2/Q^2)\}\,,\end{aligned} \tag{3.21}$$

where the factor $\left[d\sigma^{(0)}_{c\bar{c},\,F}\right]$ in Eq. (3.30) is the Born level cross section of the partonic subprocess

$$c + \bar{c} \to F\,. \tag{3.22}$$

Since the final-state F consists of colourless particles, the partonic subprocesses include quark-antiquark $q\bar{q}$ annihilation, $q + \bar{q} \to F$, and gluon fusion, $g + g \to F$. Explicitly, the Born level cross section can be written as

$$\left[d\sigma^{(0)}_{c\bar{c},\,F}\right] = \frac{d\hat{\sigma}^{(0)}_{c\bar{c},\,F}}{M^2\, d\boldsymbol{\Omega}}(x_1P_1, x_2P_2; \boldsymbol{\Omega}; \alpha_{\mathrm{S}}(M^2))\,, \tag{3.23}$$

where $x_1P_1^\mu$ and $x_2P_2^\mu$ are the momenta of the partons c and $\bar{c}$. Eq. (3.30) includes the contribution of both the $q\bar{q}$ annihilation channel and the gluon fusion channel. Depending on the specific final state F, one of these two contribution channels may be absent[†].

The function $\mathcal{H}^F_{N_1,N_2}$ in Eq. (3.21) does not depend on the impact parameter b. Therefore, it does not contain large logarithmic terms to be resummed and can be expanded in powers of $\alpha_{\mathrm{S}} = \alpha_{\mathrm{S}}(\mu_R^2)$

$$\mathcal{H}^F_{N_1,N_2}(M, \boldsymbol{\Omega}, \alpha_{\mathrm{S}}(\mu_R^2)) = 1 + \sum_{n=1}^{\infty}\left(\frac{\alpha_{\mathrm{S}}}{\pi}\right)^n \mathcal{H}^{F\,(n)}_{N_1,N_2}(M, \boldsymbol{\Omega})\,, \tag{3.24}$$

where the dependence on the ratios of scales M^2/μ_R^2, M^2/μ_F^2 and M^2/Q^2 on both sides of the equation is understood.

Contrary to $\mathcal{H}^F_{N_1,N_2}$, the function $\mathcal{G}^{(N_1,N_2)}$ contains the complete dependence on b, in particular, it includes all the terms that are logarithmically divergent when $b \to \infty$, order-by-order in α_{S}. In Eq. (3.21) we have introduced a new unphysical scale Q, the *resummation scale*. The role of the resummation scale is to parametrise the ambiguities, coming from the factorisation of constant and logarithmic terms in Eq. (3.21). More precisely, the argument of the large logarithms can always be rescaled as $\ln M^2b^2 = \ln Q^2b^2 + \ln M^2/Q^2$, provided that Q does not depend on b and $Q \sim M$. The logarithmic expansion parameter L in Eq. (3.21) is then defined as

$$L \equiv \ln\frac{Q^2b^2}{b_0^2}\,, \tag{3.25}$$

where $b_0 = 2e^{-\gamma_E}$ ($\gamma_E = 0.5772\ldots$ is the Euler number). With this definition, L becomes large when $b \to \infty$ or, equivalently, when $q_T \to 0$. However, it is also singular in the limit $b \to 0$ ($q_T \to \infty$), thus leading to unjustified impact of large logarithms in the region where the resummation is not needed. To reduce this impact, one can replace L with $\widetilde{L}$

$$L \to \widetilde{L} \equiv \ln\left(\frac{Q^2b^2}{b_0^2} + 1\right)\,. \tag{3.26}$$

The variables L and $\widetilde{L}$ are equivalent in the region $Qb \gg 1$ (where the resummation is needed), $\widetilde{L} = L + \mathcal{O}(1/(Qb)^2)$, while at small values of b (large values of q_T), we have $\widetilde{L} \to 0$ and $\exp\{\mathcal{G}(\widetilde{L})\} \to 1$.

[†]For example, in the case of Higgs boson production only the gluon fusion channel contributes, while for the production of a vector boson, like Z or W, only the $q\bar{q}$ annihilation channel contributes. Diphoton production, on the contrary, receives contribution from both channels.

In particular, since $\exp\{\mathcal{G}(\alpha_{\rm S},\widetilde{L})\}=1$ at $b=0$, using Eqs. (3.18) and (3.21) and integrating over the q_T^2, we obtain the relation

$$\int_0^\infty dq_T^2\;\frac{d\hat{\sigma}^{\rm sing.}_{a_1a_2\to F+X}}{dq_T^2\;dz_1\;dz_2\;d\boldsymbol{\Omega}}(\hat{s};q_T,M,z_1,z_2,\boldsymbol{\Omega};\alpha_{\rm S}(\mu_R^2))=\frac{M^2}{\hat{s}}\;\Big[d\sigma^{(0)}_{c\bar{c},\,F}\Big]\;\mathcal{H}^F\Big(M,\boldsymbol{\Omega},z_1,z_2,\alpha_{\rm S}(\mu_R^2)\Big)\;, \tag{3.27}$$

which simply follows from the fact that the value at $b=0$ of the (b-space) Fourier transformation of the q_T-dependent cross section is equal to the integral over q_T of the q_T-dependent cross section itself. Since the hard cross section $\mathcal{H}^F$ is evaluated in fixed-order perturbation theory, the relation (3.27) implies that the replacement in Eq. (3.26) also allows us to implement a perturbative constraint on the differential cross section $d\hat{\sigma}_{a_1a_2\to F+X}/(dz_1dz_2d\boldsymbol{\Omega})$. More precisely, the integral over q_T^2 of the $d\hat{\sigma}_{a_1a_2\to F+X}/(dq_T^2dz_1dz_2d\boldsymbol{\Omega})$ cross section at NLL+NLO (NNLL+NNLO) accuracy exactly reproduces the calculation of the differential cross section $d\hat{\sigma}_{a_1a_2\to F+X}/(dz_1dz_2d\boldsymbol{\Omega})$ at NLO (NNLO).

As we will show in Section 3.2, $\mathcal{G}(\widetilde{L})$ can be systematically organised in the following form:

$$\mathcal{G}(\alpha_{\rm S},\widetilde{L})=\widetilde{L}g^{(1)}(\alpha_{\rm S}\widetilde{L})+g^{(2)}(\alpha_{\rm S}\widetilde{L})+\sum_{n=3}^{\infty}\left(\frac{\alpha_{\rm S}}{\pi}\right)^{(n-2)}g^{(n)}(\alpha_{\rm S}\widetilde{L})\,, \tag{3.28}$$

where $\alpha_{\rm S}=\alpha_{\rm S}(\mu_R^2)$ and the functions $g^{(n)}(\alpha_{\rm S}\widetilde{L})$ are defined such that $g^{(n)}=0$ when $\alpha_{\rm S}\widetilde{L}=0$. Counting the powers of logarithms $\widetilde{L}$ with respect to powers of $\alpha_{\rm S}$, we see that the first term on the right-hand side of Eq. (3.28), $\widetilde{L}g^{(1)}$, resums the LL contributions $\alpha_{\rm S}\widetilde{L}^{n+1}$, the coefficient $g^{(2)}$ collects the NLL contributions, $\alpha_{\rm S}\widetilde{L}^n$, and so forth.

3.2 The resummed component

In Section 3.1 we sketched the structure of the resummed cross section and anticipated that in the Mellin space the logarithmically-enhanced contributions can be factorised from constant terms, as it is given by Eq. (3.21). The goal of this section is to fix the perturbative coefficients of the hard-collinear function $\mathcal{H}^F_{N_1,N_2}$ in Eq. (3.24) and the resummation coefficients $g^{(n)}$ in Eq. (3.28).

The b-space resummation approach was fully formalised in terms of perturbative coefficients in Refs. [79, 81]. According to these works the singular component of the hadronic cross section $[d\sigma_F]$ is written as:

$$[d\sigma_F]=\frac{M^2}{s}\int\frac{d^2\mathbf{b}}{(2\pi)^2}\;e^{i\mathbf{b}\cdot\mathbf{q_T}}\;W^F(s;b,y,M,\boldsymbol{\Omega};\alpha_{\rm S}(\mu_R^2),\mu_R^2,\mu_F^2)\,. \tag{3.29}$$

The factor W^F is the hadronic cross section that embodies the all-order resummation of

the large logarithms $\ln M^2 b^2$. It can be written as

$$W^F(s;b,y,M,\mathbf{\Omega};\alpha_{\rm S}(\mu_R^2),\mu_R^2,\mu_F^2) = \sum_{a_1,a_2} \int_{x_1}^1 \frac{dz_1}{z_1} \int_{x_2}^1 \frac{dz_2}{z_2}\, f_{a_1/h_1}\left(\frac{x_1}{z_1},\frac{b_0^2}{b^2}\right)\, f_{a_2/h_2}\left(\frac{x_2}{z_2},\frac{b_0^2}{b^2}\right) \times \sum_{c=q,\bar{q},g} \left[d\sigma^{(0)}_{c\bar{c},\,F}\right]\, S_c(M,b)\, \left[H^F C_1 C_2\right]_{c\bar{c};a_1a_2}\,, \tag{3.30}$$

We note that the factor W^F in Eq. (3.30) depends only on the absolute value of the impact parameter b and the inverse Fourier transformation in Eq. (3.29) can be replaced by the Bessel transformation, according to Eq. (3.16)[†]. Note also that unlike the factorisation formula in Eq. (3.6), where the parton densities $f_{a_i/h_i}(x,\mu^2)$ are calculated at the scale $\mu_F \sim M$, the parton densities entering the resummation formula in (3.30) are evaluated at the scale $\mu = b_0/b$, which depends on the impact parameter.

The factor $S_c(M,b)$ is the Sudakov form factor, and it is *universal*, it only depends on the partonic channel of the Born process. The Sudakov form factor is produced by soft and flavour-conserving collinear radiation from the initial-state partons c and $\bar{c}$, and it resums logarithmic terms $\alpha_{\rm S}^n \ln^k(Mb)$, starting from the LL contributions ($k = 2n$) to the q_T cross section. It can be expressed in the following exponential form:

$$S_c(M,b) = \exp\left\{-\int_{b_0^2/b^2}^{M^2} \frac{dq^2}{q^2}\left[A_c(\alpha_{\rm S}(q^2))\ln\frac{M^2}{q^2} + B_c(\alpha_{\rm S}(q^2))\right]\right\}\,, \tag{3.31}$$

where the functions $A_c(\alpha_{\rm S})$ and $B_c(\alpha_{\rm S})$ are perturbative functions

$$A_c(\alpha_{\rm S}) = \sum_{n=1}^{\infty}\left(\frac{\alpha_{\rm S}}{\pi}\right)^n A_c^{(n)}\,, \tag{3.32}$$

$$B_c(\alpha_{\rm S}) = \sum_{n=1}^{\infty}\left(\frac{\alpha_{\rm S}}{\pi}\right)^n B_c^{(n)}\,. \tag{3.33}$$

The symbolic factor $\left[H^F C_1 C_2\right]$ is process-dependent and has the following explicit form:

$$\left[H^F C_1 C_2\right]_{c\bar{c};a_1a_2} = H_c^F(x_1P_1,x_2P_2;\mathbf{\Omega};\alpha_{\rm S}(M^2))\; C_{ca_1}(z_1;\alpha_{\rm S}(b_0^2/b^2))\; C_{ca_2}(z_2;\alpha_{\rm S}(b_0^2/b^2))\,. \tag{3.34}$$

where H_c^F and C_{ab} are both perturbative functions:

$$H_c^F(x_1P_1,x_2P_2;\mathbf{\Omega};\alpha_{\rm S}(M^2)) = 1 + \sum_{n=1}^{\infty}\left(\frac{\alpha_{\rm S}}{\pi}\right)^n H_c^{F\,(n)}(x_1P_1,x_2P_2;\mathbf{\Omega})\,, \tag{3.35}$$

$$C_{ab}(z;\alpha_{\rm S}) = \delta_{ab}\,\delta(1-z) + \sum_{n=1}^{\infty}\left(\frac{\alpha_{\rm S}}{\pi}\right)^n C_{ab}^{(n)}(z)\,. \tag{3.36}$$

[†]We recall that this is true only for $q\bar{q}$ annihilation subprocesses. In this section, however, we assume that the structure of the transverse-momentum resummed cross section in Eq. (3.30) are the same both for the gg and the $q\bar{q}$ annihilation subprocesses. In Section 3.4, instead, we present the necessary modifications of the formulae obtained in this section for gluon fusion subprocesses.

The function H_c^F on the right-hand side of Eq. (3.34) does not depend on the impact parameter b, and, thus is free of logarithmically-enhanced contributions. On the contrary, the functions C_{ab} depend on the impact parameter through the α_S scale b_0^2/b^2. These functions originate from initial-state collinear radiation.

Both the H_c^F and C_{ab} functions, as well as the function B_c, depend on the so-called *resummation scheme*. In particular, the resummation formula (3.30) is invariant under the following resummation scheme transformations [81]:

$$\begin{aligned} H_c^F(\alpha_S) &\to H_c^F(\alpha_S)\ [\,h(\alpha_S)\,]^{-1}\ , \\ B_c(\alpha_S) &\to B_c(\alpha_S) - \beta(\alpha_S)\ \frac{d\ln h(\alpha_S)}{d\ln \alpha_S}\ , \\ C_{ab}(\alpha_S, z) &\to C_{ab}(\alpha_S, z)\ [\,h(\alpha_S)\,]^{1/2}\ . \end{aligned} \tag{3.37}$$

Depending on the choice of the resummation scheme, the process dependence of the factor $\left[H^F C_1 C_2\right]$ can be distributed among the functions H_c^F and C_{ab}. In the following, we will work in the so-called *hard scheme*, where all the process dependence of $\left[H^F C_1 C_2\right]$ is contained in the hard-virtual coefficients H_c^F, while the collinear functions C_{ab} are process-independent. More precisely, the hard scheme is the scheme, in which, order-by-order in perturbation theory, the coefficients $C_{ab}^{(n)}(z)$ with $n \geq 1$ do not contain any $\delta(1-z)$ terms.

The first-order perturbative coefficients $C_{ab}^{(1)}$ of the collinear functions in the hard scheme read

$$C_{qq}^{(1)}(z) = \frac{1}{2} C_F (1-z)\,, \tag{3.38}$$

$$C_{gq}^{(1)}(z) = \frac{1}{2} C_F z\,, \tag{3.39}$$

$$C_{qg}^{(1)}(z) = \frac{1}{2} z(1-z)\,, \tag{3.40}$$

$$C_{gg}^{(1)}(z) = C_{q\bar{q}}^{(1)}(z) = C_{qq'}^{(1)}(z) = C_{q\bar{q}'}^{(1)}(z) = 0\,. \tag{3.41}$$

The second-order coefficients $C_{ab}^{(2)}$ are also known in the hard scheme and can be found in Ref. [128].

In the hard scheme the process-dependence of H_c^F comes from the finite part of loop amplitudes. Let us denote the all-order (virtual) amplitude for the elastic parton scattering of Eq. (3.22) by $\mathcal{M}_{c\bar{c}\to F}$. In the following we work with renormalised on-shell scattering amplitudes, which are regularisid by analitic continuation in $d = 4 - 2\epsilon$ space-time dimensions in the CDR scheme. The all-order perturbative expansion of the renormalised

amplitude can be formally written as

$$\mathcal{M}_{c\bar{c}\to F}(p_1,p_2;\{q_i\}) = (\alpha_{\rm S}(\mu_R^2)\mu^{2\epsilon})^k \left[\mathcal{M}^{(0)}_{c\bar{c}\to F}(p_1,p_2;\{q_i\}) + \sum_{n=1}^{\infty}\left(\frac{\alpha_{\rm S}(\mu_R)}{2\pi}\right)^n \mathcal{M}^{(n)}_{c\bar{c}\to F}(p_1,p_2;\{q_i\};\mu_R)\right], \tag{3.42}$$

where k is the power of $\alpha_{\rm S}$ in the leading order contribution, $\mathcal{M}^{(0)}_{c\bar{c}\to F}$ is the Born-level amplitude and $\mathcal{M}^{(n)}_{c\bar{c}\to F}$ are the perturbative terms at the n-loop level, renormalised in the $\overline{\rm MS}$ scheme.

Each renormalised amplitude $\mathcal{M}^{(n)}_{c\bar{c}\to F}$ still contains poles of IR origin. The IR divergences in the loop amplitudes have a universal structure, which is known at one-loop [29, 129–131] and two-loop order [129,132,133] for the class of processes in Eq. (3.22). Exploiting this universality, one can then subtract the IR divergences in a process-independent way. To this end, we define the following auxiliary hard-virtual amplitude [128]

$$\widetilde{\mathcal{M}}_{c\bar{c}\to F}(p_1,p_2;\{q_i\}) = \left[1-\widetilde{I}_c(\epsilon,M)\right]\mathcal{M}_{c\bar{c}\to F}(p_1,p_2;\{q_i\}), \tag{3.43}$$

where $\widetilde{I}_c$ is a process-independent IR subtraction operator. The dependence of $\widetilde{I}_c$ on ϵ is fixed at the level of the poles, reproducing the infrared structure of $\mathcal{M}_{c\bar{c}\to F}$. Thus, the operator $\left[1-\widetilde{I}_c\right]$ subtracts the infrared poles of $\mathcal{M}_{c\bar{c}\to F}$ and *some* of its IR finite terms. The all-order expansion of the IR subtraction factor is

$$\widetilde{I}_c(\epsilon,M) = \sum_{n=1}^{\infty}\left(\frac{\alpha_{\rm S}(\mu_R^2)}{2\pi}\right)^n \widetilde{I}_c^{(n)}(\epsilon,M;\mu_R). \tag{3.44}$$

The perturbative expansion of $\widetilde{\mathcal{M}}_{c\bar{c}\to F}$ is completely analogous to that in Eq. (3.42). Explicitly, the first two terms of the expansion read

$$\begin{aligned}\widetilde{\mathcal{M}}^{(0)}_{c\bar{c}\to F} &= \mathcal{M}^{(0)}_{c\bar{c}\to F},\\ \widetilde{\mathcal{M}}^{(1)}_{c\bar{c}\to F} &= \mathcal{M}^{(1)}_{c\bar{c}\to F} - \widetilde{I}_c^{(1)}(\epsilon,M;\mu_R)\mathcal{M}^{(0)}_{c\bar{c}\to F}.\end{aligned} \tag{3.45}$$

At the Born level, the two amplitudes are equal, because of the absence of IR divergences. The first-order subtraction operator $\widetilde{I}_c^{(1)}$ can be written as

$$\widetilde{I}_c^{(1)}(\epsilon,M;\mu_R) = \widetilde{I}_c^{(1)\rm soft}(\epsilon,M^2/\mu_R^2) + \widetilde{I}_c^{(1)\rm coll}(\epsilon,M^2/\mu_R^2), \tag{3.46}$$

where the soft component $\widetilde{I}_c^{(1)\rm soft}$ contains the soft-collinear douple pole, and the collinear component of the subtraction operator $\widetilde{I}_c^{(1)\rm coll}$ contains the collinear (non-soft) single pole. Explicitly they read

$$\begin{aligned}\widetilde{I}_c^{(1)\rm soft}(\epsilon,M^2/\mu_R^2) &= -\frac{e^{\epsilon\gamma_E}}{\Gamma(1-\epsilon)}\left(\frac{\mu_R^2}{M^2}\right)^{\epsilon}\left(\frac{1}{\epsilon^2}+i\pi\frac{1}{\epsilon}\right)C_a,\\ \widetilde{I}_c^{(1)\rm coll}(\epsilon,M^2/\mu_R^2) &= -\left(\frac{\mu_R^2}{M^2}\right)^{\epsilon}\frac{1}{\epsilon}\gamma_a,\end{aligned} \tag{3.47}$$

where the flavour dependent coefficients γ_a are

$$\gamma_q = \gamma_{\bar{q}} = \frac{3}{2} C_F \,, \quad \gamma_g = \frac{11}{6} C_A - \frac{1}{3} n_F \,. \tag{3.48}$$

The hard-virtual resummation coefficient H_c^F can now be defined in terms of the IR-finite auxiliary amplitude $\widetilde{\mathcal{M}}_{c\bar{c}\to F}$

$$H_c^F(p_1, p_2; \alpha_{\rm S}(M^2)) = \frac{|\widetilde{\mathcal{M}}_{c\bar{c}\to F}(p_1, p_2; \{q_i\})|^2}{\alpha_{\rm S}^{2k}(M^2) \widetilde{\mathcal{M}}^{(0)}_{c\bar{c}\to F}(p_1, p_2; \{q_i\})} \,, \tag{3.49}$$

which is the last ingredient of the hadronic resummation formula in Eqs. (3.29) and (3.30).

Having defined all the ingredients entering the formula for the hadronic cross section, we can now fix the perturbative coefficients of the hard-collinear function $\mathcal{H}^F_{N_1,N_2}$ in Eq. (3.24) and the resummation coefficients $g^{(n)}$ in Eq. (3.28). To this purpose, let us first define the double N-moment of the hadronic resummation factor W^F with respect to the variables x_1 and x_2 in Eq. (3.7) at fixed M

$$W^F_{N_1,N_2}(b, M, \mathbf{\Omega}) = \int_0^1 dx_1 \; x_1^{N_1-1} \int_0^1 dx_2 \; x_2^{N_2-1} \; W^F \left(s = \frac{M^2}{x_1 x_2}; b, y = \frac{1}{2} \ln \frac{x_1}{x_2}, M, \mathbf{\Omega} \right) \,, \tag{3.50}$$

where the dependence on $\alpha_{\rm S}(\mu_R^2)$ and on the renormalisation and factorisation scales μ_R^2 and μ_F^2 is understood. In Mellin space the convolution integral of two functions are turned into into ordinary multiplications. To see this on the example of the hadronic resummation factor in Eq. (3.30) W^F, let us consider the Mellin moment $W^F_{N_1}$ with respect to x_1

$$\begin{aligned} W^F_{N_1} &= \int_0^1 dx_1 \; x_1^{N_1-1} \int_{x_1}^1 \frac{dz_1}{z_1} \; g(z_1) \; f_{a_1/h_1}(x_1/z_1) \\ &= \int_0^1 dx_1 \; x_1^{N_1-1} \int_0^1 \frac{dz_1}{z_1} \; g(z_1) \; f_{a_1/h_1}(x_1/z_1) \; \Theta(z_1 - x_1) \\ &= \int_0^1 dz_1 \; z_1^{N_1-1} \; g(z_1) \int_0^1 d(x_1/z_1) \; (x_1/z_1)^{N_1-1} \; f_{a_1/h_1}(x_1/z_1) \\ &= g_{N_1} \cdot f_{a_1/h_1, N_1} \,, \end{aligned} \tag{3.51}$$

where we have denoted by $g(z_1)$ the collective dependence on z_1 on the right-hand side of Eq. (3.30). According to Eq. (3.51), the Mellin moment of the hadronic resummation factor $W^F_{N_1}$ with respect to x_1 is given by the Mellin moment of $g(z_1)$ with respect to z_1 multiplied by the Mellin moment of the parton density $f_{a_1/h_1, N_1}$ with respect to $\xi_1 = x_1/z_1$.

To relate the Mellin moment of the hadronic resummation factor $W^F_{N_1,N_2}$ in Eq. (3.51) to the partonic one $\mathcal{W}^F_{N_1,N_2}$ in Eq. (3.21) we need to replace the parton densities $f_{a_i/h_i, N_i}(b_0^2/b^2)$ with $f_{a_i/h_i, N_i}(\mu_F^2)$. In Mellin space this is done by using

$$f_{a/h, N}(\mu^2) = \sum_b U_{ab, N}(\mu^2, \mu_0^2) f_{b/h, N}(\mu_0^2) \,, \tag{3.52}$$

where $U_{ab,\,N}(\mu^2,\mu_0^2)$ is the QCD evolution operator and fulfils the following evolution equations

$$\frac{d\,U_{ab,\,N}(\mu^2,\mu_0^2)}{d\ln\mu^2} = \sum_c \gamma_{ac,\,N}(\alpha_{\rm S}(\mu^2))\,U_{cb,\,N}(\mu^2,\mu_0^2)\,, \tag{3.53}$$

and $\gamma_{ac,\,N}(\alpha_{\rm S})$ are the parton anomalous dimensions. They are the N-moments of the customary AP splitting functions $P_{ab}(\alpha_{\rm S},z)$ in Eq. (2.78):

$$\gamma_{ab,\,N}(\alpha_{\rm S}) = \int_0^1 dz\; z^{N-1}\; P_{ab}(\alpha_{\rm S},z) = \sum_{n=1}^{\infty}\left(\frac{\alpha_{\rm S}}{\pi}\right)^n \gamma^{(n)}_{ab,\,N}\,. \tag{3.54}$$

With the replacement $f_{a_i/h_i,\,N_i}(b_0^2/b^2) \to f_{a_i/h_i,\,N_i}(\mu_F^2)$, the resummed factors $W^F_{N_1,N_2}$ and $\mathcal{W}^F_{N_1,N_2}$ are then related by

$$W^F_{N_1,N_2}(b,M,\mathbf{\Omega}) = \sum_{a_1,\,a_2} \mathcal{W}^F_{a_1a_2,\,(N_1,N_2)}(M,b,\mathbf{\Omega})\; f_{a_1/h_1,\,N_1}(\mu_F^2)\; f_{a_2/h_2,\,N_2}(\mu_F^2)\,, \tag{3.55}$$

with $\mathcal{W}^F_{N_1,N_2}$ given by

$$\begin{aligned}\mathcal{W}^F_{a_1a_2,\,(N_1,N_2)}(M,b,\mathbf{\Omega};\alpha_{\rm S}(\mu_R^2),\mu_R^2,\mu_F^2) = &\sum_{c=q,\bar q,g}\left[d\sigma^{(0)}_{c\bar c,\,F}\right] H_c^F(M,\mathbf{\Omega};\alpha_{\rm S}(M^2))S_c(M,b)\\ &\times \sum_{b_1,\,b_2} C_{cb_1,\,N_1}(\alpha_{\rm S}(b_0^2/b^2))\; C_{\bar c b_2,\,N_2}(\alpha_{\rm S}(b_0^2/b^2))\\ &\times U_{b_1a_1,\,N_1}(b_0^2/b^2,\mu_F^2)\; U_{b_2a_2,\,N_2}(b_0^2/b^2,\mu_F^2)\,.\end{aligned} \tag{3.56}$$

To bring Eq (3.56) to the anticipated factorised form of Eq. (3.21), we first write down the solution of evolution equation in Eq. (3.53) for $U_{ba,\,N}(b_0^2/b^2,\mu_F^2)$. For simplicity of the presentation we consider a scenario when there is only one species of partons. The generalisation to multiflavour case is known, and the details can be found in Ref. [82]. The solution of Eq. (3.21) in this simplified case is given by

$$U_N(b_0^2/b^2,\mu_F^2) = \exp\left\{-\int_{b_0^2/b^2}^{\mu_F^2}\frac{dq^2}{q^2}\;\gamma_N(\alpha_{\rm S}(q^2))\right\}\,. \tag{3.57}$$

Next, using the RG equation for the coupling constant $\alpha_{\rm S}$ (see Eq. (2.26)), we write $C_N(\alpha_{\rm S}(b_0^2/b^2)$ in terms of $C_N(\alpha_{\rm S}(M^2)$

$$C_N(\alpha_{\rm S}(b_0^2/b^2) = C_N(M^2)\,\exp\left\{-\int_{b_0^2/b^2}^{M^2}\frac{dq^2}{q^2}\;\beta(\alpha_{\rm S}(q^2))\;\frac{d\ln C_N(\alpha_{\rm S}(q^2))}{d\ln\alpha_{\rm S}(q^2)}\right\}\,. \tag{3.58}$$

Using Eqs. (3.56), (3.57) and (3.58), we then can write the explicit expressions for the

hard-collinear function $\mathcal{H}^F_{N_1,N_2}$ and the exponential factor $\mathcal{G}_{N_1,N_2}$ in Eq. (3.21)

$$\begin{aligned}\mathcal{H}^F_{N_1,N_2}(M,\mathbf{\Omega},\alpha_{\rm S}(\mu_R^2)) &= H_c^F(M,\mathbf{\Omega};\alpha_{\rm S}(M^2))\; C_{N_1}(\alpha_{\rm S}(M^2))\; C_{N_2}(\alpha_{\rm S}(M^2)) \\ &\times \exp\left\{\int_{M^2}^{Q^2}\frac{dq^2}{q^2}\left[A(\alpha_{\rm S}(q^2))\ln\frac{M^2}{q^2}+\frac{1}{2}\left(\widetilde{B}_{N_1}(\alpha_{\rm S}(q^2))+\widetilde{B}_{N_2}(\alpha_{\rm S}(q^2))\right)\right]\right. \\ &\left.+\int_{\mu_F^2}^{M^2}\frac{dq^2}{q^2}\left(\gamma_{N_1}(\alpha_{\rm S}(q^2))+\gamma_{N_2}(\alpha_{\rm S}(q^2))\right)\right\},\end{aligned} \tag{3.59}$$

$$\mathcal{G}_{N_1,N_2}(\alpha_{\rm S}(\mu_R^2),L) = -\int_{b_0^2/b^2}^{Q^2}\frac{dq^2}{q^2}\left[A(\alpha_{\rm S}(q^2))\ln\frac{M^2}{q^2}+\frac{1}{2}\left(\widetilde{B}_{N_1}(\alpha_{\rm S}(q^2))+\widetilde{B}_{N_1}(\alpha_{\rm S}(q^2))\right)\right]. \tag{3.60}$$

The functions $\widetilde{B}_{N_i}(\alpha_{\rm S})$ are related to the function $B_c(\alpha_{\rm S})$ entering the Sudakov form factor in Eq. (3.31) and to the collinear functions $C_{N_i}(\alpha_{\rm S})$ by the following equation

$$\widetilde{B}_N(\alpha_{\rm S}) = B(\alpha_{\rm S}) + 2\beta(\alpha_{\rm S})\,\frac{d\ln C_N(\alpha_{\rm S})}{d\ln\alpha_{\rm S}} + 2\gamma_N(\alpha_{\rm S}) = \sum_{n=1}^{\infty}\left(\frac{\alpha_{\rm S}}{\pi}\right)^n \widetilde{B}^{(n)}_{c,\,N}\,. \tag{3.61}$$

The first-order coefficient $\widetilde{B}^{(1)}_{c,\,N}$ of the universal function $\widetilde{B}_N(\alpha_{\rm S})$ is

$$\widetilde{B}^{(1)}_{c,\,N} = B^{(1)}_c + 2\gamma_{cc,\,N}\,, \tag{3.62}$$

where the coefficients $B^{(1)}_c$ are resummation scheme independent and are [75, 80]

$$B^{(1)}_q = B^{(1)}_{\bar{q}} = -\frac{3}{2}C_F\,, \qquad B^{(1)}_g = -\frac{1}{6}(11C_A - 2N_f)\,. \tag{3.63}$$

The universal second-order coefficient $\widetilde{B}^{(2)}_{c,\,N}$ is given by

$$\widetilde{B}^{(2)}_{c,\,N} = B^{(2)}_c - 2\beta_0\; C^{(1)}_{cc,\,N} + 2\gamma^{(2)}_{cc,\,N}\,. \tag{3.64}$$

The coefficient $B^{(2)}_c$ is resummation scheme dependent and in the hard scheme it reads [128]

$$B^{(2)}_c = \frac{\gamma^{(1)}_c}{16} + \pi\beta_0 C_c\zeta_2\,, \tag{3.65}$$

where $\zeta_2 = \pi^2/6$, $C_c = C_F$ for the quarks ($c = q, \bar{q}$) and $C_c = C_A$ for the gluon ($c = g$).

The universal perturbative function $A(\alpha_{\rm S})$ in Eq. (3.60) is the same function that enters the Sudakov form factor in Eq. (3.31). The first two coefficients $A^{(1)}_c$ and $A^{(2)}_c$ are given by

$$A^{(1)}_c = C_c\,, \qquad A^{(2)}_c = \frac{1}{2}C_c\left[\left(\frac{67}{18}-\frac{\pi^2}{6}C_A\right)-\frac{5}{9}N_f\right]. \tag{3.66}$$

We note that the relation (3.61) implies that both the form factor $\exp\{\mathcal{G}\}$ and the non-logarithmic function $\mathcal{H}$ in Eq. (3.59) do not depend on the resummation scheme used to express the various factors in the resummation formulae (3.30) and (3.31) (we recall that the customary Sudakov form factor $S_c(M, b)$ in Eq. (3.31) does instead depend on the resummation scheme).

To complete the resummation procedure we need to compute the coefficients $g_N^{(n)}$ in Eq. (3.28). To this purpose let us rewrite Eq. (3.60) in the following way:

$$\mathcal{G}_N(\alpha_{\rm S}(\mu_R^2), L) = -\int_{b_0^2/b^2}^{Q^2} \frac{dq^2}{q^2} \left[A(\alpha_{\rm S}(q^2)) \int_{q^2}^{M^2} \frac{d\mu^2}{\mu^2} + \widetilde{B}_N(\alpha_{\rm S}(q^2)) \right] . \tag{3.67}$$

Next, we use the renormalisation group equation (2.26) to change the integration variables $\{q^2, \mu^2\}$ to $\{\alpha = \alpha_{\rm S}(q^2)\,, \alpha' = \alpha_{\rm S}(\mu^2)\}$. Eq. (3.67) becomes

$$\mathcal{G}_N(\alpha_{\rm S}(\mu_R^2), L) = -\int_{\alpha_{\rm S}(b_0^2/b^2)}^{\alpha_{\rm S}(Q^2)} \frac{d\alpha}{\alpha} \frac{1}{\beta(\alpha)} \left[A(\alpha) \int_{\alpha}^{\alpha_{\rm S}(M^2)} \frac{d\alpha'}{\alpha'} \frac{1}{\beta(\alpha')} + \widetilde{B}_N(\alpha) \right] . \tag{3.68}$$

Truncating the expansion of the integrands (see Eqs. (2.26), (3.32) and (3.61)) to the required accuracy and computing the integrals, one obtains a result in terms of elementary functions of the perturbative coefficients $A^{(n)}$, $\widetilde{B}^{(n)}$, β_n and $\alpha_{\rm S}(k^2)$ with $k^2 = Q^2$, M^2, b_0^2/b^2. Using the RG equation (2.26), $\alpha_{\rm S}(k^2)$ then can be expressed in terms of $\alpha_{\rm S}(\mu_R^2)$ and $\ln(k^2/\mu_R^2)$. Comparing the final result with the left-hand side of Eq. (3.28), one finally obtains the resummation coefficients $g_N^{(n)}$. The LL $g_N^{(1)}$, NLL $g_N^{(2)}$ and NNLL $g_N^{(3)}$ coefficients are computed in [82, 134] and read

$$g^{(1)}(\alpha_{\rm S} L) = \frac{A^{(1)}}{\beta_0} \frac{\lambda + \ln(1-\lambda)}{\lambda} \quad , \tag{3.69}$$

$$\begin{aligned} g_N^{(2)}(\alpha_{\rm S} L) = {} & \frac{\overline{B}_N^{(1)}}{\beta_0} \ln(1-\lambda) - \frac{A^{(2)}}{\beta_0^2} \left(\frac{\lambda}{1-\lambda} + \ln(1-\lambda) \right) \\ & + \frac{A^{(1)}}{\beta_0} \left(\frac{\lambda}{1-\lambda} + \ln(1-\lambda) \right) \ln \frac{Q^2}{\mu_R^2} \\ & + \frac{A^{(1)} \beta_1}{\beta_0^3} \left(\frac{1}{2} \ln^2(1-\lambda) + \frac{\ln(1-\lambda)}{1-\lambda} + \frac{\lambda}{1-\lambda} \right) , \end{aligned} \tag{3.70}$$

$$
\begin{aligned}
g_N^{(3)}(\alpha_{\rm S}L) = &-\frac{A^{(3)}}{2\beta_0^2}\frac{\lambda^2}{(1-\lambda)^2} - \frac{\overline{B}_N^{(2)}}{\beta_0}\frac{\lambda}{1-\lambda} + \frac{A^{(2)}\beta_1}{\beta_0^3}\left(\frac{\lambda(3\lambda-2)}{2(1-\lambda)^2} - \frac{(1-2\lambda)\ln(1-\lambda)}{(1-\lambda)^2}\right) \\
&+ \frac{\overline{B}_N^{(1)}\beta_1}{\beta_0^2}\left(\frac{\lambda}{1-\lambda} + \frac{\ln(1-\lambda)}{1-\lambda}\right) - \frac{A^{(1)}}{2}\frac{\lambda^2}{(1-\lambda)^2}\ln^2\frac{Q^2}{\mu_R^2} \\
&+ \ln\frac{Q^2}{\mu_R^2}\left(\overline{B}_N^{(1)}\frac{\lambda}{1-\lambda} + \frac{A^{(2)}}{\beta_0}\frac{\lambda^2}{(1-\lambda)^2} + A^{(1)}\frac{\beta_1}{\beta_0^2}\left(\frac{\lambda}{1-\lambda} + \frac{1-2\lambda}{(1-\lambda)^2}\ln(1-\lambda)\right)\right) \\
&+ A^{(1)}\left(\frac{\beta_1^2}{2\beta_0^4}\frac{1-2\lambda}{(1-\lambda)^2}\ln^2(1-\lambda) + \ln(1-\lambda)\left[\frac{\beta_0\beta_2-\beta_1^2}{\beta_0^4} + \frac{\beta_1^2}{\beta_0^4(1-\lambda)}\right]\right. \\
&\left. + \frac{\lambda}{2\beta_0^4(1-\lambda)^2}(\beta_0\beta_2(2-3\lambda)+\beta_1^2\lambda)\right)\,, \qquad (3.71)
\end{aligned}
$$

where

$$\lambda = \frac{1}{\pi}\,\beta_0\,\alpha_{\rm S}(\mu_R^2)\,L\,, \qquad (3.72)$$

$$\overline{B}^{(n)} = \widetilde{B}^{(n)} + A^{(n)}\ln\frac{M^2}{Q^2}\,, \qquad (3.73)$$

and the dependence on the ratios M^2/μ_R^2, M^2/Q^2 on the left-hand sides of Eqs (3.70) and (3.71) is understood.

3.3 The finite component

As we have discussed in Section 3.2 the finite component of the partonic multidifferential cross section $d\hat{\sigma}^{\rm reg.}_{a_1a_2\to F}$ is computed at a given fixed order in $\alpha_{\rm S}$ according to Eq. (3.13). Moreover, by definition, the finite component $d\hat{\sigma}^{\rm reg.}_{a_1a_2\to F}$ does not contain any perturbative contributions proportional to $\delta(q_T^2)$ (these contributions and all the logarithmically-enhanced terms at small q_T are included in $d\hat{\sigma}^{\rm sing.}_{a_1a_2\to F}$. Therefore, when computing $\left[d\hat{\sigma}^{\rm reg.}_{a_1a_2\to F}\right]_{\rm f.o.}$ according to the subtraction procedure in Eq. (3.11), we can consistently neglect any terms proportional to $\delta(q_T^2)$ both in $\left[d\hat{\sigma}_{a_1a_2\to F}\right]_{\rm f.o.}$ and in $\left[d\hat{\sigma}^{\rm sing.}_{a_1a_2\to F}\right]_{\rm f.o.}$. This is formally equivalent to the evaluation of both contributions in the region where $q_T \neq 0$. In the case of $\left[d\hat{\sigma}_{a_1a_2\to F}\right]_{\rm f.o.}$ the last statement is equivalent to considering the differential cross section for the F + jet process. The expansions of $\left[d\hat{\sigma}^{\rm reg.}_{a_1a_2\to F}\right]_{\rm f.o.}$ at the first and at the second perturbative order thus give

$$\left[\frac{d\hat{\sigma}^{\rm reg.}_{a_1a_2\to F}}{dq_T^2\,dz_1\,dz_2\,d\boldsymbol{\Omega}}\right]_{\rm NLO} = \left[\frac{d\hat{\sigma}_{a_1a_2\to F+\rm jet}}{dq_T^2\,dz_1\,dz_2\,d\boldsymbol{\Omega}}\right]_{\rm LO} - \left[\frac{d\hat{\sigma}^{\rm sing.}_{a_1a_2\to F}}{dq_T^2\,dz_1\,dz_2\,d\boldsymbol{\Omega}}\right]_{\rm NLO}\,, \qquad (3.74)$$

$$\left[\frac{d\hat{\sigma}^{\rm reg.}_{a_1a_2\to F}}{dq_T^2\,dz_1\,dz_2\,d\boldsymbol{\Omega}}\right]_{\rm NNLO} = \left[\frac{d\hat{\sigma}_{a_1a_2\to F+\rm jet}}{dq_T^2\,dz_1\,dz_2\,d\boldsymbol{\Omega}}\right]_{\rm NLO} - \left[\frac{d\hat{\sigma}^{\rm sing.}_{a_1a_2\to F}}{dq_T^2\,dz_1\,dz_2\,d\boldsymbol{\Omega}}\right]_{\rm NNLO}\,, \qquad (3.75)$$

where the subscript LO (NLO) denotes the perturbative truncation of the various cross sections at the leading order (next-to-leading order) in the region where $q_T \neq 0$.

The fixed order truncation $[d\hat{\sigma}^{\text{sing.}}]_{\text{f.o}}$ of the singular component is obtained by the perturbative expansion of the singular component $d\hat{\sigma}^{\text{sing.}}$ in Eq. (3.18). To this purpose, we write the partonic resummation factor $\mathcal{W}^F_{a_1,\,a_2}$ on the right-hand side of Eq. (3.18) as follows:

$$\begin{aligned}\mathcal{W}^F_{a_1a_2}(\hat{s};b,M,\mathbf{\Omega};\alpha_{\text{S}},\mu_R^2,\mu_F^2,Q^2) \;&=\sum_c \left[d\sigma^{(0)}_{c\bar{c},\,F}\right]\Bigg\{\delta_{ca_1}\delta_{ca_2}\;\delta(1-z_1)\;\delta(1-z_2) \\ &+\sum_{n=1}^{\infty}\left(\frac{\alpha_{\text{S}}}{\pi}\right)^n\Bigg[\widetilde{\Sigma}^{F\,(n)}_{c\bar{c}\leftarrow a_1a_2}\left(z_1,z_2,\widetilde{L};\frac{M^2}{\mu_R^2},\frac{M^2}{\mu_F^2},\frac{M^2}{Q^2}\right) \\ &+\mathcal{H}^{F\,(n)}_{c\bar{c}\leftarrow a_1a_2}\left(z_1,z_2;\frac{M^2}{\mu_R^2},\frac{M^2}{\mu_F^2},\frac{M^2}{Q^2}\right)\Bigg]\Bigg\}\,,\end{aligned} \tag{3.76}$$

where $\alpha_{\text{S}}=\alpha_{\text{S}}(\mu_R^2)$. The first $\widetilde{\Sigma}^{F\,(1)}_{c\bar{c}\leftarrow a_1a_2}$ and second-order $\widetilde{\Sigma}^{F\,(2)}_{c\bar{c}\leftarrow a_1a_2}$ coefficients are polynomials of $\widetilde{L}$

$$\widetilde{\Sigma}^{F\,(1)}_{c\bar{c}\leftarrow a_1a_2}(z_1,z_2,\widetilde{L})=\sum_{p=1}^{2}\widetilde{\Sigma}^{F\,(1;n)}_{c\bar{c}\leftarrow a_1a_2}(z_1,z_2)\;\widetilde{L}^n\,, \tag{3.77}$$

$$\widetilde{\Sigma}^{F\,(1)}_{c\bar{c}\leftarrow a_1a_2}(z_1,z_2,\widetilde{L})=\sum_{p=1}^{4}\widetilde{\Sigma}^{F\,(2;n)}_{c\bar{c}\leftarrow a_1a_2}(z_1,z_2)\;\widetilde{L}^n\,, \tag{3.78}$$

where the coefficients $\widetilde{\Sigma}^{F\,(1;p)}_{c\bar{c}\leftarrow a_1a_2}$ $(p=1,2)$ and $\widetilde{\Sigma}^{F\,(2;p)}_{c\bar{c}\leftarrow a_1a_2}$ $(k=p,\ldots,4$ do not depend on the impact parameter b, and thus the Bessel transformation in Eq. (3.18) acts only on the powers of the modified large logarithms $\widetilde{L}^n$

$$Q^2\int_0^\infty db\;\frac{b}{2}\;J_0(bq_T)\;\ln^n\left(\frac{Q^2b^2}{b_0^2}+1\right)=\widetilde{I}_n(q_T/Q)\,. \tag{3.79}$$

The functions $\widetilde{I}_n(q_T/Q)$ are computed in Ref. [82].

The NLO coefficients $\widetilde{\Sigma}^{F\,(1;p)}(z_1,z_2)$, $\mathcal{H}^{F\,(1)}(z_1,z_2)$ and the NNLO coefficients $\widetilde{\Sigma}^{F\,(2;p)}(z_1,z_2)$, $\mathcal{H}^{F\,(2)}(z_1,z_2)$ have a simpler form in the Mellin space and are presented below:

$$\Sigma^{F\,(1;2)}_{c\bar{c}\leftarrow a_1a_2,\,(N_1,N_2)}=-\frac{1}{2}A_c^{(1)}\;\delta_{ca_1}\delta_{\bar{c}a_2}\;, \tag{3.80}$$

$$\Sigma^{F\,(1;1)}_{c\bar{c}\leftarrow a_1a_2,\,(N_1,N_2)}=-\left[\delta_{ca_1}\delta_{\bar{c}a_2}\;\left(B_c^{(1)}+A_c^{(1)}\,\ell_Q\right)+\delta_{ca_1}\gamma^{(1)}_{\bar{c}a_2,\,N_2}+\delta_{\bar{c}a_2}\gamma^{(1)}_{ca_1,\,N_1}\right]\;, \tag{3.81}$$

$$\begin{aligned}\mathcal{H}^{F\,(1)}_{c\bar{c}\leftarrow a_1a_2,\,(N_1,N_2)}=&\delta_{ca_1}\delta_{\bar{c}a_2}\left[H_c^{F\,(1)}-\left(B_c^{(1)}+\frac{1}{2}A_c^{(1)}\ell_Q\right)\ell_Q-k\beta_0\ell_R\right] \\ &+\delta_{ca_1}C^{(1)}_{\bar{c}a_2,\,N_2}+\delta_{\bar{c}a_2}C^{(1)}_{ca_1,\,N_1}+\left(\delta_{ca_1}\gamma^{(1)}_{\bar{c}a_2,\,N_2}+\delta_{\bar{c}a_2}\gamma^{(1)}_{ca_1,\,N_1}\right)(\ell_F-\ell_Q)\;,\end{aligned} \tag{3.82}$$

$$\Sigma^{F\,(2;4)}_{c\bar{c}\leftarrow a_1 a_2,\,(N_1,N_2)} = \frac{1}{8}\left(A_c^{(1)}\right)^2\,\delta_{ca_1}\delta_{\bar{c}a_2}\;, \tag{3.83}$$

$$\Sigma^{F\,(2;3)}_{c\bar{c}\leftarrow a_1 a_2,\,(N_1,N_2)} = -\,A_c^{(1)}\left[\frac{1}{3}\,\beta_0\,\delta_{ca_1}\delta_{\bar{c}a_2} + \frac{1}{2}\,\Sigma^{F\,(1;1)}_{c\bar{c}\leftarrow a_1 a_2,\,(N_1,N_2)}\right]\;, \tag{3.84}$$

$$\begin{aligned}\Sigma^{F\,(2;2)}_{c\bar{c}\leftarrow a_1 a_2,\,(N_1,N_2)} = &-\frac{1}{2}\,A_c^{(1)}\left[\mathcal{H}^{F\,(1)}_{c\bar{c}\leftarrow a_1 a_2,\,(N_1,N_2)} - \beta_0\,\delta_{ca_1}\delta_{\bar{c}a_2}\,(\ell_R-\ell_Q)\right]\\ &-\frac{1}{2}\sum_{b_1,b_2}\Sigma^{F\,(1;1)}_{c\bar{c}\leftarrow a_1 a_2,\,(N_1,N_2)}\left[\delta_{b_1 a_1}\gamma^{(1)}_{b_2 a_2,\,N_2} + \delta_{b_2 a_2}\gamma^{(1)}_{b_1 a_1,\,N_1}\right]\\ &-\frac{1}{2}\left[A_c^{(2)}\,\delta_{ca_1}\delta_{\bar{c}a_2} + \left(B_c^{(1)} + A_c^{(1)}\,\ell_Q - \beta_0\right)\Sigma^{F\,(1;1)}_{c\bar{c}\leftarrow a_1 a_2,\,(N_1,N_2)}\right]\;,\end{aligned} \tag{3.85}$$

$$\begin{aligned}\Sigma^{F\,(2;1)}_{c\bar{c}\leftarrow a_1 a_2,\,(N_1,N_2)} = &\;\Sigma^{F\,(1;1)}_{c\bar{c}\leftarrow a_1 a_2,\,(N_1,N_2)}\,\beta_0\,(\ell_Q-\ell_R)\\ &-\sum_{b_1,b_2}\mathcal{H}^{F\,(1)}_{c\bar{c}\leftarrow b_1 b_2,\,(N_1,N_2)}\left[\delta_{b_1 a_1}\delta_{b_2 a_2}\left(B_c^{(1)} + A_c^{(1)}\,\ell_Q\right) + \delta_{b_1 a_1}\gamma^{(1)}_{b_2 a_2,\,N_2} + \delta_{b_2 a_2}\gamma^{(1)}_{b_1 a_1,\,N_1}\right]\\ &-\left[\delta_{ca_1}\delta_{\bar{c}a_2}\,\left(B_c^{(2)} + A_c^{(2)}\,\ell_Q\right) - \beta_0\left(\delta_{ca_1}C^{(1)}_{\bar{c}a_2,\,N_2} + \delta_{\bar{c}a_2}C^{(1)}_{ca_1,\,N_1}\right) + \delta_{ca_1}\gamma^{(2)}_{\bar{c}a_2,\,N_2} + \delta_{\bar{c}a_2}\gamma^{(2)}_{ca_1,\,N_1}\right]\;,\end{aligned} \tag{3.86}$$

$$\begin{aligned}\mathcal{H}^{F\,(2)}_{c\bar{c}\leftarrow a_1 a_2,\,(N_1,N_2)} = &\;\delta_{ca_1}\delta_{\bar{c}a_2}\,H_c^{F\,(2)} + \delta_{ca_1}\,C^{(2)}_{\bar{c}a_2,\,N_2} + \delta_{\bar{c}a_2}\,C^{(2)}_{ca_1,\,N_1} + C^{(1)}_{ca_1,\,N_1}\,C^{(1)}_{\bar{c}a_2,\,N_2}\\ &+H_c^{F\,(1)}\left(\delta_{ca_1}\,C^{(1)}_{\bar{c}a_2,\,N_2} + \delta_{\bar{c}a_2}\,C^{(1)}_{ca_1,\,N_1}\right) + \frac{1}{6}\,A_c^{(1)}\,\beta_0\,\ell_Q^3\,\delta_{ca_1}\delta_{\bar{c}a_2}\\ &+\frac{1}{2}\left[A_c^{(2)}\,\delta_{ca_1}\delta_{\bar{c}a_2} + \beta_0\,\Sigma^{F\,(1;1)}_{c\bar{c}\leftarrow a_1 a_2,\,(N_1,N_2)}\right]\ell_Q^2\\ &-\left[\delta_{ca_1}\delta_{\bar{c}a_2}\,\left(B_c^{(2)} + A_c^{(2)}\,\ell_Q\right) - \beta_0\left(\delta_{ca_1}C^{(1)}_{\bar{c}a_2,\,N_2} + \delta_{\bar{c}a_2}C^{(1)}_{ca_1,\,N_1}\right) + \delta_{ca_1}\gamma^{(2)}_{\bar{c}a_2,\,N_2} + \delta_{\bar{c}a_2}\gamma^{(2)}_{ca_1,\,N_1}\right]\ell_Q\\ &+\frac{1}{2}\,\beta_0\,\left(\delta_{ca_1}\gamma^{(1)}_{\bar{c}a_2,\,N_2} + \delta_{\bar{c}a_2}\gamma^{(1)}_{ca_1,\,N_1}\right)\ell_F^2 + \left(\delta_{ca_1}\gamma^{(2)}_{\bar{c}a_2,\,N_2} + \delta_{\bar{c}a_2}\gamma^{(2)}_{ca_1,\,N_1}\right)\ell_F - \mathcal{H}^{F\,(1)}_{c\bar{c}\leftarrow a_1 a_2,\,(N_1,N_2)}\,\beta_0\ell_R\\ &+\frac{1}{2}\sum_{b_1,b_2}\left[\mathcal{H}^{F\,(1)}_{c\bar{c}\leftarrow b_1 b_2,\,(N_1,N_2)} + \delta_{cb_1}\delta_{\bar{c}b_2}\,H_c^{F\,(1)} + \delta_{cb_1}\,C^{(1)}_{\bar{c}b_2,\,N_2} + \delta_{\bar{c}b_2}\,C^{(1)}_{cb_1,\,N_1}\right]\\ &\times\left[\left(\delta_{b_1 a_1}\gamma^{(1)}_{b_2 a_2,\,N_2} + \delta_{b_2 a_2}\gamma^{(1)}_{b_1 a_1,\,N_1}\right)(\ell_F-\ell_Q) - \delta_{b_1 a_1}\delta_{b_2 a_2}\left(\left(B_c^{(1)} + \frac{1}{2}\,A_c^{(1)}\,\ell_Q\right)\ell_Q + k\,\beta_0\,\ell_R\right)\right]\\ &-\delta_{ca_1}\delta_{\bar{c}a_2}\,k\left(\frac{1}{2}\,\beta_0^2\,\ell_R^2 + \beta_1\,\ell_R\right)\;,\end{aligned} \tag{3.87}$$

where

$$\ell_R = \ln\frac{M^2}{\mu_R^2}\,,\qquad \ell_F = \ln\frac{M^2}{\mu_F^2}\,,\qquad \ell_Q = \ln\frac{M^2}{Q^2}\,, \tag{3.88}$$

and corresponding dependences on the ratios M^2/μ_R^2, M^2/μ_F^2 and M^2/Q^2 on the left-hand sides of Eqs. (3.80)–(3.87) are understood.

Inserting Eqs. (3.76)–(3.78) in Eq. (3.18), performing the integral over the impact parameter b, and removing the contributions proportional to $\delta(q_T^2)$ (for example, all the contributions coming from $\mathcal{H}^{F\,(n)}_{c\bar{c}\leftarrow ab}$ in Eq. (3.76)), we obtain the following expressions for the fixed-order contributions $\left[d\hat{\sigma}^{\text{sing.}}_{a_1a_2\to F}\right]_{\text{f.o.}}$ on the right-hand side of Eqs. (3.74) and (3.75):

$$\left[\frac{d\hat{\sigma}^{\text{sing.}}_{a_1a_2\to F}}{dq_T^2\,dz_1\,dz_2\,d\boldsymbol{\Omega}}(q_T,M,\hat{s},z_1,z_2,\boldsymbol{\Omega};\alpha_{\text{S}}(\mu_R^2))\right]_{\text{NLO}} = \frac{\alpha_{\text{S}}(\mu_R^2)}{\pi}\,\frac{z_1z_2}{Q^2}\,\sum_c\left[d\sigma^{(0)}_{c\bar{c},\,F}\right] \times\left[\Sigma^{F\,(1;2)}_{c\bar{c}\leftarrow a_1a_2}(z_1,z_2)\,\widetilde{I}_2(q_T/Q)+\Sigma^{F\,(1;1)}_{c\bar{c}\leftarrow a_1a_2}(z_1,z_2)\,\widetilde{I}_1(q_T/Q)\right]. \tag{3.89}$$

$$\left[\frac{d\hat{\sigma}^{\text{sing.}}_{a_1a_2\to F}}{dq_T^2\,dz_1\,dz_2\,d\boldsymbol{\Omega}}(q_T,M,\hat{s},z_1,z_2,\boldsymbol{\Omega};\alpha_{\text{S}}(\mu_R^2))\right]_{\text{NNLO}} = \left[\frac{d\hat{\sigma}^{\text{sing.}}_{a_1a_2\to F}}{dq_T^2\,dz_1\,dz_2\,d\boldsymbol{\Omega}}(q_T,M,\hat{s},z_1,z_2,\boldsymbol{\Omega};\alpha_{\text{S}}(\mu_R^2))\right]_{\text{NLO}} + \left(\frac{\alpha_{\text{S}}(\mu_R^2)}{\pi}\right)^2\,\frac{z_1z_2}{Q^2}\,\sum_c\left[d\sigma^{(0)}_{c\bar{c},\,F}\right]\sum_{k=1}^{4}\Sigma^{F\,(2;k)}_{c\bar{c}\leftarrow a_1a_2}(z_1,z_2)\,\widetilde{I}_k(q_T/Q)\,, \tag{3.90}$$

The finite component of the partonic cross section $d\hat{\sigma}^{\text{reg.}}_{a_1a_2\to F+X}$ at N(NLO) accuracy is then computed according to Eqs. (3.74) and (3.75).

3.4 Transverse-momentum resummation in gluon fusion processes

The resummation formula presented in Section 3.2 was originally proposed and proved for the DY process [70–79], which is mediated by the $q\bar{q}$ annihilation at the lowest order. The resummation structure that emerges in the DY process was than applied to other processes of the class in Eq. (3.2), including also processes which are controlled by the gluon fusion (or also by the gluon fusion) at LO, such as, for example, the production of the SM Higgs boson [82, 135–138]. Later works, however (see e.g. Refs. [69, 139]), showed that the transverse-momentum resummation in the gluon fusion channel has a richer structure, due to spin-correlated collinear splitting functions.

Throughout this section we follow the discussion of Ref [69] and outline the structure of gg-specific contributions to the resummed cross section. To this end, we separate the contributions from $q\bar{q}$ annihilation and gluon fusion subprocesses to the resummed cross section, and we write

$$[d\sigma_F] = [d\sigma_F]^{(q\bar{q}-\text{ann.})} + [d\sigma_F]^{(g-\text{fus.})}\,. \tag{3.91}$$

The all-order resummation formula for the gluon fusion processes can be formallly written

in the same way as in Eqs. (3.29) and (3.30)

$$[d\sigma_F]^{(g-\text{fus.})} = \frac{M^2}{s}\left[d\sigma^{(0)}_{gg,\,F}\right]\int\frac{d^2\mathbf{b}}{(2\pi)^2}\,e^{i\mathbf{b}\cdot\mathbf{q_T}}\,S_g(M,b)$$
$$\times\sum_{a_1,a_2}\int_{x_1}^1\frac{dz_1}{z_1}\int_{x_2}^1\frac{dz_2}{z_2}\left[H^F C_1 C_2\right]_{gg;a_1a_2} f_{a_1/h_1}(x_1/z_1,b_0^2/b^2)\;f_{a_2/h_2}(x_2/z_2,b_0^2/b^2)\,, \quad (3.92)$$

where the lowest-order cross section $\left[d\sigma^{(0)}_{gg,\,F}\right]$ and the gluon Sudakov form factor $S_g(M,b)$ are given in Eqs. (3.23) and (3.31). The difference between the resummation formulae for the $q\bar{q}$ annihilation and the gluon fusion is embodied in the gluon fusion factor $\left[H^F C_1 C_2\right]_{gg;a_1a_2}$. In particular, the naive expression on the right-hand side of Eq. (3.34) has to be replaced by the following result:

$$\left[H^F C_1 C_2\right]_{gg;a_1a_2} = H^F_{g;\,\mu_1\,\nu_1,\mu_2\,\nu_2}(p_1,p_2;\mathbf{\Omega};\alpha_{\rm S}(M^2))$$
$$\times\;C^{\mu_1\,\nu_1}_{g\,a_1}(z_1;p_1,p_2,\mathbf{b};\alpha_{\rm S}(b_0^2/b^2))\,C^{\mu_2\,\nu_2}_{g\,a_2}(z_2;p_1,p_2,\mathbf{b};\alpha_{\rm S}(b_0^2/b^2))\,. \quad (3.93)$$

In contrast to the case of $q\bar{q}$ annihilation, both the hard-virtual H_g^F and the collinear $C_{g\,a}$ functions entering Eq. (3.93) are Lorentz tensors. Moreover, the collinear functions $C^{\mu\,\nu}_{g\,a}$ not only depend on the absolute value b of the impact parameter through the scale of $\alpha_{\rm S}$, but admit an explicit dependence on the two-dimensional vector $\mathbf{b}$. These two features of Eq. (3.93) are unique of transverse-momentum resummation in gluon fusion processes and they have definitive physical origin, coming from the spin- and q_T-dependent gluon collinear splitting kernels in Eqs. (2.53) and (2.54). More precisely, the collinear functions $C^{\mu\,\nu}_{g\,a}$ are the Fourier transforms of these splitting kernels, and can be written as

$$C^{\mu\,\nu}_{g\,a}(z;p_1,p_2,\mathbf{b};\alpha_{\rm S}) = d^{\,\mu\,\nu}(p_1,p_2)\;C_{g\,a}(z;\alpha_{\rm S}) + D^{\,\mu\,\nu}(p_1,p_2;\mathbf{b})\;G_{g\,a}(z;\alpha_{\rm S})\,, \quad (3.94)$$

where the two tensors $d^{\,\mu\,\nu}$ and $D^{\,\mu\,\nu}$ are

$$d^{\,\mu\,\nu}(p_1,p_2) = -g^{\mu\,\nu} + \frac{p_1^\mu p_2^\nu + p_1^\nu p_2^\mu}{p_1\cdot p_2}\,, \quad (3.95)$$

$$D^{\,\mu\,\nu}(p_1,p_2;\mathbf{b}) = d^{\,\mu\,\nu}(p_1,p_2) - 2\,\frac{b^\mu\,b^\nu}{\mathbf{b}^2}\,, \quad (3.96)$$

with $\mathbf{b}^2 = -b^\mu b_\mu$, where $b^\mu = (0,\mathbf{b},0)$ is the impact parameter vector in the four-dimensional notation.

The gluonic coefficient function $C_{g\,a}(z;\alpha_{\rm S})$ has the same perturbative structure as in Eq. (3.36), while the perturbative expansion of the coefficient functions G_{ga} starts at $\mathcal{O}(\alpha_{\rm S})$ and it reads

$$G_{ga}(z;\alpha_{\rm S}) = \sum_{n=1}^{\infty}\left(\frac{\alpha_{\rm S}}{\pi}\right)^n G^{(n)}_{ga}(z)\,. \quad (3.97)$$

The first-order coefficients $G_{gg}^{(1)}(z)$ and $G_{gq}^{(1)}(z)$ differ only by the colour factor. Explicitly [69]

$$G_{gg}^{(1)}(z) = C_A \, \frac{1-z}{z} \,, \tag{3.98}$$

$$G_{gq}^{(1)}(z) = G_{g\bar{q}}^{(1)}(z) = C_F \, \frac{1-z}{z} \,. \tag{3.99}$$

The hard-virtual function H_g^F has the following expression

$$H^F_{g;\,\mu_1\,\nu_1,\mu_2\,\nu_2}(p_1,p_2;\mathbf{\Omega};\alpha_{\rm S}) = d^{\,\mu_1}_{\mu_1'}\, d^{\,\nu_1}_{\nu_1'}\, d^{\,\mu_2}_{\mu_2'}\, d^{\,\nu_2}_{\nu_2'}\, \frac{\left[\widetilde{\mathcal{M}}^{\mu_1'\,\mu_2'}_{gg\to F}(p_1,p_2;\{q_i\})\right]^\dagger \;\widetilde{\mathcal{M}}^{\nu_1'\,\nu_2'}_{gg\to F}(p_1,p_2;\{q_i\})}{\alpha_{\rm S}^{2k}\,|\mathcal{M}^{(0)}_{gg\to F}(p_1,p_2;\{q_i\})|^2} \tag{3.100}$$

and retains the following perturbative expansion:

$$\begin{aligned} H^F_{g;\,\mu_1\,\nu_1,\mu_2\,\nu_2}(p_1,p_2;\mathbf{\Omega};\alpha_{\rm S}) &= H^{F\,(0)}_{g;\,\mu_1\,\nu_1,\mu_2\,\nu_2}(p_1,p_2;\mathbf{\Omega}) \\ &\quad + \sum_{n=1}^{\infty} \left(\frac{\alpha_{\rm S}}{\pi}\right)^n H^{F\,(n)}_{g;\,\mu_1\,\nu_1,\mu_2\,\nu_2}(p_1,p_2;\mathbf{\Omega}) \,, \end{aligned} \tag{3.101}$$

with the lowest-order normalisation

$$H^{F\,(0)}_{g;\,\mu_1\,\nu_1,\mu_2\,\nu_2}\, g^{\mu_1\,\nu_1}\, g^{\mu_2\,\nu_2} = 1 \,. \tag{3.102}$$

3.4.1 Azimuthal correlations of the q_T cross section

The factorisation structure of Eq. (3.93) is due to quantum-mechanical interference between scattering amplitudes and their complex conjugates and has special physical effects. In particular, due to explicit dependence of the tensor $D^{\,\mu\,\nu}$ on the azimuthal angle $\phi(\mathbf{b})$ of the impact parameter vector $\mathbf{b}$, the differential cross section $d\sigma^F$ features *spin* and *azimuthal* correlations in $\mathbf{q_T}$, which are enhanced at small values of q_T. As a result, in the resummation formula (3.92) we cannot simply use Eq. (3.16) to perform the azimuthal integration over $\phi(\mathbf{b})$. However, as it has been shown in Ref. [69], the dependence of $\Big[H^F C_1 C_2\Big]_{gg;a_1a_2}$ on the azimuthal angle $\phi(\mathbf{b})$, which is given by the tensor $D^{\,\mu\,\nu}(p_1,p_2;\mathbf{b})$ in Eq. (3.96), is sufficiently simple and the integration over $\phi(\mathbf{b})$ can be still explicitly performed, allowing again to replace the two-dimensional Fourier transformation by one-dimensional transformations. Considering the Fourier transformation of contributions that are linear and quadratic with respect to the tensor $D^{\,\mu\,\nu}(p_1,p_2;\mathbf{b})$, we get [69]

$$\int \frac{d^2\mathbf{b}}{2\pi}\; e^{i\mathbf{b}\cdot\mathbf{q_T}}\; D^{\,\mu\nu}(p_1,p_2;\mathbf{b})\;\; F(\mathbf{b}^2) = -\; D^{\,\mu\nu}(p_1,p_2;\mathbf{q_T}) \int_0^{+\infty} db\; b\; J_2(bq_T)\;\; F(b^2) \;\;, \tag{3.103}$$

$$\int \frac{d^2\mathbf{b}}{2\pi}\; e^{i\mathbf{b}\cdot\mathbf{q_T}}\; D^{\,\mu_1\nu_1}(p_1,p_2;\mathbf{b})\; D^{\,\mu_2\nu_2}(p_1,p_2;\mathbf{b})\;\; F(\mathbf{b}^2)$$
$$= \;\; d_{(4)}^{\mu_1\,\nu_1,\,\mu_2\,\nu_2}(p_1,p_2)\;\int_0^{+\infty} db\; b\; J_0(bq_T)\;\; F(b^2)$$
$$+ \quad D_{(4)}^{\mu_1\,\nu_1,\,\mu_2\,\nu_2}(p_1,p_2;\mathbf{q_T})\;\int_0^{+\infty} db\; b\; J_4(bq_T)\;\; F(b^2)\;\;, \tag{3.104}$$

where $d_{(4)}^{\mu_1\,\nu_1,\,\mu_2\,\nu_2}$ is given by

$$d_{(4)}^{\mu_1\,\nu_1\,\mu_2\,\nu_2}(p_1,p_2) = \frac{1}{2}\left[d^{\mu_1\,\mu_2}\; d^{\nu_1\,\nu_2} + d^{\mu_1\,\nu_2}\; d^{\mu_2\,\nu_1} + d^{\mu_1\,\nu_1}\; d^{\mu_2\,\nu_2}\right]\;, \tag{3.105}$$

with $d^{\mu\nu} = d^{\mu\nu}(p_2,p_2)$ of Eq. (3.95), and the 4th-rank tensor $D_{(4)}^{\mu_1\,\nu_1,\,\mu_2\,\nu_2}$ is

$$D_{(4)}^{\mu_1\,\nu_1,\,\mu_2\,\nu_2}(p_1,p_2;\mathbf{q_T}) = D^{\,\mu_1\nu_1}(p_1,p_2;\mathbf{q_T})\; D^{\,\mu_2\nu_2}(p_1,p_2;\mathbf{q_T}) - d_{(4)}^{\mu_1\,\nu_1,\mu_2\,\nu_2}(p_1,p_2)\;\;. \tag{3.106}$$

As we see from Eqs. (3.103) and (3.104), the weight functions of the resulting one-dimensional transformations are the 0-th order Bessel function $J_0(bq_T)$ (as like in Eq. (3.16)) and higher order (2-nd and 4-th) Bessel functions, $J_2(bq_T)$ and $J_4(bq_T)$.

Using the fact that the dependence on the azimuthal angle $\phi(\mathbf{q_T})$ is explicitly factorized with respect to the dependence on the magnitude q_T, we can express the gluon fusion resummation formula in a form that manifestly exhibits the functional dependence on $\phi(\mathbf{q_T})$ of the $\mathbf{q_T}$ cross section, at small values of q_T. Explicitly, we write

$$\begin{aligned}[d\sigma_F]^{(g-\mathrm{fus.})} &= [d\sigma_F]_{\phi}^{(g-\mathrm{fus.})} \\ &+ [d\sigma_F]_{C_1G_2}\;\left[H^F(\phi(\mathbf{q_T}))\right]_{C_1G_2} + \;[d\sigma_F]_{G_1C_2}\;\left[H^F(\phi(\mathbf{q_T}))\right]_{G_1C_2} \\ &+ [d\sigma_F]_{GG}\;\left[H^F(\phi(\mathbf{q_T}))\right]_{GG}\;\;,\end{aligned} \tag{3.107}$$

where the factors $\left[H^F(\phi(\mathbf{q_T}))\right]_I$ (I is $I = C_1G_2, G_1C_2$ or GG) depend on $\mathbf{q_T}$ only through its azimuthal angle $\phi(\mathbf{q_T})$ (i.e., these factors do not depend on the magnitude of $\mathbf{q_T}$), while all the other terms on the right-hand side of Eq. (3.107) depend on q_T, but they are independent of $\phi(\mathbf{q_T})$. In particular, the contribution $[d\sigma_F]_{\phi}^{(g-\mathrm{fus.})}$ coincides with the azimuthally-averaged cross section (see the definition in Section 3.4.2), whereas the other cross section contributions, $[d\sigma_F]_I$, in Eq. (3.107) have the following form:

$$\begin{aligned}[d\sigma_F]_I = \frac{M^2}{s}\;\left[d\sigma_{gg,\,F}^{(0)}\right]\int_0^{+\infty}\frac{db}{2\pi}\;b\;\;S_g(M,b) \\ \times\;\sum_{a_1,a_2}\int_{x_1}^1\frac{dz_1}{z_1}\int_{x_2}^1\frac{dz_2}{z_2}\;\;[JC_1C_2]^I_{gg;a_1a_2}\;\;f_{a_1/h_1}(x_1/z_1,b_0^2/b^2)\;f_{a_2/h_2}(x_2/z_2,b_0^2/b^2)\;\;,\end{aligned} \tag{3.108}$$

where the integrand factors denoted by $[JC_1C_2]^I$ are given by the following explicit expressions:

$$[JC_1C_2]^{C_1G_2}_{gg;a_1a_2} = J_2(bq_T)\;\;C_{g\,a_1}(z_1;\alpha_{\mathrm{S}}(b_0^2/b^2))\;\;G_{g\,a_2}(z_2;\alpha_{\mathrm{S}}(b_0^2/b^2))\;\;, \tag{3.109}$$

$$[JC_1C_2]^{G_1C_2}_{gg;a_1a_2} = J_2(bq_T)\ G_{g\,a_1}(z_1;\alpha_{\rm S}(b_0^2/b^2))\ C_{g\,a_2}(z_2;\alpha_{\rm S}(b_0^2/b^2))\ , \tag{3.110}$$

$$[JC_1C_2]^{GG}_{gg;a_1a_2} = J_4(bq_T)\ G_{g\,a_1}(z_1;\alpha_{\rm S}(b_0^2/b^2))\ G_{g\,a_2}(z_2;\alpha_{\rm S}(b_0^2/b^2))\ . \tag{3.111}$$

The hard-scattering factors $\Big[H^F(\phi(\mathbf{q_T}))\Big]_I$ are process dependent; they are

$$\Big[H^F(\phi(\mathbf{q_T}))\Big]_{C_1G_2} = -\,H^F_{\mu_1\,\nu_1,\mu_2\,\nu_2}(p_1,p_2;\mathbf{\Omega};\alpha_{\rm S}(M^2))\ d^{\,\mu_1\,\nu_1}(p_1,p_2)\ D^{\,\mu_2\,\nu_2}(p_1,p_2;\mathbf{q_T})\,, \tag{3.112}$$

$$\Big[H^F(\phi(\mathbf{q_T}))\Big]_{G_1C_2} = -\,H^F_{\mu_1\,\nu_1,\mu_2\,\nu_2}(p_1,p_2;\mathbf{\Omega};\alpha_{\rm S}(M^2))\ D^{\,\mu_1\,\nu_1}(p_1,p_2;\mathbf{q_T})\ d^{\,\mu_2\,\nu_2}(p_1,p_2)\,, \tag{3.113}$$

$$\Big[H^F(\phi(\mathbf{q_T}))\Big]_{GG} = H^F_{\mu_1\,\nu_1,\mu_2\,\nu_2}(p_1,p_2;\mathbf{\Omega};\alpha_{\rm S}(M^2))\ D^{\,\mu_1\,\nu_1,\,\mu_2\,\nu_2}_{(4)}(p_1,p_2;\mathbf{q_T})\,. \tag{3.114}$$

We note that the $\phi(\mathbf{q_T})$ dependence of the hard-scattering factors $\Big[H^F(\phi(\mathbf{q_T}))\Big]_I$ in Eqs. (3.112)–(3.113) is embodied in the Lorentz tensors $D^{\,\mu\,\nu}(p_1,p_2;\mathbf{q_T})$ and $D^{\,\mu_1\,\nu_1,\,\mu_2\,\nu_2}_{(4)}(p_1,p_2;\mathbf{q_T})$. By the direct inspection of their explicit expressions given in Eqs. (3.96) and (3.106), it is easy to see that the azimuthal dependence of the $D^{\,\mu\,\nu}(p_1,p_2;\mathbf{q_T})$ tensor can be expressed in terms of $\cos\Big(2\phi(\mathbf{q_T})\Big)$ and $\sin\Big(2\phi(\mathbf{q_T})\Big)$ functions, while the tensor $D^{\,\mu_1\,\nu_1,\,\mu_2\,\nu_2}_{(4)}(p_1,p_2;\mathbf{q_T})$ can be written as a linear combination of $\cos\Big(4\phi(\mathbf{q_T})\Big)$ and $\sin\Big(4\phi(\mathbf{q_T})\Big)$. Thus, the $\phi(\mathbf{q_T})$ azimuthal dependence of the logarithmically-enhanced terms at small q_T is fully determined by the general structure of the transverse-momentum resummation formula. The $\mathbf{q_T}$ cross section $[d\sigma_F]^{(g-\rm fus.)}$ contains a contribution that is independent of $\phi(\mathbf{q_T})$ (namely, the term $[d\sigma_F]^{(g-\rm fus.)}_{\phi}$) plus a linear combination of the four trigonometric functions $\cos\Big(2\phi(\mathbf{q_T})\Big)$, $\sin\Big(2\phi(\mathbf{q_T})\Big)$, $\cos\Big(4\phi(\mathbf{q_T})\Big)$ and $\sin\Big(4\phi(\mathbf{q_T})\Big)$. No other functional dependence on $\phi(\mathbf{q_T})$ is allowed by the gluon fusion resummation formula.

To present the singular behaviour produced by $\Big[H^F(\phi(\mathbf{q_T}))\Big]_I$ contributions at small q_T we expand the resummation formula in powers of $\alpha_{\rm S} = \alpha_{\rm S}(\mu_R^2)$ and perform the Bessel transformations from b space to q_T space. At relative order $\alpha_{\rm S}$ we get

$$\frac{\alpha_{\rm S}}{\pi}\ \delta(1-z_1)\ \delta_{g\,a_1}\ G^{(1)}_{g\,a_2}(z_2)\ \Big[H^F(\phi(\mathbf{q_T}))\Big]_{C_1G_2}\ \frac{1}{q_T^2}\ , \tag{3.115}$$

and to an analogous contribution that is obtained by the exchange $1 \leftrightarrow 2$ of the subscripts. The term coming from the quadratic Lorentz tensor $D^{\,\mu\,\nu}(p_1,p_2;\mathbf{b})$ in Eq. (3.104) contributes first at the relative order $\alpha_{\rm S}^2$; it produces a partonic cross section contribution that is proportional to

$$\left(\frac{\alpha_{\rm S}}{\pi}\right)^2\ G^{(1)}_{g\,a_1}(z_1)\ G^{(1)}_{g\,a_2}(z_2)\left(2\ \Big[H^F(\phi(\mathbf{q_T}))\Big]_{GG}\frac{1}{q_T^2} + H^F_G\ \delta(q_T^2)\right)\ , \tag{3.116}$$

where the functions $G^{(1)}_{g\,a}(z)$ are given in Eqs. (3.98) and (3.99).

3.4.2 Azimuthally-averaged cross section

We will continue the discussion on the azimuthal correlations in Chapter 6, while in this section we consider the cross section, averaged over the azimuthal angle. To this end, we define the following azimuthally-averaged cross section:

$$\begin{aligned}\langle\frac{d\sigma_{h_1h_2\to F+X}(s;\mathbf{q_T},y,M,\mathbf{\Omega})}{d^2\mathbf{q_T}\,dM^2\,dy\,d\mathbf{\Omega}}\rangle_\phi &\equiv \int_0^{2\pi}\frac{d\phi(\mathbf{q_T})}{2\pi}\,\frac{d\sigma_{h_1h_2\to F+X}}{d^2\mathbf{q_T}\,dM^2\,dy\,d\mathbf{\Omega}}\\ &= \frac{1}{\pi}\,\frac{d\sigma_{h_1h_2\to F+X}(s;q_T^2,y,M,\mathbf{\Omega})}{dq_T^2\,dM^2\,dy\,d\mathbf{\Omega}}\,.\end{aligned} \tag{3.117}$$

We denote the singular component of the azimuthally-averaged cross section (3.117) as $[d\sigma_F]_\phi$. Since the resummed cross section (3.30) in the case of $q\bar{q}$ annihilation subprocesses is free of azimuthal correlations, the azimuthal average of $[d\sigma_F]^{(q\bar{q}-\text{ann.})}$ is trivial and $[d\sigma_F]_\phi^{(q\bar{q}-\text{ann.})}$ is obtained by the same resummation formula (3.30) and (3.34) (with $c=q,\bar{q}$). As it has been shown in Ref. [69], in the case of gluon fusion processes the resummed azimuthally-averaged cross section $[d\sigma_F]_\phi^{(g-\text{fus.})}$ is obtained by replacing in Eq. (3.92)

$$[d\sigma_F]^{(g-\text{fus.})}\to[d\sigma_F]_\phi^{(g-\text{fus.})}\,, \tag{3.118}$$

with the corresponding replacement of the $\Big[H^FC_1C_2\Big]$ factor

$$\Big[H^FC_1C_2\Big]_{gg;a_1a_2}\to\Big[H^FC_1C_2\Big]^\phi_{gg;a_1a_2}\,, \tag{3.119}$$

where $\Big[H^FC_1C_2\Big]^\phi_{gg;a_1a_2}$ retains the following form:

$$\begin{aligned}\Big[H^FC_1C_2\Big]^\phi_{gg;a_1a_2} &= H_g^F(p_1,p_2;\mathbf{\Omega};\alpha_{\rm S}(M^2))\;C_{ga_1}(z_1;\alpha_{\rm S}(b_0^2/b^2))\;C_{ga_2}(z_1;\alpha_{\rm S}(b_0^2/b^2))\\ &+ H_G^F(p_1,p_2;\mathbf{\Omega};\alpha_{\rm S}(M^2))\;G_{ga_1}(z_1;\alpha_{\rm S}(b_0^2/b^2))\;G_{ga_2}(z_1;\alpha_{\rm S}(b_0^2/b^2))\,.\end{aligned} \tag{3.120}$$

The scalar hard-scattering factor H_g^F in Eq. (3.120) is defined as follows

$$H_g^F(p_1,p_2;\mathbf{\Omega};\alpha_{\rm S})\equiv H^F_{g;\,\mu_1\,\nu_1,\mu_2\,\nu_2}(p_1,p_2;\mathbf{\Omega};\alpha_{\rm S})\;g^{\mu_1\,\nu_1}\;g^{\mu_2\,\nu_2}\,, \tag{3.121}$$

and the spin-correlated hard-scattering factor H_G^F is

$$H_G^F(p_1,p_2;\mathbf{\Omega};\alpha_{\rm S}(M^2))=H^F_{g;\,\mu_1\,\nu_1,\mu_2\,\nu_2}(p_1,p_2;\mathbf{\Omega};\alpha_{\rm S})\;d_{(4)}^{\mu_1\,\nu_1\,\mu_2\,\nu_2}(p_1,p_2)\,, \tag{3.122}$$

where the 4th-rank tensor is given in Eq. (3.105).

As one can see from Eq. (3.120), in gluon fusion processes the resummation factor of Eq. (3.34) is not complete even for the azimuthally-averaged cross sections. In particular, since the expansion of gluon coefficient functions G_{ga} starts at $\mathcal{O}(\alpha_{\rm S})$ (see Eq. (3.97)), the

gluon resummation factor $\Big[H^F C_1 C_2\Big]_{gg;a_1a_2} \to \Big[H^F C_1 C_2\Big]^{\phi}_{gg;a_1a_2}$ affects the computation of the QCD radiative corrections starting from NNLL+NNLO. In particular, the second-order hard-collinear function $\mathcal{H}^{F\,(2)}_{gg\leftarrow a_1a_2,\,(N_1,N_2)}$ of Eq. (3.87) should be replaced by

$$\mathcal{H}^{F\,(2)}_{gg\leftarrow a_1a_2,\,(N_1,N_2)} \to \mathcal{H}^{F\,(2)}_{gg\leftarrow a_1a_2,\,(N_1,N_2)} + H_G^{F\,(0)}(p_1,p_2;\boldsymbol{\Omega};\alpha_{\rm S})\; G^{(1)}_{ga_1,\,N_1}\; G^{(1)}_{ga_2,\,N_2}\,, \tag{3.123}$$

where H_G^F factor is coming from the Bessel transformation from b space to q_T space of the first line of Eq. (3.104).

Chapter 4

Transverse-momentum resummation for heavy-quark pair production

In this chapter we present our computation of the resummed spectrum of the transverse-momentum distribution of the top-quark pair. The resummation procedure for the production of a $t\bar{t}$ pair is more complicated with respect to the production of colourless high-mass systems, since the top quark can radiate additional soft gluons. Thus, in order to perform the resummation, the emission from both the initial and the final state should be taken into account, which leads to non-trivial colour correlations.

The first attempt to develop a q_T-resummation formalism at NLL accuracy for the $t\bar{t}$ production was done in Refs. [140, 141]. However, these papers failed to consider colour mixing between the singlet and octet final states and missed the initial-final gluon correlations. Besides the resummation formalism mentioned above, there is another independent approach based on the soft-collinear effective theory (SCET) [83–85]. Recently a resummed computation of the $t\bar{t}$ transverse-momentum spectrum, based on this approach, was performed in Refs. [93, 94]. The key difference with respect to the Drell-Yan and Higgs boson production is the appearance of transverse soft functions. However, in Refs. [93, 94] such functions are averaged over the azimuthal angle of the top quark ϕ_t in the transverse plane.

The complete resummation formalism for the hadroproduction of a pair of heavy quarks in QCD has been proposed in Ref. [95]. In contrast to the pioneering work in SCET [93], this work fully takes into account the colour-dependent azimuthal correlations in the small-q_T region, produced by the dynamics of soft-parton radiation. As it is discussed in Ref. [95], these azimuthal correlations and those from the gluonic collinear radiation, mentioned in Section 3.4, have different physical origin. Moreover, even though both azimuthal correlation effects vanish after averaging over the azimuthal angle at NLO accuracy, they give non-vanishing contribution even for the azimuthally-averaged cross sections starting from NNLO, due to non-trivial interference. Thus, to extend the calculation to one order higher

in QCD perturbation theory, it is important to have a full control over these correlations.

4.1 The all-order transverse-momentum resummation formula for heavy-quark pair production

In this section we review the general structure of the transverse-momentum resummation formulae for heavy-quark pair production of Ref. [95]. To this purpose, we consider the collisions of two hadrons h_1 and h_2 of momenta P_1^μ and P_2^μ, which produce two heavy quarks Q and $\bar{Q}$ with momenta p_3^μ, p_4^μ and mass $p_3^2 = p_4^2 = m^2$,

$$h_1(P_1) + h_2(P_2) \to Q(p_3) + \bar{Q}(p_4) + X\,, \tag{4.1}$$

accompanied by arbitrary and undetected final state X. In the centre-of-mass system of the collision the total momentum of the $Q\bar{Q}$ pair $q^\mu = p_3^\mu + p_4^\mu$ is fully specified by the invariant mass M ($M^2 = q^2$), the transverse-momentum vector $\mathbf{q_T}$ and the rapidity $y = \frac{1}{2}\ln\frac{q\cdot P_2}{q\cdot P_1}$. The momenta p_j^μ ($j = 3, 4$) of the heavy quarks are determined by the heavy-quark mass m, rapidity y_j and the transverse-momentum vector $\mathbf{p_{T}}_j$.

We consider the most general fully-differential cross section for the inclusive production process (4.1)

$$\begin{aligned}\frac{d\sigma_{h_1h_2\to Q\bar{Q}+X}(s;\mathbf{q_T},y,M,\mathbf{\Omega})}{d^2\mathbf{q_T}\,dM^2\,dy\,d\mathbf{\Omega}} &= \frac{1}{s}\sum_{a_1,a_2}\int_{x_1}^1\frac{dz_1}{z_1}\int_{x_2}^1\frac{dz_2}{z_2} \\ \times f_{a_1/h_1}(x_1/z_1,\mu_F^2)\,f_{a_2/h_2}(x_2/z_2,\mu_F^2)\,&\frac{d\hat{\sigma}_{a_1a_2\to Q\bar{Q}+X}(\mathbf{q_T},z_1,z_2;M,\mathbf{\Omega};\alpha_{\rm S}(\mu_R^2),\mu_R^2,\mu_F^2)}{d^2\mathbf{q_T}\,dz_1\,dz_2\,d\mathbf{\Omega}}\,,\end{aligned} \tag{4.2}$$

where $\mathbf{\Omega}$ represents a set of independent kinematical variables that specify the angular distribution of the heavy quarks Q and $\bar{Q}$ with respect to the momentum q of the $Q\bar{Q}$ pair. For example, one can use the rapidity y_3 and the azimuthal angle ϕ_3 of one of the heavy quarks, or any other equivalent pairs of kinematical variables.

Following the resummation formalism of Ref. [82], presented in Section 3.1, we decompose the hadronic cross section in Eq. (4.2) into singular and regular components

$$\frac{d\sigma_{h_1h_2\to Q\bar{Q}+X}(s;\mathbf{q_T},y,M,\mathbf{\Omega})}{d^2\mathbf{q_T}\,dM^2\,dy\,d\mathbf{\Omega}} = [d\sigma_{Q\bar{Q}}] + \frac{d\sigma^{\rm reg.}_{h_1h_2\to Q\bar{Q}+X}(s;\mathbf{q_T},y,M,\mathbf{\Omega})}{d^2\mathbf{q_T}\,dM^2\,dy\,d\mathbf{\Omega}}\,, \tag{4.3}$$

where we have introduced, analogously to Eq. (3.10), short-hand notation for the singular component:

$$[d\sigma_{Q\bar{Q}}] \equiv \frac{d\sigma^{\rm sing.}_{h_1h_2\to Q\bar{Q}+X}(s;\mathbf{q_T},y,M,\mathbf{\Omega})}{d^2\mathbf{q_T}\,dM^2\,dy\,d\mathbf{\Omega}}\,. \tag{4.4}$$

The decomposition of the hadronic cross section in Eq. (4.3) has the same formal meaning as it is discussed in Section 3.1, in particular, that the singular component $[d\sigma_{Q\bar{Q}}]$ of the hadronic cross section embodies all logarithmically-enhanced contributions that need to be resummed to all orders in $\alpha_{\rm S}$. The all-order resummation formula for heavy-quark production has the following form

$$[d\sigma_{Q\bar{Q}}] = \frac{M^2}{s} \int \frac{d^2\mathbf{b}}{(2\pi)^2}\; e^{i\mathbf{b}\cdot\mathbf{q_T}}\; W^{Q\bar{Q}}(s;\mathbf{b},y,M,\mathbf{\Omega};\alpha_{\rm S}(\mu_R^2),\mu_R^2,\mu_F^2)\,, \tag{4.5}$$

with

$$W^{Q\bar{Q}}(s;\mathbf{b},y,M,\mathbf{\Omega};\alpha_{\rm S}(\mu_R^2),\mu_R^2,\mu_F^2) = \sum_{a_1,a_2} \int_{x_1}^1 \frac{dz_1}{z_1} \int_{x_2}^1 \frac{dz_2}{z_2}\; f_{a_1/h_1}\left(\frac{x_1}{z_1},\frac{b_0^2}{b^2}\right)\; f_{a_2/h_2}\left(\frac{x_2}{z_2},\frac{b_0^2}{b^2}\right) \times \sum_{c=q,\bar{q},g} \left[d\sigma^{(0)}_{c\bar{c},\,Q\bar{Q}}\right] S_c(M,b)\;\left[(\mathbf{H}\,\mathbf{\Delta})\,C_1C_2\right]_{c\bar{c};a_1a_2}\;, \tag{4.6}$$

where the scaling variables x_1, x_2, z_1 and z_2 are defined in Eqs. (3.7) and (3.8).

The factor $\left[d\sigma^{(0)}_{c\bar{c},\,Q\bar{Q}}\right]$ in Eq. (4.6) is the Born level cross section of the partonic subprocess,

$$c(p_1) + \bar{c}(p_2) \to Q(p_3) + \bar{Q}(p_4)\,, \tag{4.7}$$

with

$$p_i = x_i P_i\,, \quad i = 1,2\,, \tag{4.8}$$

and it receives contribution from both the $q\bar{q}$ annihilation ($c = q,\bar{q}$) and the gg fusion ($c = g$) channels.

The QCD radiative corrections are embodied in the factors S_c and $[(\mathbf{H}\,\mathbf{\Delta})\,C_1C_2]$. In particular, $S_c(M,b)$ is the universal Sudakov form factor $S_c(M,b)$, defined in Eq. (3.31), while the factor $\mathbf{\Delta}$ contains all the differences with respect to the production of a colourless system F that occur in the case of $Q\bar{Q}$ production.

The expression of the symbolic factor $[(\mathbf{H}\,\mathbf{\Delta})\,C_1C_2]$ has different form for the $q\bar{q}$ annihilation and gluon-fusion channels, owing to the physical differences between the quark and gluon collinear functions discussed in Section 3.4. Explicitly, for the $q\bar{q}$ annihilation channel the factor $[(\mathbf{H}\,\mathbf{\Delta})\,C_1C_2]$ reads

$$[(\mathbf{H}\,\mathbf{\Delta})\,C_1C_2]_{q\bar{q};a_1a_2} = (\mathbf{H}\,\mathbf{\Delta})_{q\bar{q}}\,C_{qa_1}(z_1;\alpha_{\rm S}(b_0^2/b^2))\,C_{\bar{q}a_2}(z_2;\alpha_{\rm S}(b_0^2/b^2))\,, \tag{4.9}$$

whereas for the gluon fusion channel ($c = g$) we have

$$[(\mathbf{H}\,\mathbf{\Delta})\,C_1C_2]_{gg;a_1a_2} = (\mathbf{H}\,\mathbf{\Delta})_{gg;\mu_1\,\nu_1,\mu_2\,\nu_2}\;C^{\mu_1\,\nu_1}_{g\,a_1}(z_1;p_1,p_2,\mathbf{b};\alpha_{\rm S}(b_0^2/b^2))\,C^{\mu_2\,\nu_2}_{g\,a_2}(z_2;p_1,p_2,\mathbf{b};\alpha_{\rm S}(b_0^2/b^2))\,. \tag{4.10}$$

The functions C_{qa} and $C_{g\,a}^{\mu\,\nu}$, entering Eqs. (4.9) and (4.10), are the same universal collinear functions contributing to the transverse-momentum resummation formula for a colourless system F and retain the perturbative expansions given in Eqs. (3.36), (3.94) and (3.97).

The factor $(\mathbf{H}\,\mathbf{\Delta})$ in Eqs. (4.9) and (4.10) is the contribution of the factors $\mathbf{H}$ and $\mathbf{\Delta}$, which exhibit a non-trivial dependence on the colour structure of the partonic process in Eq. (4.7). According to Eq. (2.62), the dependence of the scattering amplitude $\mathcal{M}$ of the process (4.7) on the colour indices is represented by a vector $|\mathcal{M}\rangle$. Using the colour-space formalism presented in Section 2.6.2, the factor $(\mathbf{H}\,\mathbf{\Delta})$ can be represented as follows:

$$(\mathbf{H}\,\mathbf{\Delta})_{q\bar{q}} = \frac{\langle \widetilde{\mathcal{M}}_{c\bar{c}\to Q\bar{Q}} \,|\, \mathbf{\Delta} \,|\, \widetilde{\mathcal{M}}_{c\bar{c}\to Q\bar{Q}} \rangle}{\alpha_{\mathrm{S}}^2(M^2)\; |\mathcal{M}^{(0)}_{c\bar{c}\to Q\bar{Q}}(p_1,p_2;p_3,p_4)|^2}\,, \tag{4.11}$$

for the $q\bar{q}$ annihilation channel, and

$$(\mathbf{H}\,\mathbf{\Delta})_{gg;\mu_1\,\nu_1,\mu_2\,\nu_2} = \frac{\langle \widetilde{\mathcal{M}}^{\nu'_1\nu'_2}_{gg\to Q\bar{Q}} \,|\, \mathbf{\Delta} \,|\, \widetilde{\mathcal{M}}^{\mu'_1\mu'_2}_{gg\to Q\bar{Q}} \rangle \; d_{\mu'_1\mu_1}\, d_{\nu'_1\nu_1}\, d_{\mu'_2\mu_2}\, d_{\nu'_2\nu_2}}{\alpha_{\mathrm{S}}^2(M^2)\; |\mathcal{M}^{(0)}_{gg\to Q\bar{Q}}(p_1,p_2;p_3,p_4)|^2}\,, \tag{4.12}$$

in the gluon fusion channel. The polarisation tensor $d^{\mu\nu} = d^{\mu\nu}(p_1,p_2)$ in Eq. (4.12) is the one defined in Eq. (3.95), and $\{\mu'_i,\nu'_i\}$ are the gluon Lorentz indices of the scattering amplitude $\mathcal{M}_{gg\to Q\bar{Q}}$. The hard-virtual amplitude $\widetilde{\mathcal{M}}_{c\bar{c}\to Q\bar{Q}}$ is directly related to the infrared-finite part of the all-order virtual scattering amplitude $\mathcal{M}_{c\bar{c}\to Q\bar{Q}}$ by Eq. (4.27).

The factor $\mathbf{\Delta}$ is specific of heavy-quark pair production and embodies the effect of soft radiation from the $Q\bar{Q}$ final state and from the initial-state and final-state interferences. It depends on the impact parameter $\mathbf{b}$, on the invariant mass M and on the kinematics of the partonic process in Eq. (4.7). In particular, it depends on the two angular variables in $\mathbf{\Omega}$. Choosing the rapidity difference $y_{34} = y_3 - y_4$ between Q and $\bar{Q}$ and the azimuthal angle ϕ_3 of the quark Q as the two variables, the factor $\mathbf{\Delta}$ can be written in the following all-order form

$$\mathbf{\Delta}(\mathbf{b},M;y_{34},\phi_3) = \mathbf{V}^{\dagger}(b,M;y_{34})\;\; \mathbf{D}(\alpha_{\mathrm{S}}(b_0^2/b^2);\phi_{3b},y_{34})\; \mathbf{V}(b,M;y_{34})\,, \tag{4.13}$$

where the *evolution* factor $\mathbf{V}$ is obtained by the exponentiation of the integral of the so-called *soft anomalous dimension* matrix $\mathbf{\Gamma}_t$

$$\mathbf{V}(b,M;y_{34}) = \overline{P}_q\;\exp\left\{-\int_{b_0^2/b^2}^{M^2}\frac{dq^2}{q^2}\;\mathbf{\Gamma}_t(\alpha_{\mathrm{S}}(q^2);y_{34})\right\}\,, \tag{4.14}$$

The integration in Eq. (4.14) is performed over the transverse-momentum scale q^2 of the QCD running coupling. Therefore, the evolution factor $\mathbf{V}$ explicitly resums logarithmic terms $\alpha_{\mathrm{S}}^n(M^2)\ln^k(Mb)$ (with $k\le n$). The symbol $\overline{P}_q$ means that the exponential matrix is anti path-ordered with respect to the integration variable q^2. The soft anomalous dimension

operator $\mathbf{\Gamma}_t$, as well as the colour operator $\mathbf{D}$ in Eq. (4.14), are computable order-by-order in $\alpha_{\rm S}$

$$\mathbf{\Gamma}_t(\alpha_{\rm S}; y_{34}) = \frac{\alpha_{\rm S}}{\pi}\,\mathbf{\Gamma}_t^{(1)}(y_{34}) + \left(\frac{\alpha_{\rm S}}{\pi}\right)^2\,\mathbf{\Gamma}_t^{(2)}(y_{34}) + \sum_{n=3}^{\infty}\left(\frac{\alpha_{\rm S}}{\pi}\right)^n\,\mathbf{\Gamma}_t^{(n)}(y_{34})\;, \tag{4.15}$$

$$\mathbf{D}(\alpha_{\rm S}; \phi_{3b}, y_{34}) = 1 + \frac{\alpha_{\rm S}}{\pi}\,\mathbf{D}^{(1)}(\phi_{3b}, y_{34}) + \sum_{n=2}^{\infty}\left(\frac{\alpha_{\rm S}}{\pi}\right)^n\,\mathbf{D}^{(n)}(\phi_{3b}, y_{34})\;\;. \tag{4.16}$$

Note that the $\alpha_{\rm S}$ scale of the colour operator $\mathbf{D}$ in Eq. (4.14) is set to b_0^2/b^2. While the coefficients $\mathbf{D}^{(n)}$ of the perturbative expansion of the colour operator $\mathbf{D}$ in Eq. (4.16) do not contain logarithmically-enhanced contributions $\ln(Mb)$, these terms arise when expressing $\alpha_{\rm S}(b_0^2/b^2)$ in terms of $\alpha_{\rm S}(M^2)$. Thus, the colour operator $\mathbf{D}$ effectively resums $\ln(Mb)$ contributions to $\mathbf{\Delta}$.

The colour operator $\mathbf{D}$ exhibits an important feature. It depends not only on the rapidity difference y_{34}, as the soft anomalous dimension $\mathbf{\Gamma}_t$ (and thus also the evolution factor $\mathbf{V}$), but it also depends on the azimuthal angle ϕ_3 of the heavy quark Q. More specifically, it depends on $\phi_{3b} = \phi_3 - \phi(\mathbf{b})$, where $\phi(\mathbf{b})$ is the azimuth of the two dimensional impact parameter vector $\mathbf{b}$. The inverse Fourier transformation from $\mathbf{b}$ space to $\mathbf{q_T}$ space in Eq. (4.6), then leads to a consequent q_T-dependent *azimuthal correlations* of the produced $Q\bar{Q}$ pair at small q_T.

The perturbative coefficients $\mathbf{\Gamma}_t^{(1)}$ and $\mathbf{D}^{(1)}$ contribute to the transverse-momentum resummed cross section of Eq. (4.6) at NLL accuracy. Considering the kinematics of the process in Eq. (4.7), four-momentum conservation leads to the relations $y_3 - y = y - y_4 = y_{34}/2$, $\mathbf{p_T}_3^2 = \mathbf{p_T}_4^2 = \mathbf{p_T}^2$. Using these relations, $\mathbf{\Gamma}_t^{(1)}$ can be written as

$$\begin{aligned}\mathbf{\Gamma}_t^{(1)}(y_{34}) = -\frac{1}{4}\Bigg\{&(\mathbf{T}_3^2 + \mathbf{T}_4^2)\,(1 - i\pi) + \sum_{\substack{i=1,2\\ j=3,4}}\mathbf{T}_i\cdot\mathbf{T}_j\,\ln\frac{(2p_i\cdot p_j)^2}{M^2m^2}\\ &+ 2\,\mathbf{T}_3\cdot\mathbf{T}_4\left[\frac{1}{2v}\ln\left(\frac{1+v}{1-v}\right) - i\pi\left(\frac{1}{v}+1\right)\right]\Bigg\}\;,\end{aligned} \tag{4.17}$$

where the colour-charge operators $\mathbf{T}_i$ are defined by Eq. (2.64), and v is the relative velocity of Q and $\bar{Q}$,

$$v = \sqrt{1 - \left(\frac{2m^2}{M^2 - 2m^2}\right)^2}\;\;. \tag{4.18}$$

The soft-parton operator $\mathbf{D}$ in Eq. (4.16) also depends on the relative azimuthal angle ϕ_{3b}

(or, equivalently, ϕ_{4b}). Explicitly, it can be written as follows:

$$\mathbf{D}^{(1)}(\phi_{3b}, y_{34}) = (\mathbf{T}_3^2 + \mathbf{T}_4^2)\left[\frac{c_{3b}\,\mathrm{arcsinh}\,(c_{3b})}{\sqrt{1+c_{3b}^2}} - \frac{1}{2}\ln\left(\frac{m_T^2}{m^2}\right)\right] - (\mathbf{T}_3+\mathbf{T}_4)^2\left(\mathrm{arcsinh}^2\,(c_{3b}) + \frac{1}{2}\mathrm{Li}_2\left(-\frac{\mathbf{p}_\mathbf{T}^2}{m^2}\right)\right) + \frac{1}{2v}\,\mathbf{T}_3\cdot\mathbf{T}_4\,(L_{34}^{\varphi} - L_{34})\ , \tag{4.19}$$

where $m_T = \sqrt{p_T^2 + m^2}$ is the heavy-quark transverse mass, and the auxiliary variable c_{3b} is

$$c_{3b} = \frac{\sqrt{\mathbf{p}_\mathbf{T}^2}}{m}\,\cos(\phi_{3b}) = -\frac{\sqrt{\mathbf{p}_\mathbf{T}^2}}{m}\,\cos(\phi_{4b})\ . \tag{4.20}$$

The functions L_{34} and L_{34}^{φ} in Eq. (4.19) are defined as

$$L_{34} = \ln\left(\frac{1+v}{1-v}\right)\ln\left(\frac{m_T^2}{m^2}\right) - 2\,\mathrm{Li}_2\left(\frac{2v}{1+v}\right) - \frac{1}{4}\ln^2\left(\frac{1+v}{1-v}\right) + 2\left[\mathrm{Li}_2\left(1-\sqrt{\frac{1-v}{1+v}}\,e^{\,y_{34}}\right) + \mathrm{Li}_2\left(1-\sqrt{\frac{1-v}{1+v}}\,e^{-y_{34}}\right) + \frac{1}{2}\,y_{34}^2\right]\ , \tag{4.21}$$

$$L_{34}^{\varphi} = \mathrm{Sign}(c_{3b})\Big[L_\xi\left(\xi(c_{3b},\alpha_{34}),\alpha_{34}\right) - L_\xi\left(\xi(-c_{3b},\alpha_{34}),\alpha_{34}\right)\Big]\,, \tag{4.22}$$

with Li_2 being the customary dilogarithm function, $\mathrm{Li}_2(z) = -\int_0^z \frac{dt}{t}\,\ln(1-t)$, and

$$L_\xi(\xi,\alpha) = \frac{1}{2}\ln^2\frac{\xi(1+\xi)}{\alpha+\xi} - \ln^2\frac{\xi}{\alpha+\xi} + 2\left[\mathrm{Li}_2(-\xi) - \mathrm{Li}_2\left(\frac{\alpha+\xi}{\alpha-1}\right) + \ln(\alpha+\xi)\ln(1-\alpha)\right]\,, \tag{4.23}$$

$$\xi(c,\alpha) = \left(c+\sqrt{1+c^2}\right)\left(c+\sqrt{\alpha+c^2}\right) \quad , \quad \alpha_{34} = \frac{2\sqrt{1-v^2}}{1-\sqrt{1-v^2}}\,c_{3b}^2\,. \tag{4.24}$$

As one can see, the azimuthal dependence of $\mathbf{D}^{(1)}$ is more complex than that of the gluon collinear functions $C_{ga}^{\mu\nu}$ in Eq. (3.94), where the azimuthal dependence is entirely embodied in the polarisation tensor $D^{\mu\nu}(p_1,p_2;\mathbf{b})$ (3.96). Moreover, while the azimuthal correlations due to the gluon collinear functions are limited to only four Fourier harmonics $(\cos(\phi(\mathbf{q_T})), \sin(2\phi(\mathbf{q_T})), \cos(4\phi(\mathbf{q_T})), \sin(4\phi(\mathbf{q_T})))$, the azimuthal correlations due to the colour operator $\mathbf{D}$ depend on Fourier harmonics of any degrees. More detailed discussion on the azimuthal correlations of the q_T cross section can be found in Section 4.2.1 and in Chapter 6.

The first-order colour operator $\mathbf{D}^{(1)}$ in Eq. (4.19) has another important feature: its average over the azimuthal angle $\phi(\mathbf{b})$ vanishes

$$\langle \mathbf{D}^{(1)}(\phi_{3b}, y_{34})\rangle_{\mathrm{av.}} = 0\ . \tag{4.25}$$

In fact, it is always possible to define the colour operator $\mathbf{D}$ in such a way that the azimuthal average over $\mathbf{b}$ gives a trivial contribution at all orders in $\alpha_{\rm S}$

$$\langle \mathbf{D}(\alpha_{\rm S}; \phi_{3b}, y_{34}) \rangle_{\rm av.} = 1 \ . \tag{4.26}$$

The possibility of such a definition directly follows from the freedom of defining the individual components of the resummed cross section in Eq. (4.6), in particular of the factor $(\mathbf{H}\,\boldsymbol{\Delta})$, due to the resummation scheme invariance of the q_T-resummed cross section.

Analogously to Eq. (3.43), the auxiliary amplitude $\widetilde{\mathcal{M}}_{c\bar{c}\to Q\bar{Q}}$ is related to the scattering amplitude $\mathcal{M}_{c\bar{c}\to Q\bar{Q}}$ through an all-order factorisation formula

$$|\widetilde{\mathcal{M}}_{c\bar{c}\to Q\bar{Q}}(p_1,p_2;p_3,p_4)\rangle = \left[1 - \widetilde{\mathbf{I}}_{c\bar{c}\to Q\bar{Q}}(\epsilon, M, \boldsymbol{\Omega}; \mu_R)\right] |\mathcal{M}_{c\bar{c}\to Q\bar{Q}}(p_1,p_2;p_3,p_4)\rangle \ . \tag{4.27}$$

The role of the operator $\widetilde{\mathbf{I}}_{c\bar{c}\to Q\bar{Q}}$ in Eq. (4.27) is the same of $\widetilde{I}_c$ in Eq. (3.43) for the production of a colourless system F: it subtracts the infrared poles of $\mathcal{M}_{c\bar{c}\to Q\bar{Q}}$, along with *some* of its IR finite terms that are specific of the q_T cross section in eq. (4.6). Unlike the subtraction operator $\widetilde{I}_c$, however, the operator $\widetilde{\mathbf{I}}_{c\bar{c}\to Q\bar{Q}}$ is a colour operator, acting on the colour indices of the scattering amplitude $\mathcal{M}_{c\bar{c}\to Q\bar{Q}}$. The scattering amplitude $\mathcal{M}_{c\bar{c}\to Q\bar{Q}}$ and the subtraction operator $\widetilde{\mathbf{I}}_{c\bar{c}\to Q\bar{Q}}$ retain the same perturbative expansion as their counterparts for the production of a colourless system, given by Eqs. (3.42) and (3.44) respectively. Explicitly, the first-order operator $\widetilde{\mathbf{I}}^{(1)}_{c\bar{c}\to Q\bar{Q}}$ reads

$$\widetilde{\mathbf{I}}^{(1)}_{c\bar{c}\to Q\bar{Q}}(\epsilon, M, \boldsymbol{\Omega}; \mu_R) = \widetilde{I}^{(1)}_c(\epsilon, M; \mu_R) + \widetilde{\mathbf{I}}^{(1)}_{Q\bar{Q}}(\epsilon, M, \boldsymbol{\Omega}; \mu_R) \,, \tag{4.28}$$

where $\widetilde{I}^{(1)}_c(\epsilon, M; \mu_R)$ is given in Eq. (3.46) and it contains the IR poles from the initial-state soft and collinear radiation, while $\widetilde{\mathbf{I}}^{(1)}_{Q\bar{Q}}$ subtracts the poles originating from soft wide-angle radiation of partons from the final-state heavy quarks and is given by

$$\widetilde{\mathbf{I}}^{(1)}_{Q\bar{Q}}(\epsilon, M, \boldsymbol{\Omega}; \mu_R) = -\frac{1}{2}\left(\frac{\mu_R^2}{M^2}\right)^{\epsilon} \left\{ -\frac{4}{\epsilon}\,\boldsymbol{\Gamma}^{(1)}_t(y_{34}) + \mathbf{F}^{(1)}_t(y_{34}) \right\} \ . \tag{4.29}$$

The colour operator $\boldsymbol{\Gamma}^{(1)}_t(y_{34})$ in Eq. (4.29) is exactly equal to the first-order coefficient of the soft anomalous dimension operator in Eq. (4.17). The IR finite contribution $\mathbf{F}^{(1)}_t$ to Eq. (4.29) is

$$\mathbf{F}^{(1)}_t(y_{34}) = (\mathbf{T}_3^2 + \mathbf{T}_4^2)\ \ln\left(\frac{m_T^2}{m^2}\right) + \ (\mathbf{T}_3 + \mathbf{T}_4)^2\ \mathrm{Li}_2\left(-\frac{\mathbf{p_T^2}}{m^2}\right) + \mathbf{T}_3 \cdot \mathbf{T}_4\ \frac{1}{v}\, L_{34} \ . \tag{4.30}$$

The first-order coefficient $\mathbf{F}^{(1)}_t$, together with $\boldsymbol{\Gamma}^{(1)}_t$ and $\mathbf{D}^{(1)}$, completes the set of heavy-quark specific coefficients, contributing to the resummation formula in Eq. (4.6) at NLL level. Moreover, an entire class of NNLL terms is produced by the interferences between

the NLL terms in the soft factor $\mathbf{\Delta}$ and the NLO corrections to the hard-virtual amplitude $|\widetilde{M}_{c\bar{c}\to Q\bar{Q}}\rangle$. For the complete determination of the NNLL terms, the second-order coefficients $\mathbf{\Gamma}_t^{(2)}$, $\mathbf{D}^{(2)}$ and the IR finite part of $\widetilde{\mathbf{I}}_{Q\bar{Q}}^{(2)}$ are also needed. Exploiting the relation of the soft anomalous dimension operator $\mathbf{\Gamma}_t$ to the IR singularities of the virtual scattering amplitude $\mathcal{M}_{c\bar{c}\to Q\bar{Q}}$, which are explicitly known at one-loop [142] and two-loop order [143–145], the second-order function $\mathbf{\Gamma}_t^{(2)}$ has been extracted in Ref. [95]. Explicitly, up to the second order, the soft anomalous dimension operator $\mathbf{\Gamma}_t$ can be written as

$$\mathbf{\Gamma}_t(\alpha_{\mathrm{S}};y_{34}) = \frac{1}{2}\,\mathbf{\Gamma}^{\mathrm{sub.}}_{c\bar{c}\to Q\bar{Q}}(\alpha_{\mathrm{S}};y_{34}) - \left(\frac{\alpha_{\mathrm{S}}}{\pi}\right)^2\,\frac{1}{4}\Big(\,\Big[\mathbf{\Gamma}_t^{(1)}(y_{34})\,,\mathbf{F}_t^{(1)}(y_{34})\Big] + \pi\beta_0\mathbf{F}_t^{(1)}(y_{34})\Big) + \mathcal{O}(\alpha_{\mathrm{S}}^3)\,, \tag{4.31}$$

where $\mathbf{\Gamma}^{\mathrm{sub.}}_{c\bar{c}\to Q\bar{Q}}$ is given by the following relation:

$$\mathbf{\Gamma}^{\mathrm{sub.}}_{c\bar{c}\to Q\bar{Q}}(\alpha_{\mathrm{S}};y_{34}) = \mathbf{\Gamma}(\mu) - \left[\frac{1}{2}(\mathbf{T}_1^2+\mathbf{T}_2^2)\,\gamma_{\mathrm{cusp}}(\alpha_{\mathrm{S}})\left(\ln\frac{M^2}{\mu^2} - i\pi\right) + 2\gamma^c(\alpha_{\mathrm{S}})\right]\,. \tag{4.32}$$

The the terms on the right-hand side of Eq. (4.32) are written using the notation of Eq. (5) of Ref. [145].

Using Eqs. (4.31), (4.32), and Eq. (5) of Ref. [145], the second-order soft anomalous dimension matrix $\mathbf{\Gamma}_t^{(2)}$ can be written as follows:

$$\begin{aligned}\mathbf{\Gamma}_t^{(2)}(y_{34}) = -\frac{1}{4}\Bigg\{&\left[\,(\mathbf{T}_3+\mathbf{T}_4)^2\;(-i\pi) + \sum_{\substack{i=1,2\\ j=3,4}}\mathbf{T}_i\cdot\mathbf{T}_j\,\ln\frac{(2p_i\cdot p_j)^2}{M^2m^2}\right]\gamma_{\mathrm{cusp}}^{(2)}\\ &- 4\,\gamma_2^Q + 2\,\mathbf{T}_3\cdot\mathbf{T}_4\,\gamma_{\mathrm{cusp}}^{(2)}(v) + \sum_{j=1,2} i f^{abc}\,T_3^a\,T_4^b\,T_j^c\,g(v)\,\ln\frac{p_4\cdot p_j}{p_3\cdot p_j}\\ &+ \Big[\mathbf{\Gamma}_t^{(1)}(y_{34})\,,\mathbf{F}_t^{(1)}(y_{34})\Big] + \pi\beta_0\mathbf{F}_t^{(1)}(y_{34})\Bigg\}\,,\end{aligned} \tag{4.33}$$

where the term proportional to the three-parton colour correlations originates from the last term on the right-hand side of Eq. (5) of Ref. [145]. The coefficients $\gamma_{\mathrm{cusp}}^{(2)}$, γ_2^Q and $\gamma_{\mathrm{cusp}}^{(2)}(v)$ are the second-order perturbative coefficients of the anomalous dimension functions $\gamma_{\mathrm{cusp}}(\alpha_{\mathrm{S}})$, $\gamma^Q(\alpha_{\mathrm{S}})$ and $\gamma_{\mathrm{cusp}}(v;\alpha_{\mathrm{S}})$ respectively, with the following normalisation of the perturbative expansion:

$$\gamma_{\mathrm{cusp}}(\alpha_{\mathrm{S}}) = \sum_{n=1}^{\infty}\left(\frac{\alpha_{\mathrm{S}}}{\pi}\right)^n\,\gamma_{\mathrm{cusp}}^{(n)}\,, \tag{4.34}$$

$$\gamma_{\mathrm{cusp}}(v;\alpha_{\mathrm{S}}) = \sum_{n=1}^{\infty}\left(\frac{\alpha_{\mathrm{S}}}{\pi}\right)^n\,\gamma_{\mathrm{cusp}}^{(n)}(v)\,, \tag{4.35}$$

$$\gamma^Q(\alpha_{\mathrm{S}}) = \sum_{n=1}^{\infty}\left(\frac{\alpha_{\mathrm{S}}}{\pi}\right)^n\,\gamma_n^Q\,. \tag{4.36}$$

The second-order cusp anomalous dimension coefficient $\gamma^{(2)}_{\rm cusp}$ for the massless quarks and gluons is computed in Ref. [146]

$$\gamma^{(2)}_{\rm cusp} = \left(\frac{67}{36} - \frac{\pi^2}{12}\right) C_A - \frac{5}{9}\, T_R\, N_f\,. \tag{4.37}$$

For the massive partons the cusp anomalous dimension $\gamma_{\rm cusp}(v;\alpha_{\rm S})$ depends also on the relative velocity v, and its second-order coefficient $\gamma^{(2)}_{\rm cusp}(v)$ can be written as [147]

$$\begin{aligned}
\gamma^{(2)}_{\rm cusp}(v) =& \gamma^{(2)}_{\rm cusp}\, \frac{1}{v}\left[\frac{1}{2}\ln\left(\frac{1+v}{1-v}\right) - i\pi\right] \\
&+ \frac{C_A}{2}\Bigg\{\frac{1}{4}\ln^2\left(\frac{1+v}{1-v}\right) - \frac{5}{6}\pi^2 + \zeta_3 - i\pi\ln\left(\frac{1+v}{1-v}\right) \\
&\quad + \frac{1}{v^2}\Bigg[\mathrm{Li}_3\left(\frac{1-v}{1+v}\right) + \frac{1}{2}\ln\left(\frac{1+v}{1-v}\right)\mathrm{Li}_2\left(\frac{1-v}{1+v}\right) \\
&\qquad + \frac{1}{24}\ln^3\left(\frac{1+v}{1-v}\right) - \frac{5}{12}\pi^2\ln\left(\frac{1+v}{1-v}\right) - \zeta_3 \\
&\qquad + i\pi\left(-\mathrm{Li}_2\left(\frac{1-v}{1+v}\right) - \frac{1}{4}\ln^2\left(\frac{1+v}{1-v}\right) + \frac{\pi^2}{6}\right)\Bigg] \\
&\quad + \frac{1}{v}\Bigg[-\frac{1}{24}\ln^3\left(\frac{1+v}{1-v}\right) + \mathrm{Li}_2\left(\frac{1-v}{1+v}\right) - \frac{1}{4}\ln^2\left(\frac{1+v}{1-v}\right) \\
&\qquad - \ln\left(\frac{1+v}{1-v}\right)\ln\left(\frac{2v}{1+v}\right) + \frac{5}{12}\pi^2\ln\left(\frac{1+v}{1-v}\right) + \frac{5}{6}\pi^2 \\
&\qquad + i\pi\left(\frac{1}{4}\ln^2\left(\frac{1+v}{1-v}\right) + \ln\left(\frac{1+v}{1-v}\right) + 2\ln\left(\frac{2v}{1+v}\right) - \frac{\pi^2}{6}\right)\Bigg]\Bigg\},
\end{aligned} \tag{4.38}$$

where the Riemann ζ function $\zeta_3 = 1.202\ldots$ and $\mathrm{Li}_3(z) = -\int_0^z \frac{dt}{t}\,\ln(t)\ln(1-zt)$ is the usual polylogarithm function.

The second-order massive quark (anti-quark) anomalous dimension γ_2^Q in Eq. (4.33) is [147]

$$\gamma_2^Q = \frac{1}{16}\left[C_F C_A\left(\frac{2}{3}\pi^2 - \frac{98}{9} - 4\zeta_3\right) + \frac{40}{9} T_R C_F N_f\right], \tag{4.39}$$

and the $g(v)$ function can be written as [145]

$$\begin{aligned} g(v) = &-\frac{1}{4}\ln^2\left(\frac{1+v}{1-v}\right)+\frac{5}{6}\pi^2+i\pi\ln\left(\frac{1+v}{1-v}\right) \\ &+\frac{1}{v}\left[-\mathrm{Li}_2\left(\frac{1-v}{1+v}\right)+\frac{1}{4}\ln^2\left(\frac{1+v}{1-v}\right)+\ln\left(\frac{2v}{1+v}\right)\ln\left(\frac{1+v}{1-v}\right)-\frac{5}{6}\pi^2\right. \\ &\left.-i\pi\left(2\ln\left(\frac{2v}{1+v}\right)+\ln\left(\frac{1+v}{1-v}\right)\right)\right]. \end{aligned} \tag{4.40}$$

As already mentioned, the colour matrix $\mathbf{\Gamma}_t^{(2)}$ also controls the two-loop divergences of $\widetilde{\mathbf{I}}_{Q\bar{Q}}^{(2)}$. The finite terms of $\widetilde{\mathbf{I}}_{Q\bar{Q}}^{(2)}$, however, are determined by a second-order coefficient $\mathbf{F}_t^{(2)}$, which, together with the second-order coefficient $\mathbf{D}^{(2)}$, are not known at present. These coefficients cannot be derived from known results and need to be explicitly calculated.

4.2 Decomposition in azimuthal structures

In this section we present a decomposition of the resummed cross section in different azimuthal structures. The aim of such a decomposition is to make explicit the origin of azimuthal correlations and their potential contribution to the azimuthally-averaged cross section. To that purpose, we recall the definition of the azimuthally-averaged cross section

$$\begin{aligned} \Big\langle\frac{d\sigma_{h_1h_2\to Q\bar{Q}+X}(s;\mathbf{q_T},y,M,\mathbf{\Omega})}{d^2\mathbf{q_T}\,dM^2\,dy\,d\mathbf{\Omega}}\Big\rangle_\phi &\equiv \int_0^{2\pi}\frac{d\phi(\mathbf{q_T})}{2\pi}\,\frac{d\sigma_{h_1h_2\to Q\bar{Q}+X}}{d^2\mathbf{q_T}\,dM^2\,dy\,d\mathbf{\Omega}} \\ &= \frac{1}{\pi}\,\frac{d\sigma_{h_1h_2\to Q\bar{Q}+X}(s;q_T^2,y,M,\mathbf{\Omega})}{dq_T^2\,dM^2\,dy\,d\mathbf{\Omega}}, \end{aligned} \tag{4.41}$$

and we denote the singular component of the azimuthally-averaged cross section (4.41) as $[d\sigma_{Q\bar{Q}}]_\phi$. To make the presentation more explicit, we introduce the following decomposition of the singular component of the cross section:

$$[d\sigma_{Q\bar{Q}}] = [d\sigma_{Q\bar{Q}}]_\phi + [d\sigma_{Q\bar{Q}}]_{\mathrm{corr}}\,, \tag{4.42}$$

where by $[d\sigma_{Q\bar{Q}}]_\phi$ we have denoted the contribution to the resummed q_T cross section that does not depend on $\phi(\mathbf{q_T})$, and it coincides with the azimuthally-averaged cross section, while $[d\sigma_{Q\bar{Q}}]_{\mathrm{corr}}$ embodies all the dependence on the azimuthal angle $\phi(\mathbf{q_T})$. We note that

the azimuthal average over $\phi(\mathbf{q_T})$ of the singular component can be realized in the $\mathbf{b}$ space

$$
\begin{aligned}
[d\sigma_{Q\bar{Q}}]_\phi \equiv \int_0^{2\pi} \frac{d\phi(\mathbf{q_T})}{2\pi} [d\sigma_{Q\bar{Q}}] &= \frac{M^2}{s} \int_0^{2\pi} \frac{d\phi(\mathbf{q_T})}{2\pi} \int \frac{d^2\mathbf{b}}{(2\pi)^2}\; e^{i\mathbf{b}\cdot\mathbf{q_T}}\; W^{Q\bar{Q}}(s;\mathbf{b},y,M,\mathbf{\Omega}) \\
&= \frac{M^2}{s} \int \frac{d^2\mathbf{b}}{(2\pi)^2} \int_0^{2\pi} \frac{d\phi(\mathbf{q_T})}{2\pi}\; e^{i\mathbf{b}\cdot\mathbf{q_T}}\; W^{Q\bar{Q}}(s;\mathbf{b},y,M,\mathbf{\Omega}) \\
&= \frac{M^2}{s} \int_0^{\infty} db\, \frac{b}{2\pi}\, J_0(bq_T) \int_0^{2\pi} \frac{d\phi(\mathbf{b})}{2\pi}\; W^{Q\bar{Q}}(s;\mathbf{b},y,M,\mathbf{\Omega}) \\
&\equiv \frac{M^2}{s} \int_0^{\infty} db\, \frac{b}{2\pi}\, J_0(bq_T)\; \Big[W^{Q\bar{Q}}(s;\mathbf{b},y,M,\mathbf{\Omega})\Big]^{\phi(\mathbf{b})}\;.
\end{aligned}
\tag{4.43}
$$

Owing to the fact that the dependence of the resummed cross section in Eq. (4.5) on the azimuth $\phi(\mathbf{b})$ is completely embodied in the symbolic factor $[(\mathbf{H}\,\mathbf{\Delta})\,C_1C_2]_{c\bar{c};a_1a_2}$, the azimuthally-averaged resummed cross section $[d\sigma_{Q\bar{Q}}]_\phi$ can be obtained with the following replacements:

$$
\int \frac{d^2\mathbf{b}}{(2\pi)^2}\; e^{i\mathbf{b}\cdot\mathbf{q_T}} \to \int_0^{\infty} db\, \frac{b}{2\pi}\, J_0(bq_T)\,, \tag{4.44}
$$

$$
[(\mathbf{H}\,\mathbf{\Delta})\,C_1C_2]_{c\bar{c};a_1a_2} \to [(\mathbf{H}\,\mathbf{\Delta})\,C_1C_2]^{\phi(\mathbf{b})}_{c\bar{c};a_1a_2}\;, \tag{4.45}
$$

where $[(\mathbf{H}\,\mathbf{\Delta})\,C_1C_2]^{\phi(\mathbf{b})}_{c\bar{c};a_1a_2}$ is the azimuthal-average of $[(\mathbf{H}\,\mathbf{\Delta})\,C_1C_2]_{c\bar{c};a_1a_2}$ in $\mathbf{b}$ space

$$
[(\mathbf{H}\,\mathbf{\Delta})\,C_1C_2]^{\phi}_{c\bar{c};a_1a_2} = \int_0^{2\pi} \frac{d\phi(\mathbf{b})}{2\pi}\, [(\mathbf{H}\,\mathbf{\Delta})\,C_1C_2]_{c\bar{c};a_1a_2}\;. \tag{4.46}
$$

Therefore, the decomposition of the singular cross section in Eq. (4.42) implies a corresponding decomposition of the $[(\mathbf{H}\,\mathbf{\Delta})\,C_1C_2]_{c\bar{c};a_1a_2}$ factor in the $\mathbf{b}$ space:

$$
[(\mathbf{H}\,\mathbf{\Delta})\,C_1C_2]_{c\bar{c};a_1a_2} = [(\mathbf{H}\,\mathbf{\Delta})\,C_1C_2]^{\phi(\mathbf{b})}_{c\bar{c};a_1a_2} + [(\mathbf{H}\,\mathbf{\Delta})\,C_1C_2]^{\rm corr}_{c\bar{c};a_1a_2}\;. \tag{4.47}
$$

To highlight the structural differences of the $q\bar{q}$ annihilation and gluon fusion channels, we separate these contributions and write

$$
[d\sigma_{Q\bar{Q}}] = [d\sigma_{Q\bar{Q}}]^{q\bar{q}} + [d\sigma_{Q\bar{Q}}]^{gg}\,. \tag{4.48}
$$

In the case of the $[d\sigma_{Q\bar{Q}}]^{q\bar{q}}$ cross section the only dependence on the azimuth $\phi(\mathbf{b})$ is due to the soft radiation factor $\mathbf{D}$. Using Eq. (4.26), we see that the azimuthal average in Eq. (4.46) is equivalent to setting $\mathbf{D} = 1$ in Eq. (4.13). Explicitly, at all orders in $\alpha_{\rm S}$ the $[(\mathbf{H}\,\mathbf{\Delta})\,C_1C_2]^{\phi(\mathbf{b})}_{q\bar{q};a_1a_2}$ factor is given by

$$
[(\mathbf{H}\,\mathbf{\Delta})\,C_1C_2]^{\phi(\mathbf{b})}_{q\bar{q};a_1a_2} = \Big[\Big(\mathbf{H}\,\mathbf{V}^\dagger\,\mathbf{V}\Big)\,C_1C_2\Big]_{q\bar{q};a_1a_2}\;, \tag{4.49}
$$

while the azimuthal correlation contribution $[(\mathbf{H}\,\mathbf{\Delta})\,C_1C_2]^{\rm corr}_{q\bar{q};a_1a_2}$ is given by

$$
[(\mathbf{H}\,\mathbf{\Delta})\,C_1C_2]^{\rm corr}_{q\bar{q};a_1a_2} = \Big[\Big(\mathbf{H}\,\mathbf{V}^\dagger\,(\mathbf{D}-1)\,\mathbf{V}\Big)\,C_1C_2\Big]_{q\bar{q};a_1a_2}\;, \tag{4.50}
$$

where $\mathbf{V}$ is defined in Eq. (4.14). Explicitly, the symbolic factor $[(\mathbf{H}\,\mathbf{J})\,C_1C_2]_{q\bar{q};a_1a_2}$ ($\mathbf{J} = \mathbf{H}\,\mathbf{V}^\dagger\,\mathbf{V}$, $\mathbf{H}\,\mathbf{V}^\dagger\,(\mathbf{D}-1)\,\mathbf{V}$) reads

$$[(\mathbf{H}\,\mathbf{J})\,C_1C_2]_{q\bar{q};a_1a_2} = \frac{\langle\widetilde{\mathcal{M}}_{q\bar{q}\to Q\bar{Q}}\mid\mathbf{J}\mid\widetilde{\mathcal{M}}_{q\bar{q}\to Q\bar{Q}}\rangle}{\alpha_{\rm S}^2(M^2)\;|\mathcal{M}^{(0)}_{q\bar{q}\to Q\bar{Q}}(p_1,p_2;p_3,p_4)|^2}\,C_{qa_1}(z_1;\alpha_{\rm S}(b_0^2/b^2))\,C_{\bar{q}a_2}(z_2;\alpha_{\rm S}(b_0^2/b^2))\,. \tag{4.51}$$

The situation is much more involved in the gluon fusion channel, due to the additional azimuthal correlations of collinear origin. The azimuthally-averaged contribution can be symbolically written as

$$\begin{aligned}[(\mathbf{H}\,\mathbf{\Delta})\,C_1C_2]^{\phi(\mathbf{b})}_{gg;a_1a_2} &= \Big[\Big(\mathbf{H}\,\mathbf{V}^\dagger\,\mathbf{V}\Big)\,C_1C_2\Big]^{C_1C_2}_{gg;a_1a_2} \\ &+ \Big\{\Big[\Big(\mathbf{H}\,\mathbf{V}^\dagger\,\mathbf{V}\Big)\,C_1C_2\Big]^{(G_1G_2)}_{gg;a_1a_2}\Big\}^{\phi(\mathbf{b})} \\ &+ \Big\{\Big[\Big(\mathbf{H}\,\mathbf{V}^\dagger\,(\mathbf{D}-1)\,\mathbf{V}\Big)\,C_1C_2\Big]^{(C_1G_2)}_{gg;a_1a_2}\Big\}^{\phi(\mathbf{b})} + \Big\{\Big[\Big(\mathbf{H}\,\mathbf{V}^\dagger\,(\mathbf{D}-1)\,\mathbf{V}\Big)\,C_1C_2\Big]^{(G_1C_2)}_{gg;a_1a_2}\Big\}^{\phi(\mathbf{b})} \\ &+ \Big\{\Big[\Big(\mathbf{H}\,\mathbf{V}^\dagger\,(\mathbf{D}-1)\,\mathbf{V}\Big)\,C_1C_2\Big]^{(G_1G_2)}_{gg;a_1a_2}\Big\}^{\phi(\mathbf{b})}\,,\end{aligned} \tag{4.52}$$

while for the azimuthal correlation contribution we write

$$\begin{aligned}[(\mathbf{H}\,\mathbf{\Delta})\,C_1C_2]^{\rm corr}_{gg;a_1a_2} &= \Big[\Big(\mathbf{H}\,\mathbf{V}^\dagger\,(\mathbf{D}-1)\,\mathbf{V}\Big)\,C_1C_2\Big]^{(C_1C_2)}_{gg;a_1a_2} \\ &+ \Big[\Big(\mathbf{H}\,\mathbf{V}^\dagger\,\mathbf{V}\Big)\,C_1C_2\Big]^{(C_1G_2)}_{gg;a_1a_2} + \Big[\Big(\mathbf{H}\,\mathbf{V}^\dagger\,\mathbf{V}\Big)\,C_1C_2\Big]^{(G_1C_2)}_{gg;a_1a_2} \\ &+ \Big\{\Big[\Big(\mathbf{H}\,\mathbf{V}^\dagger\,(\mathbf{D}-1)\,\mathbf{V}\Big)\,C_1C_2\Big]^{(C_1G_2)}_{gg;a_1a_2}\Big\}^{\rm corr} + \Big\{\Big[\Big(\mathbf{H}\,\mathbf{V}^\dagger\,(\mathbf{D}-1)\,\mathbf{V}\Big)\,C_1C_2\Big]^{(G_1C_2)}_{gg;a_1a_2}\Big\}^{\rm corr} \\ &+ \Big\{\Big[\Big(\mathbf{H}\,\mathbf{V}^\dagger\,\mathbf{V}\Big)\,C_1C_2\Big]^{(G_1G_2)}_{gg;a_1a_2}\Big\}^{\rm corr} + \Big\{\Big[\Big(\mathbf{H}\,\mathbf{V}^\dagger\,(\mathbf{D}-1)\,\mathbf{V}\Big)\,C_1C_2\Big]^{(G_1G_2)}_{gg;a_1a_2}\Big\}^{\rm corr}.\end{aligned} \tag{4.53}$$

The notation in Eqs. (4.52) and (4.53) is a bit complicated and needs to be explained. First of all, the factors $[(\mathbf{J})\,C_1C_2]^I_{gg;a_1a_2}$ (I is $I = (C_1C_2)$, (C_1G_2), (G_1C_2), (G_1G_2) and $\mathbf{J}$ is $\mathbf{J} = \mathbf{H}\,\mathbf{V}^\dagger\,\mathbf{V}$, $\mathbf{H}\,\mathbf{V}^\dagger\,(\mathbf{D}-1)\,\mathbf{V}$) can be written as follows:

$$[(\mathbf{J})\,C_1C_2]^I_{gg;a_1a_2} = (\mathbf{J})_{gg;\mu_1\,\nu_1,\mu_2\,\nu_2}\;[I]^{\mu_1\,\nu_1,\mu_2\,\nu_2}_{gg;a_1a_2}\;, \tag{4.54}$$

with

$$(\mathbf{J})_{gg;\mu_1\,\nu_1,\mu_2\,\nu_2} = \frac{\langle\widetilde{\mathcal{M}}^{\nu_1'\nu_2'}_{gg\to Q\bar{Q}}\mid\mathbf{J}\mid\widetilde{\mathcal{M}}^{\mu_1'\mu_2'}_{gg\to Q\bar{Q}}\rangle\;d_{\mu_1'\mu_1}\;d_{\nu_1'\nu_1}\;d_{\mu_2'\mu_2}\;d_{\nu_2'\nu_2}}{\alpha_{\rm S}^2(M^2)\;|\mathcal{M}^{(0)}_{gg\to Q\bar{Q}}(p_1,p_2;p_3,p_4)|^2}\,, \tag{4.55}$$

and the symbolic factor $[I]^{\mu_1\,\nu_1,\mu_2\,\nu_2}_{gg;a_1a_2}$ has the following explicit form for different configurations

$$[C_1C_2]^{\mu_1\,\nu_1,\mu_2\,\nu_2}_{gg;a_1a_2} = d^{\,\mu_1\,\nu_1}(p_1,p_2)\;d^{\,\mu_2\,\nu_2}(p_1,p_2)\;C_{g\,a_1}(z;\alpha_{\rm S})\;C_{g\,a_2}(z;\alpha_{\rm S})\,, \tag{4.56}$$

$$[C_1G_2]^{\mu_1\,\nu_1,\mu_2\,\nu_2}_{gg;a_1a_2} = d^{\,\mu_1\,\nu_1}(p_1,p_2)\;D^{\,\mu_1\,\nu_2}(p_1,p_2;\mathbf{b})\;C_{g\,a_1}(z;\alpha_{\rm S})\;G_{g\,a_2}(z;\alpha_{\rm S})\,, \tag{4.57}$$

$$[G_1C_2]^{\mu_1\,\nu_1,\mu_2\,\nu_2}_{gg;a_1a_2} = D^{\,\mu_1\,\nu_1}(p_1,p_2;\mathbf{b})\;d^{\,\mu_2\,\nu_2}(p_1,p_2)\;G_{g\,a_1}(z;\alpha_{\rm S})\;C_{g\,a_2}(z;\alpha_{\rm S})\,, \tag{4.58}$$

$$[G_1G_2]^{\mu_1\,\nu_1,\mu_2\,\nu_2}_{gg;a_1a_2} = D^{\,\mu_1\,\nu_1}(p_1,p_2;\mathbf{b})\;D^{\,\mu_2\,\nu_2}(p_1,p_2;\mathbf{b})\;G_{g\,a_1}(z;\alpha_{\rm S})\;G_{g\,a_2}(z;\alpha_{\rm S})\,, \tag{4.59}$$

where the Lorentz tensors $d^{\mu\,\nu}$ and $D^{\mu\,\nu}$ are given in Eqs. (3.95) and (3.96), respectively.

Furthermore, the notation $\Big\{ [\dots] \Big\}^{\phi(\mathbf{b})}$ means that the azimuthal average over $\phi(\mathbf{b})$ is taken

$$\Big\{ [\dots] \Big\}^{\phi(\mathbf{b})} = \int_0^{2\pi} \frac{d\phi(\mathbf{b})}{2\pi} [\dots] \,, \tag{4.60}$$

while the notation $\Big\{ [\dots] \Big\}^{\rm corr}$ is defined as follows:

$$\Big\{ [\dots] \Big\}^{\rm corr} = [\dots] - \Big\{ [\dots] \Big\}^{\phi(\mathbf{b})} \,. \tag{4.61}$$

In the following subsections we provide some details on the azimuthally-averaged and azimuthal correlation contributions to the resummed cross section.

4.2.1 q_T-dependent azimuthal correlations

Having set the notation in the previous section, let us now consider the azimuthal correlation contributions of Eqs. (4.50) and (4.53). To illustrate the singular behaviour of the azimuthal correlations at small q_T, we expand the resummation formula in powers of $\alpha_{\rm S} = \alpha_{\rm S}(\mu_R^2)$. We first consider the azimuthal correlations of the gluon fusion cross section due to the collinear splitting, which are given on the second line of Eq. (4.53). Performing the Fourier transform from $\mathbf{b}$ space to $\mathbf{q_T}$ space we get that at relative order $\alpha_{\rm S}$ these contributions lead to a singular behaviour similar to Eq. (3.115). Explicitly, at the partonic level we get

$$\Sigma^{\rm corr}_{\rm coll} = \frac{\alpha_{\rm S}}{\pi} \Big[d\sigma^{(0)}_{c\bar{c},\,Q\bar{Q}} \Big] \; \delta(1-z_1) \; \delta_{g\,a_1} \; G^{(1)}_{g\,a_2}(z_2) \; \Big[H^{Q\bar{Q}}(\phi(\mathbf{q_T})) \Big]_{C_1 G_2} \; \frac{1}{q_T^2} \,, \tag{4.62}$$

where the factor $\Big[H^{Q\bar{Q}}(\phi(\mathbf{q_T})) \Big]_{C_1 G_2}$ is defined as in Eq. (3.112)

$$\Big[H^{Q\bar{Q}}(\phi_3 - \phi(\mathbf{q_T})) \Big]_{C_1 G_2} = - \, H^{Q\bar{Q}}_{gg;\mu_1\,\nu_1,\mu_2\,\nu_2}(p_1,p_2;\mathbf{\Omega};\alpha_{\rm S}(M^2)) \; d^{\,\mu_1\,\nu_1}(p_1,p_2) \; D^{\,\mu_2\,\nu_2}(p_1,p_2;\mathbf{q_T}) \,, \tag{4.63}$$

and $H^{Q\bar{Q}}_{gg;\mu_1\,\nu_1,\mu_2\,\nu_2}$ is defined as

$$H^{Q\bar{Q}}_{gg;\mu_1\,\nu_1,\mu_2\,\nu_2} = \frac{\langle \widetilde{\mathcal{M}}^{\nu_1'\nu_2'}_{gg\to Q\bar{Q}} \,|\, \widetilde{\mathcal{M}}^{\mu_1'\mu_2'}_{gg\to Q\bar{Q}} \rangle \; d_{\mu_1'\mu_1} \; d_{\nu_1'\nu_1} \; d_{\mu_2'\mu_2} \; d_{\nu_2'\nu_2}}{\alpha_{\rm S}^2(M^2) \; |\mathcal{M}^{(0)}_{gg\to Q\bar{Q}}(p_1,p_2;p_3,p_4)|^2} \,. \tag{4.64}$$

Note that even though the Lorentz tensor $D^{\,\mu_2\,\nu_2}(p_1,p_2;\mathbf{q_T})$ depends on the azimuth of the heavy-quark pair $\phi(\mathbf{q_T})$ the hard-scattering factor $\Big[H^{Q\bar{Q}}(\phi_3 - \phi(\mathbf{q_T})) \Big]_{C_1 G_2}$ in Eq. (4.63) retains an azimuthal correlation on $(\phi_3 - \phi(\mathbf{q_T}))$. The dependence on $(\phi_3 - \phi(\mathbf{q_T}))$ is produced

by the combination of the $\phi(\mathbf{q_T})$ dependence of the Lorentz tensor $D^{\mu_2\,\nu_2}(p_1,p_2;\mathbf{q_T})$ with the $\mathbf{\Omega}$-dependence (in particular ϕ_3-dependence) of $H^{Q\bar{Q}}(p_1,p_2;\mathbf{\Omega};\alpha_{\rm S}(M^2)$. As we discuss in Chapter 6, this is valid not only for the heavy-quark production, but it holds in general. Moreover, if the multidifferential cross section is insensitive to the azimuthal angles ϕ_i of the produced particles, like, for instance, for the inclusive production of the SM Higgs boson, the corresponding hard-scattering factors $\Big[H^F(\phi(\mathbf{q_T}))\Big]_I$ ($I = C_1G_2$, G_1C_2, G_1G_2) in Eqs. (3.112)–(3.114) vanish order-by-order in pertrubation theory.

The explicit expression of the $\Big[H^{Q\bar{Q}}(\phi_3-\phi(\mathbf{q_T}))\Big]_{C_1G_2}$ factor is

$$\Big[H^{Q\bar{Q}}(\phi_3-\phi(\mathbf{q_T}))\Big]_{C_1G_2} = -\frac{128\,\pi^3\,(N_c^2-1)\,((N_c^2-1)\,\hat{s}^2-2N_c^2\,t_1\,u_1)}{N_c\,t_1^2\,u_1^2\,|\mathcal{M}^{(0)}_{gg\to Q\bar{Q}}|^2}\,m^2\,\mathbf{p_T^2}\cos(2(\phi_3-\phi(\mathbf{q_T}))\,, \tag{4.65}$$

where we have used

$$\hat{s}=2(p_1\cdot p_2)\,,\quad u_1=-2(p_2\cdot p_3)\,,\quad t_1=-2(p_1\cdot p_3)\,. \tag{4.66}$$

As we see from Eq. (4.65), the dependence of $\Big[H^{Q\bar{Q}}(\phi_3-\phi(\mathbf{q_T}))\Big]_{C_1G_2}$ on the relative angle $(\phi_3-\phi(\mathbf{q_T}))$ is very simple, it is just given by $\cos(2(\phi_3-\phi(\mathbf{q_T}))$, which is consistent with the expectation of Eq. (3.112).

As in the case of the production of a colourless final state, the azimuthal correlations due to the collinear splitting arise only in the gluon fusion cross section. In the case of heavy-quark production both the $q\bar{q}$ annihilation and the gluon fusion cross section receive analogous azimuthally-correlated contributions (see Eq. (4.50) and the first term on the right-hand side of Eq. (4.53)) due to the soft large-angle radiation from the heavy quarks. From technical point of view, these contributions are easier to compute directly in the $\mathbf{q_T}$ space. At relative order $\alpha_{\rm S}$ we have

$$\Sigma^{\rm corr}_{\rm soft}=\frac{\alpha_{\rm S}}{\pi}\Big[d\sigma^{(0)}_{c\bar{c},\,Q\bar{Q}}\Big]\;\delta(1-z_1)\,\delta(1-z_2)\,\delta_{c\,a_1}\,\delta_{\bar{c}\,a_2}\,\frac{\langle\widetilde{\mathcal{M}}_{c\bar{c}\to Q\bar{Q}}\,|\,\mathbf{D}^{(1)}(\phi_3-\phi(\mathbf{q_T}))\,|\,\widetilde{\mathcal{M}}_{c\bar{c}\to Q\bar{Q}}\rangle}{\alpha_{\rm S}^2(M^2)\;\mathcal{M}^{(0)}_{c\bar{c}\to Q\bar{Q}}(p_1,p_2;p_3,p_4)|^2}\,\frac{1}{q_T^2}\,, \tag{4.67}$$

where $\mathbf{D}^{(1)}(\phi_3-\phi(\mathbf{q_T}))$ is given as [148]

$$\begin{aligned}\mathbf{D}^{(1)}(\phi_3-\phi(\mathbf{q_T})) = {}& (\mathbf{T}_3^2+\mathbf{T}_4^2)\left[-\frac{m^2}{2\,m_T^2\,(1-\hat{q}_3^2)}\left(1+\frac{\hat{q}_3}{\sqrt{1-\hat{q}_3^2}}\arctan\frac{\hat{q}_3}{\sqrt{1-\hat{q}_3^2}}\right)+\frac{1}{2}\right]\\ &-(\mathbf{T}_3+\mathbf{T}_4)^2\left[\frac{\hat{q}_3}{\sqrt{1-\hat{q}_3^2}}\arctan\frac{\sqrt{1-\hat{q}_3^2}}{\hat{q}_3}-\frac{\pi}{2}\,\frac{|\hat{q}_3|}{\sqrt{1-\hat{q}_3^2}}-\frac{1}{2}\,\ln\frac{m^2}{m_T^2}\right]\\ &-\mathbf{T}_3\cdot\mathbf{T}_4\left(R_{34}(\phi_3-\phi(\mathbf{q_T}))-\frac{1}{2v}\ln\frac{1+v}{1-v}\right)\,,\end{aligned} \tag{4.68}$$

where the auxiliary variable $\hat{q}_3$ is

$$\hat{q}_3 = \frac{\sqrt{\mathbf{p}_\mathbf{T}^2}}{m_T}\,\cos(\phi_3 - \phi(\mathbf{q_T})) = -\frac{\sqrt{\mathbf{p}_\mathbf{T}^2}}{m_T}\,\cos(\phi_4 - \phi(\mathbf{q_T}))\,, \tag{4.69}$$

and the function $R_{34}(\phi_3 - \phi(\mathbf{q_T}))$ has the following explicit form

$$\begin{aligned} R_{34}(\phi_3 - \phi(\mathbf{q_T})) =& \frac{M^2 - 2m^2}{4M^2\, m_T^2\,(\hat{q}_3^2 - 1) + M^4}\left[2M^2\,\frac{\hat{q}_3}{\sqrt{1-\hat{q}_3^2}}\arctan\frac{\hat{q}_3}{\sqrt{1-\hat{q}_3^2}}\right. \\ &\left. + \left(\frac{2(p_1\cdot p_3)(p_2\cdot p_4)}{M^2}\ln\frac{(p_1\cdot p_3)(p_2\cdot p_4)}{(p_2\cdot p_3)(p_1\cdot p_4)} + (3\leftrightarrow 4)\right)\right]. \end{aligned} \tag{4.70}$$

As we see from Eqs. (4.62) and (4.67) both the $q\bar{q}$ annihilation and gg fusion cross section exhibit non-trivial azimuthal correlations at small q_T. As we discuss in Chapter 6, these azimuthal correlations lead to divergent predictions for azimuthal distributions in fixed-order perturbation theory. In the following we present the resummation formula for the azimuthal-correlation cross section $[d\sigma_{Q\bar{Q}}]_{\rm corr}$, while the quantitative results and the accompanying discussion are postponed to Chapter 6. Explicitly, we write

$$[d\sigma_{Q\bar{Q}}]^{\rm corr} = \frac{M^2}{s}\int\frac{d^2\mathbf{b}}{(2\pi)^2}\;e^{i\mathbf{b}\cdot\mathbf{q_T}}\;\Big[W^{Q\bar{Q}}\Big]^{\rm corr}(s;\mathbf{b},y,M,\mathbf{\Omega};\alpha_{\rm S}(\mu_R^2),\mu_R^2,\mu_F^2)\,, \tag{4.71}$$

According to the resummation formalism of Chapter 3, we can write the resummation formula at the partonic level in the Mellin space

$$\begin{aligned} \Big[W^{Q\bar{Q}}_{N_1,N_2}\Big]^{\rm corr}(s;\mathbf{b},y,M,\mathbf{\Omega};\alpha_{\rm S}(\mu_R^2)) =& \sum_{a_1,\,a_2}\Big[\mathcal{W}^{Q\bar{Q}}_{a_1a_2,\,(N_1,N_2)}\Big]^{\rm corr}(M,\mathbf{b},\mathbf{\Omega};\alpha_{\rm S}(\mu_R^2)) \\ &\times\; f_{a_1/h_1,\,N_1}(\mu_F^2)\;f_{a_2/h_2,\,N_2}(\mu_F^2)\,. \end{aligned} \tag{4.72}$$

In the case of the $q\bar{q}$ annihilation cross section, at the first non-trivial order the partonic resummed azimuthal-correlation cross section $\Big[\mathcal{W}^{Q\bar{Q}}_{a_1a_2,\,(N_1,N_2)}\Big]^{\rm corr}_{q\bar{q}}$ can be written as

$$\begin{aligned} \Big[\mathcal{W}^{Q\bar{Q}}_{a_1a_2,\,(N_1,N_2)}\Big]^{\rm corr}_{q\bar{q}} =& \frac{\alpha_{\rm S}(b_0^2/b^2)}{\pi}\Big[d\sigma^{(0)}_{q\bar{q},\,Q\bar{Q}}\Big]\;\exp\Big\{\mathcal{G}_{N_1,N_2}(\alpha_{\rm S},L)\Big\} \\ &\times\delta_{q\,a_1}\;\delta_{\bar{q}\,a_2}\;\frac{\langle\widetilde{\mathcal{M}}^{(0)}_{q\bar{q}\to Q\bar{Q}}\mid\mathbf{V}^\dagger\,\mathbf{D}^{(1)}(\phi_{3b})\,\mathbf{V}\mid\widetilde{\mathcal{M}}^{(0)}_{q\bar{q}\to Q\bar{Q}}\rangle}{\alpha_{\rm S}^2(M^2)\;\mathcal{M}^{(0)}_{q\bar{q}\to Q\bar{Q}}(p_1,p_2;p_3,p_4)|^2}\,, \end{aligned} \tag{4.73}$$

while the corresponding gg fusion cross section $\Big[\mathcal{W}^{Q\bar{Q}}_{a_1a_2,\,(N_1,N_2)}\Big]^{\rm corr}_{gg}$ is given by

$$\begin{aligned}\Big[\mathcal{W}^{Q\bar{Q}}_{a_1a_2,\,(N_1,N_2)}\Big]^{\rm corr}_{gg} &= \frac{\alpha_{\rm S}(b_0^2/b^2)}{\pi}\,\Big[d\sigma^{(0)}_{gg,\,Q\bar{Q}}\Big]\,\exp\Big\{\mathcal{G}_{N_1,N_2}(\alpha_{\rm S},L)\Big\}\\ &\times\Bigg[\delta_{g\,a_1}\,\delta_{g\,a_2}\,\frac{\langle\widetilde{\mathcal{M}}^{(0)}_{gg\to Q\bar{Q}}\,|\,\mathbf{V}^\dagger\,\mathbf{D}^{(1)}(\phi_{3b})\,\mathbf{V}\,|\,\widetilde{\mathcal{M}}^{(0)}_{gg\to Q\bar{Q}}\rangle}{\alpha_{\rm S}^2(M^2)\,\mathcal{M}^{(0)}_{gg\to Q\bar{Q}}(p_1,p_2;p_3,p_4)|^2}\\ &\quad+\delta_{g\,a_1}\,G^{(1)}_{g\,a_2,\,N_2}\,d^{\,\mu_1\,\nu_1}\,D^{\,\mu_2\,\nu_2}(\mathbf{b})\,\frac{\langle\widetilde{\mathcal{M}}^{(0)\,\nu_1'\nu_2'}_{gg\to Q\bar{Q}}\,|\,\mathbf{V}^\dagger\,\mathbf{V}\,|\,\widetilde{\mathcal{M}}^{(0)\,\mu_1'\mu_2'}_{gg\to Q\bar{Q}}\rangle\;d_{\mu_1'\mu_1}\,d_{\nu_1'\nu_1}\,d_{\mu_2'\mu_2}\,d_{\nu_2'\nu_2}}{\alpha_{\rm S}^2(M^2)\,|\mathcal{M}^{(0)}_{gg\to Q\bar{Q}}(p_1,p_2;p_3,p_4)|^2}\\ &\quad+\delta_{g\,a_2}\,G^{(1)}_{g\,a_1,\,N_1}\,d^{\,\mu_2\,\nu_2}\,D^{\,\mu_1\,\nu_1}(\mathbf{b})\,\frac{\langle\widetilde{\mathcal{M}}^{(0)\,\nu_1'\nu_2'}_{gg\to Q\bar{Q}}\,|\,\mathbf{V}^\dagger\,\mathbf{V}\,|\,\widetilde{\mathcal{M}}^{(0)\,\mu_1'\mu_2'}_{gg\to Q\bar{Q}}\rangle\;d_{\mu_1'\mu_1}\,d_{\nu_1'\nu_1}\,d_{\mu_2'\mu_2}\,d_{\nu_2'\nu_2}}{\alpha_{\rm S}^2(M^2)\,|\mathcal{M}^{(0)}_{gg\to Q\bar{Q}}(p_1,p_2;p_3,p_4)|^2}\Bigg]\,,\end{aligned}\tag{4.74}$$

where $\mathcal{G}_{N_1,N_2}(\alpha_{\rm S},L)$ is the universal form factor of Eq. (3.60), the Lorentz tensors $d^{\,\mu\,\nu}(p_1,p_2)$ and $D^{\,\mu\,\nu}(p_1,p_2;\mathbf{b})$ are given by Eqs. (3.95) and (3.96) respectively, and the gluon collinear functions $G^{(1)}_{g\,a}$ ($a=g,\,q$) are presented in Eqs. (3.98) and (3.99).

As we see from Eqs. (4.73) and (4.74), the resummation formulae for the azimuthal-correlation component of the cross section involves the soft anomalous dimension $\mathbf{\Gamma}_t$ contribution embodied in the soft parton factor $\mathbf{V}$, which contributes starting from NLL accuracy. Due to the non-trivial colour correlations, the treatment of the soft anomalous dimension matrices in the numerical computations requires a so-called *diagonalization* procedure, which we present in Section 4.4. The numerical results for the azimuthal-correlation resummed cross section at NLL+NLO accuracy are presented in Section 6.2.

4.2.2 Azimuthally-averaged cross section

We have seen in the beginning of this section that the azimuthally-averaged $q\bar{q}$ annihilation cross section for heavy-quark production is computed by simply setting $\mathbf{D}=1$ in Eq. (4.16). The similar contribution to the gluon fusion cross section is given by the first term on the right-hand side of Eq. (4.52). Performing the contraction over the Lorentz indices, it can be written as the corresponding contribution in the $q\bar{q}$ channel

$$\Big[\Big(\mathbf{H}\,\mathbf{V}^\dagger\,\mathbf{V}\Big)\,C_1C_2\Big]^{C_1C_2}_{gg;a_1a_2} = \frac{\langle\widetilde{\mathcal{M}}_{gg\to Q\bar{Q}}\,|\,\mathbf{V}^\dagger\,\mathbf{V}\,|\,\widetilde{\mathcal{M}}_{gg\to Q\bar{Q}}\rangle}{\alpha_{\rm S}^2(M^2)\,|\mathcal{M}^{(0)}_{gg\to Q\bar{Q}}(p_1,p_2;p_3,p_4)|^2}\,C_{ga_1}(z_1;\alpha_{\rm S}(b_0^2/b^2))\,C_{ga_2}(z_2;\alpha_{\rm S}(b_0^2/b^2))\,.\tag{4.75}$$

The other terms on the right-hand side of Eq. (4.52) are coming from the interference of different contributions. The second term comes from the terms that are quadratic with respect to the tensor $D^{\,\mu_2\,\nu_2}(p_1,p_2;\mathbf{b})$, similarly to the contribution discussed in Section 3.4.

In the following we will refer to this contribution as a collinear-collinear interference term. The terms on the third and fourth lines of Eq. (4.52) are unique of heavy-quark production, and they originate from the additional interference of the soft factor $\mathbf{D}$ with either one (the terms on the third line: we will refer to it as a soft-collinear interference term) or with both (the term on the fourth line) collinear legs. To present the relative order of contribution of these terms we expand the resummation formula in powers of $\alpha_{\rm S} = \alpha_{\rm S}(\mu_R^2)$ and perform the Bessel transformation from b space to q_T space. Due to the fact that the perturbative expansion of both G_{ga} and $(\mathbf{D}-1)$ functions start at $\mathcal{O}(\alpha_{\rm S})$ (see Eqs. (3.97) and (4.16) respectively), the collinear-collinear and soft-collinear interference terms contribute at relative order $\alpha_{\rm S}^2$, while the last term on the right-hand side of Eq. (4.52) contributes starting from the relative order $\alpha_{\rm S}^3$. The contribution from the collinear-collinear interference term is proportional

$$\left(\frac{\alpha_{\rm S}}{\pi}\right)^2 \, G^{(1)}_{g\,a_1}(z_1) \, G^{(1)}_{g\,a_2}(z_2) \, H_G^{Q\bar{Q}} \, \delta(q_T^2) \,, \tag{4.76}$$

while the contribution from the soft-collinear interference terms are proportional to

$$\left(\frac{\alpha_{\rm S}}{\pi}\right)^2 \delta(1-z_1) \, \delta_{g a_1} \, G^{(1)}_{g\,a_2}(z_1) \, H_{\mathbf{D}G}^{Q\bar{Q}} \, \delta(q_T^2) \,, \tag{4.77}$$

and to analogous contribution that is obtained by the exchange $1 \leftrightarrow 2$ of the subscripts.

In accordance with the notations that we introduced in this section, the $H_G^{Q\bar{Q}}$ and $H_{\mathbf{D}G}^{Q\bar{Q}}$ factors are

$$H_G^{Q\bar{Q}} = \int_0^{2\pi} \frac{d\phi(\mathbf{b})}{2\pi} \frac{\langle \widetilde{\mathcal{M}}^{\nu_1'\nu_2'}_{gg\to Q\bar{Q}} \,|\, \widetilde{\mathcal{M}}^{\mu_1'\mu_2'}_{gg\to Q\bar{Q}} \rangle \; d_{\mu_1'\mu_1} \, d_{\nu_1'\nu_1} \, d_{\mu_2'\mu_2} \, d_{\nu_2'\nu_2}}{\alpha_{\rm S}^2(M^2) \; |\mathcal{M}^{(0)}_{gg\to Q\bar{Q}}(p_1,p_2;p_3,p_4)|^2} \; D^{\,\mu_1\,\nu_1}(\mathbf{b}) \; D^{\,\mu_2\,\nu_2}(\mathbf{b}) \,, \tag{4.78}$$

$$H_{\mathbf{D}G}^{Q\bar{Q}} = \int_0^{2\pi} \frac{d\phi(\mathbf{b})}{2\pi} \frac{\langle \widetilde{\mathcal{M}}^{\nu_1'\nu_2'}_{gg\to Q\bar{Q}} \,|\, \mathbf{D}^{(1)}(\phi_{3b}, y_{34}) \,|\, \widetilde{\mathcal{M}}^{\mu_1'\mu_2'}_{gg\to Q\bar{Q}} \rangle \; d_{\mu_1'\mu_1} \, d_{\nu_1'\nu_1} \, d_{\mu_2'\mu_2} \, d_{\nu_2'\nu_2}}{\alpha_{\rm S}^2(M^2) \; |\mathcal{M}^{(0)}_{gg\to Q\bar{Q}}(p_1,p_2;p_3,p_4)|^2} \; d^{\,\mu_1\,\nu_1} \; D^{\,\mu_2\,\nu_2}(\mathbf{b}) \,. \tag{4.79}$$

To compute these integrals we first note that the Lorentz contraction of the scattering amplitudes with the tensor $D^{\,\mu\,\nu}(p_1,p_2;\mathbf{b})$ either vanishes or produces terms proportional to $\cos^2(\phi_3 - \phi(\mathbf{b}))$. The reason is the following: the only Lorentz tensors that appear in the scattering amplitude are $p_i^\mu p_j^\mu$ $(i,j=1,2,3,4)$ and $g^{\mu\nu}$. Moreover, the dependence on p_4^μ can be replaced by p_3^μ due to the momentum conservation. On the other hand, since $D^{\,\mu\,\nu}(p_1,p_2;\mathbf{b})$ is traceless (when multiplied by $g_{\mu\nu}$) and orthogonal to p_1 and p_2, the only Lorentz structure that we can get is $p_{3\,\mu} p_{3\,\nu} D^{\,\mu\,\nu}(p_1,p_2;\mathbf{b})$, which is simply proportional to $\cos^2(\phi_3 - \phi(\mathbf{b}))$. As far as the $H_G^{Q\bar{Q}}$ factor is concerned, therefore, the integration is trivial. We naturally arrive to the same result as in Eq. (3.122):

$$H_G^{Q\bar{Q}}(p_1,p_2;\mathbf{\Omega};\alpha_{\rm S}(M^2)) = H^{Q\bar{Q}}_{g;\,\mu_1\,\nu_1,\mu_2\,\nu_2}(p_1,p_2;\mathbf{\Omega};\alpha_{\rm S}) \; d^{\,\mu_1\,\nu_1\,\mu_2\,\nu_2}_{(4)}(p_1,p_2) \,, \tag{4.80}$$

where the 4th-rank tensor is given in Eq. (3.105).

The integrals involved in the computation of the $H_{\mathbf{D}G}^{Q\bar{Q}}$ factor, on the other hand are highly non-trivial. However, we managed to compute them analytically by finding a proper integral representation for $\mathbf{D}^{(1)}$. The results of the integrals are listed below:

$$I_1 = \int_0^{2\pi} \frac{d\phi_{3b}}{2\pi} \left[\frac{c_{3b}\,\mathrm{arcsinh}(c_{3b})}{\sqrt{1+c_{3b}^2}} - \frac{1}{2}\ln\left(\frac{m_T^2}{m^2}\right)\right] \cos^2(\phi_{3b}) = \frac{1}{4}\left[1 - \frac{1}{a^2}\ln\left(1+a^2\right)\right] , \quad (4.81)$$

$$I_2 = \int_0^{2\pi} \frac{d\phi_{3b}}{2\pi} \left(\mathrm{arcsinh}^2(c_{3b}) + \frac{1}{2}\,\mathrm{Li}_2\left(-\frac{\mathbf{p_T^2}}{m^2}\right)\right) \cos^2(\phi_{3b}) = \frac{1}{4}\left[-1 + \left(1+\frac{1}{a^2}\right)\ln\left(1+a^2\right)\right] , \quad (4.82)$$

$$\begin{aligned} I_3 &= \int_0^{2\pi} \frac{d\phi_{3b}}{2\pi} \frac{1}{2v} \left(L_{34}^{\varphi} - L_{34}\right) \cos^2(\phi_{3b}) \\ &= -\frac{p_3\cdot p_4}{2\,\mathbf{p_T^2}} \left[\frac{1-\sqrt{1-v^2}}{2v}\ln\left(\frac{1+v}{1-v}\right) - \ln\left(\frac{m_T^2}{m^2}\right) - \sqrt{1-\frac{4m_T^2}{M^2}}\ln\left(\frac{1+\sqrt{1-\frac{4m_T^2}{M^2}}}{1-\sqrt{1-\frac{4m_T^2}{M^2}}}\right)\right] \\ &\quad + \frac{1}{4v}\ln\left(\frac{1+v}{1-v}\right) , \end{aligned} \quad (4.83)$$

where $a = \frac{\sqrt{\mathbf{p_T^2}}}{m}$. The integrands in Eqs. (4.81)–(4.83) correspond to the functions multiplying different colour-correlators in Eq. (4.19). Performing the Lorentz contraction and computing the colour-correlated amplitudes, we arrive at the following explicit expressions for $H_G^{Q\bar{Q}}$ and $H_{\mathbf{D}G}^{Q\bar{Q}}$

$$H_G^{Q\bar{Q}} = -64\,\pi^4\,\frac{N_c^2-1}{N_c}\,\frac{\left((N_c^2-1)\,\hat{s}^2 - 2\,N_c^2\,t_1\,u_1\right)}{t_1^2\,u_1^2\,|\mathcal{M}^{(0)}_{gg\to Q\bar{Q}}|^2}\,m^4 , \quad (4.84)$$

$$\begin{aligned} H_{\mathbf{D}G}^{Q\bar{Q}} &= \frac{128\,\pi^4\,N_c^2\,(N_c^2-1)\,(u_1^2+t_1^2)}{t_1^2\,u_1^2\,|\mathcal{M}^{(0)}_{gg\to Q\bar{Q}}|^2}\,m^2\,\mathbf{p_T^2}\,\left(I_3 - 2I_2\right) \\ &\quad - \frac{256\,\pi^4\,(N_c^2-1)\,((N_c^2-1)\,\hat{s}^2 - 2\,N_c^2\,t_1\,u_1)}{N_c\,t_1^2\,u_1^2\,|\mathcal{M}^{(0)}_{gg\to Q\bar{Q}}|^2}\,m^2\,\mathbf{p_T^2}\,\left[2\,C_F\,I_1 - 2\,N_c\,I_2 + (N_c - C_F)\,I_3\right] , \end{aligned} \quad (4.85)$$

We presented the functions that contribute to the azimuthally-averaged cross section due to the interference of the terms that depend on the azimuthal angle. These contributions arise only in the gluon fusion cross section and contribute at the relative order α_S^2. Up to $\mathcal{O}(\alpha_S^2)$ the azimuthally-averaged cross section can be computed by replacing the $[(\mathbf{H}\,\boldsymbol{\Delta})\,C_1C_2]_{c\bar{c};a_1a_2}$ factor by the expressions in Eqs. (4.12) and (4.75). Therefore, to make the presentation simple, in the rest of this Chapter we do the aforementioned replacement (in particular, in the following, when referring to the factor $\boldsymbol{\Delta}$, we will always understand $\boldsymbol{\Delta} = \mathbf{V}^\dagger\,\mathbf{V}$) and at the end we use the results in Eqs (4.65) and (4.85) to complete the final resummation formulae at NNLO for the gluon fusion cross section.

4.3 Colour-space formalism and anomalous dimension matrices

The evolution factor $\mathbf{V}(b, M; y_{34})$ in Eq. (4.14) involves an exponentiation of the soft anomalous dimension operator $\mathbf{\Gamma}_t$, which is expressed in an abstract mathematical form. In this section we present the application of the resummation formula of Eq. (4.6) to numerical calculations. The first step is to derive the explicit form of the soft anomalous dimension operator $\mathbf{\Gamma}_t$ in some colour basis of the partonic amplitudes. As such basis, we choose the s-channel singlet-octet basis, where the $Q\bar{Q}$ pair is either in a colour-singlet or colour-octet state. For the $q\bar{q}$ annihilation process $q_i + \bar{q}_j \to Q_k + \bar{Q}_l$, we therefore choose the following independent colour structures

$$c_1^{q\bar{q}} = \delta_{ij}\,\delta_{kl}\,, \quad c_2^{q\bar{q}} = t^c_{ji}\,t^c_{kl}\,. \tag{4.86}$$

For the gluon fusion process $g_a + g_b \to Q_k + \bar{Q}_l$, we choose the following colour basis

$$c_1^{gg} = \delta^{ab}\,\delta_{kl}\,, \quad c_2^{gg} = if^{abc}\,t^c_{kl}\,, \quad c_3^{gg} = d^{abc}\,t^c_{kl}\,, \tag{4.87}$$

where $i\,, j\,, k\,, l\,, a\,, b$ and c are colour indices.

Following the notations of Ref. [29], the on-shell scattering amplitude $\mathcal{M}_{c\bar{c}\to Q\bar{Q}\{a\}}$ for the partonic process in Eq. (4.7), with a given colour configuration $\{a\}$, can be written as:

$$\mathcal{M}_{\{a\}} = \langle a_1, a_2, a_3, a_4 | \mathcal{M} \rangle\ , \tag{4.88}$$

where $\mathcal{M}$ is an abstract vector in colour space. Since we are interested in colour-singlet amplitudes, we decompose the scattering amplitude into a set of basis colour structures $\{c\}$

$$|\mathcal{M}\rangle = \sum_I \mathcal{M}_i \sum_{\{a\}} (c_i)_{\{a\}}\,|\{a\}\rangle \equiv \mathcal{M}_i\,|c_i\rangle\ . \tag{4.89}$$

Note that the basis vectors defined by Eqs. (4.86), (4.87) and (4.89), are orthogonal but not normalized to 1. For later convenience we define the matrix $\mathbf{C} = |c_i\rangle\,\langle c_i|$ from the inner products of basis vectors. Explicitly, it reads for the $q\bar{q}$ and gg channels:

$$\mathbf{C}_{q\bar{q}} = \sum_{i=1}^{2} |c_i^{q\bar{q}}\rangle\,\langle c_i^{q\bar{q}}| = \frac{N_c}{2}\begin{pmatrix} 2N_c & 0 \\ 0 & C_F \end{pmatrix}\,, \tag{4.90}$$

$$\mathbf{C}_{gg} = \sum_{i=1}^{3} |c_i^{gg}\rangle\,\langle c_i^{gg}| = C_F \begin{pmatrix} 2N_c^2 & 0 & 0 \\ 0 & N_c^2 & 0 \\ 0 & 0 & N_c^2 - 4 \end{pmatrix}\,.$$

The $\mathcal{M}_i$ coefficients in Eq. (4.89) can be projected out by

$$\mathcal{M}_i = \frac{1}{\langle c_i|c_i\rangle}\,\langle c_i|\mathcal{M}\rangle\ , \tag{4.91}$$

and the square of the amplitude, summed over colours, is given as

$$\sum_{\text{colours}} |\mathcal{M}|^2 = \langle\mathcal{M}|\mathcal{M}\rangle = \sum_i (\mathcal{M}_i)^*\mathcal{M}_i\,\langle c_i|c_i\rangle\ . \tag{4.92}$$

Using the projected amplitudes of Eq. (4.91), we can introduce a colour space operator $\alpha_{\text{S}}^2\,|\mathcal{M}^{(0)}|^2\,\mathbf{H} = |\widetilde{\mathcal{M}}\rangle\,\langle\widetilde{\mathcal{M}}|$, with the following matrix representation

$$\alpha_{\text{S}}^2(M^2)\,|\mathcal{M}^{(0)}|^2\,H_{ij} = \frac{1}{\langle c_i|c_i\rangle\,\langle c_j|c_j\rangle}\,\langle c_i|\mathbf{H}|c_j\rangle = \widetilde{\mathcal{M}}_i\,\widetilde{\mathcal{M}}_j^*\,. \tag{4.93}$$

Therefore, according to Eqs. (4.9) and (4.10), the shorthand notation $(\mathbf{H}\,\boldsymbol{\Delta})$ is equivalent to $(\mathbf{H}\,\boldsymbol{\Delta}) = \text{Tr}\,[\mathbf{H}\,\boldsymbol{\Delta}]$, where the matrix elements of $\boldsymbol{\Delta}$ are defined as

$$\boldsymbol{\Delta}_{ij} = \langle c_i|\boldsymbol{\Delta}|c_j\rangle\ , \tag{4.94}$$

and 'Tr' exactly denotes the colour space trace of the colour operator $\mathbf{H}\,\boldsymbol{\Delta}$. The hard-scattering matrix $\mathbf{H}$ admits the following perturbative expansion

$$\alpha_{\text{S}}^2(M^2)\,\mathbf{H}(\alpha_{\text{S}}) = \mathbf{H}^{(0)} + \sum_{n=1}^{\infty}\left(\frac{\alpha_{\text{S}}}{\pi}\right)^n\,\mathbf{H}^{(n)}\,, \tag{4.95}$$

with the leading-order constraint

$$\text{Tr}\left[\mathbf{H}_c^{(0)}\,\mathbf{C}_{c\bar{c}}\right] = 1\,, \qquad c = q, g\,. \tag{4.96}$$

Explicitly, the leading order hard-scattering matrices are

$$\frac{|\widetilde{\mathcal{M}}^{(0)}_{q\bar{q}\to Q\bar{Q}}|^2\,\mathbf{H}_q^{Q\bar{Q}\,(0)}}{64\,\pi^2} = \begin{pmatrix} 0 & 0 \\ 0 & 2 \end{pmatrix}\left[\frac{t_1^2+u_1^2}{M^4} + \frac{2m^2}{M^2}\right]\,, \tag{4.97}$$

$$\frac{|\widetilde{\mathcal{M}}^{(0)}_{gg\to Q\bar{Q}}|^2\,\mathbf{H}_g^{Q\bar{Q}\,(0)}}{64\,\pi^2} = \begin{pmatrix} \frac{1}{N_c^2} & \frac{1}{N_c}\frac{t_1-u_1}{M^2} & \frac{1}{N_c} \\ \frac{1}{N_c}\frac{t_1-u_1}{M^2} & \frac{(t_1-u_1)^2}{M^4} & \frac{t_1-u_1}{M^2} \\ \frac{1}{N_c} & \frac{t_1-u_1}{M^2} & 1 \end{pmatrix}\frac{M^4}{2t_1u_1}\left[\frac{t_1^2+u_1^2}{M^4} + \frac{4m^2}{M^2} - \frac{4m^4}{t_1u_1}\right]\,,$$

where t_1 and u_1 are given in Eq. (4.66). The explicit expression of the first-order hard-scattering matrices $\mathbf{H}_c^{Q\bar{Q}\,(1)}$ is too long to be reported here.

Similarly to Eq. (3.49) we also define the scalar functions $H_c^{Q\bar{Q}}$ $(c = q, g)$

$$H_c^{Q\bar{Q}}(p_1, p_2; \alpha_{\rm S}(M^2)) = \frac{|\widetilde{\mathcal{M}}_{c\bar{c}\to Q\bar{Q}}(p_1, p_2; p_3, p_4)|^2}{\alpha_{\rm S}^2(M^2)|\widetilde{\mathcal{M}}^{(0)}_{c\bar{c}\to Q\bar{Q}}(p_1, p_2; p_3, p_4)|^2}\,, \tag{4.98}$$

which are equivalent to

$$H_c^{Q\bar{Q}} \equiv {\rm Tr}\left[\mathbf{H}_c^{Q\bar{Q}}\,\mathbf{C}_{c\bar{c}}\right]\,. \tag{4.99}$$

Having fixed the colour basis, we can now derive the action of colour-charge operators $\mathbf{T}_i$ on the basis states $|c\rangle$. In particular, we define the matrices $\mathbf{T}_{ij}^{c\bar{c}}$ ($c = q\,, \bar{q}\,, g$ and $i\,, j = 1, \ldots, 4$):

$$\left(\mathbf{T}_{ij}^{c\bar{c}}\right)_{IJ} \equiv [\mathbf{T}_i \cdot \mathbf{T}_j]_{IJ} = \frac{1}{\langle c_I^{c\bar{c}}|c_I^{c\bar{c}}\rangle}\,\langle c_I^{c\bar{c}}|\,\mathbf{T}_i \cdot \mathbf{T}_j\,|c_J^{c\bar{c}}\rangle\,. \tag{4.100}$$

For the quark-antiquark annihilation channel, the results are:

$$\mathbf{T}_{11}^{q\bar{q}} = \mathbf{T}_{22}^{q\bar{q}} = \mathbf{T}_{33}^{q\bar{q}} = \mathbf{T}_{44}^{q\bar{q}} = C_F\mathbf{1}_2\,,$$

$$\mathbf{T}_{12}^{q\bar{q}} = \mathbf{T}_{34}^{q\bar{q}} = -\frac{1}{2N_c}\begin{pmatrix} N_c^2-1 & 0 \\ 0 & -1 \end{pmatrix}\,,$$

$$\mathbf{T}_{13}^{q\bar{q}} = \mathbf{T}_{24}^{q\bar{q}} = -\frac{1}{2N_c}\begin{pmatrix} 0 & C_F \\ 2N_c & N_c^2-2 \end{pmatrix}\,,$$

$$\mathbf{T}_{14}^{q\bar{q}} = \mathbf{T}_{23}^{q\bar{q}} = -\frac{1}{2N_c}\begin{pmatrix} 0 & -C_F \\ -2N_c & 2 \end{pmatrix}\,. \tag{4.101}$$

For the gluon fusion channel we get:

$$\mathbf{T}_{33}^{gg} = \mathbf{T}_{44}^{gg} = C_F \mathbf{1}_3 \,,$$

$$\mathbf{T}_{11}^{gg} = \mathbf{T}_{22}^{gg} = N_c \mathbf{1}_3 \,,$$

$$\mathbf{T}_{12}^{gg} = -\frac{N_c}{2} \begin{pmatrix} 2 & 0 & 0 \\ 0 & 1 & 0 \\ 0 & 0 & 1 \end{pmatrix} ,$$

$$\mathbf{T}_{34}^{gg} = -\frac{1}{2N_c} \begin{pmatrix} N_c^2 - 1 & 0 & 0 \\ 0 & -1 & 0 \\ 0 & 0 & -1 \end{pmatrix} ,$$

$$\mathbf{T}_{13}^{gg} = \mathbf{T}_{13}^{gg} = -\frac{1}{4N_c} \begin{pmatrix} 0 & 2N_c & 0 \\ 4N_c & N_c^2 & N_c^2 - 4 \\ 0 & N_c^2 & N_c^2 \end{pmatrix} ,$$

$$\mathbf{T}_{23}^{gg} = \mathbf{T}_{14}^{gg} = -\frac{1}{4N_c} \begin{pmatrix} 0 & -2N_c & 0 \\ -4N_c & N_c^2 & -(N_c^2 - 4) \\ 0 & -N_c^2 & N_c^2 \end{pmatrix} . \tag{4.102}$$

where $\mathbf{1}_2$ and $\mathbf{1}_3$ are the identity operators in two (for the quark channel), and three (for the gluon channel) dimensions respectively.

Using the matrix representation of colour-charge operators in Eqs. (4.101) and (4.102), we can now write the anomalous dimension operator $\mathbf{\Gamma}_t$ from Eq. (4.15) in an explicit matrix form. For example, for the first-order operator $\mathbf{\Gamma}_t^{(1)}$ in the $q\bar{q}$ channel we get

$$\mathbf{\Gamma}_t^{q\bar{q},\,(1)}(y_{34}) = \Gamma_{\rm s} \begin{pmatrix} 0 & 0 \\ 0 & N_c \end{pmatrix} + \Gamma_{\rm t} \begin{pmatrix} 2C_F & -\frac{C_F}{N_c} \\ -2 & \frac{1}{N_c} \end{pmatrix} + \Gamma_{\rm I}^{q\bar{q}}\, \mathbf{1} \,, \tag{4.103}$$

while in the gg channel the result is

$$\mathbf{\Gamma}_t^{gg,\,(1)}(y_{34}) = \Gamma_{\rm s} \begin{pmatrix} 0 & 0 & 0 \\ 0 & N_c & 0 \\ 0 & 0 & N_c \end{pmatrix} + \Gamma_{\rm t} \begin{pmatrix} N_c + C_F & -1 & 0 \\ -2 & \frac{N_c}{2} + C_F & -\frac{N_c^2-4}{2N_c} \\ 0 & -\frac{N_c}{2} & \frac{N_c}{2} + C_F \end{pmatrix} + \Gamma_{\rm I}^{gg}\,\mathbf{1}\,, \quad (4.104)$$

where the coefficients $\Gamma_{\rm s}$ and $\Gamma_{\rm t}$ depend on the dynamics of the process and are given as follows:

$$\Gamma_{\rm s} = -\frac{1}{4}\left[\frac{1}{2v}\ln\left(\frac{1+v}{1-v}\right) - i\pi\left(\frac{1}{v}+1\right) - \ln\frac{(2p_1\cdot p_4)\,(2p_2\cdot p_3)}{M^2m^2}\right], \quad (4.105)$$

$$\Gamma_{\rm t} = -\frac{1}{4}\ln\frac{(2p_1\cdot p_3)\,(2p_2\cdot p_4)}{(2p_1\cdot p_4)\,(2p_2\cdot p_3)}\,, \quad (4.106)$$

and the matrices in front of $\Gamma_{\rm t}$ and $\Gamma_{\rm s}$ are the t-channel, $\mathbf{T}_t^2 = (\mathbf{T}_1 + \mathbf{T}_3)^2$, and s-channel, $\mathbf{T}_s^2 = (\mathbf{T}_1 + \mathbf{T}_2)^2$, matrices respectively. The $\Gamma_{\rm I}$ coefficients in Eqs. (4.103) and (4.103) are:

$$\Gamma_{\rm I}^{q\bar{q}} = -\frac{C_F}{2}\left(1 - \frac{1}{2v}\left[\ln\left(\frac{1+v}{1-v}\right) - 2i\pi\right] - \ln\frac{(2p_1\cdot p_3)\,(2p_2\cdot p_4)}{(2p_1\cdot p_4)\,(2p_2\cdot p_3)}\right), \quad (4.107)$$

and

$$\Gamma_{\rm I}^{gg} = -\frac{C_F}{2}\left(1 - \frac{1}{2v}\left[\ln\left(\frac{1+v}{1-v}\right) - 2i\pi\right]\right) + \frac{C_A + C_F}{4}\,\ln\frac{(2p_1\cdot p_3)\,(2p_2\cdot p_4)}{(2p_1\cdot p_4)\,(2p_2\cdot p_3)}\,, \quad (4.108)$$

4.4 RG evolution and q_T resummation

Having defined the matrix form of the anomalous dimension matrices in the previous section, we can now express the all-order resummation formula in Eq. (4.6) in factorised form of Eqs. (3.21) and (3.55). In particular, in this section we present in detail how we treat the resummation factor $[\mathbf{H}\,\mathbf{\Delta}]$, which embodies the terms unique of heavy-quark pair production. To parametrize the ambiguities coming from the factorisation of constant and logarithmic terms in Eq. (3.21), due to the factor $[\mathbf{H}\,\mathbf{\Delta}]$, we write the evolution operator $\mathbf{V}(b_0/b, M; y_{34})$ in Eq. (4.14) as

$$\mathbf{V}(b_0/b, M) = \mathbf{V}(b_0/b, Q)\,\mathbf{V}(Q, M)\,, \quad (4.109)$$

where $\mathbf{V}(b_0/b, Q; y_{34})$ is evaluated at some resummation scale $Q \sim M$. Explicitly,

$$\mathbf{V}(b_0/b, Q; y_{34}) = \overline{P}_q \exp\left\{-\int_{b_0^2/b^2}^{Q^2}\frac{dq^2}{q^2}\mathbf{\Gamma}_t(\alpha_{\rm S}(q^2); y_{34})\right\}. \quad (4.110)$$

The operator $\mathbf{V}(b_0/b, Q)$ in Eq. (4.110) satisfies the following evolution equation

$$\frac{d\,\mathbf{V}(b_0/b, Q; y_{34})}{d\,\ln\,(b_0^2/b^2)} = \mathbf{\Gamma}_t(\alpha_{\rm S}(b_0^2/b^2); y_{34})\,\mathbf{V}(b_0/b, Q; y_{34})\,. \tag{4.111}$$

In close analogy to the QCD evolution operator $\mathbf{U}$ (see Appendix C of Ref. [82]), the evolution factor $\mathbf{V}(b_0/b, Q)$ can be written in the following form:

$$\mathbf{V}(b_0/b, Q) = \mathbf{K}(\alpha_{\rm S}(b_0^2/b^2))\,\mathbf{V}^{(\rm LO)}(\alpha_{\rm S}(b_0^2/b^2), \alpha_{\rm S}(Q^2))\,\mathbf{K}^{-1}(\alpha_{\rm S}(Q^2)), \tag{4.112}$$

where the dependence on y_{34} is implicitly understood. The $\mathbf{V}^{(\rm LO)}$ is determined by the lowest-order soft anomalous dimension operator $\mathbf{\Gamma}_t^{(1)}$, while the operator $\mathbf{K}$ retains the information on the higher-order terms $\mathbf{\Gamma}_t^{(n)}$ $(n \geq 2)$. The leading order operator $\mathbf{V}^{(\rm LO)}$ fulfils the following evolution equation

$$\frac{d\,\mathbf{V}^{(\rm LO)}(\alpha_{\rm S}, \alpha'_{\rm S})}{d\,\ln\alpha_{\rm S}} = -\frac{1}{\beta_0}\,\mathbf{\Gamma}_t^{(1)}\,\mathbf{V}^{(\rm LO)}(\alpha_{\rm S}, \alpha'_{\rm S})\,, \tag{4.113}$$

where we denoted $\alpha_{\rm S} = \alpha_{\rm S}(b_0^2/b^2)$ and $\alpha'_{\rm S} = \alpha_{\rm S}(Q^2)$. The general solution to the evolution equation (4.113) is given by:

$$\mathbf{V}^{(\rm LO)}(\alpha_{\rm S}, \alpha'_S) = \exp\left\{-\frac{1}{\beta_0}\mathbf{\Gamma}_t^{(1)}\ln(\alpha_{\rm S})\right\}\widetilde{\mathbf{V}}^{(\rm LO)}\,, \tag{4.114}$$

where $\widetilde{\mathbf{V}}_{\rm LO}$ can be fixed from the initial condition

$$\mathbf{V}^{(\rm LO)}(\alpha'_{\rm S}, \alpha'_{\rm S}) = \mathbf{1}\,, \tag{4.115}$$

which brings us to the following solution for $\mathbf{V}^{(\rm LO)}$,

$$\mathbf{V}^{(\rm LO)}(\alpha_{\rm S}, \alpha'_{\rm S}) = \exp\left\{\frac{1}{\beta_0}\mathbf{\Gamma}_t^{(1)}\ln\left(\frac{\alpha'_{\rm S}}{\alpha_{\rm S}}\right)\right\}\,. \tag{4.116}$$

The operator $\mathbf{K}$ in Eq. (4.112) fulfils the following differential equation:

$$\frac{d\,\mathbf{K}(\alpha_{\rm S})}{d\,\ln\alpha_{\rm S}} = \frac{1}{\beta(\alpha_{\rm S})}\mathbf{\Gamma}_t(\alpha_{\rm S})\,\mathbf{K}(\alpha_{\rm S}) + \frac{1}{\beta_0}\mathbf{K}(\alpha_{\rm S})\,\mathbf{\Gamma}_t^{(1)}\,, \tag{4.117}$$

where $\beta(\alpha_{\rm S})$ is the QCD β function in Eq. (2.26). The Eq. (4.117) can be solved by performing a perturbative expansion,

$$\mathbf{K}(\alpha_{\rm S}) = \mathbf{1} + \sum_{n=1}^{\infty}\left(\frac{\alpha_{\rm S}}{\pi}\right)^n\mathbf{K}^{(n)}\,. \tag{4.118}$$

For example, one gets the following equation for $\mathbf{K}^{(1)}$:

$$\mathbf{K}^{(1)} = -\frac{1}{\beta_0}\left[\mathbf{\Gamma}_t^{(1)}\,\mathbf{K}^{(1)} - \mathbf{K}^{(1)}\,\mathbf{\Gamma}_t^{(1)}\right] + \frac{\beta_1\mathbf{\Gamma}_t^{(1)} - \beta_0\mathbf{\Gamma}_t^{(2)}}{\beta_0^2}\,. \tag{4.119}$$

As one can see from Eqs. (4.103) and (4.104) the first-order anomalous dimension matrix $\mathbf{\Gamma}_t^{(1)}$, is not diagonal in the basis we work. To write the solution of $\mathbf{V}^{(\mathrm{LO})}$ in Eq. (4.116) in an explicit form, we need to diagonalise the anomalous dimension matrix $\mathbf{\Gamma}_t^{(1)}$

$$\mathbf{\Gamma}_t^{(1),\,\mathrm{diag}} = \mathbf{R}^{-1}\,\mathbf{\Gamma}_t^{(1)}\,\mathbf{R}\,, \tag{4.120}$$

where $\mathbf{R}$ is the diagonalising matrix for $\mathbf{\Gamma}_t^{(1)}$, and $\mathbf{\Gamma}_t^{(1),\,\mathrm{diag}}$ is the diagonal anomalous dimension matrix, having the eigenvalues λ_I ($I = 1,\, 2$ for the $q\bar{q}$ channel and $I = 1,\, 2,\, 3$ for the gg channel) as its entries. The explicit expression of the matrix $\mathbf{R}$ and the eigenvalues λ_I are presented in Eqs. (A.1)–(A.3) and (A.6). Using the transformation of Eq. (4.120), Eq. (4.116) can be written as

$$\mathbf{V}^{(\mathrm{LO})}(\alpha_{\mathrm{S}},\alpha_{\mathrm{S}}') = \mathbf{R}\,\overline{\mathbf{V}}^{(\mathrm{LO})}(\alpha_{\mathrm{S}},\alpha_{\mathrm{S}}')\,\mathbf{R}^{-1} = \mathbf{R}\,\exp\left\{\frac{1}{\beta_0}\mathbf{\Gamma}_t^{(1),\,\mathrm{diag}}\ln\left(\frac{\alpha_{\mathrm{S}}'}{\alpha_{\mathrm{S}}}\right)\right\}\mathbf{R}^{-1}\,. \tag{4.121}$$

The transformation in Eq. (4.120) is equivalent to the basis transformation $\{c\} \xrightarrow{\mathbf{R}} \{\bar{c}\}$ as follows

$$|\bar{c}_I\rangle = \sum_j R_{jI}\,|c_j\rangle\ . \tag{4.122}$$

Note that the diagonalising matrix $\mathbf{R}$ is not unitary. As a result, the new basis is not orthogonal, and to write the matrix representation of the soft anomalous operator $\mathbf{\Gamma}_t^{(1)}$ we introduce the so-called dual vectors $|\tilde{c}\rangle$ as

$$|\tilde{c}_I\rangle = \sum_J (\bar{\mathbf{C}}^{-1})_{JI}\,|\bar{c}_J\rangle\ , \tag{4.123}$$

where $\bar{\mathbf{C}}$ is the overlap matrix of the new basis, and is defined analogously to the matrix $\mathbf{C}$ in Eq. (4.90)

$$\bar{\mathbf{C}}_{IJ} = \langle\bar{c}_I|\bar{c}_J\rangle\ . \tag{4.124}$$

It is easy to check that the overlap matrices in the original and diagonal bases are related through the following identity

$$\bar{\mathbf{C}} = \mathbf{R}^{\dagger}\,\mathbf{C}\,\mathbf{R}\,. \tag{4.125}$$

By construction, the dual states $|\tilde{c}\rangle$ and $|\bar{c}\rangle$ obey

$$\langle\tilde{c}_I|\bar{c}_J\rangle = \langle\bar{c}_J|\tilde{c}_I\rangle = \delta_{IJ}\,, \tag{4.126}$$

and, hence, the completeness relation for the new basis has the following form:

$$\sum_I |\tilde{c}_I\rangle\,\langle\bar{c}_I| = \sum_I |\bar{c}_I\rangle\,\langle\tilde{c}_I| = \sum_{I,J} |\bar{c}_I\rangle\,(\bar{\mathbf{C}}^{-1})_{IJ}\,\langle\bar{c}_J| = \mathbf{1}\,. \tag{4.127}$$

Using Eqs. (4.122) and (4.126) we see that the dual vector $\langle\tilde{c}|$ is related to the original vector $\langle c|$ by

$$\langle\tilde{c}_I| = \sum_j \frac{1}{\langle c_j|c_j\rangle}(\mathbf{R}^{-1})_{Ij}\,\langle c_j|\ . \tag{4.128}$$

Having introduced the dual states $\{\tilde{c}\}$, we can now write the matrix representation of the anomalous dimension operator, $\mathbf{\Gamma}_t$, in the new basis,

$$(\overline{\mathbf{\Gamma}}_t)_{IJ} = \langle \tilde{c}_I | \mathbf{\Gamma}_t | \bar{c}_J \rangle \ , \tag{4.129}$$

such that the anomalous dimension matrices, and hence also $\mathbf{K}$, in the diagonal and original bases are related by

$$\begin{aligned} \overline{\mathbf{\Gamma}}_t &= \mathbf{R}^{-1}\, \mathbf{\Gamma}_t\, \mathbf{R}\,, \\ \overline{\mathbf{K}} &= \mathbf{R}^{-1}\, \mathbf{K}\, \mathbf{R}\,, \end{aligned} \tag{4.130}$$

while the operator $\mathbf{H}$ transforms to

$$\mathbf{H} \to \overline{\mathbf{H}} = \mathbf{R}^{-1}\, \mathbf{H}\, (\mathbf{R}^{-1})^\dagger\,, \tag{4.131}$$

with

$$\alpha_{\rm S}^2\, |\mathcal{M}^{(0)}|^2\, \overline{\mathbf{H}}_{IJ} = \widetilde{\mathcal{M}}_I\, \widetilde{\mathcal{M}}_J^* \equiv \langle \tilde{c}_I | \widetilde{\mathcal{M}} \rangle\, \langle \widetilde{\mathcal{M}} | \tilde{c}_J \rangle \ , \tag{4.132}$$

where the hard-scattering matrix $\overline{\mathbf{H}}$ in the diagonal basis admits the same perturbative expansion as $\mathbf{H}$ in Eq. (4.95).

Using Eqs. (4.121) and (4.130), the evolution operator $\mathbf{V}$ can be written as

$$\mathbf{V}(b_0/b, Q) = \mathbf{R}\, \overline{\mathbf{V}}(b_0/b, Q)\, \mathbf{R}^{-1} = \mathbf{R}\, \overline{\mathbf{K}}(\alpha_{\rm S})\, \overline{\mathbf{V}}^{(\rm LO)}(\alpha_{\rm S}, \alpha'_{\rm S})\, \overline{\mathbf{K}}^{-1}(\alpha'_{\rm S})\, \mathbf{R}^{-1}\,. \tag{4.133}$$

The operator equation (4.119) in the diagonal basis has the following form:

$$\overline{\mathbf{K}}^{(1)}_{IJ} = -\frac{1}{\beta_0} \left[\lambda_I\, \overline{\mathbf{K}}^{(1)}_{IJ} - \lambda_J\, \overline{\mathbf{K}}^{(1)}_{IJ} \right] + \frac{\beta_1 \lambda_I \delta_{IJ} - \beta_0 \left(\overline{\mathbf{\Gamma}}^{(2)}_t \right)_{IJ}}{\beta_0^2}\,, \tag{4.134}$$

which leads to the following solution:

$$\overline{\mathbf{K}}^{(1)}_{IJ} = \frac{\beta_1}{\beta_0^2}\, \lambda_I\, \delta_{IJ} - \frac{\left(\overline{\mathbf{\Gamma}}^{(2)}_t \right)_{IJ}}{\beta_0 + \lambda_I - \lambda_J}\,. \tag{4.135}$$

Rewriting $\mathbf{V}(b_0/b, M) = \mathbf{V}(b_0/b, Q)\, \mathbf{V}(Q, M)$, the operator $(\mathbf{H}\, \mathbf{\Delta})$ can be written as

$$(\mathbf{H}\, \mathbf{\Delta}) = {\rm Tr} \left[\overline{\mathbf{V}}^{(\rm LO)}(\alpha_{\rm S}, \alpha'_{\rm S})\, \widetilde{\mathbf{H}}(\alpha'_{\rm S}; Q, M) \left(\overline{\mathbf{V}}^{(\rm LO)}(\alpha_{\rm S}, \alpha'_S) \right)^\dagger \mathbf{S}(\alpha_{\rm S}) \right] , \tag{4.136}$$

where we have defined

$$\widetilde{\mathbf{H}}(\alpha'_{\rm S}; Q, M) \equiv \overline{\mathbf{K}}^{-1}(\alpha'_{\rm S})\, \overline{\mathbf{V}}(Q, M)\, \overline{\mathbf{H}}\, \overline{\mathbf{V}}^\dagger(Q, M)\, (\overline{\mathbf{K}}^{-1}(\alpha'_{\rm S}))^\dagger\,, \tag{4.137}$$

and $\mathbf{S}(\alpha_{\rm S})$ is given as

$$\mathbf{S}(\alpha_{\rm S}) = \left(\overline{\mathbf{K}}(\alpha_{\rm S}) \right)^\dagger \bar{\mathbf{C}}\, \overline{\mathbf{K}}(\alpha_{\rm S})\,. \tag{4.138}$$

The operator $\widetilde{\mathbf{H}}(\alpha_{\rm S}';Q,M)$ in Eq. (4.136) does not depend on the impact parameter $\mathbf{b}$ and can be expanded in powers of $\alpha_{\rm S}(\mu_R^2)$

$$\widetilde{\mathbf{H}}(\alpha_{\rm S}';Q,M)=\widetilde{\mathbf{H}}^{(0)}(M)+\sum_{n=1}^{\infty}\left(\frac{\alpha_{\rm S}(\mu_R^2)}{\pi}\right)^n\widetilde{\mathbf{H}}^{(n)}(Q,M)\,. \tag{4.139}$$

The first- and second-order matrices $\widetilde{\mathbf{H}}^{(0)}$ and $\widetilde{\mathbf{H}}^{(1)}$ are

$$\widetilde{\mathbf{H}}^{(0)}=\overline{\mathbf{H}}^{(0)}\,, \tag{4.140}$$

$$\begin{aligned}\widetilde{\mathbf{H}}^{(1)}=&\overline{\mathbf{H}}^{(1)}-\beta_0\ell_R\overline{\mathbf{H}}^{(0)}-\left(\mathbf{\Gamma}_t^{(1),\,\rm diag}\,\overline{\mathbf{H}}^{(0)}+\overline{\mathbf{H}}^{(0)}\left(\mathbf{\Gamma}_t^{(1),\,\rm diag}\right)^\dagger\right)\ell_Q\\&-\left(\overline{\mathbf{K}}^{\,(1)}\,\overline{\mathbf{H}}^{(0)}+\overline{\mathbf{H}}^{(0)}\left(\overline{\mathbf{K}}^{\,(1)}\right)^\dagger\right),\end{aligned} \tag{4.141}$$

where ℓ_Q and ℓ_R are given in Eq. (3.88).

The contribution from large logarithms is embodied in $\overline{\mathbf{V}}^{(\rm LO)}$ (and its complex conjugate) and in $\mathbf{S}$. In particular, $\overline{\mathbf{V}}^{(\rm LO)}$ explicitly depends on the impact parameter b (see.Eq. (4.121)). Using the techniques discussed in the Chapter 3, the argument of the exponent of $\overline{\mathbf{V}}^{(\rm LO)}$ can be logarithmically expanded, and we write

$$\overline{\mathbf{V}}^{(\rm LO)}=\exp\{\mathcal{G}_{(\rm LO)}(\alpha_{\rm S}(\mu_R^2),L)\}\,, \tag{4.142}$$

with

$$\mathcal{G}_{(\rm LO)}(\alpha_{\rm S},L)=\boldsymbol{g}^{(2)}_{(\rm LO)}(\alpha_{\rm S}L)+\sum_{n=3}^{\infty}\left(\frac{\alpha_{\rm S}}{\pi}\right)^{(n-2)}\boldsymbol{g}^{(n)}_{(\rm LO)}(\alpha_{\rm S}L)\,, \tag{4.143}$$

and the coefficients $\boldsymbol{g}^{(n)}_{(\rm LO)}(\alpha_{\rm S}L)$ are diagonal matrices. Explicitly, the coefficients needed for the NNLL-accurate resummation, $\boldsymbol{g}^{(2)}_{(\rm LO)}$ and $\boldsymbol{g}^{(3)}_{(\rm LO)}$, are

$$\begin{aligned}(\boldsymbol{g}^{(2)}_{(\rm LO)})_{IJ}(\alpha_{\rm S}L)&=\frac{\lambda_I}{\beta_0}\ln(1-\lambda)\delta_{IJ}\,,\\(\boldsymbol{g}^{(3)}_{(\rm LO)})_{IJ}(\alpha_{\rm S}L)&=\lambda_I\left(\frac{\beta_1}{\beta_0^2}\frac{\ln(1-\lambda)}{1-\lambda}+\frac{\lambda}{1-\lambda}\ln\frac{Q^2}{\mu_R^2}\right)\delta_{IJ}\,,\end{aligned} \tag{4.144}$$

where $\lambda=\frac{1}{\pi}\beta_0\alpha_{\rm S}(\mu_R^2)L$ and should not be confused with the eigenvalues λ_I of soft anomalous dimension matrix. As anticipated, the soft wide angle emission of gluons, described by anomalous dimension matrices, results in large logarithms contributing from NLL accuracy (the logarithmic expansion in Eq. (4.143) starts with $\boldsymbol{g}^{(2)}_{(\rm LO)}(\alpha_{\rm S}L)$, as opposed to the logarithmic expansion of the resummation factor in Eq. (3.67)).

The operator $\mathbf{S}$ also resumms large logarithms, through the evolution of the strong coupling $\alpha_{\rm S}$ scale from b_0^2/b^2 to $Q\sim M$. Note that the evolution can be realised at

the level of the matrix elements S_{IJ}, and no further diagonalization procedure is needed. Explicitly, we write:

$$S_{IJ}(\alpha_{\rm S}(b_0^2/b^2)) = S_{IJ}(\alpha_{\rm S}(Q^2)) \exp\left\{\mathcal{G}_{\mathbf{S},IJ}(\alpha_{\rm S}(\mu_R^2), L; M^2/\mu_R^2, M^2/Q^2)\right\} . \tag{4.145}$$

where

$$\mathcal{G}_{\mathbf{S},IJ}(\alpha_{\rm S}(\mu_R^2), L; M^2/\mu_R^2, M^2/Q^2) = -\int_{b_0^2/b^2}^{Q^2} \frac{dq^2}{q^2}\, \beta(\alpha_{\rm S}(q^2))\, \frac{d\ln S_{IJ}(\alpha_{\rm S}(q^2))}{d\ln \alpha_{\rm S}(q^2)} , \tag{4.146}$$

and the matrix $\mathbf{S}$ has the following perturbative expansion in $\alpha_{\rm S}$

$$\mathbf{S}(\alpha_{\rm S}) = \mathbf{S}^{(0)} + \sum_{n=1}^{\infty} \left(\frac{\alpha_{\rm S}}{\pi}\right)^n \mathbf{S}^{(n)} . \tag{4.147}$$

Explicitly, the first two coefficients $\mathbf{S}^{(0)}$ and $\mathbf{S}^{(1)}$ are given by

$$\begin{aligned} \mathbf{S}^{(0)} &= \bar{\mathbf{C}} , \\ \mathbf{S}^{(1)} &= \left(\overline{\mathbf{K}}^{(1)}\right)^{\dagger} \bar{\mathbf{C}} + \bar{\mathbf{C}}\, \overline{\mathbf{K}}^{(1)} . \end{aligned} \tag{4.148}$$

Eq. (4.136) describes the all-order structure of the resummed cross section due to soft wide angle radiation of gluons from the heavy quarks. An important feature of the structure of Eq. (4.136) is that the individual ingredients, $\overline{\mathbf{V}}^{(\rm LO)}$, $\widetilde{\mathbf{H}}(\alpha_{\rm S}'; Q, M)$ and $\mathbf{S}(\alpha_{\rm S})$ are separately invariant under resummation scheme transformations order-by-order in $\alpha_{\rm S}$. As a result, one can systematically expand Eq. (4.136) to desired accuracy in an unambiguous way.

At NLL accuracy the expansion of $(\mathbf{H}\,\boldsymbol{\Delta})$ factor has the following form

$$\begin{aligned} (\mathbf{H}\,\boldsymbol{\Delta})_{\rm NLL} = {\rm Tr}\left[\exp\left\{\boldsymbol{g}^{(2)}_{(\rm LO)}\right\} \widetilde{\mathbf{H}}^{(0)} \exp\left\{\boldsymbol{g}^{(2)}_{(\rm LO)}\right\}^{\dagger} \mathbf{S}^{(0)}\right] \\ + \frac{\alpha_{\rm S}(\mu_R^2)}{\pi}\, {\rm Tr}\left[\widetilde{\mathbf{H}}^{(1)}\, \mathbf{S}^{(0)} + \widetilde{\mathbf{H}}^{(0)}\, \mathbf{S}^{(1)}\right] , \end{aligned} \tag{4.149}$$

where we kept the first-order coefficient $\boldsymbol{g}^{(2)}_{(\rm LO)}$ in the logarithmic expansion of the exponential form factor, combined with the first-order hard-scattering matrix $\widetilde{\mathbf{H}}^{(0)}$, and with the first-order coefficient $\mathbf{S}^{(0)}$, while the form factor multiplying $\widetilde{\mathbf{H}}^{(1)}$ and $\mathbf{S}^{(1)}$ is set to 1. Note that this is sufficient for resumming the large logarithms up to NLL accuracy, and the terms that have been neglected are proportional to $\alpha_{\rm S}^n L^{n-1}$, which are of NNLL accuracy. It is easy to see that the terms proportional to $\overline{\mathbf{K}}^{(1)}$ in $\widetilde{\mathbf{H}}^{(1)}$ and $\mathbf{S}^{(1)}$ cancel out in the second line of Eq. (4.149). Moreover, due to the absence of the exponential matrix in these contributions, we can explicitly carry out the trace over the colour indices and write the second line in terms of the scalar hard functions of Eqs. (4.98). We get,

$${\rm Tr}\left[\widetilde{\mathbf{H}}_c^{Q\bar{Q}\,(1)}\, \mathbf{S}^{(0)}_{c\bar{c}} + \widetilde{\mathbf{H}}_c^{Q\bar{Q}\,(0)}\, \mathbf{S}^{(1)}_{c\bar{c}}\right] = H_c^{Q\bar{Q}\,(1)} - \beta_0 \ell_R H_c^{Q\bar{Q}\,(0)} - \frac{\langle \widetilde{\mathcal{M}}^{(0)}_{c\bar{c}\to Q\bar{Q}}| \left(\boldsymbol{\Gamma}_t^{(1)} + \boldsymbol{\Gamma}_t^{(1)\dagger}\right) |\widetilde{\mathcal{M}}^{(0)}_{c\bar{c}\to Q\bar{Q}}\rangle}{|\widetilde{\mathcal{M}}^{(0)}_{c\bar{c}\to Q\bar{Q}}|^2} \ell_Q , \tag{4.150}$$

At NNLL accuracy the expansion of $(\mathbf{H}\,\boldsymbol{\Delta})$ can be written as

$$(\mathbf{H}\,\boldsymbol{\Delta})_{\text{NNLL}} = \text{Tr}\left[\exp\left\{\boldsymbol{g}^{(2)}_{(\text{LO})} + \frac{\alpha_{\text{S}}(\mu_R^2)}{\pi}\,\boldsymbol{g}^{(3)}_{(\text{LO})}\right\}\widetilde{\mathbf{H}}^{(0)}\exp\left\{\boldsymbol{g}^{(2)}_{(\text{LO})} + \frac{\alpha_{\text{S}}(\mu_R^2)}{\pi}\,\boldsymbol{g}^{(3)}_{(\text{LO})}\right\}^{\dagger}\mathbf{S}^{(0)}\right] \tag{4.151}$$

$$+ \frac{\alpha_{\text{S}}(\mu_R^2)}{\pi}\,\text{Tr}\left[\exp\left\{\boldsymbol{g}^{(2)}_{(\text{LO})}\right\}\widetilde{\mathbf{H}}^{(1)}\exp\left\{\boldsymbol{g}^{(2)}_{(\text{LO})}\right\}^{\dagger}\mathbf{S}^{(0)}\right]$$

$$+ \frac{\alpha_{\text{S}}(\mu_R^2)}{\pi}\,\text{Tr}\left[\exp\left\{\boldsymbol{g}^{(2)}_{(\text{LO})}\right\}\widetilde{\mathbf{H}}^{(0)}\exp\left\{\boldsymbol{g}^{(2)}_{(\text{LO})}\right\}^{\dagger}\mathbf{S}^{(1)}\right]\,\exp\Big\{-\ln(1-\lambda)\Big\}$$

$$+ \left(\frac{\alpha_{\text{S}}(\mu_R^2)}{\pi}\right)^2\text{Tr}\left[\widetilde{\mathbf{H}}^{(2)}\,\mathbf{S}^{(0)} + \widetilde{\mathbf{H}}^{(0)}\,\mathbf{S}^{(2)} + \widetilde{\mathbf{H}}^{(1)}\,\mathbf{S}^{(1)}\right],$$

where we kept the first- and second-order coefficients $\boldsymbol{g}^{(2)}_{(\text{LO})}$ and $\boldsymbol{g}^{(3)}_{(\text{LO})}$ in the logarithmic expansion of the exponential form factor, combined with the first-order hard-scattering matrix $\widetilde{\mathbf{H}}^{(0)}$, and with the first-order coefficient $\mathbf{S}^{(0)}$, while only the first-order coefficient $\boldsymbol{g}^{(2)}_{(\text{LO})}$ enters in the exponent multiplying $\widetilde{\mathbf{H}}^{(1)}$ and $\mathbf{S}^{(1)}$. In the last line of Eq. (4.151) the exponential form factor is set to 1, and the form factor $\exp\{-\ln(1-\lambda)\}$ in the third line of Eq. (4.151) originates from the logarithmic expansion of the form factor $\mathcal{G}_{\mathbf{S},IJ}$ in Eq. (4.146). It is easy to see that the neglected terms in Eq. (4.151) are proportional to $\alpha_{\text{S}}^n L^{n-2}$, which are of N^{3}LL accuracy.

4.5 The resummed component

In the following we present the expression for the azimuthally-averaged resummed cross section for the heavy-quark pair production process in the context of the resummation formalism sketched in Section 3.1, accordingly combined with the additional resummation factors due to the soft radiation from heavy quarks, presented in Section 4.4. Explicitly, we write

$$[d\sigma^{c\bar{c}}_{Q\bar{Q}}]_{\phi} = \frac{M^2}{s}\int_0^{\infty} db\; b\; J_0(bq_T)\; W^{c\bar{c}\to Q\bar{Q}}(s; b, y, M, \boldsymbol{\Omega}; \alpha_{\text{S}}(\mu_R^2), \mu_R^2, \mu_F^2)\,. \tag{4.152}$$

Following the steps described in Chapter 3, we can write the resummation formula at the partonic level. In particular, we introduce the double Mellin moments $W^{c\bar{c}\to Q\bar{Q}}_{N_1,N_2}(s; b, y, M, \boldsymbol{\Omega})$ of the hadronic and $\mathcal{W}^{c\bar{c}\to Q\bar{Q}}_{a_1a_2,\,(N_1,N_2)}(s; b, y, M, \boldsymbol{\Omega})$ of the partonic cross section, which are related through the factorization formula

$$W^{c\bar{c}\to Q\bar{Q}}_{N_1,N_2}(s; b, y, M, \boldsymbol{\Omega}; \alpha_{\text{S}}(\mu_R^2)) = \sum_{a_1,\,a_2}\mathcal{W}^{c\bar{c}\to Q\bar{Q}}_{a_1a_2,\,(N_1,N_2)}(M, b, \boldsymbol{\Omega}; \alpha_{\text{S}}(\mu_R^2))\; f_{a_1/h_1,\,N_1}(\mu_F^2)\; f_{a_2/h_2,\,N_2}(\mu_F^2)\,. \tag{4.153}$$

At NLL+NLO accuracy the partonic resummed cross section $\mathcal{W}^{c\bar{c}\to Q\bar{Q}}_{a_1a_2,\,(N_1,N_2)}$ can then be organized as

$$\mathcal{W}^{c\bar{c}\to Q\bar{Q}}_{N_1,N_2} = \left[d\sigma^{(0)}_{c\bar{c},\,Q\bar{Q}}\right]\left(\mathrm{Tr}\left[\exp\left\{\boldsymbol{g}^{(2)}_{(\mathrm{LO})}\right\}\boldsymbol{\mathcal{H}}^{Q\bar{Q}\,(0)}_{c\bar{c}\leftarrow a_1a_2,\,(N_1,N_2)}\exp\left\{\boldsymbol{g}^{(2)}_{(\mathrm{LO})}\right\}^{\dagger}\mathbf{S}^{(0)}_{c\bar{c}}\right] + \frac{\alpha_{\mathrm{S}}}{\pi}\mathcal{H}^{Q\bar{Q}\,(1)}_{c\bar{c}\leftarrow a_1a_2,\,(N_1,N_2)}\right)\exp\left\{\mathcal{G}_{N_1,N_2}(\alpha_{\mathrm{S}},L)\right\}, \tag{4.154}$$

with $\alpha_{\mathrm{S}} = \alpha_{\mathrm{S}}(\mu_R^2)$, and the matrix $\boldsymbol{\mathcal{H}}^{Q\bar{Q}}_{c\bar{c}\leftarrow a_1a_2,\,(N_1,N_2)}(\alpha_{\mathrm{S}})$ is defined as the hard-collinear function $\mathcal{H}^{F}_{c\bar{c}\leftarrow a_1a_2,\,(N_1,N_2)}(\alpha_{\mathrm{S}})$ in Eq. (3.59), by replacing H_c^F with $\widetilde{\mathbf{H}}_c^{Q\bar{Q}}$. Explicitly,

$$\begin{aligned}\boldsymbol{\mathcal{H}}^{Q\bar{Q}}_{c\bar{c}\leftarrow a_1a_2,\,(N_1,N_2)} &= \left[\widetilde{\mathbf{H}}^{Q\bar{Q}}\,C_{N_1}\,C_{N_2}\right]_{c\bar{c};a_1,a_2} \\ &\times\exp\left\{\int_{M^2}^{Q^2}\frac{dq^2}{q^2}\left[A(\alpha_{\mathrm{S}}(q^2))\ln\frac{M^2}{q^2}+\frac{1}{2}\left(\widetilde{B}_{N_1}(\alpha_{\mathrm{S}}(q^2))+\widetilde{B}_{N_2}(\alpha_{\mathrm{S}}(q^2))\right)\right]\right. \\ &\left.+\int_{\mu_F^2}^{M^2}\frac{dq^2}{q^2}\left(\gamma_{N_1}(\alpha_{\mathrm{S}}(q^2))+\gamma_{N_2}(\alpha_{\mathrm{S}}(q^2))\right)\right\},\end{aligned} \tag{4.155}$$

where the symbolic factor $\left[\widetilde{\mathbf{H}}^{Q\bar{Q}}\,C_{N_1}\,C_{N_2}\right]_{c\bar{c};a_1,a_2}$ is

$$\left[\widetilde{\mathbf{H}}^{Q\bar{Q}}\,C_{N_1}\,C_{N_2}\right]_{c\bar{c};a_1,a_2} = \widetilde{\mathbf{H}}_c^{Q\bar{Q}}(M,\boldsymbol{\Omega};\alpha_{\mathrm{S}}(M^2))\,C_{c\,a_1,\,N_1}(\alpha_{\mathrm{S}}(M^2))\,C_{\bar{c}\,a_2,\,N_2}(\alpha_{\mathrm{S}}(M^2)), \tag{4.156}$$

$\mathcal{H}^{Q\bar{Q}\,(1)}_{c\bar{c}\leftarrow a_1a_2,\,(N_1,N_2)}$ in Eq. (4.154) is the first-order coefficient of the perturbative function $\mathcal{H}^{Q\bar{Q}}_{c\bar{c}\leftarrow a_1a_2,\,(N_1,N_2)}$

$$\mathcal{H}^{Q\bar{Q}}_{c\bar{c}\leftarrow a_1a_2,\,(N_1,N_2)}(M,\boldsymbol{\Omega},\alpha_{\mathrm{S}}(\mu_R^2)) = 1+\sum_{n=1}^{\infty}\left(\frac{\alpha_{\mathrm{S}}(\mu_R^2)}{\pi}\right)^n\mathcal{H}^{Q\bar{Q}\,(n)}_{c\bar{c}\leftarrow a_1a_2,\,(N_1,N_2)}, \tag{4.157}$$

which is defined as

$$\mathcal{H}^{Q\bar{Q}}_{c\bar{c}\leftarrow a_1a_2,\,(N_1,N_2)} = \mathrm{Tr}\left[\boldsymbol{\mathcal{H}}^{Q\bar{Q}}_{c\bar{c}\leftarrow a_1a_2,\,(N_1,N_2)}\,\mathbf{S}_{c\bar{c}}\right]. \tag{4.158}$$

The explicit expressions of the coefficients $\mathcal{H}^{Q\bar{Q}\,(1)}_{c\bar{c}\leftarrow a_1a_2,\,(N_1,N_2)}$ and $\mathcal{H}^{Q\bar{Q}\,(2)}_{c\bar{c}\leftarrow a_1a_2,\,(N_1,N_2)}$ are presented in Eqs. (4.166) and (4.171).

At NNLL+NNLO accuracy we write for the partonic resummed cross section $\mathcal{W}^{c\bar{c}\to Q\bar{Q}}_{a_1a_2,\,(N_1,N_2)}$

$$\begin{aligned}\mathcal{W}^{c\bar{c}\to Q\bar{Q}}_{N_1,N_2} &= \left(\mathrm{Tr}\left[\exp\left\{\boldsymbol{g}^{(2)}_{(\mathrm{LO})}+\frac{\alpha_{\mathrm{S}}}{\pi}\boldsymbol{g}^{(3)}_{(\mathrm{LO})}\right\}\boldsymbol{\mathcal{H}}^{Q\bar{Q}\,(0)}_{c\bar{c}\leftarrow a_1a_2,\,(N_1,N_2)}\exp\left\{\boldsymbol{g}^{(2)}_{(\mathrm{LO})}+\frac{\alpha_{\mathrm{S}}}{\pi}\boldsymbol{g}^{(3)}_{(\mathrm{LO})}\right\}^{\dagger}\mathbf{S}^{(0)}_{c\bar{c}}\right]\right. \\ &+\frac{\alpha_{\mathrm{S}}}{\pi}\mathrm{Tr}\left[\exp\left\{\boldsymbol{g}^{(2)}_{(\mathrm{LO})}\right\}\boldsymbol{\mathcal{H}}^{Q\bar{Q}\,(1)}_{c\bar{c}\leftarrow a_1a_2,\,(N_1,N_2)}\exp\left\{\boldsymbol{g}^{(2)}_{(\mathrm{LO})}\right\}^{\dagger}\mathbf{S}^{(0)}_{c\bar{c}}\right] \\ &+\frac{\alpha_{\mathrm{S}}}{\pi}\mathrm{Tr}\left[\exp\left\{\boldsymbol{g}^{(2)}_{(\mathrm{LO})}\right\}\boldsymbol{\mathcal{H}}^{Q\bar{Q}\,(0)}_{c\bar{c}\leftarrow a_1a_2,\,(N_1,N_2)}\exp\left\{\boldsymbol{g}^{(2)}_{(\mathrm{LO})}\right\}^{\dagger}\mathbf{S}^{(1)}_{c\bar{c}}\right]\exp\left\{-\ln(1-\lambda)\right\} \\ &\left.+\left(\frac{\alpha_{\mathrm{S}}}{\pi}\right)^2\mathcal{H}^{Q\bar{Q}\,(2)}_{c\bar{c}\leftarrow a_1a_2,\,(N_1,N_2)}\right)\exp\left\{\mathcal{G}_{N_1,N_2}(\alpha_{\mathrm{S}},L)\right\},\end{aligned} \tag{4.159}$$

where the first-order matrix $\boldsymbol{\mathcal{H}}^{Q\bar{Q}\,(1)}_{c\bar{c}\leftarrow a_1a_2,\,(N_1,N_2)}$ is given by

$$\begin{aligned}\left[\boldsymbol{\mathcal{H}}^{Q\bar{Q}\,(1)}_{c\bar{c}\leftarrow a_1a_2,\,(N_1,N_2)}\right]_{\phi(\mathbf{b})} &= \delta_{ca_1}\delta_{\bar{c}a_2}\left[\widetilde{\mathbf{H}}^{Q\bar{Q}\,(1)}_c - \left(B^{(1)}_c + \frac{1}{2}A^{(1)}_c\ell_Q\right)\ell_Q\,\widetilde{\mathbf{H}}^{Q\bar{Q}\,(0)}_c\right] \\ &+ \left[\delta_{ca_1}C^{(1)}_{\bar{c}a_2,\,N_2} + \delta_{\bar{c}a_2}C^{(1)}_{ca_1,\,N_1} + \left(\delta_{ca_1}\gamma^{(1)}_{\bar{c}a_2,\,N_2} + \delta_{\bar{c}a_2}\gamma^{(1)}_{ca_1,\,N_1}\right)(\ell_F-\ell_Q)\right]\widetilde{\mathbf{H}}^{Q\bar{Q}\,(0)}_c\,.\end{aligned} \tag{4.160}$$

4.6 The finite component

In this Section we present the explicit results for the finite component of the partonic cross section $d\hat{\sigma}^{\rm reg.}_{a_1a_2\to Q\bar{Q}+X}$, which is defined as in the case of the production of colourless final system F (see Eq. (3.18)). To this purpose we expand the resummed partonic cross section in $\alpha_{\rm S}$ and write it as in Eq. (3.76).

$$\begin{aligned}\mathcal{W}^{c\bar{c}\to Q\bar{Q}}_{a_1a_2}(\hat{s};b,M,\mathbf{\Omega};\alpha_{\rm S},\mu_R^2,\mu_F^2,Q^2) &= \left[d\sigma^{(0)}_{c\bar{c},\,Q\bar{Q}}\right]\Bigg\{\delta_{ca_1}\delta_{ca_2}\,\delta(1-z_1)\,\delta(1-z_2) \\ &+ \sum_{n=1}^{\infty}\left(\frac{\alpha_{\rm S}}{\pi}\right)^n\Bigg[\widetilde{\Sigma}^{Q\bar{Q}\,(n)}_{c\bar{c}\leftarrow a_1a_2}\left(z_1,z_2,\widetilde{L};\frac{M^2}{\mu_R^2},\frac{M^2}{\mu_F^2},\frac{M^2}{Q^2}\right) \\ &+ \mathcal{H}^{Q\bar{Q}\,(n)}_{c\bar{c}\leftarrow a_1a_2}\left(z_1,z_2;\frac{M^2}{\mu_R^2},\frac{M^2}{\mu_F^2},\frac{M^2}{Q^2}\right)\Bigg]\Bigg\},\end{aligned} \tag{4.161}$$

where $\alpha_{\rm S}=\alpha_{\rm S}(\mu_R^2)$. As in the case of colourless final system, in this case also the first $\widetilde{\Sigma}^{Q\bar{Q}\,(1)}_{c\bar{c}\leftarrow a_1a_2}$ and second-order $\widetilde{\Sigma}^{Q\bar{Q}\,(2)}_{c\bar{c}\leftarrow a_1a_2}$ coefficients are polynomials of $\widetilde{L}$

$$\widetilde{\Sigma}^{Q\bar{Q}\,(1)}_{c\bar{c}\leftarrow a_1a_2}(z_1,z_2,\widetilde{L}) = \sum_{p=1}^{2}\widetilde{\Sigma}^{Q\bar{Q}\,(1;n)}_{c\bar{c}\leftarrow a_1a_2}(z_1,z_2)\;\widetilde{L}^n\,, \tag{4.162}$$

$$\widetilde{\Sigma}^{Q\bar{Q}\,(1)}_{c\bar{c}\leftarrow a_1a_2}(z_1,z_2,\widetilde{L}) = \sum_{p=1}^{4}\widetilde{\Sigma}^{Q\bar{Q}\,(2;n)}_{c\bar{c}\leftarrow a_1a_2}(z_1,z_2)\;\widetilde{L}^n\,, \tag{4.163}$$

Below we present the NLO coefficients $\widetilde{\Sigma}^{Q\bar{Q}\,(1;p)}(z_1,z_2)$, $\mathcal{H}^{Q\bar{Q}\,(1)}(z_1,z_2)$ and the NNLO coefficients $\widetilde{\Sigma}^{Q\bar{Q}\,(2;p)}(z_1,z_2)$, $\mathcal{H}^{Q\bar{Q}\,(2)}(z_1,z_2)$ in the Mellin space. The structure of the leading logarithmic contribution $\widetilde{\Sigma}^{Q\bar{Q}\,(1;2)}(z_1,z_2)$, as already mentioned, is unaffected by the soft large-angle radiation from the heavy quarks. Moreover, since it is also process-independent, $\widetilde{\Sigma}^{Q\bar{Q}\,(1;2)}(z_1,z_2)$ exactly coincides with $\widetilde{\Sigma}^{F\,(1;2)}(z_1,z_2)$ of Eq. (3.80)

$$\Sigma^{Q\bar{Q}\,(1;2)}_{c\bar{c}\leftarrow a_1a_2,\,(N_1,N_2)} = \Sigma^{F\,(1;2)}_{c\bar{c}\leftarrow a_1a_2,\,(N_1,N_2)}\,. \tag{4.164}$$

The soft large-angle radiation effects first show up at NLL, leading to the Born-level colour-correlated contribution. Explicitly, using the process-independent function $\widetilde{\Sigma}^{F\,(1;1)}(z_1,z_2)$

of Eq. (3.81), the $\widetilde{\Sigma}^{Q\bar{Q}\,(1;1)}(z_1,z_2)$ function can be written as

$$\Sigma^{Q\bar{Q}\,(1;1)}_{c\bar{c}\leftarrow a_1a_2,\,(N_1,N_2)} = \Sigma^{F\,(1;1)}_{c\bar{c}\leftarrow a_1a_2,\,(N_1,N_2)} - \delta_{ca_1}\delta_{\bar{c}a_2}\frac{\langle\widetilde{\mathcal{M}}^{(0)}_{c\bar{c}\to Q\bar{Q}}|\left(\mathbf{\Gamma}^{c\bar{c}\,(1)}_t+\mathbf{\Gamma}^{c\bar{c}\,(1)\dagger}_t\right)|\widetilde{\mathcal{M}}^{(0)}_{c\bar{c}\to Q\bar{Q}}\rangle}{|\widetilde{\mathcal{M}}^{(0)}_{c\bar{c}\to Q\bar{Q}}|^2}\,. \tag{4.165}$$

The hard function $\mathcal{H}^{Q\bar{Q}\,(1)}_{c\bar{c}\leftarrow a_1a_2,\,(N_1,N_2)}$ can be written by setting $k=1^*$ in Eq. (4.166), replacing the hard-virtual functions $H^{F\,(1)}_c$ by the corresponding hard function $H^{Q\bar{Q}\,(1)}_c$, and by accounting for resummation scale-dependent contribution from the soft anomalous dimension matrices

$$\mathcal{H}^{Q\bar{Q}\,(1)}_{c\bar{c}\leftarrow a_1a_2,\,(N_1,N_2)} = \mathcal{H}^{F\,(1)}_{c\bar{c}\leftarrow a_1a_2,\,(N_1,N_2)}|_{F=Q\bar{Q},\,k=1} - \delta_{ca_1}\delta_{\bar{c}a_2}\frac{\langle\widetilde{\mathcal{M}}^{(0)}_{c\bar{c}\to Q\bar{Q}}|\left(\mathbf{\Gamma}^{c\bar{c}\,(1)}_t+\mathbf{\Gamma}^{c\bar{c}\,(1)\dagger}_t\right)|\widetilde{\mathcal{M}}^{(0)}_{c\bar{c}\to Q\bar{Q}}\rangle}{|\widetilde{\mathcal{M}}^{(0)}_{c\bar{c}\to Q\bar{Q}}|^2}\ell_Q\,. \tag{4.166}$$

At NNLO, $\widetilde{\Sigma}^{Q\bar{Q}\,(2;4)}(z_1,z_2)$ exactly coincides with Eq. (3.83), while $\widetilde{\Sigma}^{Q\bar{Q}\,(2;3)}(z_1,z_2)$ receives contribution from the first-order anomalous dimension matrices, similar to the NLO coefficient $\widetilde{\Sigma}^{Q\bar{Q}\,(1;1)}(z_1,z_2)$.

$$\Sigma^{Q\bar{Q}\,(2;4)}_{c\bar{c}\leftarrow a_1a_2,\,(N_1,N_2)} = \Sigma^{F\,(2;4)}_{c\bar{c}\leftarrow a_1a_2,\,(N_1,N_2)}\,, \tag{4.167}$$

$$\Sigma^{Q\bar{Q}\,(2;3)}_{c\bar{c}\leftarrow a_1a_2,\,(N_1,N_2)} = -\,A^{(1)}_c\left[\frac{1}{3}\,\beta_0\;\delta_{ca_1}\delta_{\bar{c}a_2}+\frac{1}{2}\,\Sigma^{Q\bar{Q}\,(1;1)}_{c\bar{c}\leftarrow a_1a_2,\,(N_1,N_2)}\right]\,, \tag{4.168}$$

The $\widetilde{\Sigma}^{Q\bar{Q}\,(2;2)}(z_1,z_2)$ and $\widetilde{\Sigma}^{Q\bar{Q}\,(2;1)}(z_1,z_2)$ are more involved in terms of colour correlations, and therefore technically more difficult to deal with. Explicitly, they read

$$\begin{aligned}
\Sigma^{Q\bar{Q}\,(2;2)}_{c\bar{c}\leftarrow a_1a_2,\,(N_1,N_2)} =& -\frac{1}{2}\,A^{(1)}_c\left[\mathcal{H}^{Q\bar{Q}\,(1)}_{c\bar{c}\leftarrow a_1a_2,\,(N_1,N_2)}-\beta_0\;\delta_{ca_1}\delta_{\bar{c}a_2}\,(\ell_R-\ell_Q)\right] \\
&-\frac{1}{2}\sum_{b_1,b_2}\Sigma^{Q\bar{Q}\,(1;1)}_{c\bar{c}\leftarrow a_1a_2,\,(N_1,N_2)}\left[\delta_{b_1a_1}\gamma^{(1)}_{b_2a_2,\,N_2}+\delta_{b_2a_2}\gamma^{(1)}_{b_1a_1,\,N_1}\right] \\
&+\frac{1}{2}\sum_{b_1,b_2}\frac{\langle\widetilde{\mathcal{M}}^{(0)}_{c\bar{c}\to Q\bar{Q}}|\left(\mathbf{\Gamma}^{c\bar{c}\,(1)}_t+\mathbf{\Gamma}^{c\bar{c}\,(1)\dagger}_t\right)|\widetilde{\mathcal{M}}^{(0)}_{c\bar{c}\to Q\bar{Q}}\rangle}{|\widetilde{\mathcal{M}}^{(0)}_{c\bar{c}\to Q\bar{Q}}|^2}\left[\delta_{b_1a_1}\gamma^{(1)}_{b_2a_2,\,N_2}+\delta_{b_2a_2}\gamma^{(1)}_{b_1a_1,\,N_1}\right] \\
&-\frac{1}{2}\left[A^{(2)}_c\;\delta_{ca_1}\delta_{\bar{c}a_2}+\left(B^{(1)}_c+A^{(1)}_c\,\ell_Q-\beta_0\right)\Sigma^{Q\bar{Q}\,(1;1)}_{c\bar{c}\leftarrow a_1a_2,\,(N_1,N_2)}\right] \\
&+\frac{1}{2}\,\delta_{ca_1}\delta_{\bar{c}a_2}B^{(1)}_c\frac{\langle\widetilde{\mathcal{M}}^{(0)}_{c\bar{c}\to Q\bar{Q}}|\left(\mathbf{\Gamma}^{c\bar{c}\,(1)}_t+\mathbf{\Gamma}^{c\bar{c}\,(1)\dagger}_t\right)|\widetilde{\mathcal{M}}^{(0)}_{c\bar{c}\to Q\bar{Q}}\rangle}{|\widetilde{\mathcal{M}}^{(0)}_{c\bar{c}\to Q\bar{Q}}|^2} \\
&+\frac{1}{2}\,\delta_{ca_1}\delta_{\bar{c}a_2}\frac{\langle\widetilde{\mathcal{M}}^{(0)}_{c\bar{c}\to Q\bar{Q}}|\left(\mathbf{\Gamma}^{c\bar{c}\,(1)}_t+\mathbf{\Gamma}^{c\bar{c}\,(1)\dagger}_t\right)^2|\widetilde{\mathcal{M}}^{(0)}_{c\bar{c}\to Q\bar{Q}}\rangle}{|\widetilde{\mathcal{M}}^{(0)}_{c\bar{c}\to Q\bar{Q}}|^2}\,,
\end{aligned} \tag{4.169}$$

*we recall that k is the power of $\alpha_{\rm S}^2$ at the Born level, which is one in the case of heavy-quark production

$$
\begin{aligned}
\Sigma^{Q\bar{Q}\,(2;1)}_{c\bar{c}\leftarrow a_1a_2,\,(N_1,N_2)} &= \Sigma^{Q\bar{Q}\,(1;1)}_{c\bar{c}\leftarrow a_1a_2,\,(N_1,N_2)}\,\beta_0\,(\ell_Q-\ell_R) \\
&- \sum_{b_1,b_2}\mathcal{H}^{Q\bar{Q}\,(1)}_{c\bar{c}\leftarrow b_1b_2,\,(N_1,N_2)}\left[\delta_{b_1a_1}\delta_{b_2a_2}\left(B_c^{(1)}+A_c^{(1)}\,\ell_Q\right)+\delta_{b_1a_1}\gamma^{(1)}_{b_2a_2,\,N_2}+\delta_{b_2a_2}\gamma^{(1)}_{b_1a_1,\,N_1}\right] \\
&- \left[\delta_{ca_1}\delta_{\bar{c}a_2}\left(B_c^{(2)}+A_c^{(2)}\,\ell_Q\right)-\beta_0\left(\delta_{ca_1}C^{(1)}_{\bar{c}a_2,\,N_2}+\delta_{\bar{c}a_2}C^{(1)}_{ca_1,\,N_1}\right)+\delta_{ca_1}\gamma^{(2)}_{\bar{c}a_2,\,N_2}+\delta_{\bar{c}a_2}\gamma^{(2)}_{ca_1,\,N_1}\right] \\
&- \delta_{ca_1}\delta_{\bar{c}a_2}\left[\frac{\langle\widetilde{\mathcal{M}}^{(0)}_{c\bar{c}\to Q\bar{Q}}|\left(\mathbf{\Gamma}_t^{c\bar{c}\,(1)}+\mathbf{\Gamma}_t^{c\bar{c}\,(1)\dagger}\right)|\widetilde{\mathcal{M}}^{(1)}_{c\bar{c}\to Q\bar{Q}}\rangle}{|\widetilde{\mathcal{M}}^{(0)}_{c\bar{c}\to Q\bar{Q}}|^2}+\text{h.c.}\right] \\
&- \delta_{ca_1}\delta_{\bar{c}a_2}\frac{\langle\widetilde{\mathcal{M}}^{(0)}_{c\bar{c}\to Q\bar{Q}}|\left(\mathbf{\Gamma}_t^{c\bar{c}\,(2)}+\mathbf{\Gamma}_t^{c\bar{c}\,(2)\dagger}\right)|\widetilde{\mathcal{M}}^{(0)}_{c\bar{c}\to Q\bar{Q}}\rangle}{|\widetilde{\mathcal{M}}^{(0)}_{c\bar{c}\to Q\bar{Q}}|^2} \\
&- \left(\delta_{ca_1}C^{(1)}_{\bar{c}a_2,\,N_2}+\delta_{\bar{c}a_2}C^{(1)}_{ca_1,\,N_1}\right)\frac{\langle\widetilde{\mathcal{M}}^{(0)}_{c\bar{c}\to Q\bar{Q}}|\left(\mathbf{\Gamma}_t^{c\bar{c}\,(1)}+\mathbf{\Gamma}_t^{c\bar{c}\,(1)\dagger}\right)|\widetilde{\mathcal{M}}^{(0)}_{c\bar{c}\to Q\bar{Q}}\rangle}{|\widetilde{\mathcal{M}}^{(0)}_{c\bar{c}\to Q\bar{Q}}|^2} \\
&+ \delta_{ca_1}\delta_{\bar{c}a_2}\,\beta_0\frac{\langle\widetilde{\mathcal{M}}^{(0)}_{c\bar{c}\to Q\bar{Q}}|\left(\mathbf{\Gamma}_t^{c\bar{c}\,(1)}+\mathbf{\Gamma}_t^{c\bar{c}\,(1)\dagger}\right)|\widetilde{\mathcal{M}}^{(0)}_{c\bar{c}\to Q\bar{Q}}\rangle}{|\widetilde{\mathcal{M}}^{(0)}_{c\bar{c}\to Q\bar{Q}}|^2}\ell_R \\
&- \left(\delta_{ca_1}\gamma^{(1)}_{\bar{c}a_2,\,N_2}+\delta_{\bar{c}a_2}\gamma^{(1)}_{ca_1,\,N_1}\right)\frac{\langle\widetilde{\mathcal{M}}^{(0)}_{c\bar{c}\to Q\bar{Q}}|\left(\mathbf{\Gamma}_t^{c\bar{c}\,(1)}+\mathbf{\Gamma}_t^{c\bar{c}\,(1)\dagger}\right)|\widetilde{\mathcal{M}}^{(0)}_{c\bar{c}\to Q\bar{Q}}\rangle}{|\widetilde{\mathcal{M}}^{(0)}_{c\bar{c}\to Q\bar{Q}}|^2}(\ell_F-\ell_Q) \\
&+ \frac{1}{2}\,\delta_{ca_1}\delta_{\bar{c}a_2}\,A_c^{(1)}\frac{\langle\widetilde{\mathcal{M}}^{(0)}_{c\bar{c}\to Q\bar{Q}}|\left(\mathbf{\Gamma}_t^{c\bar{c}\,(1)}+\mathbf{\Gamma}_t^{c\bar{c}\,(1)\dagger}\right)|\widetilde{\mathcal{M}}^{(0)}_{c\bar{c}\to Q\bar{Q}}\rangle}{|\widetilde{\mathcal{M}}^{(0)}_{c\bar{c}\to Q\bar{Q}}|^2}\ell_Q \\
&+ \delta_{ca_1}\delta_{\bar{c}a_2}\frac{\langle\widetilde{\mathcal{M}}^{(0)}_{c\bar{c}\to Q\bar{Q}}|\left(\mathbf{\Gamma}_t^{c\bar{c}\,(1)}+\mathbf{\Gamma}_t^{c\bar{c}\,(1)\dagger}\right)^2|\widetilde{\mathcal{M}}^{(0)}_{c\bar{c}\to Q\bar{Q}}\rangle}{|\widetilde{\mathcal{M}}^{(0)}_{c\bar{c}\to Q\bar{Q}}|^2}\ell_Q\,.
\end{aligned}
\tag{4.170}
$$

In the $\widetilde{\Sigma}^{Q\bar{Q}\,(2;2)}(z_1,z_2)$ counterterm the main complication is connected with the last term, which requires the computation of the Born-level colour correlations with four colour operators. The $\widetilde{\Sigma}^{Q\bar{Q}\,(2;1)}(z_1,z_2)$ function, besides the same complication, involves also the one-loop colour-correlations, which are the technically most challenging ingredient in the computation of $\widetilde{\Sigma}^{Q\bar{Q}\,(2;p)}(z_1,z_2)$ counterterms. The second-order hard function $\mathcal{H}^{Q\bar{Q}\,(2)}_{c\bar{c}\leftarrow a_1a_2,\,(N_1,N_2)}$ is written with the same notation as the first-order hard function $\mathcal{H}^{Q\bar{Q}\,(1)}_{c\bar{c}\leftarrow a_1a_2,\,(N_1,N_2)}$ in

Eq. (4.166). Explicitly, it reads

$$\begin{aligned}\mathcal{H}^{Q\bar{Q}\,(2)}_{c\bar{c}\leftarrow a_1a_2,\,(N_1,N_2)} =& \mathcal{H}^{F\,(2)}_{c\bar{c}\leftarrow a_1a_2,\,(N_1,N_2)}\big|_{F=Q\bar{Q},\,k=1} \\ &- \delta_{ca_1}\delta_{\bar{c}a_2}\frac{\langle\widetilde{\mathcal{M}}^{(0)}_{c\bar{c}\to Q\bar{Q}}|\left(\mathbf{\Gamma}^{c\bar{c}\,(2)}_t+\mathbf{\Gamma}^{c\bar{c}\,(2)\dagger}_t\right)|\widetilde{\mathcal{M}}^{(0)}_{c\bar{c}\to Q\bar{Q}}\rangle}{|\widetilde{\mathcal{M}}^{(0)}_{c\bar{c}\to Q\bar{Q}}|^2}\ell_Q \\ &+\frac{1}{2}\,\delta_{ca_1}\delta_{\bar{c}a_2}\frac{\langle\widetilde{\mathcal{M}}^{(0)}_{c\bar{c}\to Q\bar{Q}}|\left(\mathbf{\Gamma}^{c\bar{c}\,(1)}_t+\mathbf{\Gamma}^{c\bar{c}\,(1)\dagger}_t\right)^2|\widetilde{\mathcal{M}}^{(0)}_{c\bar{c}\to Q\bar{Q}}\rangle}{|\widetilde{\mathcal{M}}^{(0)}_{c\bar{c}\to Q\bar{Q}}|^2}\ell_Q \\ &+\frac{1}{2}\,\delta_{ca_1}\delta_{\bar{c}a_2}B^{(1)}_c\frac{\langle\widetilde{\mathcal{M}}^{(0)}_{c\bar{c}\to Q\bar{Q}}|\left(\mathbf{\Gamma}^{c\bar{c}\,(1)}_t+\mathbf{\Gamma}^{c\bar{c}\,(1)\dagger}_t\right)|\widetilde{\mathcal{M}}^{(0)}_{c\bar{c}\to Q\bar{Q}}\rangle}{|\widetilde{\mathcal{M}}^{(0)}_{c\bar{c}\to Q\bar{Q}}|^2}\ell_Q^2\,,\end{aligned} \tag{4.171}$$

and corresponding dependences on the ratios M^2/μ_R^2, M^2/μ_F^2 and M^2/Q^2 on the left-hand sides of Eqs. (4.164)–(4.171) are understood.

As anticipated in Section 4.2.2, the second-order function $\mathcal{H}^{Q\bar{Q}\,(2)}_{gg\leftarrow a_1a_2,\,(N_1,N_2)}$ for the the gluon fusion cross section receives additional contributions from the azimuthal average of collinear-collinear and soft-collinear interference terms. Therefore, in this case Eq. (4.171) should be replaced by

$$\begin{aligned}\mathcal{H}^{Q\bar{Q}\,(2)}_{gg\leftarrow a_1a_2,\,(N_1,N_2)} \to& \mathcal{H}^{Q\bar{Q}\,(2)}_{gg\leftarrow a_1a_2,\,(N_1,N_2)} + H^{Q\bar{Q}}_G(p_1,p_2;\mathbf{\Omega};\alpha_{\rm S})\;G^{(1)}_{ga_1,\,N_1}\;G^{(1)}_{ga_2,\,N_2} \\ &+\delta_{ga_2}\,H^{Q\bar{Q}}_{\mathbf{D}D}(p_1,p_2;\mathbf{\Omega};\alpha_{\rm S})\;G^{(1)}_{ga_1,\,N_1}+\delta_{ga_1}\,H^{Q\bar{Q}}_{\mathbf{D}G}(p_1,p_2;\mathbf{\Omega};\alpha_{\rm S})\;G^{(1)}_{ga_2,\,N_2}\,,\end{aligned} \tag{4.172}$$

with $H^{Q\bar{Q}}_G$ and $H^{Q\bar{Q}}_{\mathbf{D}G}$ given in Eqs. (4.84) and (4.85), respectively.

The finite component $d\hat{\sigma}^{\rm reg.}_{a_1a_2\to Q\bar{Q}}$ of the q_T distribution for the $Q\bar{Q}$ production can then be written as in Eqs. (3.74) and (3.75) for the colourless final state. Explicitly, the N(NLO) truncation of the finite component reads

$$\left[\frac{d\hat{\sigma}^{\rm reg.}_{a_1a_2\to Q\bar{Q}}}{dq_T^2\;dz_1\;dz_2\;d\mathbf{\Omega}}\right]_{\rm N(NLO)} = \left[\frac{d\hat{\sigma}_{a_1a_2\to Q\bar{Q}+\rm jet}}{dq_T^2\;dz_1\;dz_2\;d\mathbf{\Omega}}\right]_{\rm N(LO)} - \left[\frac{d\hat{\sigma}^{\rm sing.}_{a_1a_2\to Q\bar{Q}}}{dq_T^2\;dz_1\;dz_2\;d\mathbf{\Omega}}\right]_{\rm N(NLO)}\,, \tag{4.173}$$

where the resummed component at N(NLO) has the similar form as in Eqs. (3.89) and (3.90).

$$\begin{aligned}\left[\;\frac{d\hat{\sigma}^{\rm sing.}_{a_1a_2\to Q\bar{Q}}}{dq_T^2\;dz_1\;dz_2\;d\mathbf{\Omega}}(q_T,M,\hat{s},z_1,z_2,\mathbf{\Omega};\alpha_{\rm S}(\mu_R^2))\;\right]_{\rm NLO} &= \frac{\alpha_{\rm S}(\mu_R^2)}{\pi}\;\frac{z_1z_2}{Q^2}\;\sum_c\left[d\sigma^{(0)}_{c\bar{c},\,Q\bar{Q}}\right] \\ &\times\left[\Sigma^{Q\bar{Q}\,(1;2)}_{c\bar{c}\leftarrow a_1a_2}(z_1,z_2)\;\widetilde{I}_2(q_T/Q)+\Sigma^{Q\bar{Q}\,(1;1)}_{c\bar{c}\leftarrow a_1a_2}(z_1,z_2)\;\widetilde{I}_1(q_T/Q)\right]\,.\end{aligned} \tag{4.174}$$

$$\begin{aligned}\left[\;\frac{d\hat{\sigma}^{\rm sing.}_{a_1a_2\to Q\bar{Q}}}{dq_T^2\;dz_1\;dz_2\;d\mathbf{\Omega}}(q_T,M,\hat{s},z_1,z_2,\mathbf{\Omega};\alpha_{\rm S}(\mu_R^2))\;\right]_{\rm NNLO} &= \left[\;\frac{d\hat{\sigma}^{\rm sing.}_{a_1a_2\to Q\bar{Q}}}{dq_T^2\;dz_1\;dz_2\;d\mathbf{\Omega}}(q_T,M,\hat{s},z_1,z_2,\mathbf{\Omega};\alpha_{\rm S}(\mu_R^2))\;\right]_{\rm NLO} \\ &+\left(\frac{\alpha_{\rm S}(\mu_R^2)}{\pi}\right)^2\;\frac{z_1z_2}{Q^2}\;\sum_c\left[d\sigma^{(0)}_{c\bar{c},\,Q\bar{Q}}\right]\sum_{k=1}^{4}\Sigma^{Q\bar{Q}\,(2;k)}_{c\bar{c}\leftarrow a_1a_2}(z_1,z_2)\;\widetilde{I}_k(q_T/Q)\,.\end{aligned} \tag{4.175}$$

4.7 Results

In this Section we present numerical results for the azimuthally-averaged q_T spectrum of the $t\bar{t}$ pair, produced in pp collisions. The results are obtained with a numerical program which is based on the q_T-resummation programs `HRes` [124, 149] and `DYRes` [125, 150], for the Higgs boson and vector boson productions, respectively. We have implemented the new contributions related to the soft wide angle radiation off the heavy quarks according to the results presented in previous sections of this chapter. Due to missing contributions at NNLL, we limit ourselves to the presentation of the results at NLL+NLO accuracy (see Eq. (4.154)). In particular, we compare our resummed results with the fixed-order results at NLO and with the latest experimental data by ATLAS collaboration [24].

To compute the $t\bar{t}$ cross section we use the MSTW2008 [151] PDFs with the QCD running coupling and α_S evaluated at two-loop order. The pole mass of the top quark is $m_t = 173.3$ GeV. As discussed in previous sections, our resummed predictions depend on renormalization, factorization and resummation scales. Our convention to compute factorization and renormalization scale uncertainties is to consider independent variations of μ_F and μ_R by a factor of two around the central values $\mu_F = \mu_R = m_t$ (i.e. we consider the range $m_t/2 \leq \{\mu_F, \mu_R\} \leq 2\, m_t$), with the constraint $0.5 \leq \mu_F/\mu_R \leq 2$. Similarly, we choose $Q = m_t$ as central value of the resummation scale, considering scale variations in the range $m_t/2 < Q < 2m_t$.

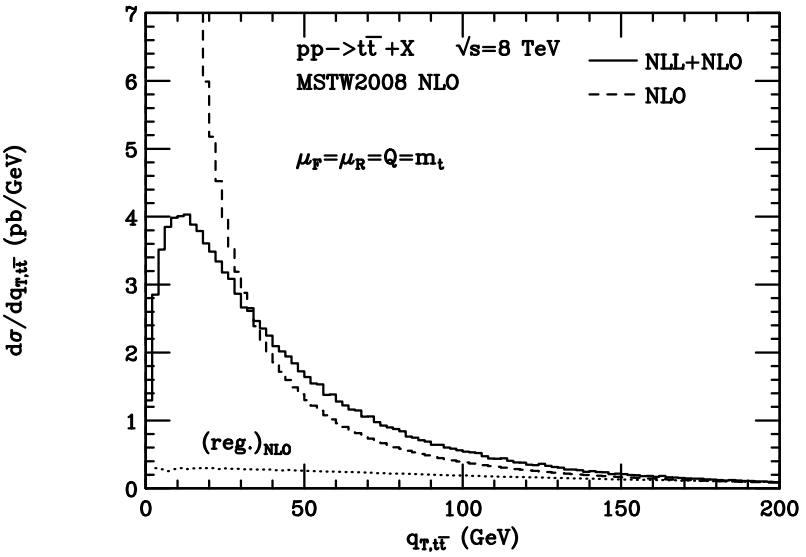

Figure 4.1: *The transverse momentum spectrum of the $t\bar{t}$ pair at the LHC ($\sqrt{s} = 8$ TeV) computed at NLL+NLO accuracy (solid line). The result is compared to the corresponding (NLO) fixed-order result (dashed line) and to the regular component (dotted line).*

In Fig. 4.1 the NLL+NLO q_T spectrum (solid line) at the default scales ($\mu_F = \mu_R =$

$Q = m_t$) is compared to the corresponding NLO result (dashed line) and to the regular component of the resummed cross section (dotted line) (see Eq. (4.3)). We see that the the NLO result diverges to $+\infty$ as $q_T \to 0$. The resummation of the small-q_T logarithms leads to a well-behaved distribution at small transverse momenta, with a kinematical peak at $q_T \sim 10\,\text{GeV}$, and tends to the corresponding NLO result at large values of q_T. In the low-q_T region the NLL+NLO result is dominated by resummation, the regular component being of the order of $\sim 7\,\%$. In the region of intermediate values of q_T (say, around 100 GeV), the contribution of the regular component increases to $\sim 30\,\%$, while at large values of q_T the contribution of the NLO finite component sizeably increases, indicating that the logarithmic terms are no longer dominant and that the resummed calculation cannot improve upon the predictivity of the fixed-order expansion.

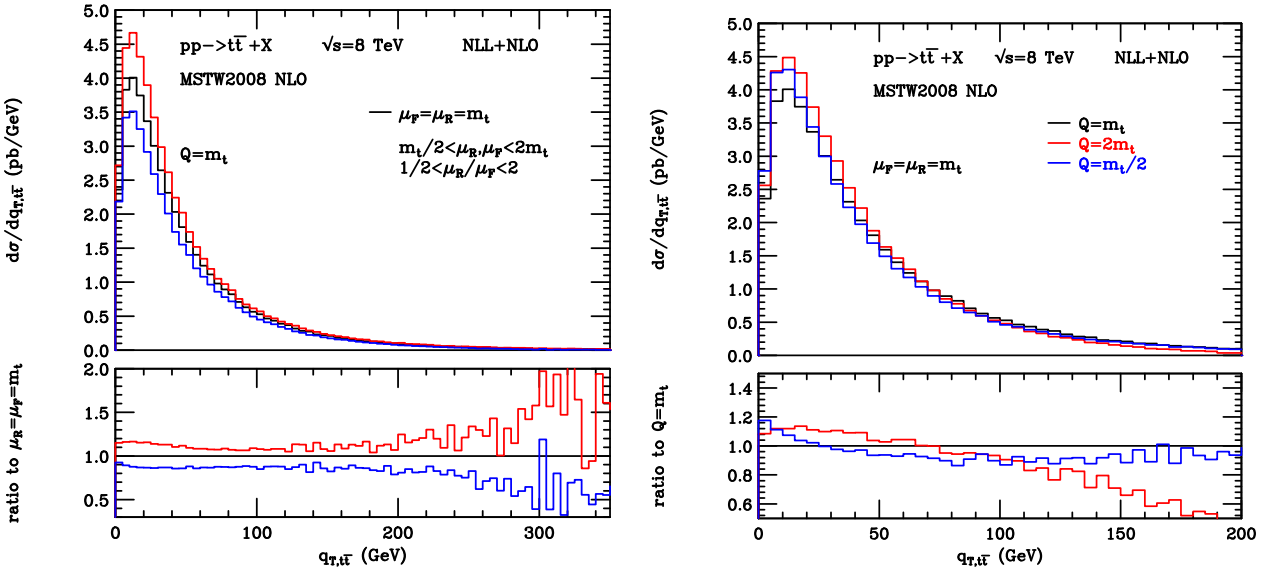

(a) (b)

Figure 4.2: *The q_T spectrum of the $t\bar{t}$ pair at the LHC ($\sqrt{s} = 8$ TeV) computed at NLL+NLO accuracy. The bands are obtained by varying μ_F and μ_R (left plot) and Q (right plot) as described in the text. The lower panels present the scale variation bands relative to the central result.*

In Fig. 4.2 we show the scale dependence of our results. In the left plot we consider variations of the renormalization and factorization scales with the default resummation scale. The bands are obtained by varying μ_R and μ_F as previously described in this section. The scale variation in the peak region is of the order of $\pm 15\%$. At intermediate values of q_T the scale variation shrinks a bit, while in the region of large values of q_T the scale variation increases dramatically, reaching even to $\pm 100\%$.

In the right panel of Fig. 4.2 we consider resummation scale variation. The bands are obtained by fixing $\mu_R = \mu_F = m_t$ and varying Q between $m_t/2$ and $2m_t$. Performing variations of the resummation scale, we can get further insight on the size of yet uncalculated

$q_{T,t\bar{t}}$ [GeV]	$\frac{1}{\sigma}\frac{d\sigma}{dq_{T,t\bar{t}}}$ [TeV^{-1}] ATLAS	$\frac{1}{\sigma}\frac{d\sigma}{dq_{T,t\bar{t}}}$ [TeV^{-1}] NLL+NLO
0-30	14.3 ± 1.0	14.96 ± 0.99
30-70	7.60 ± 0.16	7.81 ± 0.36
70-120	2.94 ± 0.28	2.84 ± 0.28
120-180	1.14 ± 0.12	0.99 ± 0.08
180-250	0.42 ± 0.04	0.34 ± 0.02
250-350	0.143 ± 0.018	0.096 ± 0.020
350-1000	0.0099 ± 0.0015	0.0062 ± 0.0040

Table 4.1: *Normalized $q_{T,t\bar{t}}$ distribution at $\sqrt{s} = 8\,\text{TeV}$.*

higher-order logarithmic contributions at small and intermediate values of q_T. We find that in the peak region the resummation scale dependence is about 15% and positive, while at very large transverse momenta the variation is negative and very large.

The integral over q_T of the resummed NLL+NLO spectrum is in agreement (for any values of μ_R, μ_F and Q) with the value of the NLO total cross section to better than 0.5%, thus checking the numerical accuracy of the code. For example, for the default scales, out NLL+NLO cross section is 226.3 pb, and agrees with the NLO one (226.6 pb) better than 0.2%.

Finally, we compare our results with the recent measurement of ATLAS experiment [24]. The dataset corresponds to an integrated luminosity of 20.2 fb^{-1} at 8 TeV, recorded with the ATLAS detector at the LHC. The results of this comparison are shown in Table 4.1. One can see that the theoretical predictions obtained with our program agree well with the experimental results along the whole range of transverse momenta. One can also see that the uncertainties of the NLL+NLO calculation, obtained by taking the envelope of the seven-point scale variation of μ_R and μ_F for the central resummation scale $Q = m_t$ and the variation of Q by factor of two with central μ_R and μ_F, are of the order of the experimental uncertainties. The experimental uncertainties will decrease with the new data, accumulated during the second run of LHC, and more precise theoretical computations will be of utmost importance. Our resummation formalism and the developed program is well suited for this task, provided that the two-loops amplitudes, which contribute at the next perturbative order, will be computed.

Chapter 5

q_T subtraction for heavy-quark pair production

The implementation of the various scattering amplitudes in a complete NNLO calculation at the fully differential (exclusive) level is a highly non-trivial task because of the presence of infrared (IR) divergences at intermediate stages of the calculation. In particular, these divergences do not permit a straightforward implementation of numerical techniques. As we have mentioned in the Introduction, various methods have been proposed and used to overcome these difficulties at the NNLO level [35–51].

The q_T subtraction formalism [48] is one of these methods to handle and cancel the IR divergences at the NLO and NNLO level. The method has been successfully applied to the fully differential computation of NNLO QCD corrections to several hard-scattering processes [48,97–107]. It uses IR subtraction counterterms that are constructed by considering and explicitly computing the transverse-momentum (q_T) distribution of the produced final-state system in the limit $q_T \to 0$. If the produced final-state system is composed of non-QCD (colourless) partons (e.g., leptons, vector bosons or Higgs bosons), the behaviour of the q_T distribution in the limit $q_T \to 0$ has a universal (process-independent) structure that is explicitly known up to the NNLO level through the formalism of transverse-momentum resummation [128], presented in Chapter 3. These results on transverse-momentum resummation are sufficient to fully specify the q_T subtraction formalism for this entire class of processes. Therefore, up to now, the applications of the q_T subtraction formalism have been limited to the production of colourless high-mass systems in hadron collisions.

In this Chapter we present our results on the application of the q_T subtraction method to the NNLO computation of heavy-quark production in hadron collisions. To this purpose, we use the recent progress on transverse-momentum resummation for heavy-quark production [93–95]. We exploit the formulation of transverse-momentum resummation in Ref. [95], presented in Section 4.1, that includes the *complete* dependence on the kinemat-

ics of the heavy-quark pair. This dependence and, in particular, the complete control on the heavy-quark azimuthal correlations are essential (see below) to extract all the NNLO counterterms of the q_T subtraction method.

In the following, on the example of the $Q\bar{Q}$ production process, we present the main building blocks of the q_T subtraction method. The q_T cross section $d\sigma_{h_1h_2\to Q\bar{Q}}/dq_T^2$ for the inclusive production process $h_1(P_1) + h_2(P_2) \to Q(p_3) + \bar{Q}(p_4) + X$ of Eq. (4.1) is computable by convoluting the corresponding partonic cross sections $d\hat{\sigma}_{a_1a_2\to Q\bar{Q}}/dq_T^2$ of the various partonic channels with the parton distribution functions of the colliding hadrons. We first note that, at LO, the transverse momentum $\mathbf{q_T} = \mathbf{p_{3T}} + \mathbf{p_{4T}}$ of the $Q\bar{Q}$ pair is exactly zero. As a consequence, as long as $q_T \neq 0$, the (N)NLO contributions are actually given by the (N)LO contributions to the $Q\bar{Q}$ + jet(s) process. Thus, we can write the partonic differential cross section as

$$\left[d\hat{\sigma}_{a_1a_2\to Q\bar{Q}}\right]_{(N)NLO}|_{q_T\neq 0} = \left[d\hat{\sigma}_{a_1a_2\to Q\bar{Q}+\text{jets}}\right]_{(N)LO} . \tag{5.1}$$

Applying Eq. (5.1) at NLO, the LO cross section $\left[d\hat{\sigma}_{a_1a_2\to Q\bar{Q}+\text{jets}}\right]_{LO}$ can be directly obtained by integrating the corresponding tree-level scattering amplitudes. Applying Eq. (5.1) at NNLO, $\left[d\hat{\sigma}_{a_1a_2\to Q\bar{Q}+\text{jets}}\right]_{NLO}$ can be evaluated by using any available NLO method (e.g., Refs. [28, 30, 31]) to handle and cancel the corresponding IR divergences. Therefore, $\left[d\hat{\sigma}_{a_1a_2\to Q\bar{Q}+\text{jets}}\right]_{(N)LO}$ is IR finite *provided* $q_T \neq 0$. The only remaining singularities of NNLO type are associated to the limit $q_T \to 0$. As we have shown in Section 4.6, where we have constructed the regular component $d\hat{\sigma}^{\text{reg.}}_{a_1a_2\to Q\bar{Q}}$ of the partonic cross section $d\hat{\sigma}_{a_1a_2\to Q\bar{Q}}$, the singular behaviour of the $\left[d\hat{\sigma}_{a_1a_2\to Q\bar{Q}+\text{jets}}\right]_{(N)LO}$ cross section in the limit $q_T \to 0$ is given by the expansion of the singular cross section $d\hat{\sigma}^{\text{sing.}}_{a_1a_2\to Q\bar{Q}}$ at N(NLO) (see Eq. (4.173)). This fact is the key point of the q_T subtraction method. More precisely, the analytical knowledge of the singular limit at low q_T is used to construct an IR subtraction counterterm to cancel the divergencies in the $\left[d\hat{\sigma}_{a_1a_2\to Q\bar{Q}+\text{jets}}\right]_{(N)LO}$ cross section.

Explicitly, according to the q_T subtraction method [48], the (N)NLO partonic cross section $d\hat{\sigma}^{(N)NLO}_{a_1a_2\to Q\bar{Q}}$ can be written as

$$d\hat{\sigma}^{(N)NLO}_{a_1a_2\to Q\bar{Q}} = \mathcal{H}^{(N)NLO}_{a_1a_2\to Q\bar{Q}} \otimes d\sigma^{LO}_{c\bar{c},\,Q\bar{Q}} + \left[d\hat{\sigma}^{(N)LO}_{a_1a_2\to Q\bar{Q}+\text{jet}} - d\hat{\sigma}^{Q\bar{Q},\,CT}_{(N)NLO\,a_1a_2}\right] , \tag{5.2}$$

where a sum over the Born level partonic channels $c\bar{c} = q\bar{q}$ and $c\bar{c} = gg$ is understood.

The square bracket term of Eq. (5.2) is IR finite in the limit $q_T \to 0$, but its individual contributions, $d\sigma^{(N)LO}_{Q\bar{Q}+\text{jet}}$ and $d\sigma^{Q\bar{Q},\,CT}_{(N)NLO}$ are separately divergent. The IR subtraction counterterm $d\sigma^{Q\bar{Q},\,CT}_{(N)NLO}$ is obtained from the (N)NLO perturbative expansion of the resummation formula of the logarithmically-enhanced contributions to the q_T distribution of the $Q\bar{Q}$ pair, given by Eqs. (4.174) and (4.175) at NLO and NNLO respectively. Explicitly,

the IR subtraction counterterm $d\sigma^{Q\bar{Q},CT}_{(N)NLO}$ in the partonic channel $a_1a_2 \to t\bar{t} + X$ is

$$d\sigma^{Q\bar{Q},CT}_{NLO} = \sum_{c=q,\bar{q},g} \frac{\alpha_S}{\pi} \widetilde{\Sigma}^{Q\bar{Q}\,(1)}_{c\bar{c}\leftarrow a_1a_2}(z_1,z_2;q_T/M)\,\frac{dq_T^2}{M^2} \otimes d\hat{\sigma}^{Q\bar{Q}}_{LO\,c\bar{c}}\,, \tag{5.3}$$

$$d\sigma^{Q\bar{Q},CT}_{NNLO} = \sum_{c=q,\bar{q},g} \left(\frac{\alpha_S}{\pi}\right)^2 \widetilde{\Sigma}^{Q\bar{Q}\,(2)}_{c\bar{c}\leftarrow a_1a_2}(z_1,z_2;q_T/M)\,\frac{dq_T^2}{M^2} \otimes d\hat{\sigma}^{Q\bar{Q}}_{LO\,c\bar{c}}\,. \tag{5.4}$$

The explicit forms of $\widetilde{\Sigma}^{Q\bar{Q}\,(1)}_{c\bar{c}\leftarrow a_1a_2}$ and $\widetilde{\Sigma}^{Q\bar{Q}\,(2)}_{c\bar{c}\leftarrow a_1a_2}$ are worked out in Section (4.6). Here we recall that they are organised in the following form:

$$\widetilde{\Sigma}^{Q\bar{Q}\,(1)}_{c\bar{c}\leftarrow a_1a_2}(z_1,z_2;q_T/M) = \sum_{n=1}^{2} \widetilde{\Sigma}^{Q\bar{Q}\,(1;n)}_{c\bar{c}\leftarrow a_1a_2}(z_1,z_2)\; I_n(q_T/M)\,, \tag{5.5}$$

$$\widetilde{\Sigma}^{Q\bar{Q}\,(2)}_{c\bar{c}\leftarrow a_1a_2}(z_1,z_2;q_T/M) = \sum_{n=1}^{4} \widetilde{\Sigma}^{Q\bar{Q}\,(2;n)}_{c\bar{c}\leftarrow a_1a_2}(z_1,z_2)\; I_n(q_T/M)\,, \tag{5.6}$$

where the coefficients $\widetilde{\Sigma}^{Q\bar{Q}\,(1;n)}_{c\bar{c}\leftarrow a_1a_2}$ and $\widetilde{\Sigma}^{Q\bar{Q}\,(2;n)}_{c\bar{c}\leftarrow a_1a_2}$ are given in Eqs. (4.164)–(4.165) and (4.167)–(4.170), respectively. The expressions in (5.3) and (5.4) involve convolutions (which are denoted by the symbol $\otimes$) with respect to the longitudinal-momentum fractions z_1 and z_2 of the colliding partons c and $\bar{c}$ in $d\hat{\sigma}^{Q\bar{Q}}_{LO\,c\bar{c}}$. The integration variable q_T in Eqs. (5.3) and (5.4) corresponds, in the limit $q_T \to 0$, to the transverse momentum of the produced $Q\bar{Q}$ pair in the cross section $d\hat{\sigma}^{Q\bar{Q}+\text{jet}}_{(N)LO}$ on the right-hand side of Eq. (5.2). Together, the term in the square bracket of Eq. (5.2) accounts for all the contribution to the partonic cross section $d\hat{\sigma}^{(N)NLO}_{Q\bar{Q}}$ at $q_T \neq 0$ and is fully known up to NNLO.

The contribution at $q_T = 0$ is embodied in the hard-collinear (IR-finite) factors $\mathcal{H}^{(N)NLO}_{a_1a_2\to Q\bar{Q}}$, given by Eqs. (4.166) and (4.171). In general, they receive contributions of both process-independent and process-dependent nature. As we have already discussed, the process-independent contributions to $\mathcal{H}^{Q\bar{Q}}_{N(NLO)}$ are analogous to those that contribute to Higgs boson [48] and vector boson [98] production, and they are explicitly known [128, 152–154]. The process-dependent contributions in $\mathcal{H}^{(N)NLO}_{a_1a_2\to Q\bar{Q}}$ are embodied in the hard-virtual functions $H^{Q\bar{Q}}_c$ ($c = q, g$), defined in Eq. (4.98). We recall that the n-th order hard-virtual functions $H^{Q\bar{Q}\,(n)}_c$ depend on the n-loop virtual corrections and on the n-th order IR counterterms $\widetilde{\mathbf{I}}^{(n)}_{c\bar{c}\to Q\bar{Q}}$, more importantly, on the n-th order IR finite contribution $\mathbf{F}^{(n)}_t$.

More precisely, the NLO hard-collinear counterterms $\mathcal{H}^{NLO}_{a_1a_2\to Q\bar{Q}}$ depend on the Born amplitudes, and on the one-loop virtual amplitudes, and are completely known [93–95] for all the partonic channels. The NNLO hard-collinear counterterms $\mathcal{H}^{NNLO}_{a_1a_2\to Q\bar{Q}}$ in the off-diagonal partonic channels derive from the knowledge of at most one-loop virtual amplitudes and from the explicit results on the NLO *azimuthal correlation* terms in the transverse-momentum resummation formalism [95]. The analytical computation of latter terms, presented in Section 4.2.2 (see Eqs. (4.84) and (4.85)), therefore, is absolutely

crucial for the explicit determination of the $\mathcal{H}^{NNLO}_{a_1a_2\to Q\bar{Q}}$ counterterms in general, and for all the off-diagonal partonic channels, in particular. The second-order hard-collinear counterterms in the diagonal channels $\mathcal{H}^{NNLO}_{c\bar{c}\to Q\bar{Q}}$, in addition, depend also on the two-loop virtual amplitudes and on the second-order IR finite contribution $\mathbf{F}^{(2)}_t$, which are currently unknown.

Therefore, in the NNLO calculation of the cross section in this Chapter we present numerical results for all the flavour off-diagonal channels $a_1a_2 \to t\bar{t} + X$, with $a_1a_2 = qg(\bar{q}g), qq(\bar{q}\bar{q}), qq'(\bar{q}\bar{q}'), q\bar{q}'(\bar{q}q')$ (q and q' denote quarks with different flavour), while for the flavour diagonal partonic channels $q\bar{q} \to t\bar{t} + X$ and $gg \to t\bar{t} + X$ we limit ourselves to show the cancellation of IR singularities at small q_T.

5.1 Implementation and checks

Up to NLO accuracy our numerical implementation is based on the tree-level scattering amplitudes and phase space generation of the MCFM program [155], suitably modified for q_T subtraction along the lines of the corresponding numerical programs for Higgs boson [48] and vector boson [98] production. At NNLO accuracy the $t\bar{t}$+jet cross section is evaluated by using the MUNICH code [109]. MUNICH provides a fully automated implementation of the NLO dipole subtraction formalism [28, 30] as well as an interface to the one-loop generator OPENLOOPS [32], which can also be used to obtain the spin- and colour-correlated tree-level matrix elements needed for the dipole terms. For the evaluation of tensor integrals we rely on the COLLIER library [156], which is based on the Denner–Dittmaier reduction techniques [157] of tensor integrals and on the scalar integrals of Ref. [158]. In OPENLOOPS problematic phase space points are addressed with a rescue system that uses the quadruple-precision implementation of the OPP method in CUTTOOLS [159] with scalar integrals from ONELOOP [160]. The computation of the hard-collinear $\mathcal{H}^{t\bar{t}}_{(N)NLO}$ and IR subtraction $d\hat{\sigma}^{t\bar{t},CT}_{(N)NLO}$ counterterms is based on our private implementation of analytical colour-correlated Born-level and one-loop amplitudes.

Based on the MUNICH NLO framework, recently the MATRIX NNLO framework [161] was developed, which includes an automated implementation of q_T-subtraction and resummation. This automated framework is limited only by the two-loop amplitudes entering the hard-collinear counterterm $\mathcal{H}^{F}_{NNLO}$, and has already been used, in combination with the two-loop scattering amplitudes of Refs. [162–164], for the calculations of $Z\gamma$ [101, 105], $W^{\pm}\gamma$ [105], ZZ [103, 165], W^+W^- [104, 166], $W^{\pm}Z$ [106] and HH [107] production at NNLO QCD as well as in the resummed computations of the ZZ and W^+W^- transverse-momentum spectra [127] at NNLL+NNLO. MATRIX has inherited such features of the MUNICH framework as the automatic computation of scale uncertainties both for total cross sections and for distributions, the computation of arbitrarily many single-differential

distributions in a single run, and a natural parallelisation of the computation into partonic channels. In view of exploiting these nice features in our heavy-quark production computation and, more importantly, of the prospect on future automation of the NNLO computations for processes with additional colourless final-state particles, we have started implementing the relevant counterterms of the q_T subtraction method for heavy-quark production process in the MATRIX framework. Up to NLO accuracy we already have the full implementation, while at NNLO accuracy we have finished the implementation of the $d\hat{\sigma}^{t\bar{t},CT}_{NNLO}$ counterterm contribution for all the off-diagonal partonic channels. We find full agreement between the results obtained with MATRIX and our original implementation in Fortran. At this stage the implementation of the $d\hat{\sigma}^{t\bar{t},CT}_{NNLO}$ counterterms in the diagonal partonic channels is not possible in the MATRIX framework due to the yet unavailable one-loop colour-correlated amplitudes in OPENLOOPS [32]. Together with the OPENLOOPS team we are working on fixing the colour-bases and in the near future we will be able to complete the implementation also for the diagonal partonic channels.

As we have already mentioned, the transverse-momentum resummation for heavy-quark production has been also worked out in SCET [93,94]. In particular, the paper [94] provides the expansion of the resummation formula at NNLO accuracy in a Mathematica notebook file, as a function of the kinematical variables of the process. We have checked our results against the results in this Mathematica file for fixed phase space points and found perfect agreement for the terms contributing to the $d\hat{\sigma}^{t\bar{t},CT}_{(N)NLO}$ counterterms at (N)NLO and to the hard-collinear functions $\mathcal{H}^{t\bar{t}}_{NLO}$ at NLO accuracy. The NNLO hard-collinear counterterm $\mathcal{H}^{t\bar{t}}_{NNLO}$ can not be fully constructed from the expansion of the resummation formula of Refs. [93, 94] even for the off-diagonal partonic channels, due to the missing contributions from the azimuthal correlation terms (see Eq. (4.172)).

In the practical implementation of the q_T subtraction method we treat the terms in the square bracket of Eq. (5.2), $d\hat{\sigma}^{(N)LO}_{a_1a_2\to Q\bar{Q}+\text{jet}}$ and $d\hat{\sigma}^{Q\bar{Q},CT}_{(N)NLO\,a_1a_2}$ separately from each other, by introducing a technical cut on q_T, which renders both terms separately finite. In this way, the q_T-subtraction method works very similarly to a phase-space slicing method. In practice, it turns out to be more convenient to use a cut, r_{cut}, on the dimensionless quantity $r = q_{T,t\bar{t}}/M_{t\bar{t}}$.

The counterterm $d\hat{\sigma}^{Q\bar{Q},CT}_{(N)NLO\,a_1a_2}$ cancels all divergent terms from the real-emission contributions at small q_T, implying that the r_{cut} dependence of their difference should vanish in the $r_{\text{cut}} \to 0$ limit. In practice, however, as both the counterterm and the real-emission contribution grow arbitrarily large for $r_{\text{cut}} \to 0$, the statistical accuracy of the Monte Carlo integration degrades, preventing one from going to very low values of r_{cut}. On the other hand, the r_{cut} dependence of the cross section can be used as a tool to check the correctness of the computation, since any significant mismatch between the counterterm and the real contribution would result in a divergent cross section in the limit $r_{\text{cut}} \to 0$. We also use the numerical information on the r_{cut} dependence of the cross section to quantify the uncertainty due to finite r_{cut} values.

5.2 Results

Having discussed the content of Eq. (5.2), we are in a position to apply it to $t\bar{t}$ production and to obtain the complete NLO results plus the NNLO corrections in all the flavour off-diagonal partonic channels. As we have mentioned in the beginning of this chapter, we have the full information needed to construct the counterterm $d\hat{\sigma}^{Q\bar{Q},CT}_{NNLO}$ also in the flavour diagonal partonic channels $q\bar{q} \to t\bar{t} + X$ and $gg \to t\bar{t} + X$. Therefore, we also present the stability of the q_T subtraction method in these partonic channels. Our NLO implementation of the calculation has the main purpose of illustrating the applicability of the q_T subtraction method to heavy-quark production and, in particular, of cross-checking the q_T subtraction methodology by numerical comparisons with NLO calculations performed by using more established NLO methods. Our NNLO results on $t\bar{t}$ production represent a first step (due to the missing flavour diagonal partonic channels) towards the complete NNLO calculation for this production process.

5.2.1 Results at NLO

We start the presentation of our results by considering pp collisions at $\sqrt{s} = 8$ TeV. We use the MSTW2008 [151] PDFs with the QCD running coupling α_S evaluated at each corresponding order (i.e., we use $(n+1)$-loop α_S at N^{n}LO, with $n = 1, 2$). The pole mass of the top quark is $m_t = 173.3$ GeV. The renormalization and factorization scales, μ_R and μ_F, are fixed at $\mu_R = \mu_F = m_t$.

In Fig. 5.1 we show the $r_{\rm cut}$ dependence of our NLO results for all the partonic channels contributing at this order, as well as for the full NLO cross section (all partonic channels combined). These results are obtained with the MATRIX framework, which allows for simultaneous cross-section evaluations at variable $r_{\rm cut}$ values, without the need of repeated runs. In the upper panels of Fig. 5.1, the $r_{\rm cut}$ dependence in the diagonal partonic channels ($q\bar{q}$ and gg) are presented, while the lower left panel plot depicts the $r_{\rm cut}$ dependence in the qg channel, which contributes first at relative order α_S. In the lower right panel we show the $r_{\rm cut}$ dependence of the full NLO cross section. We vary the technical cut variable $r_{\rm cut}$ in the range from 0.01 % to 1 %. The $r_{\rm cut}$-independent cross section in the corresponding partonic channels, obtained with Catani-Seymour subtraction is used as a reference for the validation of the q_T-subtraction result. As we see from Fig. 5.1, the $r_{\rm cut}$ dependence is of the order of -0.3 % and -0.6 % for the $q\bar{q}$ and gg channels, respectively, while the cross section in the qg channel exhibits much larger $r_{\rm cut}$ dependence, of the order of -7 %. The relatively larger $r_{\rm cut}$ dependence in the qg channel is due to the fact that this channel starts to contribute only from NLO. In general, the $r_{\rm cut}$ dependence is due to the power-suppressed contributions that are left after the cancellation of the logarithmic singularity at small $r_{\rm cut}$. We observe relatively larger power corrections for the $t\bar{t}$ production cross

section compared to the production processes of colourless systems, which do not involve photons (see. e.g. the $r_{\rm cut}$ dependence studies for the W^+W^- production in Ref. [166]). As we have discussed in the previous sections, the IR singularity structure for the heavy-quark production process is richer than that of the production of colourless high-mass systems, due to the soft large-angle radiation of partons from the heavy quarks. Thus, it is most likely that the relatively larger power corrections that we see in Fig. 5.1 originate from these additional singularities. Despite the relatively larger $r_{\rm cut}$ dependence, our NLO results in all partonic channels reproduce the Catani-Seymour results for very low $r_{\rm cut}$ values, providing, thus, a strong check on our results.

In Figs. 5.2 and 5.3 we compare the NLO differential distributions obtained by using MCFM (which implements the dipole subtraction method [28, 30]) with those obtained by using our numerical program. In particular in Fig. 5.2 we consider the invariant mass ($m_{t\bar{t}}$) distribution (left) and the rapidity ($y_{t\bar{t}}$) distribution (right) of the $t\bar{t}$ pair. In Fig. 5.3 we consider the rapidity (y_t) distribution (left) and the transverse-momentum ($p_{T,t}$) distribution (right) of the top quark. We clearly see that the distributions obtained with q_T subtraction are in excellent agreement with those obtained with MCFM. We have checked that the agreement persists also for different choices of μ_R and μ_F.

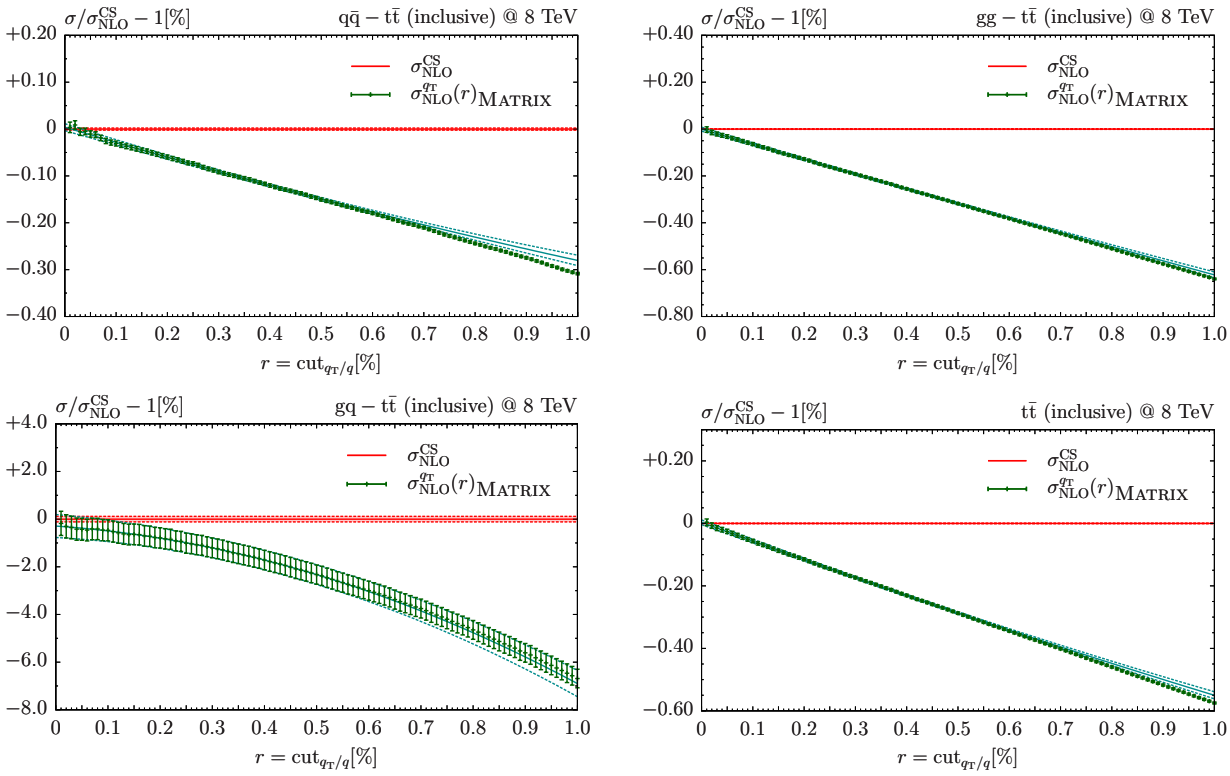

Figure 5.1: *Dependence of the NLO $pp \to t\bar{t}+X$ cross section at* 8 TeV *on the q_T subtraction cut, $r_{\rm cut}$, for $q\bar{q}$ (upper left plot), gg (upper right plot) and qg (lower central plot) partonic channels. The results are normalized to the $r_{\rm cut}$-independent NLO cross section computed with Catani-Seymour subtraction.*

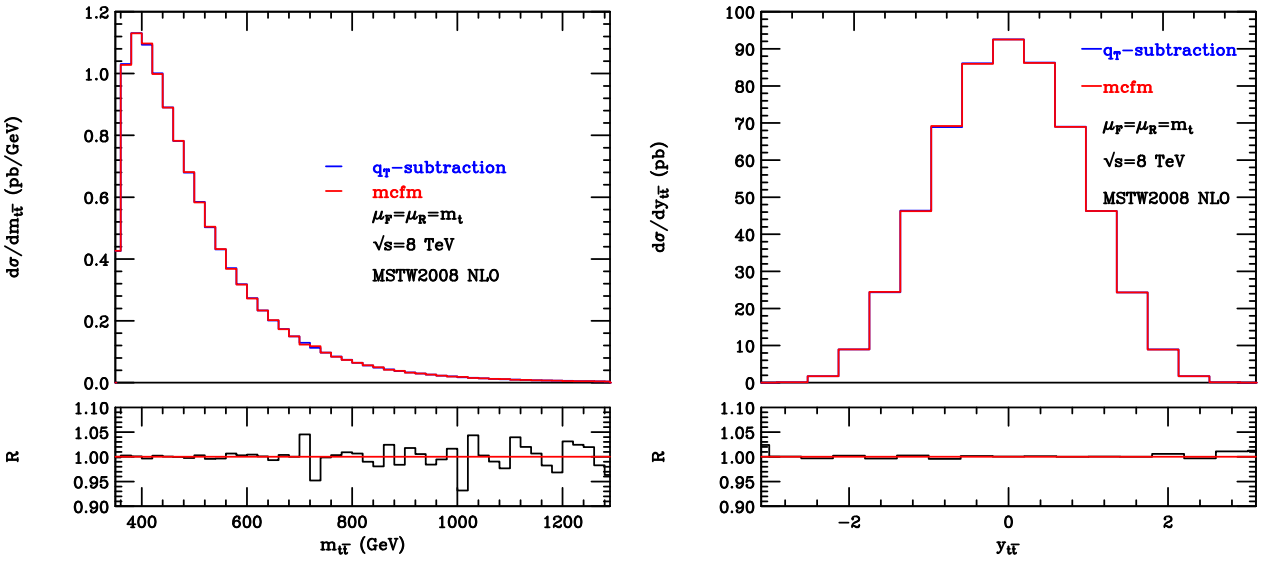

(a) (b)

Figure 5.2: *The invariant mass (left) and rapidity (right) distributions of the $t\bar{t}$ pair at the LHC ($\sqrt{s} = 8$ TeV) computed at NLO accuracy. Comparison of our results (blu) with the MCFM results (red). The lower panel presents the ratio of our results over the MCFM results.*

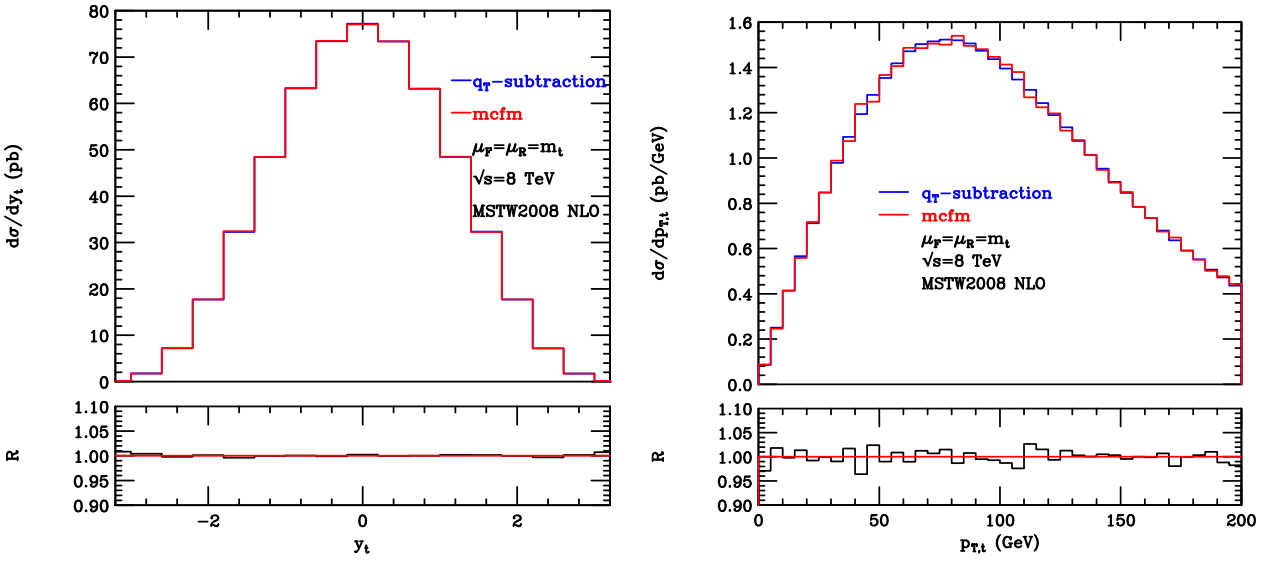

(a) (b)

Figure 5.3: *The rapidity (left) and transverse-momentum (right) distributions of the top quark at the LHC ($\sqrt{s} = 8$ TeV) computed at NLO accuracy. Comparison of our results (blu) with the MCFM results (red). The lower panel presents the ratio of our results over the MCFM results.*

5.2.2 Results at NNLO

We now move to consider the NNLO contributions. We first consider contributions to the NNLO cross section from the flavour off-diagonal partonic channels $ab \to t\bar{t} + X$. The contribution from all the channels with $ab = qg, \bar{q}g$ is labelled by the subscript qg, and the contribution from all the channels with $ab = qq, \bar{q}\bar{q}, qq', \bar{q}\bar{q}', q\bar{q}', \bar{q}q'$ is labelled by the subscript $q(\bar{q})q'$. We note that the partonic channels $q(\bar{q})q'$ contribute first at NNLO, while the qg channel contributes starting from NLO.

In Fig. 5.4 we show the r_{cut} dependence of the NNLO cross section contribution from the term in the square bracket of Eq. (5.2) in these partonic channels. Moreover, in order to concentrate on the r_{cut} dependence of the terms contributing at relative order α_{S}^2, and in particular to avoid possible cancellation of r_{cut} dependence from the $\mathcal{O}(\alpha_{\text{S}})$ contribution, in the case of the qg channel (right panel) the contribution to the NNLO cross section at relative order α_{S} is computed with r_{cut}-independent Catani-Seymour subtraction. The two histograms in Fig. 5.4 correspond to the different implementations of the IR subtraction counterterms. In particular, the green histogram is obtained in the MATRIX framework, while the one in magenta is obtained with the Fortran implementation. The two results are in a good agreement at small r_{cut} values, while at higher r_{cut} the results for the $q(\bar{q})q'$ partonic channel exhibit some differences. The difference has a statistical origin and related to the different mechanisms of obtaining the r_{cut} dependence results. While the MATRIX framework allows for simultaneous cross-section evaluations at variable r_{cut} values, the Fortan implementation does not have this feature. Up to $r_{\text{cut}} = 0.1\,\%$ we perform separate runs for every value of r_{cut} variable, while the prediction at higher r_{cut} values is obtained through the r-distribution of the cross section, which has a lower statistical accuracy and apparently a bit underestimated statistical error at larger values of the r_{cut} variable for the $q(\bar{q})q'$ channel.

As one can see from the right plot of Fig. 5.4, the r_{cut} dependence in the qg channel at NNLO is about $8\,\%$ and is opposite in sign of that at NLO, presented in Fig. 5.1. The r_{cut} dependence in the $q(\bar{q})q'$ partonic channels is much smaller, at the order of $0.5\,\%$. We note that even though the cross section in the qg channel starts at relative order α_{S}, the contribution at relative order α_{S}^2 is by far the dominating one. Therefore, we do not see the characteristic suppression of the r_{cut} dependence that we have seen for the NLO cross section in the diagonal partonic channels. We also recall that at this order the IR subtraction counterterm $d\hat{\sigma}^{Q\bar{Q},CT}_{(N)NLO\,qg}$ in the qg channel receives contribution from the soft anomalous dimension matrices, originating from the final-state soft radiation, while the cross section in the $q(\bar{q})q'$ partonic channels is free of such contribution, which might explain the relatively larger r_{cut} dependence in the qg channel with respect to the $q(\bar{q})q'$ channel. We finally note, most importantly, that we do not observe any significant r_{cut} dependence below $r_{\text{cut}} = 0.1\,\%$, which provides a stringent check on the correct cancellation of the IR singularities in the $d\sigma^{NLO}_{Q\bar{Q}+\text{jet}}$ cross section. We therefore use the finite-r_{cut} results

to extrapolate to $r_{\rm cut} = 0$, taking into account the breakdown of predictivity for very low $r_{\rm cut}$ values, and conservatively assign an additional numerical error to our results due to this extrapolation, which is of the order of 0.2 % and 1 % for the $q(\bar{q})q'$ and qg channels, respectively.

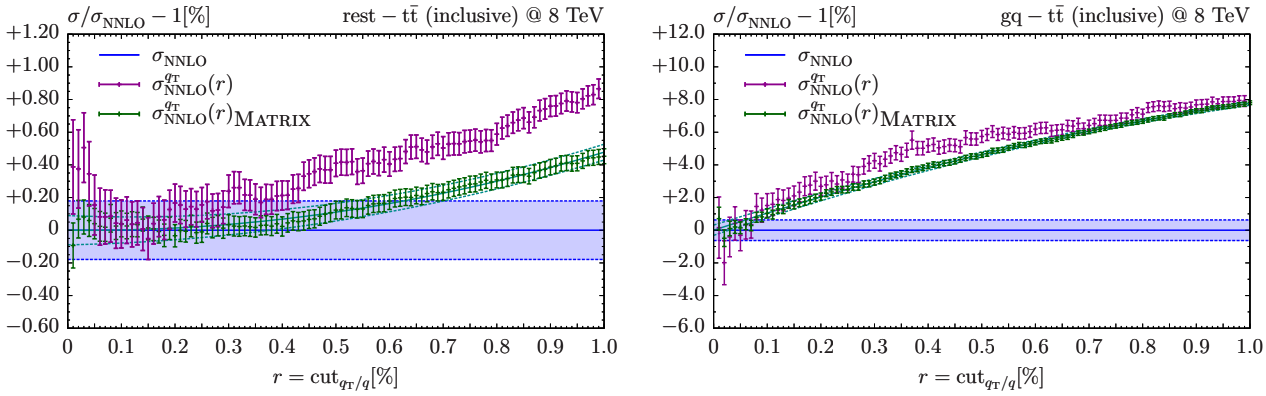

Figure 5.4: *Dependence of the $q_T \neq 0$ contribution to the NNLO $pp \to t\bar{t} + X$ cross section at* 8 TeV *on the q_T subtraction cut, $r_{\rm cut}$, for $q(\bar{q})q'$ (left plot), and qg (right plot) partonic channels, obtained with* MATRIX *(green) and our Fortran implementation (magenta). The results are normalized to their values at $r_{\rm cut} \to 0$, with a conservative extrapolation-error indicated by the blue bands.*

Having presented the $r_{\rm cut}$ dependence of the cross section contribution from the term in the square bracket of Eq. (5.2), we can now combine this term with the contribution from hard-collinear counterterms $\mathcal{H}^{NNLO}_{a_1 a_2 \to t\bar{t}}$, which are explicitly known for these off-diagonal partonic channels, thanks to the analytical computation of the azimuthal correlation contribution, given in Eqs. (4.65), (4.85). In Table 5.1 we report our results and we compare them with the corresponding results from the numerical program TOP++ [167], which implements the NNLO calculation of Ref. [57]. Specifically, we report the complete NLO results and the $\mathcal{O}(\alpha_{\rm S}^4)$ contributions to the NNLO cross section from the flavour off-diagonal partonic channels. From Table 5.1 we see that the results obtained by using q_T subtraction are in agreement with those from TOP++. We note that the numerical uncertainties of our $\mathcal{O}(\alpha_{\rm S}^4)$ results are at the 2% level. This is partially due to the uncertainty that we assign from our $r_{\rm cut}$ dependence analysis and partially due to the fact that in both the qg and $q(\bar{q})q'$ channels at $\sqrt{s} = 8$ TeV there is a strong quantitative cancellation between the contributions of the two terms in the right-hand side of Eq. (5.2) (the term that is proportional to $\mathcal{H}^{t\bar{t}}_{NNLO}$ and the term in the square bracket). The numerical uncertainties of our $\mathcal{O}(\alpha_{\rm S}^4)$ calculation can be reduced by considering different centre–of–mass energies. In particular, the numerical cancellation that we have mentioned is reduced by decreasing the centre–of–mass energy of the collision. We have computed the total cross section for $p\bar{p}$ collisions at $\sqrt{s} = 2$ TeV and we report the corresponding results in Table 5.2. We note that the numerical agreement between our calculation and the TOP++ result is still

satisfactory, and the numerical uncertainties of our $\mathcal{O}(\alpha_S^4)$ results are reduced below the 1% level. Using TOP++ we can compute the complete NNLO result and we note that the flavour off-diagonal partonic channels contribute to about 10% of the total result at $\mathcal{O}(\alpha_S^4)$ for both collision energies considered in Tables 5.1 and 5.2.

Cross section [pb]	NLO	$\mathcal{O}(\alpha_S^4)\|_{qg}$	$\mathcal{O}(\alpha_S^4)\|_{q(\bar{q})q'}$
q_T subtraction	226.2(1)	−2.25(5)	0.151(3)
TOP++	226.3	−2.253	0.148

Table 5.1: *Total cross sections for $t\bar{t}$ production. NLO and (partial) NNLO results from q_T subtraction compared with the corresponding results from* TOP++ *for pp collisions at $\sqrt{s} = 8$ TeV.*

Cross section [fb]	NLO	$\mathcal{O}(\alpha_S^4)\|_{qg}$	$\mathcal{O}(\alpha_S^4)\|_{q(\bar{q})q'}$
q_T subtraction	7083(3)	−61.5(5)	1.33(1)
TOP++	7086	−61.53	1.33

Table 5.2: *Total cross sections for $t\bar{t}$ production. NLO and (partial) NNLO results from q_T subtraction compared with the corresponding results from* TOP++ *for $p\bar{p}$ collisions at $\sqrt{s} = 2$ TeV.*

We finally move to consider the contribution to the NNLO cross section from the diagonal partonic channels $q\bar{q}$ and gg. As we have mentioned in the beginning of this chapter, at this stage we are not able to compute the full NNLO cross section in these channels, due to the missing information in the hard-collinear counterterms $\mathcal{H}^{NNLO}_{c\bar{c}\to t\bar{t}}$. However, we have the full analytical knowledge of the IR subtraction counterterm $d\hat{\sigma}^{t\bar{t},CT}_{NNLO\,c\bar{c}}$ to cancel the IR singularities in the $d\sigma^{NLO}_{t\bar{t}+\text{jet}}$ cross section in these partonic channels, which exhibit much more complex structure, compared to the off-diagonal ones, involving the second-order anomalous dimension matrix and the one-loop colour-correlations. Moreover, this task also required the completion of the massive Dipole subtraction implementation for these channels in the MUNICH code. To test the prediction of the $d\sigma^{NLO}_{t\bar{t}+\text{jet}}$ cross section obtained with the new version of MUNICH, we also computed it with the SHERPA Monte Carlo event generator [168], operating with the COMIX [169] matrix-element generator and found nice agreement.

In Fig. 5.5 we show the r_{cut} dependence of the NNLO cross section contribution in the diagonal partonic channels from the term in the square bracket of Eq. (5.2). As in the case of qg channel, the contribution to the NNLO cross section at relative order α_S is

computed with $r_{\rm cut}$-independent Catani-Seymour subtraction. We see from Fig. 5.5 that the $r_{\rm cut}$ dependence both in the $q\bar{q}$ channel (left plot) and in the gg channel (right plot) is smaller in the absolute value (about 0.15 % in the $q\bar{q}$ channel and 0.4 % in the gg channel) than that at NLO, and is opposite in sign. Most importantly, the results in both cases nicely converge at small $r_{\rm cut}$. We follow the same procedure for assigning a numerical uncertainty due to the $r_{\rm cut}$ dependence as in the case of off-diagonal channels. As we can see from the blue bands of Fig. 5.5, we control the subtraction at the level of 0.05 % and 0.2 % for the $q\bar{q}$ and gg channels, respectively. The cancellation of the IR singularities in the diagonal partonic channels represents the first non-trivial step towards the extension of our framework to the computation of the full NNLO QCD corrections to the $t\bar{t}$ production process at hadron colliders.

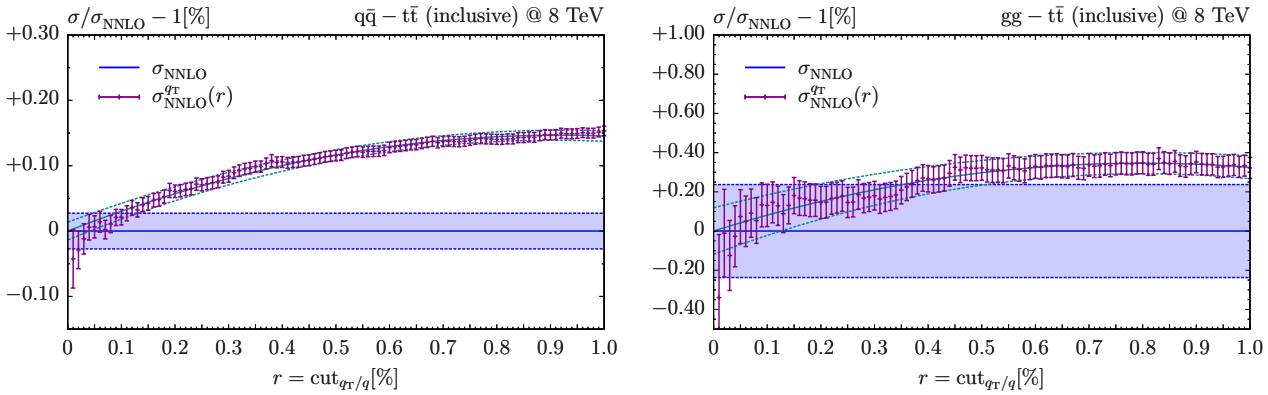

Figure 5.5: *Dependence of the $q_T \neq 0$ contribution to the NNLO $pp \to t\bar{t} + X$ cross section at 8 TeV on the q_T subtraction cut, $r_{\rm cut}$, for $q\bar{q}$ (left plot), and gg (right plot) partonic channels. The results are normalized to their values at $r_{\rm cut} \to 0$, with a conservative extrapolation-error indicated by the blue bands.*

Chapter 6

Azimuthal asymmetries

In this chapter we come back to the issue of azimuthal correlations at small q_T. To simplify the illustration of the key points we begin our detailed discussion by considering the simplest class of processes, in which the produced high-mass system in the final state is formed by only two 'particles' in generalized sense (point-like particles and/or jets).

We consider the inclusive hard-scattering hadroproduction process

$$h_1(P_1) + h_2(P_2) \to F(\{p_3, p_4\}) + X \quad , \tag{6.1}$$

in which the collision of the two hadrons h_1 and h_2 with momenta P_1 and P_2 produces the triggered final state F, and X denotes the accompanying final-state radiation. The observed final state F is a generic system that is formed by two 'particles', f_3 and f_4, with four momenta p_3 and p_4, respectively. The two particles can be point-like particles or hadronic jets (j), which are reconstructed by a suitable (infrared and collinear safe) jet algorithm. As for the case of point-like particles, the most topical process is the production of a high-mass lepton pair $\ell\ell'$ through the DY mechanism of quark–antiquark annihilation. We can consider many other cases such as, for instance, the production of a photon pair ($\gamma\gamma$), a pair of top quark and antiquark ($t\bar{t}$) or a pair of vector bosons (VV), in addition to dijet production (jj) and associated production processes such as vector boson plus jet (Vj). The invariant masses of the two particles have a little role in the context of our discussion (and they do not affect any conceptual aspects of our discussion). The system F has *total* invariant mass M ($M^2 = (p_3 + p_4)^2$), transverse momentum $\mathbf{q_T}$ and rapidity y (transverse momenta and rapidities are defined in the centre–of–mass frame of the colliding hadrons). We require that M is large ($M \gg \Lambda_{QCD}$, Λ_{QCD} being the QCD scale), so that the process in Eq. (6.1) can be treated within the customary perturbative QCD framework. We use $\sqrt{s}$ to denote the centre–of–mass energy of the colliding hadrons, which are treated in the massless approximation ($s = (P_1 + P_2)^2 = 2P_1 \cdot P_2$).

The dynamics of the production process in Eq. (6.1) can be described in terms of five

kinematical variables: the total mass M, transverse momentum q_T and rapidity y of the system F and two independent angular variables that specify the kinematics of the two particles f_3 and f_4 with respect to the total momentum $q = p_3 + p_4$ of F. These two angular variables are a polar-angle variable and an azimuthal-angle variable. To be definite and to avoid the use of 'exotic' variables, we refer to a widely-used set of angular variables and we use the polar angle θ and the azimuthal angle φ (of particle f_3) in the Collins–Soper (CS) rest frame[†] [170] of the system F.

The variable φ is the relevant variable for our discussion of azimuthal correlations. We remark that φ specifies the azimuth of one of the two paricles in the system F with respect to the total momentum of the system. In particular, we also remark that we are not considering the relative azimuthal separation $\Delta\phi = \phi_3 - \phi_4$ ($\phi_i = \phi(\boldsymbol{p_T}_i)$, with $i = 3, 4$, is the azimuthal angle of the transverse-momentum vector $\boldsymbol{p_T}_i$ in the centre–of–mass frame of the colliding hadrons) between the two particles. However, we can anticipate (we postpone comments on this point) that our main findings are not specific of the CS frame, and they are equally valid for other azimuthal variables with respect to the system F (for instance, we can consider the azimuthal angle in a different rest frame of F or, simply, the azimuthal difference $\phi(\boldsymbol{p_T}_i) - \phi(\mathbf{q_T})$, where $\phi(\mathbf{q_T})$ is the azimuthal angle of $\mathbf{q_T}$ in the centre–of–mass frame of the colliding hadrons).

Using the kinematical variables in the CS frame, we can consider azimuthal distributions for the process in Eq. (6.1). The most elementary azimuthal-dependent observable is the azimuthal cross section at fixed invariant mass,

$$\frac{d\sigma}{dM^2\, d\varphi} \quad , \tag{6.2}$$

and we can also consider less inclusive observables such as, for instance, the q_T-dependent azimuthal cross section in Eq. (6.3) and the multidifferential (five-fold) cross section in Eq. (6.4):

$$\frac{d\sigma}{dM^2\, dq_T^2\, d\varphi} \quad , \tag{6.3}$$

$$\frac{d\sigma}{dM^2\, dy\, dq_T^2\, d\cos\theta\, d\varphi} \quad . \tag{6.4}$$

All these quantities are related (from the less inclusive to the more inclusive case) through integration of kinematical variables (for instance, the azimuthal cross section in Eq. (6.2) is obtained by integrating Eq. (6.3) over q_T^2) and, in particular, the azimuthal integration of Eq. (6.2) gives the total cross section (at fixed invariant mass) of the process:

$$\frac{d\sigma}{dM^2} = \int_0^{2\pi} d\varphi \; \frac{d\sigma}{dM^2\, d\varphi} \quad . \tag{6.5}$$

[†]Since we are dealing with a rest frame of F, the two particles are exactly (by definition) back–to–back in that frame. In particular, the relative azimuthal separation is $\Delta\varphi = \pi$.

Obviously, we can also consider differential cross sections that are integrated over a certain range of values of the invariant mass.

Since all the cross sections that we have just mentioned are infrared and collinear safe quantities [171], they can be computed perturbatively within the customary QCD factorization framework (see Ref. [172] and references therein). The only non-perturbative (strictly speaking) input is the set of parton distribution functions (PDFs) of the colliding hadrons. The PDFs are convoluted with corresponding partonic differential cross sections $d\hat{\sigma}$ that can be evaluated as a power series expansion in the QCD running coupling $\alpha_{\rm S}(M)$ (see Eq. (2.76)).

This perturbative QCD framework is applicable at any finite (and arbitrary) fixed perturbative order. Despite this statement, the first main observation that we want to make is that the *fixed-order* (f.o.) perturbative calculation of the azimuthal distributions can lead to divergent (and, hence, unphysical and useless) results. More specifically, the f.o. calculation of the azimuthal cross section of Eq. (6.2) gives the following results:

$$\frac{d\sigma}{dM^2\,d\varphi} = \begin{cases} \text{finite at any f.o.} & \text{(DY production process)} \\ \\ \text{divergent for any } \varphi \text{ at some f.o.} & (t\bar{t}, Vj, jj, \gamma\gamma, ..., \text{production process}) \end{cases} . \tag{6.6}$$

We mean that the perturbative computation of $d\sigma/dM^2\,d\varphi$ for the DY process gives a finite result order–by–order in QCD perturbation theory[†], while in most of the other cases (some of them are listed in the right-hand side of Eq. (6.6)) the computation gives a divergent (meaningless) result for *any* values of the azimuthal angle φ starting from *some* perturbative order. We note that the integration over φ of $d\sigma/dM^2\,d\varphi$ gives the total cross section (see Eq. (6.5)), which is known to be finite at any f.o.. Therefore, the divergent behaviour that is highlighted in Eq. (6.6) originates from the *azimuthal-correlation*[‡] component, $d\sigma^{\rm corr}/dM^2\,d\varphi$, of the azimuthal cross section:

$$\frac{d\sigma^{\rm corr}}{dM^2\,d\varphi} \equiv \frac{d\sigma}{dM^2\,d\varphi} - \langle\frac{d\sigma}{dM^2\,d\varphi}\rangle_{\rm av.} = \frac{d\sigma}{dM^2\,d\varphi} - \frac{1}{2\pi}\,\frac{d\sigma}{dM^2} \quad , \tag{6.7}$$

where the notation $\langle\cdots\rangle_{\rm av.}$ denotes the azimuthal average and $d\sigma/dM^2$ is the total cross section in Eq. (6.5).

To understand the origin of the divergent behaviour in Eq. (6.6), we first comment about kinematics. If the system F has vanishing transverse momentum ($q_T = 0$), the rest

[†]As we will see in the following discussion this is due to the helicity-conserving nature of the collinear radiation from the quarks and the trivial colour structure of the underlying Born process $q\bar{q} \to Z$.

[‡]Using the shorthand notation $d\sigma(\varphi)$ to denote a generic multidifferential cross section with azimuthal dependence (e.g., the cross sections in Eqs. (6.3) and (6.4)), its azimuthal average is $\langle d\sigma(\varphi)\rangle_{\rm av.}$ and we can define the corresponding correlation component as $d\sigma^{\rm corr}(\varphi) \equiv d\sigma(\varphi) - \langle d\sigma(\varphi)\rangle_{\rm av.}$, analogously to the definition in Eq. (6.7).

frame of F is obtained by simply applying a longitudinal boost to the centre–of–mass frame of the colliding hadrons. Any additional rotation in the transverse plane of the collison leaves the system F at rest and makes the particle azimuthal angle φ ambiguously defined. Owing to the azimuthal symmetry of the collision process, if $q_T = 0$ there is no preferred direction to define φ. In other words, considering the azimuthal angle φ (as defined in the CS frame or any other rest frame of F) and performing the limit $q_T \to 0$, we have

$$\cos\varphi = \cos(\phi_3 - \phi(\mathbf{q_T})) + \mathcal{O}(q_T/M) \ , \tag{6.8}$$

where $\phi_3 = \phi(\boldsymbol{p_{T3}})$ and $\phi(\mathbf{q_T})$ are the azimuthal angles of the corresponding transverse-momentum vectors in the centre–of–mass frame of the colliding hadrons. If $q_T = 0$, $\phi(\mathbf{q_T})$ is not defined and, consequently, φ is not (unambiguously) defined. At the strictly formal level, to define the azimuthal correlation we have to exclude the phase space point at $q_T = 0$. In practical terms, the azimuthal correlation is defined provided $q_T \neq 0$. If we want to consider q_T integrated azimuthal correlations (such as, for instance, the cross section in Eq. (6.7)), we have to introduce a minimum value of q_T ($q_T > q_{\rm cut}$) and eventually perform the limit $q_{\rm cut} \to 0$. The divergences that are highlighted in Eq. (6.6) do not appear by considering azimuthal correlations at fixed and finite values of q_T (e.g., the azimuthal-dependent cross sections in Eq. (6.3) and (6.4)). These divergences are related to the limit $q_{\rm cut} \to 0$ after integration of the azimuthal correlations over q_T.

Our discussion on the limit $q_{\rm cut} \to 0$ reconciles the appearence of divergences in Eq. (6.6) with the perturbative criterion of infrared and collinear safety at the formal level: no divergence occurs provided $q_T \neq 0$, namely, provided the azimuthal-correlation observable is well (unambiguously) defined. However, a single phase space point at $q_T = 0$ is physically harmless. Therefore, the q_T integrated azimuthal correlations (i.e., their limiting behaviour as $q_{\rm cut} \to 0$) are finite and measurable quantities. Moreover, they are also finite and measurable if $q_{\rm cut}$ is non-vanishing, or, equivalently if q_T is not vanishing and fixed at an arbitrarily small value. The divergence in Eq. (6.6) implies that the q_T dependent azimuthal correlations become *singular* at small values of q_T, and that this singular behaviour is *not integrable* over q_T in the limit $q_T \to 0$. This unphysical behaviour of f.o. perturbative QCD at small values of q_T and the divergence of the q_T integrated azimuthal correlations certainly require some deeper understanding to have a QCD theory of physically measurable azimuthal correlations. As a possible shortcut, one can still use f.o. perturbative QCD but avoid the region of small values of q_T. In this case one still needs some understanding of the phenomenon in order to assess the extent of the dangerous small-q_T region where the f.o. predictions are 'unphysical' or, anyhow, not reliable at the quantitative level.

We note that the kinematical relation in Eq. (6.8) implies that the azimuthal angle in the CS frame has no privileged role in the context of our discussion of azimuthal correlations in the small-q_T region. The main features of the small-q_T behaviour of azimuthal correlations that are discussed here are basically unaffected by using azimuthal angles as defined in other rest frames of the system F, or, by using other related definitions of azimuthal angles. For instance, one can simply replace the CS frame angle φ with one of the relative

azimuthal angles $\phi(\boldsymbol{p_T}_i) - \phi(\mathbf{q_T})$ $(i = 3, 4)$ in the centre–of–mass frame of the colliding hadrons. Alternatively, one can use the difference between the azimuthal angles (in the centre–of–mass frame of the colliding hadrons) of the two transverse-momentum vectors $\boldsymbol{p_T}_3 - \boldsymbol{p_T}_4$ and $\mathbf{q_T}$. All these definitions of the relevant (for our purposes) azimuthal-angle variable turn out to be equivalent (because of Eq. (6.8)) in the limit $q_T \to 0$ (or, at very small values of $q_{\rm cut}$). In the following we continue to mainly refer ourselves to the azimuthal angle in the CS frame, although all the basic feature that we discuss are unchanged by considering the other definitions of the azimuthal angle.

We also note that the discussion that we have presented so far about azimuthal correlations can be generalized in a straightforward way to consider the case in which the system F is formed by more than two particles. In the multiparticle case, we can simply examine azimuthal correlations that are defined by using the azimuthal angles of the various particles in F in a specified rest frame of F (such as the CS frame), by simply using the various relative azimuthal angles $\phi(\boldsymbol{p_T}_i) - \phi(\mathbf{q_T})$ in the centre–of–mass frame of the colliding hadrons, or by using some other related (i.e., equivalent in the limit $q_T \to 0$) azimuthal variables. Since the multiparticle cases do not present any additional conceptual issues with respect to the two-particle case, in the following we continue to explicitly consider (for the sake of technical simplicity) only systems F that are formed by two particles.

The f.o. perturbative divergences of the azimuthal correlations originate from QCD radiative corrections due to emission of final-state parton with low transverse momentum (soft and collinear partons). Since the azimuthal correlations behave differently in different processes (as stated in Eq. (6.6)), we recall the conditions that produce the divergent behaviour.

Azimuthal correlations can have f.o. divergences if at some order in the strong coupling the final-state system $F(\{p_3, p_4\})$ can be produced by the partonic subprocess $c_1\, c_2 \to F$ where either

- at least one of the initial−state colliding partons c_1 and c_2 is a gluon, (6.9)
- at least one of the final−state particles carry QCD colour charge. (6.10)

The conditions in (6.9) and (6.10) follow from a generalization of the results in Refs. [69, 95] (see Section 4.2.1). The divergences arise from the computation of the QCD radiative corrections to the partonic process $c_1\, c_2 \to F$ (they do not arise in the computation of that partonic subprocess itself!). Specifically, the f.o. divergences originate from collinear-parton radiation [69] in the case of the condition (6.9) and from soft-parton radiation [95] in the case of the condition (6.10). We remark that one of the conditions in (6.9) and (6.10) is sufficient to produce the f.o. divergences. In particular, the condition (6.10) *necessarily* produces f.o. divergences, while the condition (6.9) produce divergences with some 'exception' (words of caution) in few specific cases (see below). Having discussed the source of f.o. divergences in general terms, we can comment on some specific processes.

The production of heavy-quark pairs such as, for instance, $t\bar{t}$ can occur through the partonic subprocesses of quark-antiquark annihilation ($q\bar{q} \to t\bar{t}$) and gluon fusion ($gg \to t\bar{t}$). One of these subprocesses has initial-state gluons and, moreover, both t and $\bar{t}$ have QCD colour charge. Therefore, if $F = \{t\bar{t}\}$ both conditions (6.9) and (6.10) are fulfilled and the corresponding azimuthal correlations have f.o. divergences (as stated in Eq. (6.6)). The same reasoning and conclusions apply to the production of $F = \{Vj\}$ and $F = \{jj\}$ (for instance, $F = \{Vj\}$ can be produced through $qg \to Vj$, where at the lowest-order $j = q$ carries QCD colour charge). In the case of $F = \{\gamma\gamma\}$ production the final-state photons do not carry QCD colour charge. However, diphoton production at the next-to-next-to-leading order (NNLO) can occur through the subprocess $gg \to \gamma\gamma$ (the interaction is mediated by a quark loop): therefore, due to the condition (6.9), the azimuthal correlations for diphoton production diverge starting from the N^{3}LO computation. The cases $F = \{ZZ\}$ and $F = \{W^+W^-\}$ behave similarly to $F = \{\gamma\gamma\}$, and they also lead to azimuthal correlation that have f.o. divergences.

We consider the DY process, where $F = \{\ell\ell'\}$ and the high-mass lepton pair originates from the decay of a vector boson V ($V \to \ell\ell'$). The final-state leptons have no QCD colour charge and, therefore, the condition (6.10) is not fulfilled. The partonic subprocesses $qg \to V(\ell\ell')$ and $\bar{q}g \to V(\ell\ell')$ are forbidden by colour conservation, and the partonic subprocess $gg \to V(\ell\ell')$ is forbidden by the spin 1 of the vector boson. The DY lepton pair can be produced through $q\bar{q} \to V(\ell\ell')$, but this partonic subprocess has no initial-state gluons. Therefore, also the condition (6.9) is not fulfilled and the azimuthal correlation for the DY process have no f.o. divergences in the computation of QCD radiative corrections (as it is well known and recalled in Eq. (6.6)).

We can comment on the production of a system of colourless particles, such as $F = \{\gamma\gamma\}$ or $F = \{ZZ\}$, in the specific case (or, better, within the approximation) in which those particles originate from the decay of a spin-0 boson, such as the Standard Model Higgs boson H (e.g., $H \to \gamma\gamma$ or $H \to ZZ$). In this case the production mechanism $gg \to H$ (followed by the H decay) is allowed. However, due to the spin-0 nature of H, the H decay dynamically decouples from the H production mechanism: the angular distribution of the final-state particles ($\gamma\gamma$ or ZZ) with momenta p_3 and p_4 is dynamically flat (it has no dynamical dependence on the decay angles, since it can only depend on the Lorentz invariant $2p_3 \cdot p_4 = M^2$, namely, on the invariant mass M of the produced pair of particles). As a consequence, although the condition (6.9) is fulfilled, there are no azimuthal correlations in this specific case and, hence, there are no accompanying f.o. divergences. The absence of azimuthal correlations follows from the requirement that the two final-state particles are due to the decay of a spin-0 boson. As a matter of principle at the conceptual level we note that, considering the final-state system $F = \{\gamma\gamma\}$ or $F = \{ZZ\}$, the various subprocesses that contribute to the production mechanism $gg \to F$ (subprocesses with and without an intermediate H, and corresponding interferences) are not physically distinguishable (this is, strictly speaking, correct although the applied kinematical cuts can sizeably affect the relative size of the various contributing subprocesses). As we have previously discussed,

the production of such systems without the intermediate decay of a spin-0 boson leads to azimuthal correlations with f.o. perturbative divergences. Therefore, if the condition (6.9) is fulfilled, we can conclude that sooner or later (in the computation of subsequent perturbative orders) QCD radiative corrections produce non-vanishing azimuthal correlations and ensuing f.o. divergences.

To the purpose of studying azimuthal correlations and presenting corresponding quantitative results in the following parts of the paper, we find it convenient to introduce harmonic components of azimuthal-dependent cross sections. In particular, we define the n-th harmonic:

$$\frac{d\sigma_n}{dM^2} \equiv \int_0^{2\pi} d\varphi \, \cos(n\varphi) \int_0^{+\infty} dq_T^2 \, \frac{d\sigma}{dM^2 \, dq_T^2 \, d\varphi} \, \Theta(q_T - q_{\rm cut}) \;\; , \qquad q_{\rm cut} = r_{\rm cut} \, M \;\; , \tag{6.11}$$

where n is a positive integer ($n = 1, 2, 3, \dots$). Note that, in view of our previous discussion on the origin of the divergences that are mentioned in Eq. (6.6), we have introduced a minimum value $q_{\rm cut}$ of q_T ($q_T > q_{\rm cut}$). We usually consider values of $q_{\rm cut}$ that are proportional to the invariant mass M of the system F ($q_{\rm cut} = r_{\rm cut} M$, with a fixed parameter $r_{\rm cut}$), although also fixed values of $q_{\rm cut}$ can be used. One can also consider n-th harmonics of more differential cross sections (e.g., differential with respect to y and $\cos\theta$ as in Eq. (6.4)). The n-th harmonic in Eq. (6.11) is defined by using the weight function $\cos(n\varphi)$; n-th harmonics with respect to the sine function can also be considered by simply replacing $\cos(n\varphi) \to \sin(n\varphi)$ in the integrand of Eq. (6.11). In particular, the knowledge of the harmonics with respect to both $\cos(n\varphi)$ and $\sin(n\varphi)$ for *all* integer values of n ($n = 1, 2, 3, \dots$) is equivalent to the complete knowledge of the azimuthal-correlation cross section in Eq. (6.7). Note that the n-th harmonic in Eq. (6.11) is not a positive definite quantity. Although the physical azimuthal cross section $d\sigma/dM^2 \, dq_T^2 \, d\varphi$ is positive definite, the weight function $\cos(n\varphi)$ (or $\sin(n\varphi)$) has no definite sign.

The n-th harmonic with weight $\cos(n\varphi)$ (or $\sin(n\varphi)$) gives a direct measurement of the $\cos(n\varphi)$ (or $\sin(n\varphi)$) *asymmetry* of the azimuthal-dependent cross section. The QCD computation of the n-th harmonic gives a finite result provided $q_{\rm cut}$ is not vanishing. On the basis of Eq. (6.6), in the limit $q_{\rm cut} \to 0$ some harmonics (asymmetries) can be divergent if computed at some f.o. in QCD perturbation theory. We cannot draw general conclusions on harmonics with odd n ($n = 1, 3, 5, \dots$), but from the results in Refs. [69, 95] we know that harmonics with *even* n ($n = 2, 4, 6, \dots$) can have f.o. divergences. Specifically, if the condition (6.9) is fulfilled the harmonics with $n = 2$ and $n = 4$ have f.o. divergences [69], and if the condition (6.10) is fulfilled *all* the n-even ($n = 2, 4, 6, 8$ and so forth) $\cos(n\varphi)$ asymmetries have f.o. divergences [95]. In Sect. 6.1 we explicitly show quantitative results on f.o. computations of harmonics for the DY and $t\bar{t}$ processes. The f.o. divergences of the azimuthal asymmetries can be cured by the all-order perturbative resummation of QCD radiative corrections. The resummed computation leads to azimuthal correlations and asymmetries that are finite, as it is the case of the corresponding physical (and measurable) quantities (see Sect. 6.3).

6.1 Examples

The lepton angular distribution of the DY process is a much studied subject both experimentally and theoretically. Recent measurements of the lepton angular distribution for Z production at LHC energies ($\sqrt{s} = 8$ TeV) are presented in Refs. [173, 174], together with corresponding QCD predictions from Monte Carlo event generators and f.o. calculations. A very recent phenomenological study of the DY lepton angular distribution is performed in Ref. [68]. As for previous literature on the subject, we mainly refer the reader to the list of references in Refs. [68, 173, 174].

The QCD structure of the DY lepton angular distribution is well known, and it is a consequence of the spin-1 nature of the vector bosons ($V = Z, \gamma^*, W^\pm$) involved in the DY mechanism. To be definite we consider the DY process at the Born level with respect to electroweak (EW) interactions. Within this Born level framework, the DY differential cross section is expressed in terms of a leptonic tensor (for the EW leptonic decay of the vector boson) and a hadronic tensor (for the hadroproduction of the vector boson). The QCD production dynamics is embodied in the hadronic tensor and the two tensors are coupled through the spin (helicity) correlations of the vector boson. Owing to quantum interferences, we are dealing with 9 helicity components of the five-fold differential cross section in Eq. (6.4) (the hadronic tensor is a 3×3 helicity polarization matrix, due to the 3 polarization states of the vector boson), which, therefore, can be expressed [175] as a linear combination of 9 spherical harmonics or, better, harmonic polynomials (the leptonic tensor has a polynomial dependence of rank 2 on the lepton momenta) of the lepton angles θ and φ (we specifically use the CS frame). For the illustrative purposes of our discussion of azimuthal correlations, it is sufficient to consider the four-fold differential cross section $d\sigma/(dM^2\, dy\, dq_T^2\, d\varphi)$, which is obtained by integrating Eq. (6.4) over $\cos\theta$. We write

$$2\pi \frac{d\sigma_{DY}}{dM^2\, dy\, dq_T^2\, d\varphi} = \frac{d\sigma_{DY}}{dM^2\, dy\, dq_T^2} + [d\sigma]_3 \cos(\varphi) + [d\sigma]_2 \cos(2\varphi) + [d\sigma]_7 \sin(\varphi) + [d\sigma]_5 \sin(2\varphi)\,, \tag{6.12}$$

where $d\sigma/(dM^2\, dy\, dq_T^2)$ is the DY differential cross section integrated over φ, and the shorthand notation $[d\sigma]_I$ denotes differential cross section components that only depends on M, y, q_T. The azimuthal dependence of Eq. (6.12) is *entirely* given by the four harmonics $\{\cos(\varphi), \cos(2\varphi), \sin(\varphi), \sin(2\varphi)\}$ that are explicitly written in the right-hand side of Eq. (6.12). The subscript I in $[d\sigma]_I$ is defined according to a customary notation in the literature [173–176], such that $[d\sigma]_I \equiv C_I A_I(M, y, q_T) \times d\sigma/(dM^2\, dy\, dq_T^2)$, where the functions $A_I(M, y, q_T)$ ($I = 0, 1, \ldots, 7$) are known as 'DY angular coefficients' and C_I are normalization factors (specifically, we have $C_2 = 1/4, C_5 = 1/2, C_3 = C_7 = 3\pi/16$). A point that we would like to remark is that the QCD dependence of the azimuthal correlations of the DY cross section involves *only* four harmonics. The five-fold cross section in Eq. (6.4) for the DY process is expressed in terms of 9 harmonic polynomials of θ and φ: however, their dependence on φ is given only in terms of the four harmonics that also appear in Eq. (6.12).

At the leading order (LO) in QCD perturbation theory, the DY cross section is due to the partonic subprocess $q\bar{q} \to V(\to \ell\ell')$, which is of $\mathcal{O}(\alpha_S^0)$. At this order in α_S, there is no azimuthal dependence. Azimuthal correlations start to appear at the next-to-leading order (NLO) through the *tree-level* partonic processes at $\mathcal{O}(\alpha_S)$ ($q\bar{q} \to V + g$ and its crossing related channels, such as $qg \to V + q$). At this order only the cross section components $[d\sigma]_3$ and $[d\sigma]_2$ in Eq. (6.12) are not vanishing. The azimuthal harmonics $\sin(\varphi)$ and $\sin(2\varphi)$ receives non-vanishing contributions only starting from NNLO processes. More precisely, these non-vanishing contributions [177] are entirely due to *one-loop* absorptive (and time reversal odd) corrections to the partonic subprocess $q\bar{q} \to V + g$ and its crossing related channels. Azimuthal correlations up to NNLO were first computed in Ref. [175]. Azimuthal-correlation results at N^{3}LO can be obtained, in principle, by exploiting recent progress on the computation of the NNLO corrections to '$V + 1\,jet$' production [49, 178].

We recall that the cross section component $[d\sigma]_2$ in Eq. (6.12) is parity conserving, while $[d\sigma]_3$, $[d\sigma]_5$ and $[d\sigma]_7$ are parity violating. If $V = \gamma^*$, only the $\cos(2\varphi)$ harmonic contributes in Eq. (6.12), while in the case of the five-fold differential cross section of Eq. (6.4) there is an additional non-vanishing azimuthal contribution that is proportional to $\sin(2\theta)\cos(\varphi)$ and it is due to $[d\sigma]_1$.

All the quantitative results that are presented in this paper refer to pp collisions at the LHC energy $\sqrt{s} = 8$ TeV. In the QCD calculations we use the set MSTW2008 [151] of PDFs at NLO.

To present some illustrative results for the DY process we consider on-shell Z production and its leptonic decay $Z \to e^+e^-$ in an electron–positron pair. Our QCD calculation is performed by using the numerical Monte Carlo program `DYNNLO` [98]. The EW parameters are specified in the G_μ scheme and we use the following values: the Fermi constant is $G_F = 1.1663787 \cdot 10^{-5}$ GeV^{-2}, the mass of the Z boson is $M_Z = 91.1876$ GeV and the mass of the W boson is $M_W = 80.385$ GeV. We use equal values of the factorization (μ_F) and renormalization (μ_R) scales and we set $\mu_F = \mu_R = M_Z$.

We specifically consider the numerical calculation of various $\cos(n\varphi)$ asymmetries (see Eq. (6.11)), and φ is the azimuthal angle of the electron in the CS frame. We evaluate the asymmetries at their non-trivial lowest order in f.o. perturbation theory and, therefore, we compute all the NLO tree-level partonic processes whose final state is '$Z(e^+e^-) + jet$', where the jet is a single parton at this perturbative order. Our numerical results are presented in Fig. 6.1-left.

The n-th harmonics are integrated over the transverse-momentum q_T of the e^+e^- pair and they are computed as a function of $r_{\rm cut} = q_{\rm cut}/M_Z$, where $q_{\rm cut}$ is the minumm value of q_T ($q_T > q_{\rm cut}$). The results in Fig. 6.1 are obtained for very small values of $r_{\rm cut}$ in the range $5 \cdot 10^{-4} < r_{\rm cut} < 5 \cdot 10^{-3}$. As we have already recalled, the azimuthal asymmetries for the DY process have no f.o. divergences. Indeed, the results for $n = 1, 2, 4$ that are presented

in Fig. 6.1-left show that the corresponding $\cos(n\varphi)$ asymmetries are basically independent of $r_{\rm cut}$ for very small values of $r_{\rm cut}$ and finite (the results in Fig. 6.1-left practically coincide with the numerical evaluation at $r_{\rm cut} = 0$). The result for the $n = 4$ asymmetry (blue line) in Fig. 6.1-left is consistent with a vanishing value, in agreement with the general expression in Eq. (6.12) (the very small deviations that are observed for $n = 4$ in Fig. 6.1-left give an idea of the numerical uncertainties in our calculation of the various asymmetries). The result for the $n = 1$ asymmetry (black line) gives a non-vanishing value (it corresponds to the integral of the differential cross section component $[d\sigma]_3$ in Eq. (6.12)). A non-vanishing value is obtained also for $n = 2$ (red line), and it corresponds to the computation of the cross section component $[d\sigma]_2$ in Eq. (6.12). Note that the $n = 2$ result reported in Fig. 6.1-left is rescaled by a factor of 0.1. Therefore, by inspection of Fig. 6.1-left we can see that the $\cos(2\varphi)$ asymmetry is approximately a factor of 5 larger than the $\cos(\varphi)$ asymmetry.

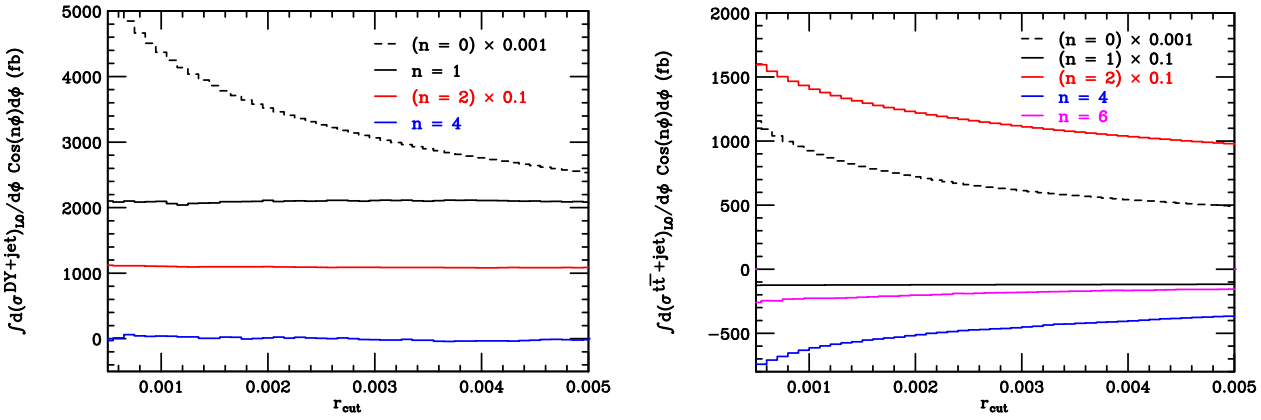

(a) (b)

Figure 6.1: *Azimuthal asymmetries for various n as a function of $r_{\rm cut}$: $DY/Z(e^+e^-)$ (left) $t\bar{t}$ (right)*

In Fig. 6.1-left we also report the result for the $n = 0$ harmonic (dashed line) of '$Z+jet$' production. The $n = 0$ harmonic corresponds to the total (azimuthally integrated) cross section, and it receives contributions from both real and virtual emission subprocesses. Real and virtual terms are separately divergent and their divergences cancel in the total contribution. In Fig. 6.1-left we report the result of the $n = 0$ harmonic computed exactly as specified in Eq. (6.11), namely, by applying a non-vanishing lower limit $q_{\rm cut} = r_{\rm cut} M$ on q_T. Therefore, our computation selects only the real-emission term due to the '$Z + jet$' subprocesses. As is well known, this real-emission term diverges in the limit $q_{\rm cut} \to 0$ and the divergent behaviour is proportional to $\ln^2 r_{\rm cut}$: in Fig. 6.1-left we clearly see the increasing behaviour of the $n = 0$ harmonic as $r_{\rm cut} \to 0$. In the actual computation of the total cross section, the $n = 0$ result in Fig. 6.1-left has to be combined with the NLO real-emission term at still smaller values of $r_{\rm cut}$ and with the LO and NLO virtual terms, thus leading to a total finite result. For the sake of completeness, we report the value (including

the numerical error of the Monte Carlo integration) of the NLO total cross section σ_{DY}^{NLO} that we obtain by using the same parameters as used in the results of Fig.6.1-left: it is $\sigma_{DY}^{NLO} = 1100 \pm 1$ pb. We note that σ_{DY}^{NLO} is roughly 100 times larger than the value of the $\cos(2\phi)$ asymmetry in Fig.6.1-left.

The DY process is quite 'special' with respect to azimuthal correlations: the azimuthal correlations are finite order-by-order in QCD perturbation theory and their general QCD structure involves only 4 azimuthal harmonics (as shown in Eq. (6.12)). For most of the other hard-scattering processes (with few possible exceptions such as $H \to \gamma\gamma, ZZ$ production, as discussed in Section 4.2.1) azimuthal correlations behaves differently: usually they have an azimuthal dependence that involves an infinite set of harmonics (all values of n) and in many cases f.o. QCD computations lead to divergences.

We consider the production of heavy-quark $Q\bar{Q}$ pairs and we treat the heavy quark and antiquark as on-shell particles. Our discussion equally applies to any heavy quark, but we specifically consider top quarks since the on-shell treatment is more suitable in this case. In Fig. 6.1-right we present results for $t\bar{t}$ production that are obtained analogously to the DY results presented in Fig. 6.1-left.

Our QCD computation of $t\bar{t}$ production is performed by using the numerical Monte Carlo program of Chapter 5, which includes QCD radiative corrections at NLO and part of the NNLO contributions. We set $\mu_F = \mu_R = m_t$ and we use the value $m_t = 173.3$ GeV for the mass m_t of the top quark. We consider the azimuthal angle φ of the top quark in the CS frame, and in Fig. 6.1-right we present the numerical results of various $\cos(n\varphi)$ asymmetries (see Eq. (6.11)) after their integration over the invariant mass M of the $t\bar{t}$ pair. The azimuthal asymmetries are evaluated (as a function of $r_{\rm cut} = q_{\rm cut}/M$) at their non-trivial lowest order (i.e., $\mathcal{O}(\alpha_{\rm S}^3)$) in f.o. perturbation theory and, therefore, we compute all the NLO *tree-level* partonic processes whose final state is '$t\bar{t} + 1$ *parton*'.

Before presenting comments on the results in Fig. 6.1-right, we recall (see Eqs. (4.62) and (4.67)) that the q_T-dependent azimuthal-correlation cross section $d\sigma^{\rm corr}/dq_T^2 d\varphi$ behaves proportionally to $1/q_T^2$ in the limit $q_T \to 0$ and, hence, it is not integrable over q_T down to the region where $q_T = 0$. The $1/q_T^2$ behaviour is proportional to a non-polynomial function of $\cos^2\varphi$ that, therefore, leads to divergent $\cos(n\varphi)$ harmonics for even values of n ($n = 2, 4, 6, \dots$). The q_T spectra of harmonics with odd values of n have instead a less singular q_T behaviour and they are integrable over q_T in the limit $q_T \to 0$.

The numerical results in Fig. 6.1-right are consistent with the convergent or divergent behaviour predicted in Ref. [95]. The harmonic with $n = 1$ (black line) is not vanishing and basically independent of $r_{\rm cut}$ for very small values of $r_{\rm cut}$. The sign of the $n = 1$ harmonic is negative (the $n = 1$ harmonic of $\bar{t}$ would be positive, analogously to the corresponding harmonic of the electron in the DY case of Fig. 6.1-left), and its abolute size (note that it is rescaled by a factor of 0.1 in Fig. 6.1-right) is roughly a factor of

two smaller than the size of the $n = 1$ harmonic for $Z(e^+e^-)$ production (Fig. 6.1-left). The harmonics with $n = 2$ (red line), $n = 4$ (blue line) and $n = 6$ (magenta line) in Fig. 6.1-right have instead an increasing (in absolute value) size for small and decreasing values of $r_{\rm cut}$: this behaviour is consistent with a $\ln r_{\rm cut}$ dependence, as expected from the analytical results in Eqs. (4.62) and (4.67). The results for $n = 2, 4$ and 6 in Fig. 6.1-right have no straightforward quantitative implications for physical azimuthal asymmetries since they refer to small values of $r_{\rm cut}$ (and they eventually diverge in the limit $r_{\rm cut} \to 0$). Nonetheless we observe that the absolute magnitude of the n-even $\cos(n\varphi)$ asymmetries decreases as n increases. As in the case of Fig. 6.1-left for the DY process, in Fig. 6.1-right we also present the $\mathcal{O}(\alpha_{\rm S}^3)$ result of the $n = 0$ harmonic (dashed line) for the real-emission process '$t\bar{t}+jet(1\ parton)$'. Analogously to the DY process, the '$t\bar{t}+1\ parton$' contribution to the $n = 0$ harmonic diverges in the limit $r_{\rm cut} \to 0$, and its dominant behaviour at small $r_{\rm cut}$ is proportional to $\ln^2 r_{\rm cut} + \mathcal{O}(\ln r_{\rm cut})$. At small values of $r_{\rm cut}$ the shape of the $r_{\rm cut}$-dependence of the $n = 0$ result is thus steeper than that of the results for the harmonics with $n = 2, 4$ and 6. After combining real and virtual contributions, the $n = 0$ harmonic gives the total cross section, reported in Table 5.1.

To cure the f.o. perturbative divergences of azimuthal correlations one may advocate non-perturbative strong-interactions dynamics and related non-perturbative QCD effects, which can be sizeable in the small-q_T region. However, in the case of q_T-integrated azimuthal correlations (see Eq. (6.7)) the non-perturbative QCD dynamics should cancel divergent terms proportional to some powers of $\alpha_{\rm S}(M)$, and this would imply that non-perturbative QCD effects scale logarithmically with M (i.e., these effects would not be suppressed by some power of Λ_{QCD}/M in the hard-scattering regime $M \gg \Lambda_{QCD}$), thus spoiling not only the *finiteness* but also the *infrared safety* of the azimuthal correlations. In the next Section we show that the problem of f.o. divergences in azimuthal correlations has a satisfactory solution entirely within the context of perturbation theory. Namely, the resummation of perturbative corrections to all orders leads to (q_T integrated) azimuthal asymmetries that are finite and computable. Such solution does not imply that the non-perturbative effects have a negligible quantitative role in the small-q_T region.

6.2 Resummation

The azimuthally-dependent perturbative contributions that diverge at small q_T can be resummed to all orders. As discussed in Chapters 3 and 4 the general structure of the transverse-momentum resummation formula involves an inverse Fourier transform from impact parameter $\mathbf{b}$ space. When considering the azimuthally averaged transverse-momentum cross section, the two-dimensional Fourier integral turns into a one-dimensional Bessel transformation

$$\frac{d\sigma^{(\rm res)}_{\rm av.}}{dq_T^2} \sim \int_0^{+\infty} db\ b\ J_0(bq_T)\ \Sigma_{\rm av.}(M, b)\,. \tag{6.13}$$

Analogously, the computation of the n-harmonic projects out the Bessel function of n-order

$$\frac{d\sigma_n^{(\mathrm{res})}}{dq_T^2} \sim \int_0^{+\infty} db\, b\, J_n(bq_T)\, \Sigma_n(M,b)\,. \tag{6.14}$$

We now discuss the small q_T limit of the resummed expressions in Eqs. (6.13,6.14). Due to the Sudakov suppression of the function $\Sigma_n(M,b)$ at large b, the small-q_T limit can be extracted by approximating the n-order Bessel function around the origin ($J_n(bq_T) \sim (bq_T)^n$) and we have

$$\frac{d\sigma_n^{(\mathrm{res})}}{dq_T^2} \propto (q_T)^n \qquad\qquad (q_T \to 0)\,. \tag{6.15}$$

When considering the azimuthally averaged cross section, the resummation procedure leads to the well-known effect that the $d\sigma_{\mathrm{av.}}/dq_T^2 \sim 1/q_T^2$ divergent behavior of the fixed order cross section is turned into $d\sigma_{\mathrm{av.}}^{(\mathrm{res})}/dq_T^2 \sim$ const. It is interesting to note that, for the n-order harmonics, the effect of resummation is even more dramatic, since it turns the $d\sigma_n/dq_T^2 \sim 1/q_T^2$ divergent behavior into the behavior of Eq. (6.15). We thus anticipate that the shape of the resummed q_T spectrum $d\sigma_n^{(\mathrm{res})}/dq_T$ for the n-order harmonic can be substantially different from the shape of the q_T spectrum for the azimuthally averaged cross section.

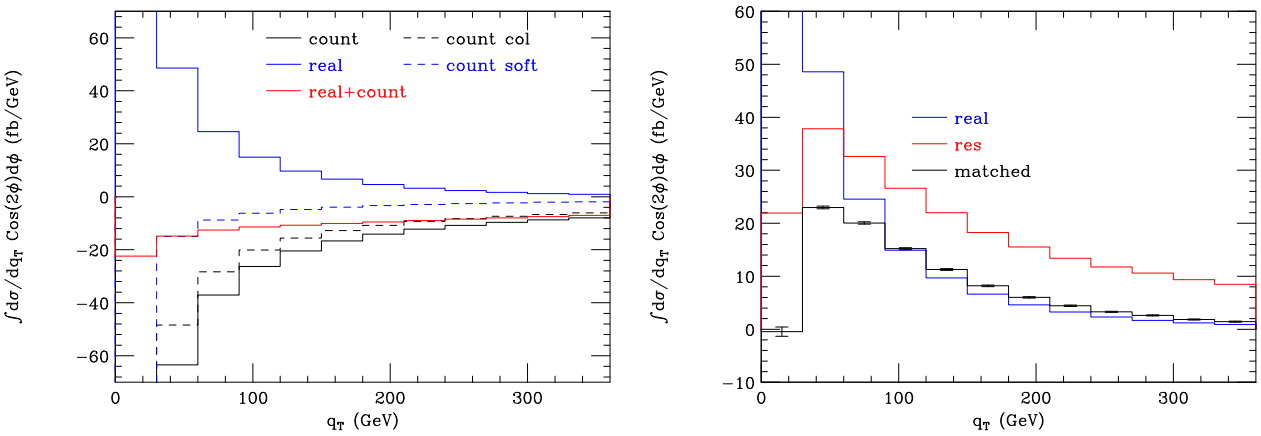

(a) (b)

Figure 6.2: *Transverse momentum spectrum for the second harmonic. Left: the real contribution (solid blue) is compared with the expansion of the resummation formula, split into collinear (black dashed) and soft (blue dashed) contributions. The finite sum of the real and counterterm contribution is also shown (red solid). Right: the purely resummed contribution (red solid) is compared with the fixed order result (blue solid) and with the matched prediction (black solid).*

In the following, we focus on the $t\bar{t}$ case and, in particular on the $n = 2$ harmonic. We have seen in Fig. 6.1 that for $n = 2$ the Z + jet cross section is finite, while the $t\bar{t}$ + jet is divergent in the limit in which $r_{\mathrm{cut}} \to 0$. This is confirmed in Fig. 6.2(a), where the $t\bar{t}$ + jet

cross section (denoted as *real*) as a function of q_T is shown to diverge to $+\infty$ as $q_T \to 0$. The setup is the same as in the previous section. The divergent behavior is cured through the resummation procedure discussed in Section 4.2.1 (see Eqs. (4.73) and (4.74)). The purely resummed contribution is shown in Fig. 6.2(b) (red solid line). According to the previous discussion (see Eq. (6.15)), we expect $d\sigma_2^{\rm res}/dq_T \sim (q_T)^3$ as $q_T \to 0$. The result in Fig. 6.2(b) is consistent with this expectation: the resummed histogram is peaked in the region $q_T \sim 45$ GeV, i.e., at much larger transverse momenta with respect to the ordinary q_T distribution shown in Fig. 4.1, which behaves as $d\sigma^{\rm res}/dq_T \sim q_T$ as $q_T \to 0$.

To provide a meaningful prediction the resummed computation must be combined with the fixed order result, valid at large q_T. The expansion of the resummation formula (denoted as *count* in Fig. 6.2) is supposed to cancel the divergent behavior of the fixed order contribution. At $\mathcal{O}(\alpha_{\rm S}^3)$ the expansion contains purely *collinear* contributions (see Eq. (4.62)) and additional large-angle *soft* contributions (see Eq. (4.67)). We see that it is only the sum of the *collinear* and *soft* contributions that ensures the cancellation. The matched contribution is reported in Fig. 6.2(b) (black solid line). Comparing the matched and fixed order contributions we see that the resummation is important in the low and intermediate q_T region, while at large values of q_T the matched prediction nicely approaches to the fixed order result.

In summary, the resummation procedure allows us to reconcile the appearence of divergences in the fixed-order perturbative computation of the n-harmonics with the criterion of infrared and collinear safety. After the resummation procedure is carried out, $d\sigma_n/dq_T$ is *integrable* at $q_T \to 0$, thereby leading to a finite perturbative prediction for $d\sigma_n/dM^2$.

Chapter 7

Conclusions and outlook

The production of heavy-quark pairs at hadron colliders is a benchmark process in QCD perturbation theory, and, at the same time, a crucial background for NP searches. In this thesis we have addressed the computation of higher-order perturbative contributions to this process, its transverse-momentum spectrum, and the corresponding azimuthal correlations.

After a brief introduction to the main aspects of perturbative QCD and infrared factorization in Chapter 2, in Chapter 3 we have reviewed the transverse-momentum resummation formalism for the production of colourless high-mass systems. In Chapter 4 we have presented the structure of the transverse-momentum resummed cross section for heavy-quark production. As we have shown in Section 4.2.2, the full control over the azimuthal correlations is crucial, due to their non-trivial interference effects on the azimuthally-averaged cross section, which we have computed analytically. The numerical computation of the transverse-momentum spectrum of the heavy-quark pair is complicated by the existence of colour-correlated contributions, which render the implementation of the resummed cross section substantially more complicated with respect to the colourless case. In Section 4.4 we provided a general algorithm for dealing with the exponentiation of colour-correlated quantities in numerical computations. In particular, we have discussed the diagonalization procedure of the soft anomalous dimension matrices, which resulted in defining kinematics-dependent colour bases vectors. In order to fully resum the large logarithmic contributions due to large-angle soft-gluon radiation from the heavy quarks, the scattering amplitudes must then be projected on this new basis, which requires the computation of the Born-level and one-loop hard matrices at NLL and NNLL accuracy, respectively. Although the structure of the transverse-momentum resummed spectrum is fully worked out, it is not yet possible to obtain complete quantitative predictions at NNLL+NNLO accuracy, due to the missing IR-finite contributions. Therefore, in Section 4.7 we limited ourselves to the presentation of our numerical results at NLL+NLO accuracy. We also compared our results with the recent experimental measurement of the $t\bar{t}$ transverse-momentum spectrum of the ATLAS collaboration [24] and found a good

agreement in a wide region of transverse momenta.

In Chapter 5 we have presented the first application of the q_T subtraction method to top-quark pair production at hadron colliders, which is based on the analytical knowledge of the IR singularities at low q_T. The latter can be extracted from the transverse-momentum resummation program, as presented In Section 4.6. Our computation is accurate at NLO in QCD perturbation theory and it includes all the off-diagonal partonic channels at NNLO accuracy. The computation of the azimuthal correlation terms is the key part of the calculation. We have also shown in Section 5.2.2, for the first time, the cancellation of the singularities between the NLO $t\bar{t}$+jet cross section and the corresponding subtraction counterterm, which is the first step towards the NNLO extension of our computation to include the missing diagonal channels. The complete extension requires the evaluation of the second-order hard-collinear functions $\mathcal{H}^{t\bar{t}}_{NNLO}$ [95], and an implementation of the two-loop virtual amplitudes, which, at present, are known only in numerical form [179, 180]. At NLO we have compared our results for various kinematical distributions with those obtained by using the MCFM program, and we find good agreement. At NNLO our results for the $t\bar{t}$ total cross section agree with the corresponding results obtained by using the Top++ program. The computation that we have performed in this Chapter can straightforwardly be extended to the production of massive-quark pairs of different flavour (e.g. bottom-quark pair). Moreover, the extension to the production processes with additional colourless final-state particle(s) is feasible.

In Chapter 6 we discussed the issue of azimuthal asymmetries. In particular, we have pointed out that for a large class of processes, fixed-order perturbation theory fails to provide physically meaningful prediction for azimuthal distributions. We have also shown that this issue is directly related to the azimuthal correlations of the transverse-momentum spectrum. We presented a possible solution to this problem in the framework of the transverse-momentum resummation program. In particular, we have shown that the transverse-momentum resummation of the azimuthal asymmetries provides a finite prediction for the azimuthal distributions that can be compared to experimental data.

Acknowledgments

After an intensive period of almost four years, today is the day: writing this note of acknowledgement is the finishing touch on my thesis. Writing this thesis has had a big impact on me and I would like to reflect on the people who have supported and helped me so much throughout this period.

First and foremost, I would like to thank my supervisor Massimiliano Grazzini for trusting me with this project and guiding me throughout the whole course of it. Despite the very tight schedule he always found time for discussions. Every time I walked out from his office I had more knowledge than when I walked in. He taught me to be patient and not to give up when facing difficulties. The joy and the enthusiasm he has for his research was contagious and motivational for me, especially during the tough times in the Ph.D. pursuit.

I am indebted to Stefano Catani whose insightful knowledge on many aspects of this project and the impact of useful discussions I had had with him is impossible to overestimate. I am very happy that our paths crossed in this life. You will always have a special place in my memory.

I am also very grateful to my collaborators Roberto Bonciani and Alessandro Torre for lending me their expertise and intuition to my scientific and technical problems. It was a honour working with you.

I would also like to thank all the members of Physik-Institut at the University of Zurich who made this period of my studies an unforgettable memory. A special acknowledgement goes to Thomas Gehrmann, Stefano Pozzorini, Adrian Signer and Gino Isidori who are always ready to share their experience and knowledge with us. I am also very grateful to Regina, Esther and Carmelina, who were always there for me to help with all kinds of issues both within and outside the Institute. I would also like to specifically thank Dominik, who has become a real friend to me. I will never forget the time we spent together at summer schools and conferences. And thank you for translating the Abstract of this thesis into German. I am also grateful to my officemates at different periods of my time in the Institute: Alessandro, Timo, Dirk, Javier, Leandro and Simone, it is thanks to

you that I enjoyed my time in the office.

I am grateful to Niccolo Moretti, Jonas Lindert and Marek Schönherr for the useful discussions and their help in using OPENLOOPS and SHERPA. I would also like to express my sincere gratitude to Stefan Kallweit for the first-hand guidance through the MUNICH code.

Last but not least, I would like to thank my family for all their love and encouragement. For my parents who raised me with a love for science and supported me in all my pursuits. For my sister Hasmik for her unwavering support throughout the years, even over time-zones. For my loving, encouraging, and patient wife Sona, whose faithful support during the final stages of this Ph.D. is so appreciated. And for my little daughter Sone who filled our life with joy and happiness. Thank you.

Appendices

Appendix A

Eigenvalues of the soft anomalous dimension matrices

In this appendix we present the explicit expressions of the diagonalising matrices $\mathbf{R}^{c\bar{c}}$ and the eigenvalues $\lambda_I^{c\bar{c}}$ of the soft anomalous dimension matrices $\mathbf{\Gamma}_t^{c\bar{c}\,(1)}$ $(c = q, g)$. The explicit matrix representation of the soft anomalous dimension matrices are given in Eqs. (4.103) and (4.104).

Below we present the eigenvalues of the quark-channel anomalous dimension matrix $\mathbf{\Gamma}_t^{c\bar{c}\,(1)}$ of Eq. (4.103)

$$\begin{aligned}\lambda_1^{q\bar{q}} &= \frac{1}{2}\left(N_c(\Gamma_{\rm s}+\Gamma_{\rm t}) + \sqrt{N_c^2(\Gamma_{\rm t}-\Gamma_{\rm s})^2 + 4\Gamma_{\rm s}\Gamma_{\rm t}}\right) + \Gamma_{\rm I}^{q\bar{q}}\,, \\ \lambda_2^{q\bar{q}} &= \frac{1}{2}\left(N_c(\Gamma_{\rm s}+\Gamma_{\rm t}) - \sqrt{N_c^2(\Gamma_{\rm t}-\Gamma_{\rm s})^2 + 4\Gamma_{\rm s}\Gamma_{\rm t}}\right) + \Gamma_{\rm I}^{q\bar{q}}\,,\end{aligned} \tag{A.1}$$

where the coefficient-functions $\Gamma_{\rm s}$, $\Gamma_{\rm t}$ and $\Gamma_{\rm I}^{q\bar{q}}$ are given in Eqs. (4.105), (4.105) and (4.107) respectively. The diagonalising matrix $\mathbf{R}^{c\bar{c}}$ of the soft anomalous dimension matrix $\mathbf{\Gamma}_t^{c\bar{c}\,(1)}$ can be constructed by solving the eigenvalue equation $\mathbf{\Gamma}_t^{c\bar{c}\,(1)}\mathbf{v}_i^{c\bar{c}} = \lambda^{c\bar{c}}\mathbf{v}_i^{c\bar{c}}$, where $\mathbf{v}_i^{c\bar{c}}$ are the eigenvectors of the $\mathbf{\Gamma}_t^{q\bar{q}\,(1)}$ matrix, and hence, the columns of the diagonalising matrix. Explicitly, for the quark channel we find

$$\mathbf{R}^{q\bar{q}} = \frac{1}{4\Gamma_{\rm t}}\begin{pmatrix} N_c\Gamma_{\rm s} - \frac{N_c^2-2}{N_c}\Gamma_{\rm t} - \sqrt{N_c^2(\Gamma_{\rm t}-\Gamma_{\rm s})^2 + 4\Gamma_{\rm s}\Gamma_{\rm t}} & N_c\Gamma_{\rm s} - \frac{N_c^2-2}{N_c}\Gamma_{\rm t} + \sqrt{N_c^2(\Gamma_{\rm t}-\Gamma_{\rm s})^2 + 4\Gamma_{\rm s}\Gamma_{\rm t}} \\ 4\Gamma_{\rm t} & 4\Gamma_{\rm t} \end{pmatrix}. \tag{A.2}$$

We now move on to consider the soft anomalous dimension matrix $\mathbf{\Gamma}_t^{gg\,(1)}$ in the gluon

channel. The eigenvalues can be written in the following form:

$$\begin{aligned}
\lambda_1^{gg} &= \frac{1}{6}\left[X^{1/3} + Y + 2\,(A_{11} + 2\,A_{22})\right] + \Gamma_{\rm I}^{gg}\,,\\
\lambda_2^{gg} &= \frac{1}{12}\left[-X^{1/3} - Y + \sqrt{3}\,i\,(X^{1/3} - Y) + 4(A_{11} + 2\,A_{22})\right] + \Gamma_{\rm I}^{gg}\,,\\
\lambda_3^{gg} &= \frac{1}{12}\left[-X^{1/3} - Y - \sqrt{3}\,i\,(X^{1/3} - Y) + 4(A_{11} + 2\,A_{22})\right] + \Gamma_{\rm I}^{gg}\,,
\end{aligned} \tag{A.3}$$

where $\Gamma_{\rm I}^{gg}$ is given in Eq. (4.108), and the functions X and Y are defined as follows

$$\begin{aligned}
X =& -18\,A_{12}^2\,(N_c^2 - 8)(A_{11} - A_{22}) + 8\,(A_{11} - A_{22})^3 +\\
&+ \Big\{4\,(A_{11} - A_{22})^2\left[4\,(A_{11} - A_{22})^2 - 9\,A_{12}^2\,(N_c^2 - 8)\right]^2\\
&- \left[4\,(A_{11} - A_{22})^2 + 3\,A_{12}^2\,(N_c^2 + 4)\right]^3\Big\}^{1/2}\,,
\end{aligned}$$

$$Y = \left[4\,(A_{11} - A_{22})^2 + 3\,A_{12}^2\,(N_c^2 + 4)\right] X^{-1/3}\,, \tag{A.4}$$

with

$$A_{ij} = \left(\mathbf{\Gamma}_t^{gg,\,(1)}\right)_{ij} - \Gamma_{\rm I}^{gg}\,\delta_{ij}\,. \tag{A.5}$$

Solving the eigenvalue equation for the gluon channel, we find that the soft anomalous dimension matrix $\mathbf{\Gamma}_t^{gg,\,(1)}$ can be diagonalised by the following matrix $\mathbf{R}^{gg}$:

$$\mathbf{R}^{gg} = \begin{pmatrix}
\frac{A_{12}}{\lambda_1^{gg} - \Gamma_{\rm I}^{gg} - A_{11}} & \frac{A_{12}}{\lambda_2^{gg} - \Gamma_{\rm I}^{gg} - A_{11}} & \frac{A_{12}}{\lambda_3^{gg} - \Gamma_{\rm I}^{gg} - A_{11}}\\[2ex]
1 & 1 & 1\\[2ex]
\frac{N_c\,A_{12}}{2(\lambda_1^{gg} - \Gamma_{\rm I}^{gg} - A_{22})} & \frac{N_c\,A_{12}}{2(\lambda_2^{gg} - \Gamma_{\rm I}^{gg} - A_{22})} & \frac{N_c\,A_{12}}{2(\lambda_3^{gg} - \Gamma_{\rm I}^{gg} - A_{22})}
\end{pmatrix}. \tag{A.6}$$

References

[1] S. L. Glashow. Partial Symmetries of Weak Interactions. *Nucl. Phys.*, 22:579–588, 1961.

[2] Steven Weinberg. A Model of Leptons. *Phys. Rev. Lett.*, 19:1264–1266, 1967.

[3] Abdus Salam. Weak and Electromagnetic Interactions. *Conf. Proc.*, C680519:367–377, 1968.

[4] S. Tomonaga. On a relativistically invariant formulation of the quantum theory of wave fields. *Prog. Theor. Phys.*, 1:27–42, 1946.

[5] Julian S. Schwinger. Quantum electrodynamics. I A covariant formulation. *Phys. Rev.*, 74:1439, 1948.

[6] R. P. Feynman. Space-time approach to nonrelativistic quantum mechanics. *Rev. Mod. Phys.*, 20:367–387, 1948.

[7] F. J. Dyson. The Radiation theories of Tomonaga, Schwinger, and Feynman. *Phys. Rev.*, 75:486–502, 1949.

[8] David J. Gross and Frank Wilczek. Ultraviolet Behavior of Nonabelian Gauge Theories. *Phys. Rev. Lett.*, 30:1343–1346, 1973.

[9] H. David Politzer. Reliable Perturbative Results for Strong Interactions? *Phys. Rev. Lett.*, 30:1346–1349, 1973.

[10] H. Fritzsch, Murray Gell-Mann, and H. Leutwyler. Advantages of the Color Octet Gluon Picture. *Phys. Lett.*, B47:365–368, 1973.

[11] Peter W. Higgs. Broken Symmetries and the Masses of Gauge Bosons. *Phys. Rev. Lett.*, 13:508–509, 1964.

[12] Peter W. Higgs. Spontaneous Symmetry Breakdown without Massless Bosons. *Phys. Rev.*, 145:1156–1163, 1966.

[13] F. Englert and R. Brout. Broken Symmetry and the Mass of Gauge Vector Mesons. *Phys. Rev. Lett.*, 13:321–323, 1964.

[14] G. S. Guralnik, C. R. Hagen, and T. W. B. Kibble. Global Conservation Laws and Massless Particles. *Phys. Rev. Lett.*, 13:585–587, 1964.

[15] T. W. B. Kibble. Symmetry breaking in nonAbelian gauge theories. *Phys. Rev.*, 155:1554–1561, 1967.

[16] Georges Aad et al. Observation of a new particle in the search for the Standard Model Higgs boson with the ATLAS detector at the LHC. *Phys. Lett.*, B716:1–29, 2012.

[17] Serguei Chatrchyan et al. Observation of a new boson at a mass of 125 GeV with the CMS experiment at the LHC. *Phys. Lett.*, B716:30–61, 2012.

[18] Eldad Gildener. Gauge Symmetry Hierarchies. *Phys. Rev.*, D14:1667, 1976.

[19] Steven Weinberg. Gauge Hierarchies. *Phys. Lett.*, B82:387–391, 1979.

[20] S. Abachi et al. Observation of the top quark. *Phys. Rev. Lett.*, 74:2632–2637, 1995.

[21] Serguei Chatrchyan et al. Measurement of differential top-quark pair production cross sections in pp colisions at $\sqrt{s} = 7$ TeV. *Eur. Phys. J.*, C73(3):2339, 2013.

[22] Georges Aad et al. Measurements of normalized differential cross sections for $t\bar{t}$ production in pp collisions at $\sqrt{s} = 7$ TeV using the ATLAS detector. *Phys. Rev.*, D90(7):072004, 2014.

[23] Vardan Khachatryan et al. Measurement of the differential cross section for top quark pair production in pp collisions at $\sqrt{s} = 8\,\text{TeV}$. *Eur. Phys. J.*, C75(11):542, 2015.

[24] Morad Aaboud et al. Measurement of top quark pair differential cross-sections in the dilepton channel in pp collisions at $\sqrt{s} = 7$ and 8 TeV with ATLAS. 2016.

[25] F. Bloch and A. Nordsieck. Note on the Radiation Field of the electron. *Phys. Rev.*, 52:54–59, 1937.

[26] T. Kinoshita. Mass singularities of Feynman amplitudes. *J. Math. Phys.*, 3:650–677, 1962.

[27] T. D. Lee and M. Nauenberg. Degenerate Systems and Mass Singularities. *Phys. Rev.*, 133:B1549–B1562, 1964. [,25(1964)].

[28] S. Catani and M. H. Seymour. The Dipole formalism for the calculation of QCD jet cross-sections at next-to-leading order. *Phys. Lett.*, B378:287–301, 1996.

[29] S. Catani and M. H. Seymour. A General algorithm for calculating jet cross-sections in NLO QCD. *Nucl. Phys.*, B485:291–419, 1997. [Erratum: Nucl. Phys.B510,503(1998)].

[30] Stefano Catani, Stefan Dittmaier, Michael H. Seymour, and Zoltan Trocsanyi. The Dipole formalism for next-to-leading order QCD calculations with massive partons. *Nucl. Phys.*, B627:189–265, 2002.

[31] S. Frixione, Z. Kunszt, and A. Signer. Three jet cross-sections to next-to-leading order. *Nucl. Phys.*, B467:399–442, 1996.

[32] Fabio Cascioli, Philipp Maierhofer, and Stefano Pozzorini. Scattering Amplitudes with Open Loops. *Phys. Rev. Lett.*, 108:111601, 2012.

[33] J. Alwall, R. Frederix, S. Frixione, V. Hirschi, F. Maltoni, O. Mattelaer, H. S. Shao, T. Stelzer, P. Torrielli, and M. Zaro. The automated computation of tree-level and next-to-leading order differential cross sections, and their matching to parton shower simulations. *JHEP*, 07:079, 2014.

[34] Gavin Cullen et al. G*OSAM*-2.0: a tool for automated one-loop calculations within the Standard Model and beyond. *Eur. Phys. J.*, C74(8):3001, 2014.

[35] Gabor Somogyi, Zoltan Trocsanyi, and Vittorio Del Duca. Matching of singly- and doubly-unresolved limits of tree-level QCD squared matrix elements. *JHEP*, 06:024, 2005.

[36] Vittorio Del Duca, Claude Duhr, Gábor Somogyi, Francesco Tramontano, and Zoltán Trócsányi. Higgs boson decay into b-quarks at NNLO accuracy. *JHEP*, 04:036, 2015.

[37] David A. Kosower. Antenna factorization of gauge theory amplitudes. *Phys. Rev.*, D57:5410–5416, 1998.

[38] David A. Kosower. Multiple singular emission in gauge theories. *Phys. Rev.*, D67:116003, 2003.

[39] David A. Kosower. Antenna factorization in strongly ordered limits. *Phys. Rev.*, D71:045016, 2005.

[40] A. Gehrmann-De Ridder, T. Gehrmann, and E. W. Nigel Glover. Antenna subtraction at NNLO. *JHEP*, 09:056, 2005.

[41] A. Daleo, T. Gehrmann, and D. Maitre. Antenna subtraction with hadronic initial states. *JHEP*, 04:016, 2007.

[42] James Currie, E. W. N. Glover, and Steven Wells. Infrared Structure at NNLO Using Antenna Subtraction. *JHEP*, 04:066, 2013.

[43] M. Czakon. A novel subtraction scheme for double-real radiation at NNLO. *Phys. Lett.*, B693:259–268, 2010.

[44] M. Czakon. Double-real radiation in hadronic top quark pair production as a proof of a certain concept. *Nucl. Phys.*, B849:250–295, 2011.

[45] M. Czakon and D. Heymes. Four-dimensional formulation of the sector-improved residue subtraction scheme. *Nucl. Phys.*, B890:152–227, 2014.

[46] Charalampos Anastasiou, Kirill Melnikov, and Frank Petriello. A new method for real radiation at NNLO. *Phys. Rev.*, D69:076010, 2004.

[47] T. Binoth and G. Heinrich. An automatized algorithm to compute infrared divergent multiloop integrals. *Nucl. Phys.*, B585:741–759, 2000.

[48] Stefano Catani and Massimiliano Grazzini. An NNLO subtraction formalism in hadron collisions and its application to Higgs boson production at the LHC. *Phys. Rev. Lett.*, 98:222002, 2007.

[49] Radja Boughezal, Christfried Focke, Xiaohui Liu, and Frank Petriello. W-boson production in association with a jet at next-to-next-to-leading order in perturbative QCD. *Phys. Rev. Lett.*, 115(6):062002, 2015.

[50] Radja Boughezal, Xiaohui Liu, and Frank Petriello. N-jettiness soft function at next-to-next-to-leading order. *Phys. Rev.*, D91(9):094035, 2015.

[51] Jonathan Gaunt, Maximilian Stahlhofen, Frank J. Tackmann, and Jonathan R. Walsh. N-jettiness Subtractions for NNLO QCD Calculations. *JHEP*, 09:058, 2015.

[52] P. Nason, S. Dawson, and R. Keith Ellis. The Total Cross-Section for the Production of Heavy Quarks in Hadronic Collisions. *Nucl. Phys.*, B303:607–633, 1988.

[53] W. Beenakker, H. Kuijf, W. L. van Neerven, and J. Smith. QCD Corrections to Heavy Quark Production in p anti-p Collisions. *Phys. Rev.*, D40:54–82, 1989.

[54] P. Nason, S. Dawson, and R. Keith Ellis. The One Particle Inclusive Differential Cross-Section for Heavy Quark Production in Hadronic Collisions. *Nucl. Phys.*, B327:49–92, 1989. [Erratum: Nucl. Phys.B335,260(1990)].

[55] W. Beenakker, W. L. van Neerven, R. Meng, G. A. Schuler, and J. Smith. QCD corrections to heavy quark production in hadron hadron collisions. *Nucl. Phys.*, B351:507–560, 1991.

[56] Michelangelo L. Mangano, Paolo Nason, and Giovanni Ridolfi. Heavy quark correlations in hadron collisions at next-to-leading order. *Nucl. Phys.*, B373:295–345, 1992.

[57] Peter Bärnreuther, Michal Czakon, and Alexander Mitov. Percent Level Precision Physics at the Tevatron: First Genuine NNLO QCD Corrections to $q\bar{q} \to t\bar{t} + X$. *Phys. Rev. Lett.*, 109:132001, 2012.

[58] Michal Czakon and Alexander Mitov. NNLO corrections to top-pair production at hadron colliders: the all-fermionic scattering channels. *JHEP*, 12:054, 2012.

[59] Michal Czakon and Alexander Mitov. NNLO corrections to top pair production at hadron colliders: the quark-gluon reaction. *JHEP*, 01:080, 2013.

[60] Michał Czakon, Paul Fiedler, and Alexander Mitov. Total Top-Quark Pair-Production Cross Section at Hadron Colliders Through $\mathcal{O}(\alpha_S^4)$. *Phys. Rev. Lett.*, 110:252004, 2013.

[61] Valentin Ahrens, Andrea Ferroglia, Matthias Neubert, Ben D. Pecjak, and Li Lin Yang. Renormalization-Group Improved Predictions for Top-Quark Pair Production at Hadron Colliders. *JHEP*, 09:097, 2010.

[62] Michal Czakon, Paul Fiedler, and Alexander Mitov. Resolving the Tevatron Top Quark Forward-Backward Asymmetry Puzzle: Fully Differential Next-to-Next-to-Leading-Order Calculation. *Phys. Rev. Lett.*, 115(5):052001, 2015.

[63] Michal Czakon, David Heymes, and Alexander Mitov. High-precision differential predictions for top-quark pairs at the LHC. *Phys. Rev. Lett.*, 116(8):082003, 2016.

[64] Michal Czakon, Paul Fiedler, David Heymes, and Alexander Mitov. NNLO QCD predictions for fully-differential top-quark pair production at the Tevatron. *JHEP*, 05:034, 2016.

[65] G. Abelof and A. Gehrmann-De Ridder. Antenna subtraction for the production of heavy particles at hadron colliders. *JHEP*, 04:063, 2011.

[66] Gabriel Abelof, Aude Gehrmann-De Ridder, Philipp Maierhofer, and Stefano Pozzorini. NNLO QCD subtraction for top-antitop production in the $q\bar{q}$ channel. *JHEP*, 08:035, 2014.

[67] Gabriel Abelof and Aude Gehrmann-De Ridder. Light fermionic NNLO QCD corrections to top-antitop production in the quark-antiquark channel. *JHEP*, 12:076, 2014.

[68] Martin Lambertsen and Werner Vogelsang. Drell-Yan lepton angular distributions in perturbative QCD. *Phys. Rev.*, D93(11):114013, 2016.

[69] Stefano Catani and Massimiliano Grazzini. QCD transverse-momentum resummation in gluon fusion processes. *Nucl. Phys.*, B845:297–323, 2011.

[70] Yuri L. Dokshitzer, Dmitri Diakonov, and S. I. Troian. Hard Processes in Quantum Chromodynamics. *Phys. Rept.*, 58:269–395, 1980.

[71] G. Parisi and R. Petronzio. Small Transverse Momentum Distributions in Hard Processes. *Nucl. Phys.*, B154:427–440, 1979.

[72] G. Curci, Mario Greco, and Y. Srivastava. QCD Jets From Coherent States. *Nucl. Phys.*, B159:451–468, 1979.

[73] John C. Collins and Davison E. Soper. Back-To-Back Jets in QCD. *Nucl. Phys.*, B193:381, 1981. [Erratum: Nucl. Phys.B213,545(1983)].

[74] John C. Collins and Davison E. Soper. Back-To-Back Jets: Fourier Transform from B to K-Transverse. *Nucl. Phys.*, B197:446–476, 1982.

[75] Jiro Kodaira and Luca Trentadue. Single Logarithm Effects in electron-Positron Annihilation. *Phys. Lett.*, B123:335–338, 1983.

[76] Guido Altarelli, R. Keith Ellis, Mario Greco, and G. Martinelli. Vector Boson Production at Colliders: A Theoretical Reappraisal. *Nucl. Phys.*, B246:12–44, 1984.

[77] C. T. H. Davies and W. James Stirling. Nonleading Corrections to the Drell-Yan Cross-Section at Small Transverse Momentum. *Nucl. Phys.*, B244:337–348, 1984.

[78] C. T. H. Davies, B. R. Webber, and W. James Stirling. Drell-Yan Cross-Sections at Small Transverse Momentum. *Nucl. Phys.*, B256:413, 1985. [1,I.95(1984)].

[79] John C. Collins, Davison E. Soper, and George F. Sterman. Transverse Momentum Distribution in Drell-Yan Pair and W and Z Boson Production. *Nucl. Phys.*, B250:199–224, 1985.

[80] S. Catani, E. D'Emilio, and L. Trentadue. The Gluon Form-factor to Higher Orders: Gluon Gluon Annihilation at Small Q^{-}transverse. *Phys. Lett.*, B211:335–342, 1988.

[81] Stefano Catani, Daniel de Florian, and Massimiliano Grazzini. Universality of nonleading logarithmic contributions in transverse momentum distributions. *Nucl. Phys.*, B596:299–312, 2001.

[82] Giuseppe Bozzi, Stefano Catani, Daniel de Florian, and Massimiliano Grazzini. Transverse-momentum resummation and the spectrum of the Higgs boson at the LHC. *Nucl. Phys.*, B737:73–120, 2006.

[83] Christian W. Bauer, Sean Fleming, Dan Pirjol, and Iain W. Stewart. An Effective field theory for collinear and soft gluons: Heavy to light decays. *Phys. Rev.*, D63:114020, 2001.

[84] Christian W. Bauer, Dan Pirjol, and Iain W. Stewart. Soft collinear factorization in effective field theory. *Phys. Rev.*, D65:054022, 2002.

[85] M. Beneke, A. P. Chapovsky, M. Diehl, and T. Feldmann. Soft collinear effective theory and heavy to light currents beyond leading power. *Nucl. Phys.*, B643:431–476, 2002.

[86] Yang Gao, Chong Sheng Li, and Jian Jun Liu. Transverse momentum resummation for Higgs production in soft-collinear effective theory. *Phys. Rev.*, D72:114020, 2005.

[87] Sonny Mantry and Frank Petriello. Factorization and Resummation of Higgs Boson Differential Distributions in Soft-Collinear Effective Theory. *Phys. Rev.*, D81:093007, 2010.

[88] Thomas Becher and Matthias Neubert. Drell-Yan Production at Small q_T, Transverse Parton Distributions and the Collinear Anomaly. *Eur. Phys. J.*, C71:1665, 2011.

[89] Miguel Garcia-Echevarria, Ahmad Idilbi, and Ignazio Scimemi. SCET, Light-Cone Gauge and the T-Wilson Lines. *Phys. Rev.*, D84:011502, 2011.

[90] Jui-Yu Chiu, Ambar Jain, Duff Neill, and Ira Z. Rothstein. A Formalism for the Systematic Treatment of Rapidity Logarithms in Quantum Field Theory. *JHEP*, 05:084, 2012.

[91] John C. Collins and Ted C. Rogers. Equality of Two Definitions for Transverse Momentum Dependent Parton Distribution Functions. *Phys. Rev.*, D87(3):034018, 2013.

[92] Thomas Becher, Matthias Neubert, and Daniel Wilhelm. Higgs-Boson Production at Small Transverse Momentum. *JHEP*, 05:110, 2013.

[93] Hua Xing Zhu, Chong Sheng Li, Hai Tao Li, Ding Yu Shao, and Li Lin Yang. Transverse-momentum resummation for top-quark pairs at hadron colliders. *Phys. Rev. Lett.*, 110(8):082001, 2013.

[94] Hai Tao Li, Chong Sheng Li, Ding Yu Shao, Li Lin Yang, and Hua Xing Zhu. Top quark pair production at small transverse momentum in hadronic collisions. *Phys. Rev.*, D88:074004, 2013.

[95] Stefano Catani, Massimiliano Grazzini, and A. Torre. Transverse-momentum resummation for heavy-quark hadroproduction. *Nucl. Phys.*, B890:518–538, 2014.

[96] S. Catani, M. Grazzini, and H. Sargsyan. Azimuthal assymmetries in QCD hard scattering: infrared safe but divergent. *In preparation.*

[97] Massimiliano Grazzini. NNLO predictions for the Higgs boson signal in the H —> WW —> lnu lnu and H —> ZZ —> 4l decay channels. *JHEP*, 02:043, 2008.

[98] Stefano Catani, Leandro Cieri, Giancarlo Ferrera, Daniel de Florian, and Massimiliano Grazzini. Vector boson production at hadron colliders: a fully exclusive QCD calculation at NNLO. *Phys. Rev. Lett.*, 103:082001, 2009.

[99] Stefano Catani, Leandro Cieri, Daniel de Florian, Giancarlo Ferrera, and Massimiliano Grazzini. Diphoton production at hadron colliders: a fully-differential QCD calculation at NNLO. *Phys. Rev. Lett.*, 108:072001, 2012. [Erratum: Phys. Rev. Lett.117,no.8,089901(2016)].

[100] Giancarlo Ferrera, Massimiliano Grazzini, and Francesco Tramontano. Associated WH production at hadron colliders: a fully exclusive QCD calculation at NNLO. *Phys. Rev. Lett.*, 107:152003, 2011.

[101] Massimiliano Grazzini, Stefan Kallweit, Dirk Rathlev, and Alessandro Torre. $Z\gamma$ production at hadron colliders in NNLO QCD. *Phys. Lett.*, B731:204–207, 2014.

[102] Giancarlo Ferrera, Massimiliano Grazzini, and Francesco Tramontano. Associated ZH production at hadron colliders: the fully differential NNLO QCD calculation. *Phys. Lett.*, B740:51–55, 2015.

[103] F. Cascioli, T. Gehrmann, M. Grazzini, S. Kallweit, P. Maierhöfer, A. von Manteuffel, S. Pozzorini, D. Rathlev, L. Tancredi, and E. Weihs. ZZ production at hadron colliders in NNLO QCD. *Phys. Lett.*, B735:311–313, 2014.

[104] T. Gehrmann, M. Grazzini, S. Kallweit, P. Maierhöfer, A. von Manteuffel, S. Pozzorini, D. Rathlev, and L. Tancredi. W^+W^- Production at Hadron Colliders in Next to Next to Leading Order QCD. *Phys. Rev. Lett.*, 113(21):212001, 2014.

[105] Massimiliano Grazzini, Stefan Kallweit, and Dirk Rathlev. $W\gamma$ and $Z\gamma$ production at the LHC in NNLO QCD. *JHEP*, 07:085, 2015.

[106] Massimiliano Grazzini, Stefan Kallweit, Dirk Rathlev, and Marius Wiesemann. $W^{\pm}Z$ production at hadron colliders in NNLO QCD. *Phys. Lett.*, B761:179–183, 2016.

[107] Daniel de Florian, Massimiliano Grazzini, Catalin Hanga, Stefan Kallweit, Jonas M. Lindert, Philipp Maierhöfer, Javier Mazzitelli, and Dirk Rathlev. Differential Higgs Boson Pair Production at Next-to-Next-to-Leading Order in QCD. *JHEP*, 09:151, 2016.

[108] Roberto Bonciani, Stefano Catani, Massimiliano Grazzini, Hayk Sargsyan, and Alessandro Torre. The q_T subtraction method for top quark production at hadron colliders. *Eur. Phys. J.*, C75(12):581, 2015.

[109] S. Kallweit. MUNICH is the abbreviation of "MUlti-chaNnel Integrator at Swiss (CH) precision"–an automated parton level NLO generator. *In preparation.*

[110] R. Bonciani, S. Catani, M. Grazzini, and H. Sargsyan. Transverse-momentum resummation for heavy-quark pair production at hadron colliders. *In preparation.*

[111] P. L. Anthony et al. Determination of the neutron spin structure function. *Phys. Rev. Lett.*, 71:959–962, 1993.

[112] K. Abe et al. Precision measurement of the proton spin structure function g1(p). *Phys. Rev. Lett.*, 74:346–350, 1995.

[113] O. V. Tarasov, A. A. Vladimirov, and A. Yu. Zharkov. The Gell-Mann-Low Function of QCD in the Three Loop Approximation. *Phys. Lett.*, B93:429–432, 1980.

[114] K. A. Olive et al. Review of Particle Physics. *Chin. Phys.*, C38:090001, 2014.

[115] K. G. Chetyrkin. Quark mass anomalous dimension to $\mathcal{O}(\alpha_s^4)$. *Phys. Lett.*, B404:161–165, 1997.

[116] J. A. M. Vermaseren, S. A. Larin, and T. van Ritbergen. The four loop quark mass anomalous dimension and the invariant quark mass. *Phys. Lett.*, B405:327–333, 1997.

[117] A. Bassetto, M. Ciafaloni, and G. Marchesini. Jet Structure and Infrared Sensitive Quantities in Perturbative QCD. *Phys. Rept.*, 100:201–272, 1983.

[118] Yuri L. Dokshitzer, Valery A. Khoze, Alfred H. Mueller, and S. I. Troian. *Basics of perturbative QCD*. 1991.

[119] Stefano Catani and Massimiliano Grazzini. The soft gluon current at one loop order. *Nucl. Phys.*, B591:435–454, 2000.

[120] Isabella Bierenbaum, Michal Czakon, and Alexander Mitov. The singular behavior of one-loop massive QCD amplitudes with one external soft gluon. *Nucl. Phys.*, B856:228–246, 2012.

[121] V. N. Gribov and L. N. Lipatov. Deep inelastic e p scattering in perturbation theory. *Sov. J. Nucl. Phys.*, 15:438–450, 1972. [Yad. Fiz.15,781(1972)].

[122] Yuri L. Dokshitzer. Calculation of the Structure Functions for Deep Inelastic Scattering and e^+e^- Annihilation by Perturbation Theory in Quantum Chromodynamics. *Sov. Phys. JETP*, 46:641–653, 1977. [Zh. Eksp. Teor. Fiz.73,1216(1977)].

[123] Guido Altarelli and G. Parisi. Asymptotic Freedom in Parton Language. *Nucl. Phys.*, B126:298–318, 1977.

[124] D. de Florian, G. Ferrera, M. Grazzini, and D. Tommasini. Higgs boson production at the LHC: transverse momentum resummation effects in the H->2gamma, H->WW->lnu lnu and H->ZZ->4l decay modes. *JHEP*, 06:132, 2012.

[125] Stefano Catani, Daniel de Florian, Giancarlo Ferrera, and Massimiliano Grazzini. Vector boson production at hadron colliders: transverse-momentum resummation and leptonic decay. *JHEP*, 12:047, 2015.

[126] Leandro Cieri, Francesco Coradeschi, and Daniel de Florian. Diphoton production at hadron colliders: transverse-momentum resummation at next-to-next-to-leading logarithmic accuracy. *JHEP*, 06:185, 2015.

[127] Massimiliano Grazzini, Stefan Kallweit, Dirk Rathlev, and Marius Wiesemann. Transverse-momentum resummation for vector-boson pair production at NNLL+NNLO. *JHEP*, 08:154, 2015.

[128] Stefano Catani, Leandro Cieri, Daniel de Florian, Giancarlo Ferrera, and Massimiliano Grazzini. Universality of transverse-momentum resummation and hard factors at the NNLO. *Nucl. Phys.*, B881:414–443, 2014.

[129] Stefano Catani. The Singular behavior of QCD amplitudes at two loop order. *Phys. Lett.*, B427:161–171, 1998.

[130] W. T. Giele and E. W. Nigel Glover. Higher order corrections to jet cross-sections in e+ e- annihilation. *Phys. Rev.*, D46:1980–2010, 1992.

[131] Zoltan Kunszt, Adrian Signer, and Zoltan Trocsanyi. Singular terms of helicity amplitudes at one loop in QCD and the soft limit of the cross-sections of multiparton processes. *Nucl. Phys.*, B420:550–564, 1994.

[132] Robert V. Harlander. Virtual corrections to g g —> H to two loops in the heavy top limit. *Phys. Lett.*, B492:74–80, 2000.

[133] V. Ravindran, J. Smith, and W. L. van Neerven. Two-loop corrections to Higgs boson production. *Nucl. Phys.*, B704:332–348, 2005.

[134] Stefano Frixione, Paolo Nason, and Giovanni Ridolfi. Problems in the resummation of soft gluon effects in the transverse momentum distributions of massive vector bosons in hadronic collisions. *Nucl. Phys.*, B542:311–328, 1999.

[135] C. Balazs and C. P. Yuan. Higgs boson production at the LHC with soft gluon effects. *Phys. Lett.*, B478:192–198, 2000.

[136] Qing-Hong Cao, Chuan-Ren Chen, Carl Schmidt, and C. P. Yuan. Improved Predictions for Higgs Q(T) at the Tevatron and the LHC. 2009.

[137] Edmond L. Berger and Jian-wei Qiu. Differential cross-section for Higgs boson production including all orders soft gluon resummation. *Phys. Rev.*, D67:034026, 2003.

[138] Anna Kulesza, George F. Sterman, and Werner Vogelsang. Joint resummation for Higgs production. *Phys. Rev.*, D69:014012, 2004.

[139] Pavel M. Nadolsky, C. Balazs, Edmond L. Berger, and C. P. Yuan. Gluon-gluon contributions to the production of continuum diphoton pairs at hadron colliders. *Phys. Rev.*, D76:013008, 2007.

[140] Edmond L. Berger and Rui-bin Meng. Transverse momentum distributions for heavy quark pairs. *Phys. Rev.*, D49:3248–3260, 1994.

[141] S. Mrenna and C. P. Yuan. Effects of QCD resummation on distributions of top - anti-top quark pairs produced at the Tevatron. *Phys. Rev.*, D55:120–129, 1997.

[142] Stefano Catani, Stefan Dittmaier, and Zoltan Trocsanyi. One loop singular behavior of QCD and SUSY QCD amplitudes with massive partons. *Phys. Lett.*, B500:149–160, 2001.

[143] Alexander Mitov, George F. Sterman, and Ilmo Sung. The Massive Soft Anomalous Dimension Matrix at Two Loops. *Phys. Rev.*, D79:094015, 2009.

[144] Andrea Ferroglia, Matthias Neubert, Ben D. Pecjak, and Li Lin Yang. Two-loop divergences of scattering amplitudes with massive partons. *Phys. Rev. Lett.*, 103:201601, 2009.

[145] Andrea Ferroglia, Matthias Neubert, Ben D. Pecjak, and Li Lin Yang. Two-loop divergences of massive scattering amplitudes in non-abelian gauge theories. *JHEP*, 11:062, 2009.

[146] G. P. Korchemsky and A. V. Radyushkin. Renormalization of the Wilson Loops Beyond the Leading Order. *Nucl. Phys.*, B283:342–364, 1987.

[147] Thomas Becher and Matthias Neubert. Infrared singularities of QCD amplitudes with massive partons. *Phys. Rev.*, D79:125004, 2009. [Erratum: Phys. Rev.D80,109901(2009)].

[148] A. Torre. Soft-Gluon Resummation for Multiparton Hard-Scattering Processes: One-Particle Inclusive Cross Section and Heavy-Quark Pair Production at Hadron Colliders. *PhD Thesis*.

[149] Massimiliano Grazzini and Hayk Sargsyan. Heavy-quark mass effects in Higgs boson production at the LHC. *JHEP*, 09:129, 2013.

[150] Giuseppe Bozzi, Stefano Catani, Giancarlo Ferrera, Daniel de Florian, and Massimiliano Grazzini. Production of Drell-Yan lepton pairs in hadron collisions: Transverse-momentum resummation at next-to-next-to-leading logarithmic accuracy. *Phys. Lett.*, B696:207–213, 2011.

[151] A. D. Martin, W. J. Stirling, R. S. Thorne, and G. Watt. Parton distributions for the LHC. *Eur. Phys. J.*, C63:189–285, 2009.

[152] S. Catani and M. Grazzini. Higgs Boson Production at Hadron Colliders: Hard-Collinear Coefficients at the NNLO. *Eur. Phys. J.*, C72:2013, 2012. [Erratum: Eur. Phys. J.C72,2132(2012)].

[153] Thomas Gehrmann, Thomas Lubbert, and Li Lin Yang. Transverse parton distribution functions at next-to-next-to-leading order: the quark-to-quark case. *Phys. Rev. Lett.*, 109:242003, 2012.

[154] Thomas Gehrmann, Thomas Luebbert, and Li Lin Yang. Calculation of the transverse parton distribution functions at next-to-next-to-leading order. *JHEP*, 06:155, 2014.

[155] John M. Campbell, R. Keith Ellis, and Walter T. Giele. A Multi-Threaded Version of MCFM. *Eur. Phys. J.*, C75(6):246, 2015.

[156] Ansgar Denner, Stefan Dittmaier, and Lars Hofer. COLLIER - A fortran-library for one-loop integrals. *PoS*, LL2014:071, 2014.

[157] Ansgar Denner and S. Dittmaier. Reduction of one loop tensor five point integrals. *Nucl. Phys.*, B658:175–202, 2003.

[158] A. Denner and S. Dittmaier. Scalar one-loop 4-point integrals. *Nucl. Phys.*, B844:199–242, 2011.

[159] Giovanni Ossola, Costas G. Papadopoulos, and Roberto Pittau. CutTools: A Program implementing the OPP reduction method to compute one-loop amplitudes. *JHEP*, 03:042, 2008.

[160] A. van Hameren. OneLOop: For the evaluation of one-loop scalar functions. *Comput. Phys. Commun.*, 182:2427–2438, 2011.

[161] M. Grazzini, S. Kallweit, D. Rathlev, and M. Wiesemann. MATRIX is the abbreviation of "MUNICH Automates q_T subtraction and Resummation to Integrate Cross Sections". *In preparation.*

[162] Thomas Gehrmann and Lorenzo Tancredi. Two-loop QCD helicity amplitudes for $q\bar{q} \to W^{\pm}\gamma$ and $q\bar{q} \to Z^0\gamma$. *JHEP*, 02:004, 2012.

[163] Thomas Gehrmann, Andreas von Manteuffel, and Lorenzo Tancredi. The two-loop helicity amplitudes for $q\overline{q}' \to V_1V_2 \to 4$ leptons. *JHEP*, 09:128, 2015.

[164] Daniel de Florian and Javier Mazzitelli. Two-loop virtual corrections to Higgs pair production. *Phys. Lett.*, B724:306–309, 2013.

[165] Massimiliano Grazzini, Stefan Kallweit, and Dirk Rathlev. ZZ production at the LHC: fiducial cross sections and distributions in NNLO QCD. *Phys. Lett.*, B750:407–410, 2015.

[166] Massimiliano Grazzini, Stefan Kallweit, Stefano Pozzorini, Dirk Rathlev, and Marius Wiesemann. W^+W^- production at the LHC: fiducial cross sections and distributions in NNLO QCD. *JHEP*, 08:140, 2016.

[167] Michal Czakon and Alexander Mitov. Top++: A Program for the Calculation of the Top-Pair Cross-Section at Hadron Colliders. *Comput. Phys. Commun.*, 185:2930, 2014.

[168] T. Gleisberg, Stefan. Hoeche, F. Krauss, M. Schonherr, S. Schumann, F. Siegert, and J. Winter. Event generation with SHERPA 1.1. *JHEP*, 02:007, 2009.

[169] Claude Duhr, Stefan Hoeche, and Fabio Maltoni. Color-dressed recursive relations for multi-parton amplitudes. *JHEP*, 08:062, 2006.

[170] John C. Collins and Davison E. Soper. Angular Distribution of Dileptons in High-Energy Hadron Collisions. *Phys. Rev.*, D16:2219, 1977.

[171] George F. Sterman and Steven Weinberg. Jets from Quantum Chromodynamics. *Phys. Rev. Lett.*, 39:1436, 1977.

[172] John C. Collins, Davison E. Soper, and George F. Sterman. Factorization of Hard Processes in QCD. *Adv. Ser. Direct. High Energy Phys.*, 5:1–91, 1989.

[173] Vardan Khachatryan et al. Angular coefficients of Z bosons produced in pp collisions at $\sqrt{s} = 8$ TeV and decaying to $\mu^+\mu^-$ as a function of transverse momentum and rapidity. *Phys. Lett.*, B750:154–175, 2015.

[174] Georges Aad et al. Measurement of the angular coefficients in Z-boson events using electron and muon pairs from data taken at $\sqrt{s} = 8$ TeV with the ATLAS detector. *JHEP*, 08:159, 2016.

[175] E. Mirkes. Angular decay distribution of leptons from W bosons at NLO in hadronic collisions. *Nucl. Phys.*, B387:3–85, 1992.

[176] M. Chaichian, M. Hayashi, and K. Yamagishi. Angular Distributions of High Mass Dileptons With Finite Transverse Momentum in High-energy Hadronic Collisions. *Phys. Rev.*, D25:130, 1982. [Erratum: Phys. Rev.D26,2534(1982)].

[177] Kaoru Hagiwara, Ken-ichi Hikasa, and Naoyuki Kai. Parity Odd Asymmetries in W Jet Events at Hadron Colliders. *Phys. Rev. Lett.*, 52:1076, 1984.

[178] A. Gehrmann-De Ridder, T. Gehrmann, E. W. N. Glover, A. Huss, and T. A. Morgan. Precise QCD predictions for the production of a Z boson in association with a hadronic jet. *Phys. Rev. Lett.*, 117(2):022001, 2016.

[179] M. Czakon. Tops from Light Quarks: Full Mass Dependence at Two-Loops in QCD. *Phys. Lett.*, B664:307–314, 2008.

[180] P. Bärnreuther, M. Czakon, and P. Fiedler. Virtual amplitudes and threshold behaviour of hadronic top-quark pair-production cross sections. *JHEP*, 02:078, 2014.